The role of fibrin clots in cardiovascular disease and infection control

Fraser Lawrence Macrae

Thrombosis and Tissue Repair Group

Discovery and Translational Science Department

Leeds Institute of Cardiovascular and Metabolic Medicine (LICAMM)

School of Medicine

University of Leeds

Submitted in accordance with the requirements for the degree of Doctor of Philosophy

January 2019

Intellectual Property and Publication Statements

The candidate confirms that the work submitted is their own, except where work which has formed part of jointly authored publications has been included. The contribution of the candidate and the other authors to this work has been explicitly indicated below. The candidate confirms that appropriate credit has been given within the thesis where reference has been made to the work of others.

Publications and proposed publications which have arisen from the work presented in this thesis are:

- **A fibrin biofilm covers blood clots and protects from microbial invasion.** Macrae FL, Duval C, Papareddy P, Baker SR, Yuldasheva N, Kearney KJ, McPherson HR, Asquith N, Konings J, Casini A, Degen JL, Connell SD, Philippou H, Wolberg AS, Herwald H, Ariëns RA. J Clin Invest. 2018 Aug 1; 128(8):3356-3368. doi: 10.1172/JCI98734. Methods from this paper appear in the methods section on formation of the fibrin film (chapter 2.3) and roles of the fibrin film (chapter 2.4). Results, adapted figures and discussion from this paper appear in Chapter 4 and Chapter 5. Robert Ariëns and I conceived the idea for this project. I performed all the experiments in this section unless stated otherwise. Cedric Duval and Helen McPherson expressed all mutant fibrinogens. Cedric Duval, Praveen Papareddy and Nadira Yuldasheva performed *in vivo* murine experiments. Stephen Baker performed AFM experiments. Katherine Kearney along with myself performed Affimer experiments. Katherine Kearney performed all SDS-page and western blot experiments. I performed all data analysis, wrote and submitted the manuscript for publication. All authors on the paper critically reviewed the manuscript prior to publication. Robert Ariëns helped plan the work, design experiments, interpret results and edit the manuscript.
- **The prothrombotic state in paroxysmal nocturnal haemoglobinuria: a multifaceted source.** Peacock-Young B, Macrae FL, Newton DJ, Hill A, Ariëns RAS. Haematologica. 2018 Jan; 103(1):9-17. doi: 10.3324/haematol.2017.177618. (Review). A pre-publication version of a figure from this review appears in chapter 1.4.1. I co-authored this review with Barnaby Peacock-Young, Darren Newton, Anita Hill and Robert Ariëns. Barnaby Peacock-Young and I wrote the review and I created the diagrams. Robert Ariëns, Anita Hill and Darren Newton were involved in the planning of the review and revision of the manuscript.
- **The (patho)physiology of fibrinogen γ'.** Macrae FL, Domingues MM, Casini A, Ariëns RAS. Semin Thromb Hemost. 2016 Jun; 42(4):344-55. doi: 10.1055/s-0036-1572353 (Review). Two figures from this review appear in chapter 1.2. I co-authored this review with Marco Domingues, Alessandro Casini and Robert Ariëns. Marco Domingues, Alessandro Casini wrote sections for the review on 'Interaction with Factor XIII' and 'Clinical Implications' respectively. I wrote the remaining parts of the review and I created the

diagrams. Robert Ariëns was involved in the planning of the review and revision of the manuscript.

- **Common FXIII and fibrinogen polymorphisms in abdominal aortic aneurysms.** Macrae FL, Evans HL, Bridge KI, Johnson A, Scott DJ, Ariëns RA. PLoS One. 2014 Nov; 10;9(11):e112407. doi: 10.1371/journal.pone.0112407. Methods from this paper appear in the methods section on clotting in AAA (chapter 2.5). Results, tables and discussion from this paper appear in Chapter 6. Robert Ariëns, Julian Scott and I conceived the idea for this study and designed the experiments. Hannah Lee Evans, Katherine Paradine and I extracted blood from DNA samples. I carried out all genotyping and analysis of data in this study. Anne Johnson recruited patients. I wrote the manuscript with the help of Robert Ariëns and submitted the manuscript for publication. All authors on the paper critically reviewed the manuscript prior to publication.
- **The relationship between PNH clone size, eculizumab treatment and fibrin clot structure.** Macrae FL, Peacock-Young B, Bowman P, Quested S, Linton E, Clarke D, McKinley C, Riley K, Copeland N, Arnold L, Newton D, Hill A, Ariëns RA (in preparation). Robert Ariëns, Anita Hill, Darren Newton and I conceived the idea for this study and designed the experiments. Barnaby Peacock-Young, Polly Bowman and Sam Quested each carried out turbidity and lysis, permeation and confocal on between 10-15 patients as part of an intercalated BSc project. Emma Linton carried out fibrinogen level measurements on 33 patients. I carried out all other experiments within the paper. Deborah Clarke, Claire McKinley, Kathryn Riley, Nicola Copeland and Louise Arnold helped recruit patients, take blood samples and prepare plasma samples. Barnaby Peacock-Young and I are writing the paper. Robert Ariëns, Anita Hill and Darren Newton are helping interpret results and edit the manuscript.

Acknowledgements

I would like to start by thanking all those who played a role in the formation of this PhD thesis. I would like to thank my supervisors Prof Robert Ariëns, Prof Helen Philippou and Prof Julian Scott for their guidance, support and intellectual discussion during my PhD. A big thank you goes to the Ariëns group for putting up with me for so long! You have provided valuable laboratory guidance and friendship over the last 5 years. Particular thanks go to Dr Amy Cilia La Corte and Dr Cedric Duval who helped me at the very beginning by guiding and teaching me, providing the foundations of my scientific career.

I would like to acknowledge our collaborators Prof Johan Heemskerk, Dr Frauke Swieringa and Dr Constance Baaten at the University of Maastricht for giving their time to host me in an intense week of flow experiments. I look forward to continuing this collaboration in the future. I would like to thank Prof Heiko Herwald and Dr Praveen Papareddy at the University of Lund in Sweden and Dr Cedric Duval, for a very fruitful collaboration, producing great data that contributed greatly to the publication of our paper in JCI. I would also like to thank all the other authors on this paper for their contributions.

I would like to thank all those involved in the Leeds Aneurysm Development Study (LEADS). Having access to one of the largest collections of data and samples relating to abdominal aortic aneurysm patients in the world contributed greatly to my PhD. A special mention goes to Mrs Anne Johnson, who dedicated ten years to the recruitment of new patients and the ongoing management of the study database. This study and my PhD would not have been possible without the generous support of the Garfield Weston Foundation.

I would like to thank Dr Anita Hill, my three iBSc students, Polly Bowman, Barnaby Peacock-Young, Sam Quested and FY2 Dr Emma Linton for their assistance in the study of thrombosis in PNH. Without their hard work recruiting patients, collecting blood samples and analysis of clot structure in these patients, this study would not have been possible.

While reading this thesis it will become clear that my PhD has included many different projects, and this has resulted in there being too many people to mention individually. I apologise if you haven’t made the list above, but you have all contributed to making the last five years a success. To all the people who have had to put up with my scientific babble outside of work, I apologise, especially to Katherine Kearney who will probably never want to hear about fibrin films ever again!

Finally, I would like to offer my heartfelt thanks to the Garfield Weston Foundation and the British Heart Foundation for funding my multiple projects throughout my PhD.

Publication list

Recurrent venous thromboembolism patients form clots with lower elastic modulus than those with non-recurrent disease. S. R. Baker, M. Zabczyk, F. L. Macrae, C. Duval, A. Undas, R. A. S. Ariëns. J Thromb Haemost. 2019 Jan (In press)

Assessment and determinants of whole blood and plasma fibrinolysis in patients with mild bleeding symptoms. Minka J.A. Vries, Fraser Macrae, Patricia J. Nelemans, Gerhardus J.A.J.M. Kuiper, Rick J.H. Wetzels, Polly Bowman, Paul W.M. Verhezen, Hugo ten Cate, Robert A.S. Ariëns, Yvonne M.C. Henskens. Thromb Res 2018 Dec; 174:88-94, doi: 10.1016/j.thromres.2018.12.004

Affimer Proteins as a Tool to Modulate Fibrinolysis, Stabilize the Blood Clot and Reduce Bleeding Complications. Katherine J Kearney, Nikoletta Pechlivani, Rhodri King, Christian Tiede, Fladia Phoenix, Ramsah Cheah, Fraser L Macrae et al. Blood 2018 Dec; doi: 10.1182/blood-2018-06-856195.

Impact of γ′γ′ fibrinogen interaction with red blood cells on fibrin clots. Guedes AF, Carvalho FA, Domingues MM, Macrae FL, McPherson HR, Sabban A, Martins IC, Duval C, Santos NC, Ariëns RA. Nanomedicine 2018 Oct; 13(19):2491-2505. doi: 10.2217/nnm-2018-0136

A fibrin biofilm covers blood clots and protects from microbial invasion. Macrae FL et al. J Clin Invest. 2018 Aug; 1;128(8):3356-3368. doi: 10.1172/JCI98734 (Cover article with 3-page commentary)

The $_{95}$RGD$_{97}$ sequence on the Aα chain of fibrinogen is essential for binding to its erythrocyte receptor. Carvalho FA, Guedes AF, Duval C, Macrae FL, Swithenbank L, Farrell DH, Ariëns RA, Santos NC. Int J Nanomedicine. 2018 Apr; 3;13:1985-1992. doi: 10.2147/IJN.S154523

Sensing adhesion forces between erythrocytes and γ' fibrinogen, modulating fibrin clot architecture and function. Guedes AF, Carvalho FA, Domingues MM, Macrae FL, McPherson HR, Santos NC, Ariëns RAS. Nanomedicine. 2018 Apr; 14(3):909-918. doi: 10.1016/j.nano.2018.01.006

Atherothrombosis and Thromboembolism: Position Paper from the Second Maastricht Consensus Conference on Thrombosis. Spronk HMH, Padro T, Siland JE, Prochaska JH, Winters J, van der Wal AC, Posthuma JJ, Lowe G, d'Alessandro E, Wenzel P, Coenen DM, Reitsma PH, Ruf W, van Gorp RH, Koenen RR, Vajen T, Alshaikh NA, Wolberg AS, Macrae FL, Asquith N, Heemskerk J, Heinzmann A, Moorlag M, Mackman N, van der Meijden P, Meijers JCM, Heestermans M, Renné T, Dólleman S, Chayouâ W, Ariëns RAS, Baaten CC, Nagy M, Kuliopulos A, Posma JJ, Harrison P, Vries MJ, Crijns HJGM, Dudink EAMP, Buller HR, Henskens YMC, Själander A, Zwaveling S, Erküner O, Eikelboom JW, Gulpen A, Peeters FECM, Douxfils J, Olie RH, Baglin T, Leader A, Schotten U, Scaf B, van Beusekom HMM, Mosnier LO, van der Vorm L, Declerck P, Visser M, Dippel DWJ, Strijbis VJ, Pertiwi K, Ten Cate-Hoek AJ, Ten Cate H. Thromb Haemost. 2018 Feb; 118(2):229-250. doi: 10.1160/TH17-07-0492.

The prothrombotic state in paroxysmal nocturnal haemoglobinuria: a multifaceted source. Peacock-Young B, Macrae FL, Newton DJ, Hill A, Ariëns RAS. Haematologica. 2018 Jan; 103(1):9-17. doi: 10.3324/haematol.2017.177618.

Thrombin-activatable fibrinolysis inhibitor in human abdominal aortic aneurysm disease. Bridge KI, Bollen L, Zhong J, Hesketh M, Macrae FL, Johnson A, Philippou H, Scott DJ, Gils A, Ariëns RAS. J Thromb Haemost. 2017 Nov; 15(11):2218-2225. doi: 10.1111/jth.13804

Characterization of the I4399M variant of apolipoprotein(a): implications for altered prothrombotic properties of lipoprotein(a). Scipione CA, McAiney JT, Simard DJ, Bazzi ZA, Gemin M, Romagnuolo R, Macrae FL, et al. J Thromb Haemost. 2017 Sep; 15(9):1834-1844. doi: 10.1111/jth.13759.

Inhibition of plasmin-mediated TAFI activation may affect development but not progression of abdominal aortic aneurysms. Bridge K, Revill C, Macrae F et al. PLoS One. 2017 May; 4;12(5):e0177117. doi: 10.1371/journal.pone.0177117

The (Patho)physiology of Fibrinogen γ'. Macrae FL, Domingues MM, Casini A, Ariëns RA. Semin Thromb Hemost. 2016 Jun; 42(4):344-55. doi: 10.1055/s-0036-1572353.

Procoagulant changes in fibrin clot structure in patients with cirrhosis are associated with oxidative modifications of fibrinogen. Hugenholtz GC, Macrae F, Adelmeijer J, Dulfer S, Porte RJ, Lisman T, Ariëns RA. J Thromb Haemost. 2016 Feb; 14(5):1054-66. doi: 10.1111/jth.13278.

Thrombin and fibrinogen γ' impact clot structure by marked effects on intrafibrillar structure and protofibril packing. Domingues MM, Macrae FL, Duval C, McPherson HR, Bridge KI, Ajjan RA, Ridger VC, Connell SD, Philippou H, Ariëns RA. Blood. 2016 Jan;127(4):487-95. doi: 10.1182/blood-2015-06-652214.

Common FXIII and fibrinogen polymorphisms in abdominal aortic aneurysms. Macrae FL, Evans HL, Bridge KI, Johnson A, Scott DJ, Ariëns RA. PLoS One. 2014 Nov; 9(11):e112407. doi: 10.1371/journal.pone.0112407.

The alpha-2-antiplasmin Arg407Lys polymorphism is associated with abdominal aortic aneurysm. Bridge KI, Macrae F, Bailey MA, Johnson A, Philippou H, Scott DJ, Ariëns RA. Thromb Res. 2014 Sep; 134(3):723-8. doi: 10.1016/j.thromres.2014.06.019.

Abstract

Coagulation plays an important role in the haemostatic process, forming a blood clot to prevent blood loss. Changes in formation, structure or breakdown of these clots can result in the pathogenesis of thrombotic disorders. These imbalances can be caused by changes to the fibrin(ogen) molecule, inflammation and levels of other plasma proteins. This thesis focusses on different mechanisms that effect clot structure, and how these prevent or promote disease, with the aim of uncovering new pathways to target therapeutically.

This study revealed the vast range of physiological fibrinogen γ' levels present in 1164 patients, fluctuating between 0.8 % and 39.5 % of total fibrinogen. Furthermore, it demonstrated that changes of fibrinogen γ' levels within this physiological range plays an important role in modulating clot structure, with fibrinogen γ' significantly increasing height and volume of clots under flow. It also found that the FXIII-B Arg95 variant is associated with an increased risk of AAA, suggesting a possible role for FXIII in AAA pathogenesis. It showed how PNH patients with increased clone size have a more thrombotic phenotype, with faster forming, more stable clots, but these changes do not appear to be caused by changes in the fibrin clot. In addition, it showed that the antithrombotic effects of eculizumab treatment appear to function in part due to a reduction in fibrinogen and thrombin levels. And finally the discovery of a remarkable aspect of blood clotting in which fibrin forms a protective film at the air-blood interface covering the external surface of the clot, retaining blood cells and providing an instant barrier against microbial invasion.

Together these data provide new insight into some of the main modulators of clot structure, providing previously unknown mechanisms of haemostasis and possible new pathways to target in the prevention and treatment of thrombosis and infection.

Contents

List of Tables

List of Figures

Abbreviations

°C - Degrees centigrade

3D - 3 dimensional

AAA - Abdominal aortic aneurysm

Abs - Absorbance

Afib - Afibrinogenemia

AFM - Atomic force microscopy

Ala - Alanine

Arg - Arginine

Asp - Aspartic acid

ATP - Adenosine triphosphate

Bac - Bacteria

BMI - Body mass index

BSA - Bovine serum albumin

BU - Batroxobin unit

$C_2H_6AsNaO_2$ - Sodium cacodylate

Ca^{2+} - Calcium ions

$CaCl_2$ - Calcium chloride

CAD - Coronary artery disease

CAT - Calibrated automated thrombogram

CFE - Cold field emission

CFU - Colony forming unit

CHO - Chinese hamster ovary cells

cm - Centimetre

CO_2 - Carbon dioxide

CR - Clotting rate

CTI - Corn trypsin inhibitor

CVA/TIA - Cerebrovascular accident/transient ischemic attack

CVD - Cardiovascular disease

ddH_2O - Distilled water

df - Degrees of freedom

DM - Diabetes mellitus

DNA - Deoxyribose nucleic acid

DTT - Dithiothreitol

DVT - Deep vein thrombosis

Dysfib - Dysfibrinogenemia

Ecu - Eculizumab

EDTA - Ethylenediaminetetraacetic acid

EGR-1 - Early growth response protein 1

ELISA - Enzyme linked immunosorbent assay

ERL - Enzyme research laboratories

ETP - Endogenous thrombin potential

F - Force

FD - Fibrinogen deficient

$FeCl_3$ - Ferric chloride

FGA - Fibrinogen alpha chain

FGB - Fibrinogen beta chain

FGG - Fibrinogen gamma chain

Fgn - Fibrinogen

Fib - Fibrinogen

FIX - Factor IX

FIXa - Factor IXa

FLAER - Fluorescein-labelled proaerolysin

Fluor - Fluorescence

FpA - Fibrinopeptide A

FpB - Fibrinopeptide B

FV - Factor V

FVa - Factor Va

FVII - Factor VII

FVIIa - Factor VIIa

FVIII - Factor VIII

FVIIIa - Factor VIIIa

FX - Factor X

FXa - Factor Xa

FXI - Factor XI

FXIa - Factor XIa

FXII - Factor XII

FXIII - Factor XIII

FXIIIa - Factor XIIIa

g - G-force/Relative centrifugal force

g - Gram

GPI - Glycosylphosphatidylinositol

GPI-Aps - Glycosylphosphatidylinositol-Anchored Proteins

GPIb - Glycoprotein Ib

GPIIb/IIIa - Glycoprotein IIb/IIIa

GPRP - Glycine-Proline-Arginine-Proline

h - Hour

H_2SO_4 - Sulphuric acid

Hb - Haemoglobin

HCL - Hydrochloric acid

His - Histadine

HMWK - High molecular weight kininogen

HRP - Horseradish peroxidase

IHC - Immunohistochemistry

IIa - Thrombin

ILT - Intraluminal thrombus

IQR - Interquartile range

IU - International units

IVC - Inferior vena cava

k - Calibration coefficient

K_2EDTA - Dipotassium ethylenediaminetetraacetic acid

KCL - Potassium chloride

kDa - Kilodalton

Kg - Kilogram

kPa - Kilopascals

LDH - Lactate dehydrogenase

LEADS - Leeds Aneurysm Development Study

Leu - Leucine

LSCM - Laser scanning confocal microscopy

Lys - Lysine

M - Molar

mAb - Monoclonal antibody

MAC - Membrane attack complex

MASP-1 - Mannan-binding lectin serine protease 1

MaxV - Maximum rate

MCF - Maximum clot firmness

mg - Milligram

$MgCl_2$ - Magnesium chloride

MI - Myocardial infarction

min - Minute

ml - Millilitre

mm - Millimetre

mM - Millimolar

mmHg - Millimetre of mercury

MMPs - Matrix metalloproteinases

mN - Millinewton

mRNA - Messenger ribonucleic acid

MSF - Mean sheet fluorescence

MW - Molecular weight

N/A - Not applicable

NaCl - Sodium chloride

NETs - Neutrophil extracellular traps

ng - Nanogram

NHS - National health service

NIHU - National institute of health units

nm - Nanometer

NO - Nitric oxide

NP - Normal pool

NPP - Normal pooled plasma

OD - Optical density

P - Photons

PAI-1 - Plasminogen activator inhibitor-1

PAI-2 - Plasminogen activator inhibitor-2

PBS - Phosphate buffered saline

PCR - Polymerase chain reaction

PE - Pulmonary embolism

PIG-A - Phosphatidylinositol N-acetylglucosaminyltransferase subunit A

PK - Prekallikrein

plg - Plasminogen

pM - Picomolar

PMPs - Platelet microparticles

PNH - Paroxysmal nocturnal haemoglobinuria

PPP - Platelet poor plasma

PRP - Platelet rich plasma

PVD - Peripheral vascular disease

PVDF - Polyvinylidene fluoride

RBC - Red blood cell

ROS - Reactive oxygen species

ROTEM - Rotational thromboelastography

rpm - Revolutions per minute

S^{-1} - Reciprocal second

SD - Standard deviation

SDS-PAGE - Sodium dodecyl sulphate polyacrylamide gel electrophoresis

Sec - Seconds

SEM - Scanning electron microscopy

Ser - Serine

SNP - Single nucleotide polymorphism

SOC - Super optimal broth with catabolite repression

SP - Surface pressure

Sr - Steradian

SV - Splice variant

T101 - 1,3,4,5-Tetramethyl-2-[(2-oxopropyl)thio]imidazolium chloride

TAFI - Thrombin-activatable fibrinolysis inhibitor

TBS - Tris buffered saline

TF - Tissue factor

TFPI - Tissue factor pathway inhibitor

TH - Todd Hewitt

Thr - Threonine

TMB - 3,3',5,5'-Tetramethylbenzidine

tPA - Tissue plasminogen activator

U - Units

ULBP1 - UL16 binding protein 1

uPA - Urokinase-type plasminogen activator

Val - Valine

Vmax - Maximum rate

vWF - von Willebrand factor

WPB - Weibel–Palade bodies

WT - Wildtype

X^2 - Chi squared

α2AP - α2-antiplasmin

µg - Microgram

µl - Microliter

µM - Micrometre

µN - Micronewton

Chapter 1 - Introduction

The coagulation and fibrinolytic cascades play important roles in both the prevention of blood loss and infection control. Damage to the vessel wall and exposure of the subendothelium triggers complex pathways that result in the formation of a blood clot that helps to prevent blood loss. Imbalances in the formation, stability or breakdown of these clots can result in the pathogenesis of thrombotic or bleeding disorders.

1.1 Haemostasis

The ultimate goal in the haemostatic process is to prevent the loss of blood. This is achieved by blocking breaches in the vessel wall with the formation of a blood clot. This occurs through a chain of enzymatic reactions known as the coagulation cascade. The initial step, primary haemostasis, occurs due to the activation and aggregation of platelets to form a platelet plug. This is followed by secondary haemostasis, which refers to the formation of the fibrin 3D network, which helps to stabilise the platelet plug. This occurs through two pathways, the ‘Extrinsic’ or ‘Tissue Factor’ pathway which is triggered by tissue factor (TF), or the ‘Intrinsic’ or ‘Contact Factor’ pathway which is triggered by the exposure of collagen or a negatively charged surface, activation of prekallikrein, high molecular weight kininogen (HMWK) and Factor XII (FXII).

1.1.1 Coagulation initiation

Upon injury to the vessel wall, endothelial cells in close proximity to the site of injury become activated. This results in P-selectin being released from the Weibel-Palade storage bodies (WPB) and becoming exposed on the cell surface (McEver et al., 1989). Exposure of the subendothelium immediately

begins to activate platelets, with P-selectin also being exposed on the platelet surface from within the alpha granules, where it plays an important role in the initial adhesion and rolling of platelets to areas of injury and inflammation. Activated platelets also begin to adhere to the exposed collagen and fibronectin via GPVI and α2β1 (Roskam et al., 1959). Simultaneously von Willebrand Factor (vWF) is released from the body of endothelial cells and platelets. This plays two roles, under high shear rates (arterial flow) vWF recruits platelets to the site of injury by binding collagen in the subendothelium and glycoprotein Ib (GPIb) on the platelet surface (Bergmeier et al., 2006). vWF also binds to glycoprotein IIb/IIIa (GPIIb/IIIa) on the activated platelet surface which helps to increase platelet aggregation (Naimushin and Mazurov, 2004). Tissue factor, a transmembrane glycoprotein, is expressed on stromal fibroblasts and smooth muscle cells and is exposed upon vascular injury. Circulating Factor VII (FVII) binds to TF forming an active TF-FVIIa complex, which can then activate Factor X (FX). Factor Xa (FXa) activates prothrombin to thrombin, and this small quantity of thrombin feeds back to propagate further thrombin production in the amplification phase (Monroe and Hoffman, 2006).

1.1.2 Thrombin amplification

Thrombin produced from FXa activation leads to the activation of Factor V (FV) and Factor XI (FXI). Thrombin also releases Factor VIII (FVIII) from its circulating complex with vWF and activates it. FVIIIa then comes together with Factor IXa (FIXa) and calcium on platelet surfaces to form a tenase complex, which activates FX (Dahlback, 2000).

The tenase complex goes on to produce vast quantities of FXa, this forms a partnership with FVa forming the prothrombinase complex. The prothrombinase complex results in a thrombin burst, producing large quantities of thrombin (Dahlback, 2000). The thrombin produced continues to activate FV, FVIII and FXI resulting in further thrombin production. The activation of FXI results in the activation of Factor IX (FIX) which also contributes to thrombin production. The thrombin produced goes on to convert fibrinogen to fibrin and activate Factor XIII (FXIII) to help stabilise the clot.

1.1.3 Intrinsic pathway

The intrinsic pathway is initiated by the exposure of collagen or other negatively charged surfaces to FXII. Small amounts of FXII are auto-activated and along with HMWK, leads to the activation of prekallikrein (PK) to kallikrein (Kaplan et al., 2002, Renne et al., 2012). Further activation of FXII by kallikrein, and PK by FXIIa results in a positive feedback loop. The generated FXIIa subsequently activates FXI. FXIa activates FIX, which along with FVIII, activates FX (Smith et al., 2015), leading to the activation of prothrombin.

Both the intrinsic and extrinsic pathways continue their feedback loops with activation of FV, FVIII and FIX producing more thrombin, until they are downregulated by anticoagulants or the fibrinolysis pathways.

1.1.4 Fibrinogen to fibrin

Fibrinogen is the third most abundant of human plasma proteins, and normally circulates at around 2-4 $mg.ml^{-1}$. Fibrinogen expression can be upregulated in response to pro-inflammatory agents such as interleukin-6

and other cytokines, resulting in increased plasma levels (Dalmon et al., 1993, Lane et al., 1991). Increased levels of fibrinogen are associated with cardiovascular disease including stroke, peripheral vascular disease, pulmonary embolism and abdominal aortic aneurysms (AAA) (Danesh et al., 2005, Bartlett et al., 2009, Klovaite et al., 2013, Parry et al., 2009). Whether these elevated fibrinogen levels are part of the cause or an effect of the disease is still unknown.

Fibrinogen is a 340 kDa complex glycoprotein made up of three pairs of polypeptide chains, Aα, Bβ and γ held together by 29 disulfide bonds (Doolittle, 1984, Henschen and McDonagh, 1986). It is 45 nm long, consisting of three globular regions, two D regions at each end and one E region in the centre connected by α-helical coiled-coil rods (Hall and Slayter, 1959, Weisel et al., 1985). The C-terminal ends of the Aα-chains extend out from the D regions in a coiled-coil, ending in the αC globular region (Weisel and Medved, 2001). The N-terminal ends of the Aα- and Bβ-chains, fibrinopeptide A and B, are located in the central E region.

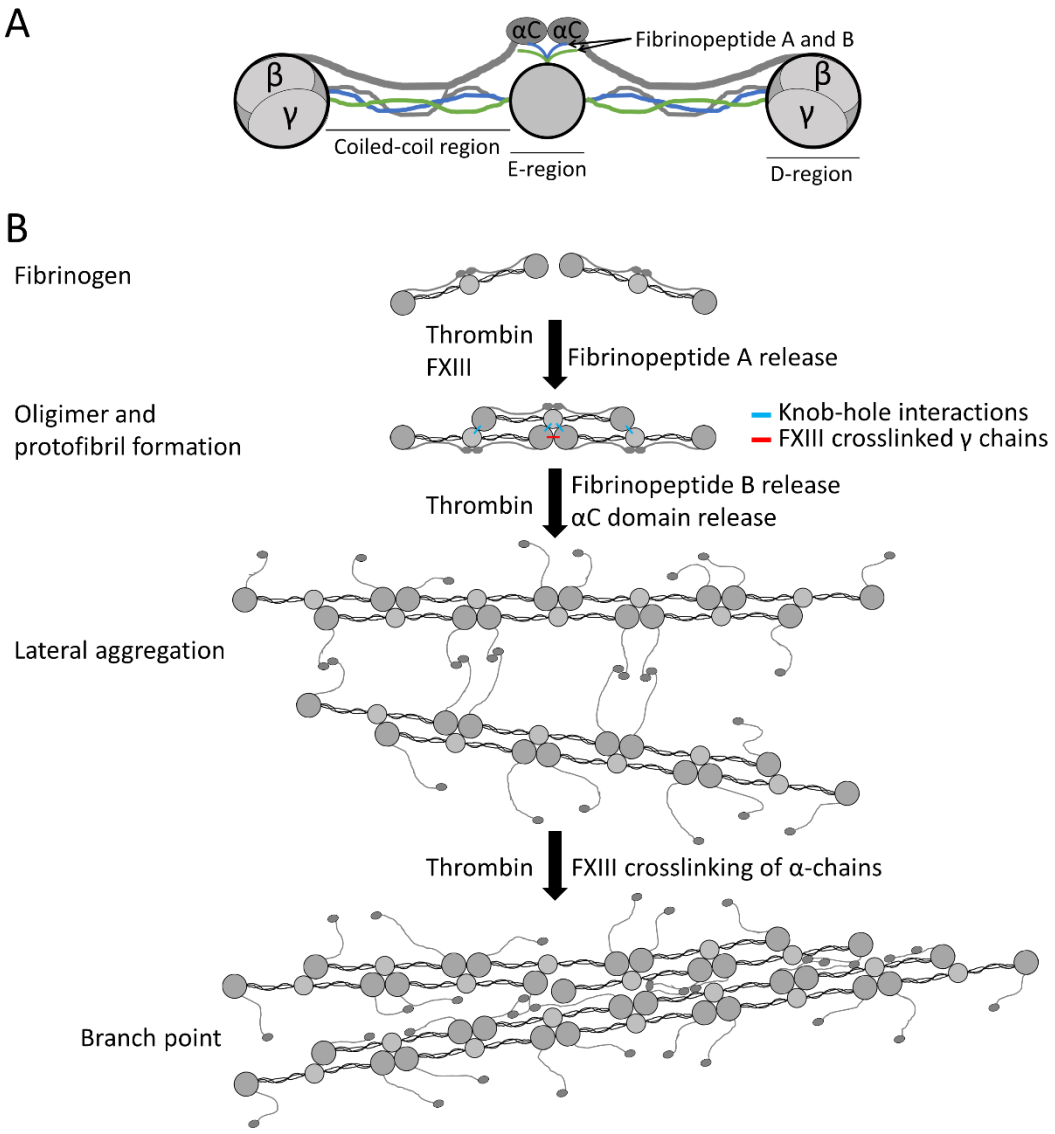

Figure 1 Structure of fibrinogen and conversion to fibrin. A, A diagram of fibrinogen structure. Fibrinogen consists of three pairs of polypeptide chains, Aα, Bβ and γ held together by 29 disulfide bonds. All three chains converge in a central E region, which contains the cleavage sites for thrombin (Fibrinopeptides A and B). The chains extend out of this central E region through a coil-coiled region to the D regions, where the beta and gamma chains reach their C-terminus. The alpha chain extends beyond this D region, as the alpha-C chain. **B,** Fibrinopeptide A is cleaved by thrombin from fibrinogen which aggregate via knob-hole interactions forming oligomers and then protofibrils. Fibrinopeptide B is then cleaved by thrombin, releasing the αC regions, which allows lateral aggregation to occur forming fibres. Factor XIIIa initially crosslinks γ chains, followed by α chains. Branch points are initiated by the divergence of two protofibrils. Adapted from Weisel (2005).

Fibrin polymerization is initiated when the fibrinopeptides are cleaved specifically by thrombin, a serine protease (Figure 1). The newly exposed ‘‘knobs’’ in the E region, due to fibrinopeptide removal, interact with the ‘‘holes’’ that are always exposed in the D regions (Doolittle, 1984, Shainoff and Dardik, 1983). This results in the conversion of soluble fibrinogen to an insoluble fibrin polymer. These tightly controlled binding interactions result in fibrin polymerizing in a repeating 22.5 nm half-staggered conformation producing oligomers that lengthen into protofibrils (Weisel, 1986, Fowler et al., 1981). Protofibrils laterally aggregate, enhanced by αC regions, to form fibres, forming a branching 3D network that is essential for haemostasis (Hantgan and Hermans, 1979, Weisel and Medved, 2001). Finally FXIII, also activated by thrombin, covalently binds together fibrin molecules through specific glutamine-lysine residue interactions via isopeptide bonds (Henschen and McDonagh, 1986, Lorand, 2001). This helps to stabilize the clot against mechanical, and proteolytic interventions. The mechanical properties of clots are essential to fibrin’s functions in haemostasis.

A blood clot is only a temporary plug during haemostasis, so mechanisms are in place to remove fibrin and remove the clot after it has served its purpose. The breakdown of fibrin occurs when the zymogen plasminogen is activated to the active enzyme plasmin by tissue-type plasminogen activator (tPA), which results in the digestion of fibrin at specific lysine residues (Marder et al., 1969). This process is augmented by the co-localization of plasminogen and tPA on fibrin (Thorsen, 1992). As fibrin cleavage occurs new binding sites for plasminogen and tPA are created when new C-terminal lysine residues are exposed (Suenson et al., 1984). This leads to a positive

feedback mechanism that accelerates lysis ensuring a rapid and efficient breakdown of the clot.

1.1.5 Factor XIII

Factor XIII is a protransglutaminase consisting of two A-subunits, which contain the active site, and two B-subunits, which protect the hydrophobic A subunits, arranged as a heterotetramer (Schwartz et al., 1973). The activation of FXIII begins with thrombin cleaving a 37 amino acid activation peptide from the A-subunit. The presence of calcium then leads to the dissociation of the B-subunits, exposing the activated enzyme FXIIIa (Ariens et al., 2002). The activated FXIII plays a vital role in stabilising the fibrin clot by crosslinking fibrin monomers together and also crosslinking anti-fibrinolytic proteins, such as alpha-2-antiplasmin (α2AP) into the clot. Crosslinking of fibrin occurs through the α- and γ-chains, with γ-chain crosslinking happening first between Gln398 or 399 of one molecule and Lys406 on another molecule during protofibril formation (Duval et al., 2014, Spraggon et al., 1997). This is followed by slower α-chain crosslinking between Gln221, Gln328 and Gln355 in one molecule with one of 15 Lys residues in another molecule during lateral aggregation (Lorand, 2001). Crosslinking by FXIIIa leads to a clot with increased density and thinner fibres that is harder to break down (Smith et al., 2013), increases fibre stiffness and reduces deformation (Duval et al., 2014) and slows fibrinolysis (Mutch et al., 2010b). FXIIIa also crosslinks α2AP (Tamaki and Aoki, 1981), plasminogen activator inhibitor-2 (PAI-2) (Ritchie et al., 2001) and thrombin activatable fibrinolysis inhibitor (TAFI)(Valnickova and Enghild, 1998).

1.1.6 Changes in clot structure

The role of altered fibrin clot structure in cardiovascular disease has been the focus of many previous studies (Bridge et al., 2014). Some of the main characteristics of fibrin clots that have been analysed previously include fibre density and thickness, fibre branching, protofibril packing (protein density of fibre), clot permeability and viscoelastic properties (Table 1). Changes in these structural properties have been linked to increased thrombotic risk.

Increased fibrinogen concentration has been shown to be a risk factor for CVD (van Holten et al., 2013), and is one of the major modulators of fibrin clot structure. Increasing fibrinogen concentration is thought to effect polymerisation resulting in an increased fibre density and thickness (Standeven et al., 2005). Elevated fibrinogen levels have been shown to reduce time to vascular occlusion *in vivo*, and increase clot fibrin content, network density and resistance to fibrinolysis in a murine model (Machlus et al., 2011). Alterations in the molecular structure of fibrinogen have also been shown to play a role in clot structure. Splice variant fibrinogen γ' (discussed in more detail in chapter 1.2) has been shown to result in clots with thinner fibres, reduced protofibril packing, increased number of fibre branch points and reduced pore size (Cooper et al., 2003, Domingues et al., 2016). Another common fibrinogen sequence variant, Fib-β Arg448Lys also effects clot structure resulting in clots with thinner fibres, smaller pores and increased stiffness that are more resistant to lysis (Ajjan et al., 2008).

However fibrinogen alone does not account for all alterations to clot structure. Another major factor in alterations to clot architecture is thrombin concentration. Low thrombin concentrations (< 1 nM) lead to clots with thick,

loosely woven fibres, while high concentrations (> 100nM) lead to clots with thin, densely packed fibres (Wolberg, 2007). Thrombin concentration during coagulation varies from < 1nM up to > 500 nM, although low levels of thrombin (~ 2 nM) are sufficient for fibrin polymerisation (Brummel et al., 2002). Thrombin concentration has also been shown to modulate protofibril packing, with increased thrombin concentrations resulting in a decrease in protofibril packing (Domingues et al., 2016). Thrombin generation is mostly localized to the cell surface and this leads to spatial heterogeneity in clot structure correlated with the distance of fibrin from the cell surface (Campbell et al., 2008).

As previously mentioned FXIII has also been shown to influence clot structure, with fibrin crosslinking resulting in fibrin clots with increased density, reduced pore size and thinner fibres, with increased resistance to lysis (Hethershaw et al., 2014). However, changes to FXIII have also been associated with changes to fibrin clot structure. FXIII-A Val34Leu results in faster activation of FXIII by thrombin, with the resulting clots forming faster with thinner and smaller pores (Ariens et al., 2000, Schroeder et al., 2001).

Blood flow has also been shown to profoundly affect clot structure, leading to fibrin fibres aligning in the direction of flow, increasing clot stiffness in that direction (Gersh et al., 2010). One study reported thick fibres in the direction of flow, with thinner interconnecting fibres (Campbell et al., 2010).

Platelets can alter clot properties via proteins they release, particularly at sites of platelet aggregation. Platelet factor 4 release is associated with the formation of a compact clot structure (Amelot et al., 2007). Polyphosphates

lead to the formation of tight fibre aggregates interspaced with large pores (Mutch et al., 2010a).

Table 1 Modifiers of fibrin clot structure.

Clot modifier	Functional effects
Fibrinogen concentration	↑concentration: Risk factor for CVD, ↑fibrin content, ↑density and ↑resistance to lysis.
Fibrinogen sequence variants	Fibrinogen γ': ↑clot stiffness, ↓fibre diameter, ↓protofibril packing, ↓clot pore size, ↑fibrin branching, ↑resistance to fibrinolysis. BβArg448Lys: ↓fibre diameter, ↓clot pore size, ↑clot stiffness, ↑resistance to fibrinolysis.
Thrombin concentration	↑thrombin: ↓fibre diameter, ↓protofibril packing, ↑clot density, ↑resistance to fibrinolysis.
FXIII	↑clot density, ↓clot pore size, ↓fibre diameter, ↑resistance to fibrinolysis
FXIII Val34Leu	↑rate of clot formation, ↓ fibre diameter, ↓clot pore size.
Blood flow	Alignment of fibres in direction of flow, ↑clot stiffness, Thick fibres in direction of flow with thin interconnecting fibres.
Platelets	Platelet factor 4: ↑clot density, Polyphosphates: tight fiber aggregates interspaced with large pores.

CVD – Cardiovascular disease

1.1.7 Fibrinolysis

Fibrin breakdown mainly occurs through cleavage by plasmin. Plasmin is produced when plasminogen is activated by tissue- or urokinase-type plasminogen activators. This process is upregulated 1000-fold in the presence of fibrin by providing a surface for co-localisation of tPA and plasminogen (Collen, 1980b). Fibrinolysis is inhibited directly by inhibition of plasmin through α2AP and α2-macroglobulin (α2M), and indirectly through plasminogen activator inhibitor-1 (PAI-1) which blocks plasmin production, and through TAFI, which cleaves C-terminal lysines in fibrin inhibiting the fibrin enhancement of plasmin generation (Figure 2) (Collen, 1980a, Cesarman-Maus and Hajjar, 2005).

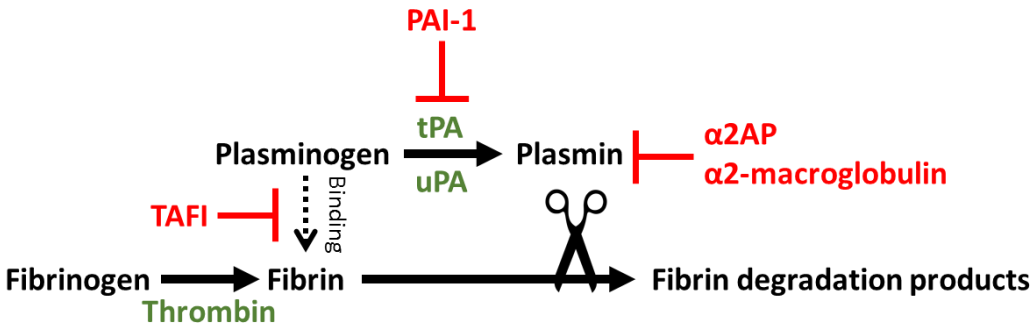

Figure 2 The fibrinolysis cascade. Plasminogen is converted to plasmin by tissue plasminogen activator (tPA) and urokinase-type plasminogen activator (uPA). Plasmin breaks down fibrin. Fibrinolysis is prevented or slowed by the inhibition of plasmin by alpha-2-antiplasmin (α2AP) and α2-macroglobulin (α2M), or through plasminogen activator inhibitor-1 (PAI-1) and thrombin activatable fibrinolysis inhibitor (TAFI) preventing plasmin generation. Adapted from Bridge et al. (2014).

1.2 Fibrinogen γ'

Fibrinogen is the product of three closely linked genes: fibrinogen α (FGA), fibrinogen β (FGB) and fibrinogen γ (FGG) which are located in a region of approximately 50 kb on chromosome 4q31.3 (Kant et al., 1985). Many common mutations, splice variations and post translational modifications make fibrinogen a very heterogeneous protein. One of the most common heterogeneities is fibrinogen γ'. This fibrinogen variant is the result of a splice variation in the γ-chain, leading to a bulky negatively charged extension at the C-terminus of the γ-chain in about 10-12 % of total fibrinogen (Figure 3). This extension produces numerous functional effects, related to protein binding and modulation of fibrin network formation. Clinically, fibrinogen γ′ levels have been associated with thrombotic diseases, but the relationship with arterial and venous thrombosis appear different. In view of this splice variant being present in all individuals so far and its functional effects, many studies have investigated the role of fibrinogen γ′ in pathophysiology.

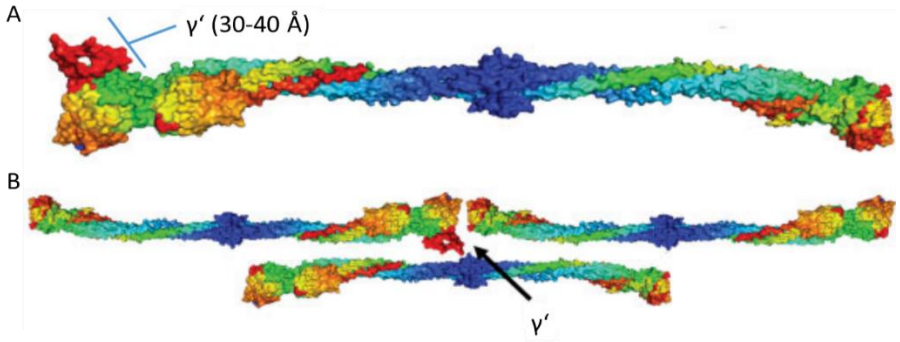

Figure 3 The bulky extension of fibrinogen γ'. A Fibrinogen molecule with the location and proposed model of the γ′-chain. **A,** The 20 amino acid extension of the γ′-chain is located at the C-terminus of the γ-chain (red) and may extend up to 30 to 40 Å or more from the D region. **B,** When fibrinogen polymerizes through D–E–D interactions, the γ′ extension is at the D–D interface and could stretch to the E region of a neighbouring molecule affecting longitudinal polymerization (colours represent progression from N-terminus (blue) through to C-terminus (red) for each chain). The fibrinogen molecule crystal structure was taken from Kollman et al (Kollman et al., 2009) and the γ′-chain extension was created using PyMOL Molecular Graphics System (New York, NY). From Macrae et al. (2014).

1.2.1 Splicing mechanisms and genetics

In 1972, Mosesson et al discovered fibrinogen γ' when noticing a subspecies of fibrinogen with a γ-chain that had a higher molecular weight (Mosesson et al., 1972). They also showed that fibrinogen's heterogeneity in size and charge was due to this minor variation of the γ-chain. Over the next few years other groups made similar findings calling it a number of different names including γB, γ′, or γ57.5. (Francis et al., 1980, Fornace et al., 1984, Peerschke et al., 1986) The predominant wildtype γA chain is made up of 10 exons and 9 introns. Normally polyadenylation occurs at the polyadenylation site (AATAAA) downstream of exon 10. However, the variant γ′-chain is produced when an alternative processing and polyadenylation site in the ninth intron is used instead. This results in the precursor mRNA being terminated and polyadenylated within the ninth intron (Chung et al., 1983, Chung and Davie, 1984). This alternative precursor matures into the mRNA that codes for the 20 unique amino acids at the terminal end of the γ′-chain

(γ′408–427; VRPEHPAETEYDSLYPEDDL), substituting the 4 γA amino acids (γA408– 411) of exon 10 (Wolfenstein-Todel and Mosesson, 1980, Wolfenstein-Todel and Mosesson, 1981)(Figure 4).

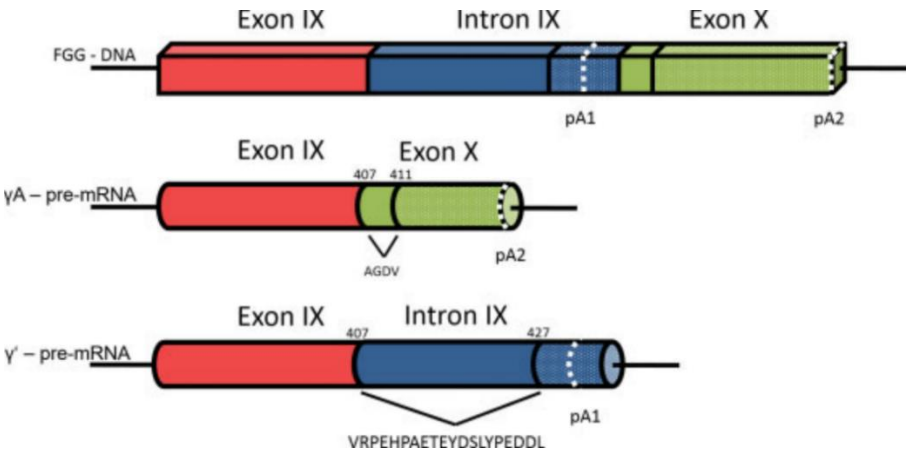

Figure 4 Alternative FGG pre-mRNA processing. The predominant γA chain is formed when polyadenylation occurs at the polyadenylation site 2 (pA2) downstream of exon 10. The γ′-chain is formed when an alternative polyadenylation site 1 (pA1), which occurs in the ninth intron, is selected. This precursor molecule matures into the mRNA that codes for the 20 unique amino acids at the terminal end of the γ′-chain, substituting the 4 γA amino acids of exon 10. From Macrae et al. (2014).

1.2.2 Thrombin interactions

Fibrinogen γ′ has been shown to bind thrombin with high affinity through exosite II on thrombin (Lovely et al., 2003), while thrombin exosite I interacts with the fibrinogen E region, where the fibrinopeptides reside. When bound to thrombin, fibrinogen γ′ adopts a β-turn structure between residues 422 and 425 (Sabo et al., 2006, Pineda et al., 2007). Within these residues there are two negatively charged, sulphated tyrosines that are particularly important for thrombin binding. When bound to thrombin, γ′ Tyr418 is positioned in a groove between Lys235, Lys236, and Arg126, and γ′ Tyr422 closely interacts with Lys240 within exosite II (Pineda et al., 2007). These

interactions consolidate the high affinity interaction of fibrinogen γ′ with thrombin.

The interaction of γ′ with thrombin is normally associated with thrombin inhibition. In fact, fibrinogen γ′ was also called antithrombin I in view of its inhibitory effect on thrombin (de Bosch et al., 2002). However, the effects of fibrinogen γ′ on thrombin activity are complex. It is thought that the antithrombin I activity of fibrinogen γ′ is due to the sequestering of thrombin via γ′ into the forming fibrin clot, reducing the amount of thrombin in the remaining plasma solution. Furthermore, the presence of the γ′ sequence was found to reduce fibrinopeptide B (FpB) cleavage, which resulted in reduced lateral aggregation of the fibrin fibres (Cooper et al., 2003). However, γ′ has no effect on fibrinopeptide A (FpA) cleavage, and when bound to γ′, thrombin is also relatively protected against inhibition by antithrombin and heparin (Cooper et al., 2003, Moaddel et al., 2000, Fredenburgh et al., 2008). It appears therefore that thrombin activity remains normal when thrombin is associated with fibrin(ogen) γ′, at least toward some of the above-mentioned substrates. Finally, the presence of fibrinogen significantly increases thrombin generation in plasma, and the fibrinogen γ′ variant is particularly capable in this respect, largely by decreasing α2M-dependent thrombin degradation (Kremers et al., 2014). The binding of γ′ to thrombin does not just inhibit thrombin activity, but rather modulates the activity of thrombin by localizing it to the growing fibrin clot and by protecting it against degradation.

1.2.3 Interactions with other proteins and pathways

FXIII is a zymogen of the transglutaminase FXIIIa that helps to stabilize blood clots in both mechanical aspects (Lorand, 2001) and its resistance to lysis (Gaffney and Whitaker, 1979, Siebenlist and Mosesson, 1994). It is known that FXIII associates with fibrinogen (K_d 10^{-8} M), and on the basis of this affinity constant, it is thought that practically all FXIII in circulation is bound to fibrinogen (Greenberg and Shuman, 1982). FXIII co-purifies with fibrinogen γA/γ′ on anion-exchange chromatography, and when separated from fibrinogen γA/γA, FXIII was only found in the second peak of γA/γ′ (Mosesson and Finlayson, 1963). Fibrinogen γA/γ′ has been shown to bind to the B-subunit of plasma FXIII with 20-fold higher affinity than fibrinogen γA/γA (Siebenlist et al., 1996). However, two studies have opposed this, with one showing no difference in FXIII binding between γA/γ′ and γA/γA fibrinogen (Gersh et al., 2006). The second more recent study found that the FXIII zymogen binds to fibrinogen residues γ390-396 via the B subunits (Byrnes et al., 2016). They also suggest that all excess plasma FXIII-B_2 circulates bound to fibrinogen, suggesting that this may reveal part of a stepwise mechanism that leads to production of fibrinogen/FXIII-A_2B_2 complexes. The effects of γ′ fibrin on FXIII activation and crosslinking have not been fully established. One study shows that γA/γ′ increases the activation kinetics of FXIII leading to enhanced FXIII A- and B-subunit dissociation (Moaddel et al., 2000). Three other studies all have opposing views on the effect of fibrinogen γA/γ′ on FXIII crosslinking, suggesting it upregulates (Moaddel et al., 2000), downregulates (Siebenlist et al., 2001) or has no effect at all (Allan et al., 2012) on the crosslinking of the fibrinogen γ-chain.

Fibrinogen γ′ has also been shown to cause effects on other proteins in the coagulation system. Its interaction with thrombin has been shown to inhibit FVIII and FV activation, which also depend on binding with thrombin exosite II (Lovely et al., 2007, Omarova et al., 2013a). Fibrinogen γ’ has also been shown to increase plasma activated Protein C sensitivity and increase histidine-rich glycoprotein binding (Omarova et al., 2013b, Vu et al., 2011).

The carboxy-terminal end of the fibrinogen γA-chain is involved in binding to the platelet integrin GPIIb/IIIa (Hawiger et al., 1982, Kloczewiak et al., 1982). The γ′-chain lacks the γA residues 408 to 411 required for platelet adhesion (Harfenist et al., 1984). This results in the γ′-chain reducing thrombin-induced platelet aggregation in both static and flow conditions and *in vivo* γA:γ′ ratios have been shown to modify platelet activation (Lancellotti et al., 2008). Platelets do not contain γA/γ′ fibrinogen, the reason for this is currently unknown and further studies are needed to elucidate why α-granules only contain γA/γA fibrinogen (Francis et al., 1984).

1.2.4 Fibrinogen γ′ effects on clot structure

Changes in fibrin clot architecture have been closely associated with cardiovascular disease (CVD), and are thought to contribute to their pathogenesis and progression (Undas and Ariens, 2011). The structural changes that occur with fibrinogen γ′ have been found to associate with some CVDs. Elevated levels have been described in patients with myocardial infarction (MI) (Mannila et al., 2007), coronary artery disease (CAD) (Lovely et al., 2002), and acute phase ischemic stroke (Cheung et al., 2008), while a reduction in levels has been related to increased risk of venous thrombosis (Uitte de Willige et al., 2005). In view of these

associations with CVD, it is important to fully elucidate the role of fibrinogen γ′ on fibrin clot structure. There have been several studies that have demonstrated that fibrinogens γA/γA and γA/γ′ display different clotting characteristics. Plasma purified γA/γ′ fibrin has been shown to clot at a slower rate, and form clots with thinner fibrin fibres and smaller pores than γA/γA fibrin (Cooper et al., 2003, Siebenlist et al., 2005). Using microrheometer magnetic tweezers, γA/γ′ were shown to have reduced stiffness and increased viscosity compared to γA/γA clots both in the presence and absence of cross-linking by FXIIIa (Allan et al., 2012). This suggested that the γA/γ′ fibres are softer and more viscous and could result in increased propensity to embolize. Early stages of clot formation were studied and showed that fibrinogen γA/γ′ produced shorter oligomers compared with fibrinogen γA/γA, which may help to explain the highly branched γA/γ′ fibrin fibres. A model was suggested whereby shorter, more numerous protofibrils could lead to earlier gelling of γ′ clots. Subsequently, this produces γA/γ′ clots that are composed of thinner, shorter fibres interspersed by large pores.

The rate at which thrombin removes the fibrinopeptides plays a role in clotting characteristics. FpB release has been shown to be decreased in γA/γ′ compared to γA/γA fibrinogen (Cooper et al., 2003, Kim et al., 2014). The timing of FpB release coincides with lateral aggregation of protofibrils and a delay in its release γA/γ′ could affect fibre thickness. In turbidity experiments, γA/γ′ fibrin clots produced with reptilase, a snake venom enzyme that release FpA but not FpB, showed decreased polymerization rates and reduced maximum absorbance. This demonstrates that the effects of γ′ on fibrin structure are independent of the electrostatic binding between

fibrinogen γ′ and exosite II in thrombin, and that the negatively charged region in fibrinogen γ′ directly influences fibrin formation (Allan et al., 2012).

Clots containing fibrinogen γ′ are more resistant to breakdown by the fibrinolytic pathway. Fibrinolysis assays in the presence of FXIII have shown that plasma purified γA/γ′ fibrin is more resistant to fibrinolysis than γA/γA fibrin (Falls and Farrell, 1997). This was thought to be due to increased FXIII cross-linking and that γA/γ′ fibrinogen localizes FXIII to the fibrin clot to increase its stability. Reduced fibrinolysis rates with γA/γ′ have also been attributed to delayed FpB release, which results in delayed activation of plasminogen (Kim et al., 2014). The effects of γA/γ′ fibrinogen on lysis have also been shown in patient plasma, with patients with increased γA/γ′ levels presenting delayed clot lysis (Pieters et al., 2013).

1.3 Abdominal Aortic Aneurysms

An Abdominal Aortic Aneurysm is a permanent, localised dilatation of the descending abdominal aorta. The aorta is classed as aneurysmal when it is 1.5 times its normal diameter or greater than 3 cm (Johnston et al., 1991). AAA commonly occurs in men over the age of 65 and accounts for up 1.8 % of all deaths in England and Wales (Parry et al., 2009). The natural progression of an untreated AAA is rupture with the risk increasing significantly as the size of the aneurysm increases (Brewster et al., 2003). Currently, the only treatment available is surgical intervention and the placement of a stent, which is offered electively once the AAA reaches the intervention threshold. This threshold is currently set at 55 mm, where the risk of rupture exceeds the risk of mortality from surgery (Filardo et al.,

2012). An AAA rupture occurs when the stress on the aortic wall becomes too great and the aortic wall dissects. Two thirds of patients who experience a ruptured AAA end up dying before they reach hospital, and only 40-50 % of those that reach hospital survive (Dillavou et al., 2006). Even with a screening program in place in the UK for men over the age of 65, ruptured AAA is still responsible for over 6000 deaths per year.

Studies have shown that some of the risk factors for AAA include smoking, and male gender and that diabetes mellitus is protective against AAA (Lederle et al., 1997). A genetic familial link has been suggested in AAA, where at least one first degree relative has also developed an AAA (Larsson et al., 2009, Linne et al., 2012). A number of candidate genes have been suggested as a means of inheritance, but no individual gene has been implicated (Sandford et al., 2007). AAA is a multifactorial disease, and it is likely that the disease and its progression is due to both genetic and environmental factors. Previous studies have indicated family history of AAA as a risk factor (Johansen and Koepsell, 1986), and strong links between AAA development and MMP9 (Duellman et al., 2012). Environmental factors such as smoking and obesity are known to be significant risk factors for the development of AAA (Blanchard et al., 2000, Stackelberg et al., 2013).

1.3.1 Formation and progression of AAA

Formation and progression of AAAs is not yet fully understood. In the presence of AAA it has been shown that matrix metalloproteinases (MMPs), other proteases from aortic smooth muscle cells and macrophages are secreted into the extracellular matrix. This leads to the proteolytic breakdown of the elastin and collagen that provide the structure of the aortic wall. There

is also an increase in the infiltration of lymphocytes and macrophages (Rizas et al., 2009), a loss of smooth muscle cells (Thompson et al., 1997) and neovascularisation (Thompson et al., 1996) occurring within the aortic wall. Studies have demonstrated that in AAA patients there is an increase in elastase and collagenase expression including MMP-2, -9, and -12 and MMP-1 and MMP-13 (Annabi et al., 2002, Curci et al., 1998, Knox et al., 1997, Mao et al., 1999, Reeps et al., 2009). The role of inflammation and immune response have also been linked to AAA formation and progression. The increase in the number of macrophages and lymphocytes may lead to an increase in the number of cytokines that are released, and these can activate proteases leading to the breakdown of the aortic wall (Lindholt and Shi, 2006). The infiltration mechanisms of the leucocytes is not fully understood, but it has been suggested that elastin degradation products may act as a chemoattractant (Ailawadi et al., 2003). The influence of biomechanical stress on the aortic wall is thought to contribute to the progression of AAA expansion. With reduced elastin within the aortic wall, the aorta becomes much stiffer (He and Roach, 1994), and with fewer smooth muscle cells it becomes less resistant to pressure of arterial flow. The stress on the aortic wall was found to correlate with aortic diameter but also to asymmetry of the vessel, possibly due to disturbed flow within the aneurysm (Vorp et al., 1998). Figure 5 shows a schematic representation of the current understanding of AAA pathophysiology.

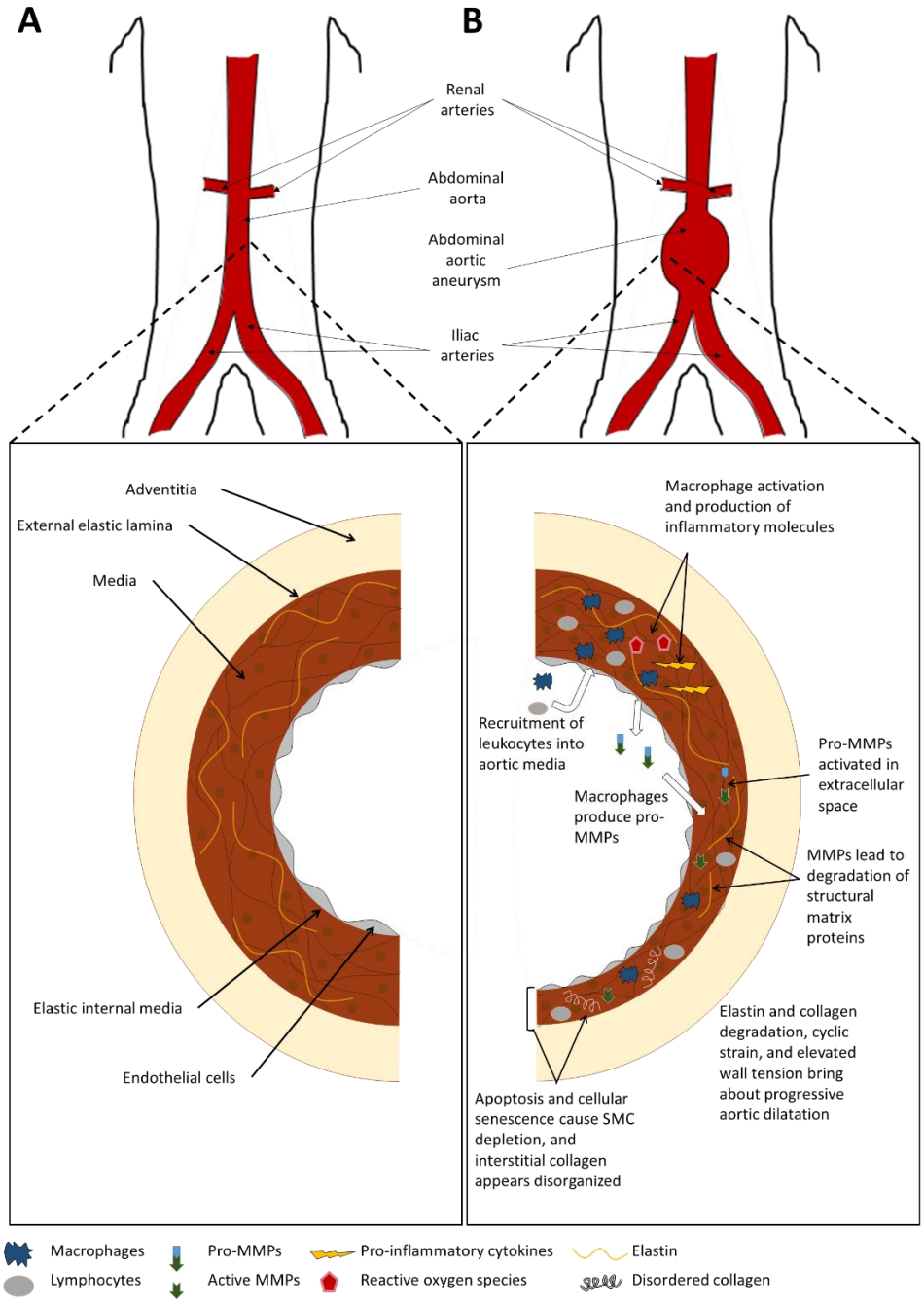

Figure 5 The pathophysiology of abdominal aortic aneurysms. A schematic diagram presenting the events that contribute to the formation and development of an AAA. **A,** A normal aortic wall with the three layers of intima, media and adventitia. The combination of collagen, elastin and smooth muscle cells help to maintain wall integrity. **B,** Following damage to the aortic wall leukocytes are recruited into the aortic media. Macrophages are activated and begin to release proinflammatory molecules, such as cytokines and reactive oxygen species. Macrophages also begin to produce pro-MMPs which are activated in the extracellular space. The active MMPs proceed to degrade elastin and collagen and over many years the degradation of elastin and collagen, the strain and tension from arterial blood pressure gradually leads to aortic dilatation. Smooth muscle cells and fibroblasts attempt to repair the damage, and this results in the deposition of disordered collagen. However, smooth muscle cells become senescent and undergo apoptosis resulting in the loss of smooth muscle cells. In an advanced AAA the medial layer of the aortic wall is found to be thinner.

1.3.2 The intra-luminal thrombus

Around 75 % of larger aneurysms have been shown to possess an intra-luminal thrombus (ILT) (Wang et al., 2002). Its role in AAA formation and progression is not fully understood. The ILT is not a stagnant structure and active secretion of proteolytic factors such as plasmin result in constant remodelling at the luminal surface (Houard et al., 2007). This results in the clot being biologically active. The wall underlying the ILT has been shown to have decreased tensile strength (Vorp and Vande Geest, 2005) and decreased wall thickness (Kazi et al., 2003). This in part, is thought to be due to the release of proteolytic factors which contribute to the thinning of the vessel wall (Folkesson et al., 2011, Fontaine et al., 2002, Coutard et al., 2010). Increased plasmin production results in increased MMP activation, and a faster rate of collagen and elastin breakdown resulting in quicker aneurysm growth. (Carrell et al., 2006). This was supported by a study that showed an increase in ILT thickness resulted in increased MMP levels and elastin breakdown within the aortic wall (Koole et al., 2013). The ILT is also thought to mediate the weakening of the aortic wall by creating localised hypoxia, which intensifies as thrombus thickness increases (Vorp et al., 2001). A couple of observational studies have found that larger ILTs are associated with a greater rate of AAA expansion and risk of rupture, and that this increased rate leads to higher risk of rupture (Wolf et al., 1994, Stenbaek et al., 2000). However, the mechanisms behind the effect of the ILT on expansion rate are still not fully understood. To highlight this, a number of studies have demonstrated a protective effect of the ILT, showing it to be protective against rupture by altering stress distribution and decreasing peak wall stress, providing a ‘cushioning’ effect to the underlying

wall (Inzoli et al., 1993, Mower et al., 1997, Wang et al., 2002). Although it appears that this protective effect is far outweighed by the negative influences of the ILT, with one study finding that the ILT is usually found at the point of AAA rupture (Simao da Silva et al., 2000).

The ILT is made up of fibrin, platelets, erythrocytes, leucocytes and neutrophils. It is usually composed of three distinct layers: The luminal layer, which is a vibrant red due to large numbers of fresh erythrocytes. This is the main location of remodelling and protease activity. The medial layer, which is yellow/pink in colour. And the abluminal layer which is a dark yellow-brown and is closest to the aortic wall. This can nicely be seen in a cross section of very large ILT that was removed from a patient with a 12 cm abdominal aortic aneurysm in Figure 6A.

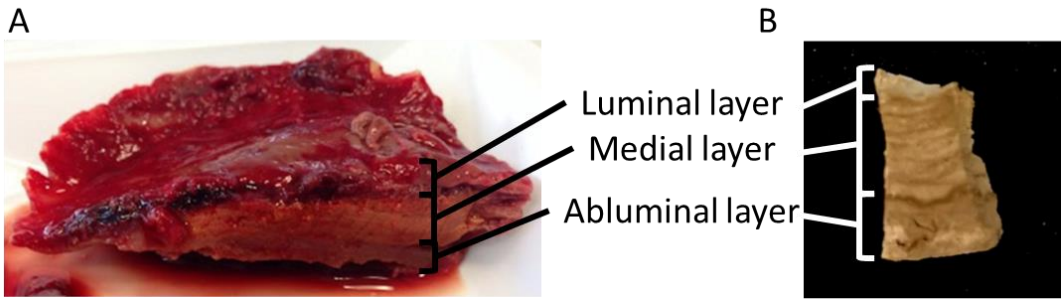

Figure 6 Intra-luminal thrombus. A, An ILT was removed from a patient having an open repair on a 12 cm abdominal aortic aneurysm. **B,** A cross section of this clot was taken and prepared for scanning electron microscopy (SEM).

A cross section of this clot was prepared for scanning electron microscopy (SEM, Figure 6B) and the clot was imaged from the luminal surface across to the aortic wall (Figure 7). This figure shows how heterogeneous the ILT is from luminal surface to the aortic wall, and the continuous network of

interconnected canaliculi (channels and pores) can be seen traversing through the clot. This allows for the movement of proteases and fluid through the ILT (Adolph et al., 1997).

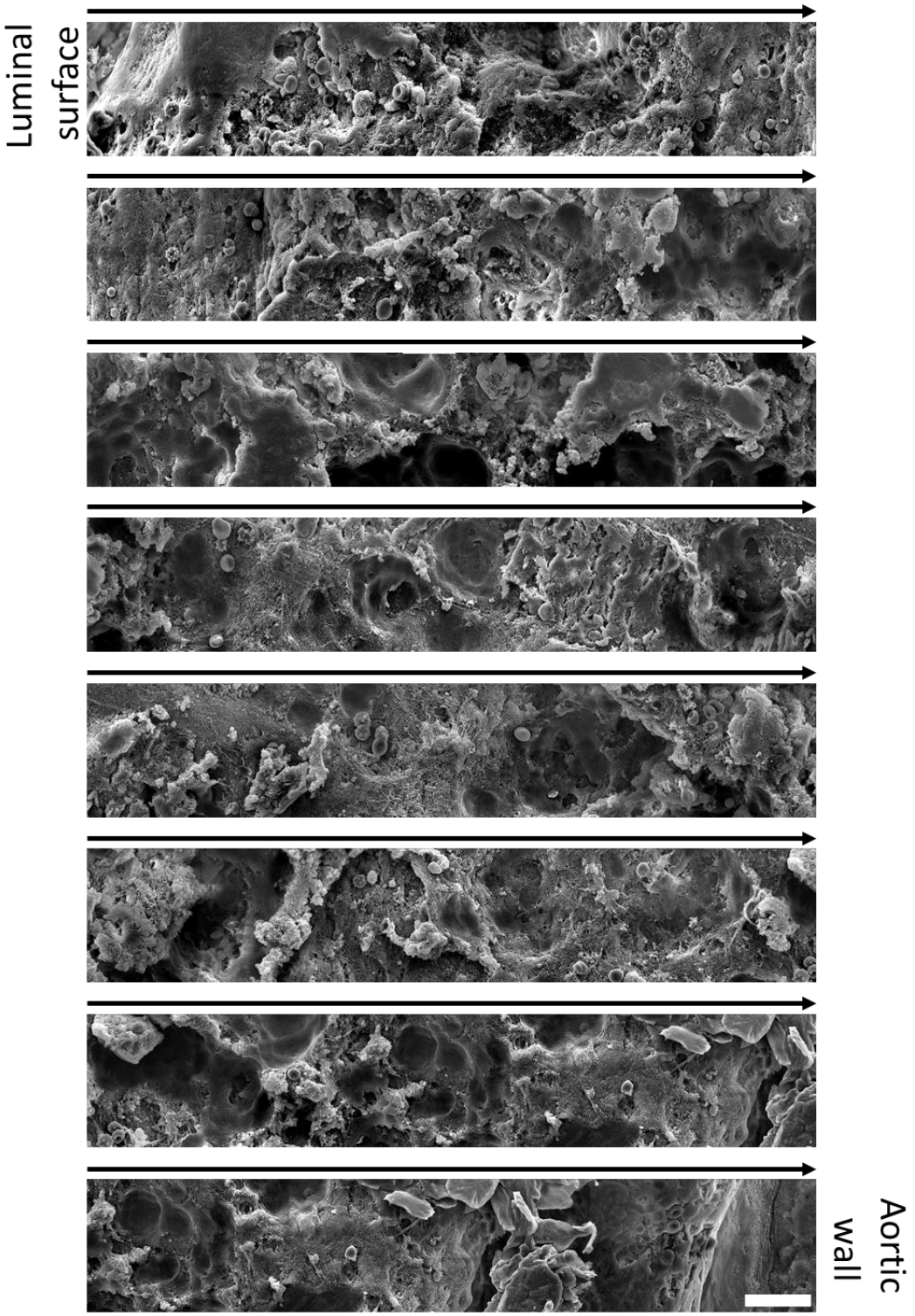

Figure 7 Cross section of an intra-luminal thrombus. A cross section of an ILT was imaged from the luminal surface to the aortic wall using scanning electron microscopy (SEM). Scale bar – 20 μm.

1.4 Paroxysmal Nocturnal Heamoglobinuria

Paroxysmal nocturnal haemoglobinuria (PNH) is a rare disorder of haematopoietic stem cells. It occurs due to an acquired mutation in the X-linked phosphatidylinositol glycan class A gene (PIG-A). The PIG-A gene codes for an enzyme involved in the formation of the N-acetylglucosaminyl phosphatidylinositol biosynthetic protein which is necessary for the first step in the biosynthesis of glycosylphosphatidyinositol (GPI) anchors (Miyata et al., 1993). GPI, a glycolipid moiety, anchors numerous proteins to the cell surface, with more than 12 GPI-anchored proteins (GPI-APs) located on haemopoietic cells (Brodsky, 2014). Mutations in this gene result in stem cell progeny (mature blood cells) lacking complement regulatory proteins on their surface and leads to them being vulnerable to complement attack (Brodsky, 2014). Thrombosis is the most common cause of morbidity and mortality in PNH and accounts for between 40-67 % of deaths. Forty percent of these patients have suffered a thromboembolic event before diagnosis and 29-44 % of patients suffer at least one event throughout the course of their disease (Socie et al., 1996). Despite playing such a large role in PNH, the mechanisms involved in PNH driven thrombosis are poorly understood, and so elucidating a link between PNH and thrombosis is important to improve the treatment of these patients. Multiple proposed mechanisms behind the increased incidence of thrombosis suggest a prothrombotic state in conjunction with platelet abnormalities and impaired fibrinolysis (Hill et al., 2013, Grunewald et al., 2003).

1.4.1 Pathophysiology

The incidence of PNH is very rare, estimated at 0.1 – 0.2/ 100,000 persons per year (Devalet et al., 2015). Studies have shown that a small number of GPI anchor deficient cells are present in the blood of healthy controls as well as in patients with PNH (Bessler et al., 1994). This suggests that the presence of a mutation in the PIG-A gene alone is not sufficient to allow the PNH clone to dominate. The process by which the clonal expansion of the mutated PIG-A stem cells in PNH patients occurs is not fully understood.

Two combined hypotheses exist to explain the clonal expansion of PNH cells; one involves immune selection-mediated expansion and the second predicts that dominant PNH clones acquire a growth advantage (Nakakuma and Kawaguchi, 2003). The UL16 binding protein 1 (ULBP1), a stress-induced ligand for the natural killer cell receptor NKG2D, is a GPI-linked glycoprotein thought to be lost on PNH stem cells. Loss of ULBP1 may prevent their destruction of ULBP1 deficient stem cells by $NKG2D^{+}$ lymphocytes allowing for immune-escape from ULBP-NKG2D engagement in the bone marrow (Kawaguchi and Nakakuma, 2007). PIG-A mutant cells have been demonstrated to be less sensitive to T lymphocytes and, along with leukemic cells with the same mutation, possess increased resistance to natural killer cells (Kawaguchi and Nakakuma, 2007, Hanaoka et al., 2006). The growth phenotype is thought to be due to upregulation of early growth response factor 1 gene (EGR-1) and ectopic expression of the high mobility transcription factor coding genes HMGA2 (Inoue et al., 2006, Lyakisheva et al., 2002, Murakami et al., 2012).

The two most significant GPI-APs thought to play a major role in the pathophysiology of PNH are complement regulatory proteins CD55 and CD59 (Schubert and Roth, 2015). CD55 prevents complement proteins C4b and C3b from catalysing the conversion of C2 and Factor B to active C2a and Bb, preventing the formation of C4b2a and C3bBb (both forms of C3 convertase). CD59 inhibits the formation of the membrane attack complex (MAC), formed as a product of the complement cascade, preventing pore formation and cell lysis (Rollins and Sims, 1990). Without these complement regulatory proteins, complement attack leads to erythrocyte lysis, platelet activation and a loss of thrombotic modulators on granulocytes, causing many of the symptoms of PNH (Jankowska et al., 2011, Hugel et al., 1999, Wiedmer et al., 1993) (Figure 8).

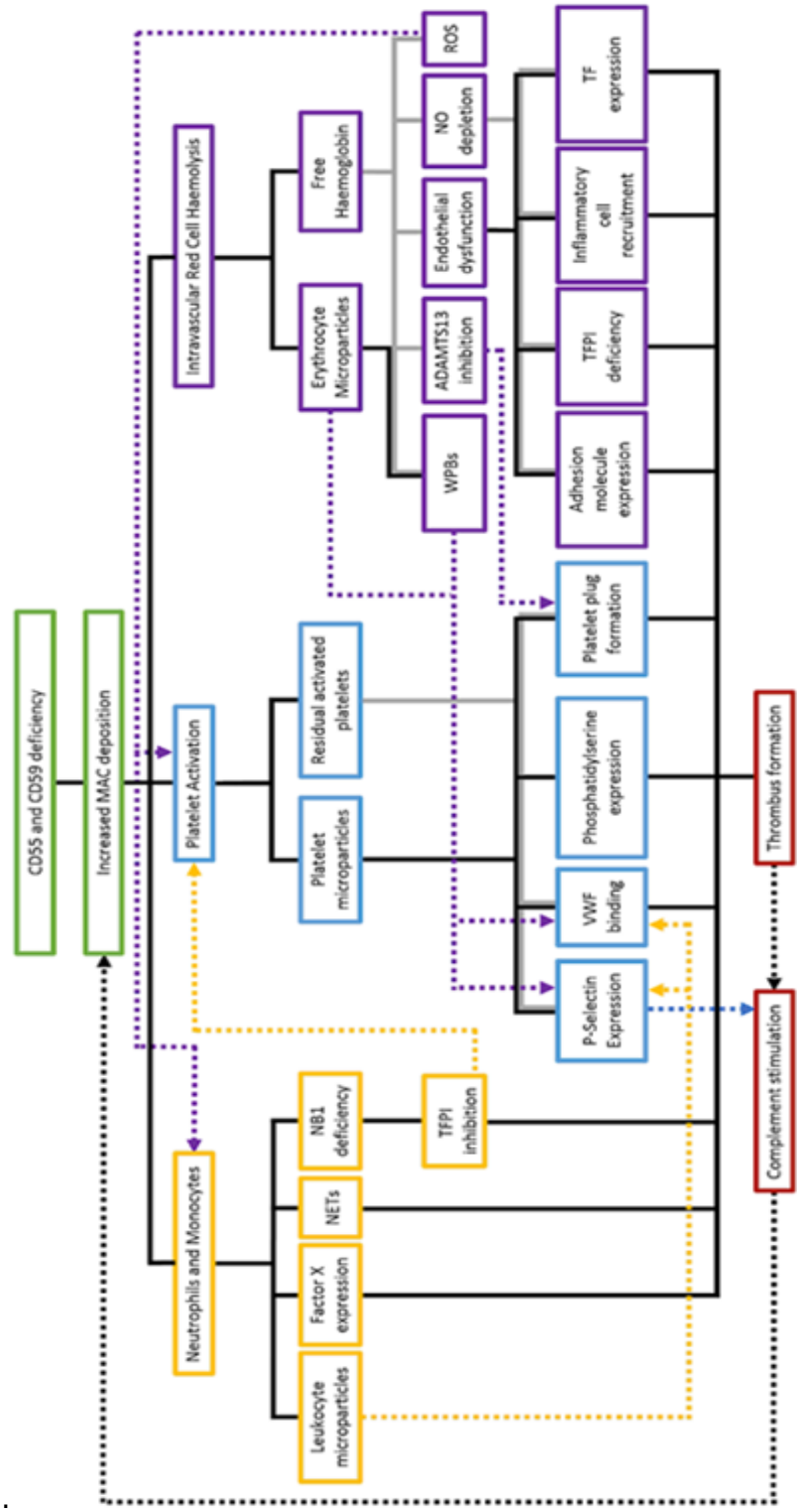

Figure 8 Multiple factors that contribute to the prothrombotic state in paroxysmal nocturnal haemoglobinuria (PNH). MAC: membrane attack complex; NET: neutrophil extracellular traps; TFPI: tissue factor pathway inhibitor; vWF: von Willebrand factor; WPB: Weibel-Palade storage bodies; NO: nitric oxide; ROS: reactive oxygen species; TF: tissue factor. Adapted from Peacock-Young et al. (2018).

1.4.2 Clinical presentation

Patients can present with ‘classical’ PNH characterized by clinical and laboratory evidence of intravascular haemolysis with no clinical evidence of an underlying bone marrow disorder. Others have evidence of haemolytic PNH as well as clinical evidence of bone marrow disorder, such as myelodysplasia or aplastic anaemia. A further group may be defined as ’subclinical PNH’ where a small proportion of PNH cells are found but with no evidence of haemolysis or thrombosis (Parker et al., 2005). The presence of PNH cells are identified using flow cytometry, determining the proportion of GPI negative granulocytes, monocytes and erythrocytes (Parker et al., 2005). The proportion of PNH granulocytes are normally used as a marker of disease severity as the numbers of granulocytes is not affected by haemolysis or transfusions. PNH RBCs are labelled type I, II or III; type I cells have normal expression of GPI-APs, type II have partial deficiency and type III lack all GPI-Aps (Hill et al., 2007b).

Clinical manifestations of PNH are variable; the main symptoms include intravascular haemolysis, thrombosis and anaemia, however, other symptoms may be present (Brodsky, 2014). Schrezenmeier et al. analysed 1610 patients and showed the proportion of symptoms, such as fatigue (80 %), dyspnea (64 %), haemoglobinuria (62 %), abdominal pain (44 %), chest pain (33 %) and impaired renal function (14 %), with only 16 % of patients having a history of thrombotic events (Schrezenmeier et al., 2014). However, it has been shown that the presence of subclinical thrombosis is significantly underestimated (Hill et al., 2007a).

Thrombosis is the most serious complication associated with PNH. Venous thrombosis accounts for 85 % of cases, arterial in 15 % of cases and cases involving thrombosis at more than one site at the same time occurring in 20.5 % of cases (Devalet et al., 2015). Thrombosis is thought to be able to occur at any site, with deep vein thrombosis (DVT), pulmonary embolism (PE), MI or cerebral vascular attack all commonly observed complications (Moyo et al., 2004). There appears to be an increased incidence of thrombosis at atypical sites, such as the hepatic vein resulting in Budd-Chiari syndrome, occurring in 40-44 % of PNH patients, in addition to thrombosis in the vasculature of the central nervous system, mesenteric, dermal veins and the cavernous sinus (Ziakas et al., 2007). The proportion of PNH cells and clone size has also been associated with thrombotic complications. It has been shown that patients with more than 50 % of their granulocytes affected by PNH have a 44 % risk of thrombosis over 10 years, but in patients with less than 50 % PNH granulocytes, the risk was only 5.8 % (Hall et al., 2003). Moyo et al. showed a 1.64 increase in odds ratio of developing thrombosis for every 10 % increase in the proportion of PNH cells (Moyo et al., 2004). These findings correlate with other studies which have shown that the occurrence of thrombosis is noticeably elevated in PNH patients with a proportion of PNH cells as low as 10 % when compared to normal population controls (Hoekstra et al., 2009, Fowkes et al., 2003).

1.4.3 Induction of a prothrombotic state

The mechanisms behind thrombus formation in PNH are complex and subject to continued research. Interactions between the complement system, platelets and coagulation are thought to explain some of the increased risk

of thrombosis. The multifactorial and variable nature of the disease mean that a combination of several factors may contribute to the increased incidence of thrombus formation and associated mortality (Figure 8).

1.4.3.1 Platelet activation

Platelets have been reported to play a significant role in thrombus formation in PNH patients, by both contributing to a prothrombotic state and initiating clot formation (Gralnick et al., 1995). Due to the deficiency of CD55 and CD59, lysis of platelets would be expected leading to thrombocytopenia, however, the lifespan of platelets in PNH patients is normal (Devine and Rosse, 1987). Rather than complement resulting in the lysis of platelets, an intrinsic mechanism of adaption and resistance to complement attack has been shown which contributes to the prothrombotic state (Wiedmer et al., 1986). Increased deposition of MAC (C5b-9) on the membrane of platelets, results in morphological changes (Hugel et al., 1999). The loss of platelet membrane phospholipid asymmetry through the action of adenosine triphosphate (ATP) -dependent enzymes, gelsolin, aminophospholipid translocase, lipid scramblase and calpain allow for cytoskeletal and phospholipid bilayer changes (Bevers et al., 1999). The now activated platelet secretes α-granules, and in conjunction with membrane depolarization, α-granules fuse with the platelet membrane (Blair and Flaumenhaft, 2009). This results in exocytosis of the vesiculated MAC and the production of prothrombotic platelet-derived microparticles (PMPs), which are also thought to contribute to thrombosis (Hugel et al., 1999).

1.4.3.2 Haemolysis

Intravascular haemolysis is responsible for causing a large number of the symptoms in PNH (Figure 8), and many of these are due to the release of free haemoglobin. Free haemoglobin is normally cleared by haptoglobin, haemopexin and the scavenger CD163. These clearing mechanisms are overwhelmed in PNH and lead to the accumulation of high levels of free haemoglobin in the plasma, which then leads to the depletion of nitric oxide (NO) (L'Acqua and Hod, 2015). The subsequent excess of haemoglobin leads to visible haemoglobinuria, while the depletion of NO, a potent vasodilator, results in vasoconstriction, decreased regional blood flow and muscular contraction, causing chest and abdominal pain, amongst other symptoms (Hill et al., 2013). Free haemoglobin can also lead to a prothrombotic state, with recent studies showing that it can rapidly stimulate the release of WPBs from the vascular endothelium resulting in the release of vWF and P-selectin onto the surface of endothelial cells, stimulating coagulation and the complement cascade (Ballarin et al., 2011, Belcher et al., 2014). Free haemoglobin has also been observed to directly bind to vWF exposed on the endothelium which increases the affinity of vWF for the glycoprotein Ib (GPIb) receptor on the surface of platelets (Da et al., 2015). Free haemoglobin can also inhibit ADAMTS13, reducing vWF cleavage, further promoting a prothrombotic state (Zhou et al., 2009, Studt et al., 2005). In agreement with this, animal and human studies have both demonstrated that the infusion of haemoglobin or haem into the blood stream resulted in a prothrombotic state, with animal models showing increased platelet aggregation and adhesion to the endothelium of an injured vessel wall (Olsen et al., 1996) and healthy volunteers presenting with

thrombophlebitis, vascular inflammation and obstruction (Simionatto et al., 1988). It has also been suggested that the increased oxidative status of PNH cells may be due to increased haemoglobin levels. Haemoglobin is known to produce reactive oxygen species (ROS), and these can go on to cause phospholipid disorganisation, induce cytotoxicity, promote inflammation and enhance platelet activation (L'Acqua and Hod, 2015, Iuliano et al., 1994).

The lysis of erythrocytes have been reported to produce microparticles as a result of MAC-induced apoptosis (Kozuma et al., 2011). Although, other studies have shown that the concentration of erythrocyte derived microparticles were much lower than platelet derived microparticles (Hugel et al., 1999), and are at similar levels to healthy controls (Simak et al., 2006), so their contribution to thrombosis in PNH may be minimal.

1.4.3.3 Reciprocal activation of complement and coagulation

Thrombin has been observed to independently activate complement proteins C3 and C5 (Huber-Lang et al., 2006). Plasmin, an enzyme involved in fibrin clot degradation and stimulated by fibrin itself, has also recently been shown to cleave C5 (Leung and Morser, 2016). This suggests a feedback mechanism in which thrombin generation, fibrin deposition and fibrinolysis may in turn activate the complement system, which reciprocally leads to more platelets and coagulation activation, exacerbating the thrombotic response.

1.4.3.4 Fibrin clot structure

Previous studies have shown that individuals with an increased risk of thrombosis form fibrin clots with an altered fibrin network (Bridge et al., 2014). Their clots are formed of thinner, more tightly packed fibrin fibres that

are stiffer, more resistant to mechanical deformation, and have an increased resistance to fibrinolysis. Resistance to fibrinolysis is due to the increased number of fibres that need to be lysed and a reduced permeation of the lytic enzymes into the denser clot structure (Collet et al., 2000). There have been no studies to date that have investigated clot structure in patients with PNH. Abnormal clot structure could be an additional mechanism by which the risk of thrombosis is increased in PNH. Complement activation and factors have previously been associated with effects on fibrin clot structure and function. Alternative complement pathway activation has been associated with the production of denser, more tightly packed clots (Shats-Tseytlina et al., 1994); furthermore, C3 has been shown to be incorporated into the fibrin clot, leading to thinner fibrin fibres and a stiffer clot with increased resistance to fibrinolysis (Howes et al., 2012). Mannan-binding lectin serine protease 1 (MASP-1) has been shown to influence clot formation and activate FXIII, leading to an increased resistance of the clot to fibrinolysis (Hess et al., 2012). Other unidentified mechanisms of complement activation may also play a role in clot structure and function.

1.4.3.5 Animal models

The use of mouse models to replicate the thrombotic phenotype caused by the deficiency of CD55 and CD59 in PNH has proven difficult to replicate. Generating the thrombotic phenotype via PIG-A mutations has also proven difficult. Two models, one in murine embryonic stem cells and another in a mouse model have attempted to inactivate the PIG-A gene, giving rise to blood cells with the PNH phenotype (Rosti et al., 1997, Tremml et al., 1999). In both cases this mutation of the PIG-A gene did not lead to the expansion

of the PNH clone, suggesting other additional factors are required for PNH symptoms. Limited knowledge of the clonal expansion mechanism has made it difficult to create animal models in which the thrombotic mechanisms in PNH can be analysed.

1.4.3.6 Treatment

The current treatment for PNH is a monoclonal antibody directed against C5, called eculizumab (Seregina et al., 2015). It helps prevent C5 cleavage to C5a and C5b, stopping uncontrolled complement system activation by inhibiting the terminal steps of the complement cascade, and reducing complement mediated complications, such as thrombosis. Studies have shown a reduction in thromboembolic incidents from 7.37 to 1.07 events per 100 patient's years when observing patients pre and post eculizumab treatment (Hillmen et al., 2007). Eculizumab's therapeutic effects are reduced with a heterozygous C5 Arg885His polymorphism (Nishimura and Kanakura, 2015), and this has led to the development of Coversin, another C5 inhibitor for the treatment of PNH and other complement-mediated disorders (Weston-Davies et al., 2014).

1.5 Hypotheses

Fibrin(ogen) plays many important roles in the human body. Physiologically, fibrinogen contributes to the prevention of blood loss through clot formation, and plays a role in infection control. Pathologically, however fibrinogen may play a role in forming thrombi in the vasculature leading to heart attacks or strokes. I hypothesize that by examining the role of fibrin(ogen) in the different settings of thrombosis and haemostasis I will uncover new mechanisms that promote or prevent disease, improving our understanding of the complex mechanisms underpinning diseases of bleeding and thrombosis.

1. **Fibrinogen γ'.** Previous studies of fibrinogen γ' have shown it plays a role in clot structure and breakdown, but many of these studies have been on purified protein comparing 100 % fibrinogen γ' to 100 % fibrinogen γA in static conditions. I hypothesise that effects of fibrinogen γ' will persist at physiological levels, with differences in clot formation, structure and breakdown being seen in patient samples with different fibrinogen γ' levels. Fibrinogen γ' will also form clots with different structural properties from fibrinogen γA when clots are formed under flow conditions.
2. **Fibrin film.** A major conundrum after decades of fibrin polymer research is that fibrin fibres in blood clots appear endless, with little evidence of fibre ends. Thus, the mechanisms and structures that determine the external boundary of an extravascular (haemostatic) blood clot are unknown. I hypothesise that the structures at the external boundaries of clots will differ from the normal fibrin fibre

network. The architecture of this interface is important because it forms a distinction between host and the environment.

3. **Fibrinogen and FXIII in AAA.** Analysis of genetic polymorphisms of FXIII and Fibrinogen in AAA patients will help to identify high risk genotypes and potential disease mechanisms.
4. **Clotting in PNH.** Patients with an increased cardiovascular risk present with altered clot structures. I hypothesise that patients with PNH will also present with an altered clot structure, and patients with a larger clone size will have denser clots and increasing fibrinolysis resistance, and this may contribute to the disease mechanism. Patients on eculizumab will possess hallmarks of a less pro-thrombotic fibrin clot structure.

1.6 Aims

1. **Fibrinogen γ'**
    a. Measure fibrinogen and fibrinogen γ' in a large number of patient samples and select three groups of patients with low, normal and high levels of fibrinogen γ'.
    b. Carry out clot structure assays on the three groups and compare them with purified and repleted plasma clots with similar fibrinogen γ' levels.
    c. Carry out rotational thromboelastometry (ROTEM) assays on a selection of patients with known fibrinogen γ' levels.
    d. Investigate the role of fibrinogen γ' on clot structure under flow.

2. **Fibrin film**
    a. Investigate the edge of clots and characterise structures that form at external boundaries.
    b. Uncover how these structures form and elucidate any roles they may have.
3. **Fibrinogen and FXIII in AAA**
    a. In view of the central role of FXIII and fibrinogen in thrombus formation and the complications of ILT in AAA, investigate genetic polymorphisms of FXIII and Fibrinogen in AAA to identify high risk genotypes and potential disease mechanisms.
    b. Measure fibrinogen levels, fibrinogen γ' levels and fibrinogen γ' percentage in AAA and control patients, and investigate its relationship with AAA size, clinical outcomes.
4. **Clotting in PNH**
    a. Analyse fibrin clot structure and function in PNH patients and how it is effected by clone size.
    b. Investigate the anti-thrombotic effects of eculizumab treatment on clot structure.

Chapter 2 - Experimental Design, Materials and Methods

2.1 General methods

2.1.1 Materials

Many of the materials in this study were used in multiple different experiments. Tris buffered saline (TBS) was used as a buffer for dilutions in many experiments, it consisted of 50 mM Tris-base (Sigma-Aldrich, Dorset, UK) 150 mM NaCl (Fisher Scientific, Loughborough, UK), pH 7.4. Human thrombin (Merck Millipore, Watford, UK) was diluted in distilled water (ddH_2O) to a stock concentration of 250 NIHU/ml (NIHU - National Institute of Health standard Unit). 1 NIHU/ml = 9.16 nM of active units of thrombin (Ariens et al., 2000). Thrombin was aliquoted on ice and immediately stored at -80ºC to prevent activity loss. Thrombin was defrosted and diluted in TBS to the required concentration and kept on ice for a maximum of 30mins for each experiment. Experiments were also performed using Reptilase (Diagnostica Stago; Theale, UK), a snake venom enzyme which only cleaves FpA, but not FpB, from fibrinogen. This was reconstituted in ddH2O to 20 BU/ml and kept on ice and used within 8 hours. Many experiments required the use of purified human fibrinogen. Commercially available human plasma fibrinogen that had been plasminogen-depleted (Merck Millipore, Watford, UK) was used for this. This fibrinogen is purified from frozen plasma and lyophilised. It was reconstituted in TBS and diluted to a stock concentration of 2 mg/ml and then aliquoted and stored at -80ºC. Fibrinogen concentration was quantified with a Nanodrop Spectrophotometer (Labtech International, UK) at 280 nm using an extinction coefficient of 1.51 (Mihalyi, 1968). tPA, (Pathway Diagnostics, Dorking, UK) and Glu-plasminogen (Enzyme Research Laboratories,

Swansea, UK) were diluted in TBS to 1 mg/ml and 990 µg/ml, respectively and stored at -80 ºC. Human FXIII-A_2B_2 was isolated from Fibrogammin P (Zedira) by Sepharose-6B gel filtration to remove contaminating albumin and glucose as described previously (Standeven et al., 2007), diluted to 110 g/ml, aliquoted and stored at -80 ºC. Alexa Fluor 488 or Alexa Fluor 594 fluorescently labelled fibrinogen (Invitrogen, Paisley, UK) used for confocal microscopy imaging was prepared by dissolution in ddH2O to a concentration of 2.5 mg/ml, aliquoted and stored at -80 ºC. Fibrinogen-deficient plasma (Merck Millipore, Watford, UK) was thawed by heating to 37 ºC in a water bath for 5 minutes before use.

2.1.2 Whole blood and plasma collection

Collection of whole blood and plasma samples from patients in the Leeds Aneurysm Development Study (LEADS), a large case-control cohort study, were used to provide whole blood and plasma samples for some of the experiments within this thesis. The inclusion and exclusion criteria, as well as the study protocol, consent form and patient information sheet can be found in Appendices 1-3. Patients were recruited and their samples collected by a senior research nurse, Mrs Anne Johnson.

Free flowing venous blood was collected from the antecubital vein of patients. Ten millilitres of blood was collected into 10 % sodium citrate (9 parts of blood to 1 part of citrate) or into a K_2EDTA coated blood collection tubes for DNA extraction. Blood taken into K_2EDTA tubes was stored at -20 °C. Citrated whole blood was used within 4 hours of the blood draw. For platelet poor plasma (PPP) whole blood was centrifuged at 2,400 g for 20 minutes. The plasma supernatant was divided into 0.5 ml aliquots, flash

frozen in liquid nitrogen and stored at -80°C until analysis. For platelet rich plasma (PRP) whole blood was centrifuged at 200 g for 10 minutes. PRP was used within 4 hours of the blood draw

Whole blood and plasma samples were also collected as per above protocol from healthy volunteers for other experiments within this thesis. Ethical approval for blood taking was obtained from the University of Leeds Medical School or the University Hospitals of Geneva and Faculty of Medicine review board. Written informed consent was received from each patient and volunteer prior to inclusion in the study in accordance with the declaration of Helsinki.

2.1.3 Normal pool plasma

Normal pool plasma (NPP) was used as a control for of a number of assays, and also for the establishment of a standard curve in the fibrinogen γ' enzyme-linked immunosorbent assays (ELISAs). This was produced by the collection of free-flowing venous blood from the antecubital fossa of 25 healthy individuals. Collection of the NPP was approved by the Leeds NHS Trust Research Ethics Committee (HSLTM/12/045 and HSLT/09/020). Blood was collected onto 10 % sodium citrate (9 parts blood to 1 part citrate), centrifuged for 20 minutes at 2,400 g to separate plasma, which was pooled together to create a mixture of all 25 individuals' plasmas. Aliquots of 0.5-1 ml were flash frozen using liquid nitrogen, and stored at -80°C until required.

2.1.4 Fibrinogen levels

Fibrinogen concentrations were measured in PPP by the Clauss method using a Start 4 haemostasis analyser (Diagnostica Stago; Theale, UK) and the Fibri-prest automate kit (Diagnostica Stago; Theale, UK) according to the

manufacturer's instructions. In brief, under excess thrombin concentrations, the rate limiting step to clotting time is fibrinogen concentration. Therefore clotting time can be used to quantify the fibrinogen concentrations in plasma samples. Two plasma controls (control N and P), Unicalibrator (plasma with known fibrinogen concentration) for use as a standard curve and Fibri-prest automate reagent (Human thrombin, ~100 NIH units.ml^{-1}, with heparin inhibitor and calcium) provided with the kit were reconstituted with ddH_2O. The standard curve was prepared by diluting Unicalibrator in the supplied buffer (STA-Owren-Koller buffer, pH 7.35 veronal acetate saline buffer) to 1/7/ 1/10, 1/20 and 1/40. Controls N and P and plasma samples for fibrinogen level determination were diluted to 1/20 in STA-Owren-Koller buffer. Cuvette strips (Diagnostica Stago; Theale, UK) were pre-warmed to 37°C, and a steel ball bearing (Diagnostica Stago; Theale, UK) was placed in each well. 100 µl of standard/control/plasma sample was added to wells of the cuvette strip in duplicate. The cuvette strips were then placed into the Start 4 haemostasis analyser which oscillates the steel ball bearings from side to side. Fifty microliters of Fibri-prest automate solution was added to each well of the cuvette strip to initiate clot formation. The time taken for clot formation to impede the movement of the steel ball bearing was recorded. The concentration of the plasma sample can be quantified by comparing it to the standard curve.

2.1.5 Purification of fibrinogen γA/γ' and γA/γA

γA/γ' and γA/γA fibrinogen were purified from commercially available plasma purified human fibrinogen as previously described (Cooper et al., 2003, Domingues et al., 2016, Wolfenstein-Todel and Mosesson, 1980). Plasma

purified human fibrinogen was initially purified to remove any FXIII by immunoaffinity chromatography (IF-1 mAb, 10 mg; Kamiya Biomedical; Seattle, USA) as previously described (Duval et al., 2014). Using the purified IF-1 fibrinogen the different fibrinogen variants were separated by anion-exchange chromatography on a DE-52 column using an AKTAavant 25 (GE Healthcare, Little Chalfont, UK). Prior to chromatography, the Enzyme Research Laboratory (ERL) fibrinogen was dialyzed into 39 mM Tris, 65 mM H_3PO_4, 0.5 mM phenylmethylsulfonyl fluoride (PMSF), 1 mM benzamidine and 5 mM ε-aminocaproic acid, pH 8.6. Samples were eluted from the column using a concave gradient from 0-100 % over 13 column volumes (5 % increments over the first 6 column volumes and 10 % over the next 7 column volumes) of 500 mM tris, 650 mM H_3PO_4, 0.5 mM PMSF, 1 mM benzamidine and 5 mM ε-aminocaproic acid, pH 4.2 (Appendices 4).

Purity of the γA/γA and γA/γ' preparations was checked by sodium dodecyl sulphate–polyacrylamide gel electrophoresis (SDS-PAGE) analysis on a NuPAGE unit with 4-12 % Bis-Tris gradient gels (Figure 9). The gel revealed a single band at the location of the γ chain for γA/γA fibrinogen, showing that only γA fibrinogen was present. For the γA/γ' fibrinogen two bands of equal intensity but different molecular weights were present. This indicated the presence of both γA and γ' chains and therefore γA/γ' fibrinogen. Aliquots of the prepared fibrinogens were stored at -80°C. Fibrinogen concentration was determined by absorbency ($E^{280\,nm}_{1\,mg.mL^{-1}} = 1.51$).

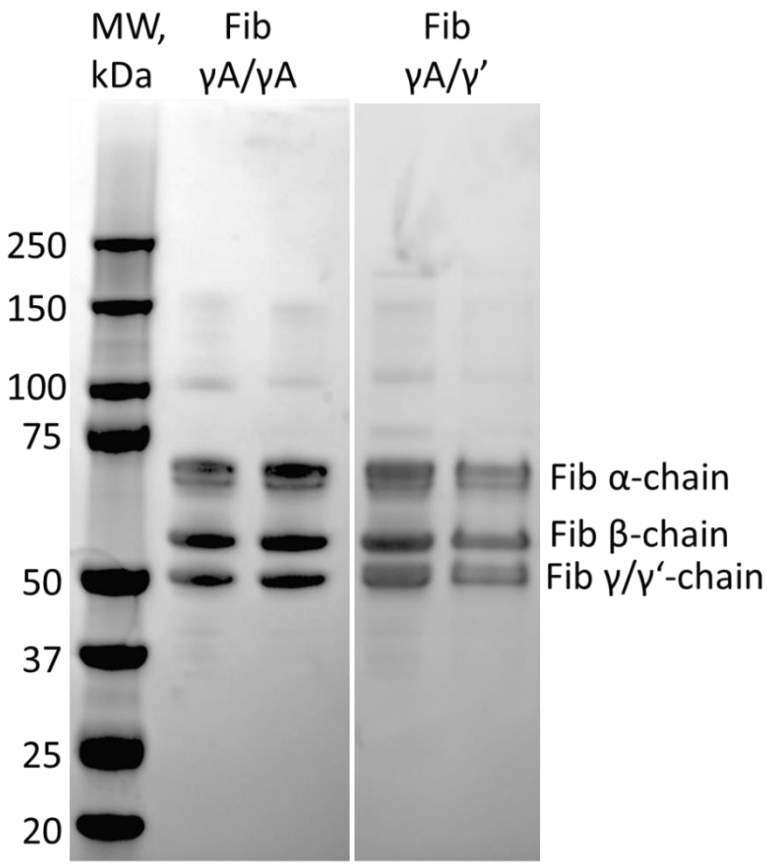

Figure 9 γA/γA and γA/γ' purification. SDS-PAGE analysis of γA/γA and γA/γ' isolated from ERL fibrinogen by anion-exchange chromatography on a DE-52 column. All lanes were run on the same gel. MW – Molecular weight, Fib – fibrinogen.

2.1.6 Measurement of fibrinogen γ' levels

An ELISA based on a previously described method was set up to measure fibrinogen γ' levels in plasma samples (Uitte de Willige et al., 2005). Initially, a standard curve of NPP was created in order to quantitate the fibrinogen γ' levels within plasma samples. A Nunc MaxiSorp 96 well plate (Thermo Scientific, Waltham, MA) was coated with fibrinogen γ' specific 2.G2.H9 monoclonal antibody (Santa Cruz Biotech, CA, 200 $\mu g.ml^{-1}$) in 50 mM sodium carbonate pH 9.5 overnight at 4°C, and then blocked with blocking buffer (1 % bovine serum albumin (BSA), 50 mM Triethanolamine, 100 mM NaCl, 10 mM Ethylenediaminetetraacetic acid (EDTA), 0.1 % Tween-20, pH

7.5) for an hour. Purified γA/γ' was diluted in dilution buffer (50 mM triethanolamine, 100 mM NaCl, 10 mM EDTA, 0.1 % Tween-20, 10 mM benzamidine, pH 7.5) to a range of concentrations from 0.9 to 0.03 $mg.L^{-1}$ and each concentration was added to the plate in six replicates. Normal pool plasma was diluted in a range from 1/400 to 1/12800 and each dilution was also added to the plate in six repeats, and the plate was then incubated for 1 hour at room temperature. A horseradish peroxidase (HRP) conjugated goat polyclonal antibody against human fibrinogen (1/20000) (Abcam, Cambridge, MA) was added to each well and incubated for 1 hour at room temperature. 100 µL 3,3',5,5'-Tetramethylbenzidine (TMB) substrate buffer was added and the reaction was stopped after 10 minutes with 50 µL 1 M H2SO4. The plate was read at 450 nm at 37°C in a Thermo Fisher Multiscan Go Microplate reader (Thermo Fisher Scientific, Waltham, MA). After blocking and between each incubation step, the plate was washed three times with washing buffer. The fibrinogen γ' level of the six NPP repeats were calculated at each dilution, using the quadratic equation in comparison with a standard curve produced with purified γA/γ' (Figure 10, Table 2). From these values the fibrinogen γ' level in the NPP was calculated as 304.48 $mg.L^{-1}$, and this NPP was then used as a standard curve for all future ELISAs.

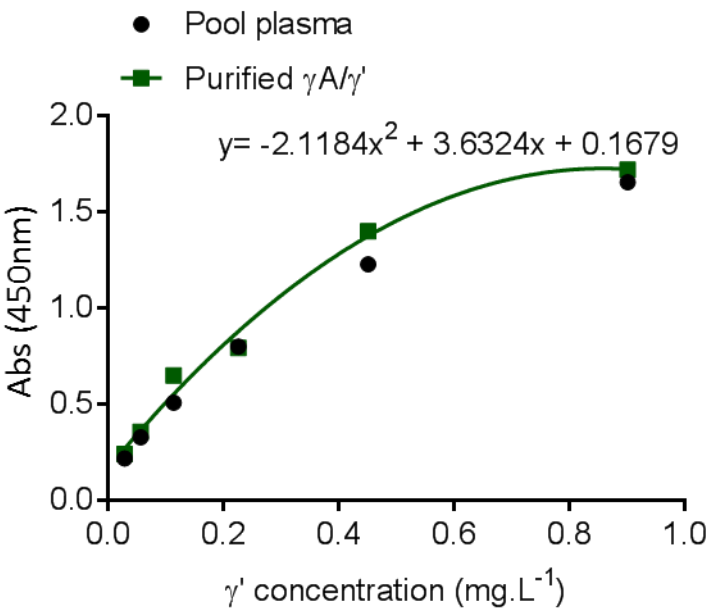

Figure 10 Average absorbance of pool plasma compared to purified γA/γ'. Average absorbance of six NPP curves at a range of dilutions (1/400-12800) compared to purified γA/γ' in increasing concentrations (0.9-0.03), measured at 450 nm.

Table 2 Creating a plasma standard curve.

γ' Concentration ($mg.L^{-1}$)	Pool plasma (Average Abs)	Purified γA/γ' (Average Abs)
0.900	1.654	1.719
0.450	1.227	1.400
0.225	0.799	0.793
0.113	0.508	0.649
0.056	0.327	0.356
0.028	0.217	0.241

To measure fibrinogen γ' levels in plasma samples, PPP was prepared as described above. Nunc MaxiSorp 96 well plates were coated with the 2.G2.H9 monoclonal antibody (200 $\mu g.ml^{-1}$) in 50 mM sodium carbonate pH 9.5 overnight at 4°C. Plates were then blocked for 1 hour at room temperature with blocking buffer (1 % BSA, 50 mM Triethanolamine, 100

mM NaCl, 10 mM EDTA, 0.1 % Tween-20, pH 7.5). A standard curve of NPP from 1/400 to 1/12800 was added to the plate in duplicate. Plasma samples were diluted to 1/1600 and 1/3200 in dilution buffer and added to the plate in duplicate and incubated for 1 hour at room temperature. The HRP conjugated goat polyclonal antibody against human fibrinogen (1/20.000 in dilution buffer) was added to the plate and incubated for 1 hour at room temperature to detect bound fibrinogen γ'. One hundred microliters of TMB substrate was added and the reaction was stopped after 10 minutes with 50 µL 1M H_2SO_4. The plate was read at 450 nm at 37°C in the Microplate reader. After blocking and between each incubation step, the plate was washed three times with washing buffer.

Fibrinogen γ' ratio (%) was calculated by dividing the fibrinogen γ' level by the total fibrinogen level (measured as described in chapter 2.1.4).

2.1.7 Confocal microscopy

To assess fibrin clot structure laser scanning confocal microscopy (LSCM) was carried out on purified fibrinogen or plasma clots.

For purified samples, fibrinogen (0.5 $mg.ml^{-1}$) with or without FXIII (3.7 $\mu g.ml^{-1}$), was spiked with 25 $\mu g.ml^{-1}$ of Alexa fluor-488 fluorescein isothiocyanate (FITC) -labelled fibrinogen. Plasma samples were diluted by half and spiked with 25 $\mu g.ml^{-1}$ of the Alexa fluor-488 FITC-labelled fibrinogen. Clotting was initiated with the addition of 5 mM $CaCl_2$ and 0.5 $U.ml^{-1}$ of human thrombin. Immediately after the initiation of clotting, 30 µl of the solution was transferred to a channel of an uncoated Ibidi slide (Thistle Scientific, UK). Once prepared the samples were stored in a dark humidity chamber for at least 4 hours to ensure full clot formation. Slides were then imaged using an

inverted Zeiss LSM880 microscope (Carl Zeiss; Welwyn Garden City, UK) with a 40× oil immersion objective lens. Fibrin clots were prepared in duplicate and six images were taken for each clot, Z-stacks (20 µm, 30 slices) were combined to form 3D images (ZEN 2.1 black, Carl Zeiss, Cambridge, UK). Fibre density was calculated using an in-house macro I designed as part of this thesis (Appendices 5), which calculates the number of fibres crossing 10 horizontal and 10 vertical lines drawn on top of a confocal image of the clots. From this the average number of fibres/100 µm can be calculated.

2.1.8 Turbidity and lysis assay

Clot formation and breakdown were analysed by the turbidity and lysis assay as previously described (Scott et al., 2011). To analyse clot formation in a purified system, fibrinogen was made up to 0.5 $mg.ml^{-1}$ with or without FXIII (3.7 $\mu g.ml^{-1}$). Plasma samples were diluted 1/6 with TBS. They were then added to the well of a 96-well Greiner bio-one microtiter plate (Greiner Bio One International GmbH) and an activation mix (thrombin – 0.5 $U.ml^{-1}$, $CaCl_2$ – 10 mM) was added to initiate clotting. To analyse clot breakdown, the assays were set up as above but with the addition of plasminogen (25 $\mu g.ml^{-1}$) and tPA (85 $ng.ml^{-1}$) for purified clots, or just tPA (85 $ng.ml^{-1}$) for plasma clots. Changes in absorbance at 340 nm was measured every 12 seconds for 3 hours at 37°C in a ThermoFisher Multiscan Go Microplate reader (ThermoFisher Scientific, Waltham, MA). Investigated parameters were lag time, Max OD, time to Max OD, average clotting rate and time between 25 and 75 %, time to 50 % lysis (time from Max OD to 50 % lysis) and average

lysis rate and time between 25 and 75 % lysis (Figure 11). Duplicates were measured for each sample and averaged.

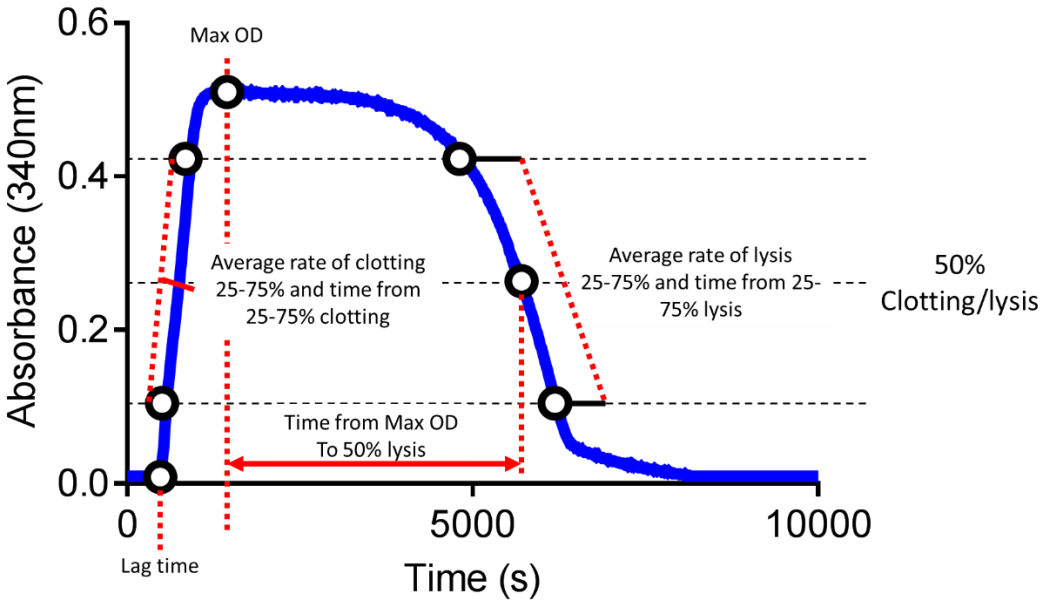

Figure 11 Turbidity and lysis curve. An example trace of a turbidity and lysis curve with the different measured parameters indicated on the curve.

2.1.9 Rotational thromboelastometry

Rotational thromboelastometry was carried out on samples of whole blood that were collected as previously described (chapter 2.1.2). The experiments were carried out using The ROTEM®-delta system (ROTEM, Tem International GmBH) combined with the Cup and Pin pro measurement cells (ROTEM, Tem International GmBH). Clotting was initiated with the addition of 20 µl of star-tem® reagent (re-calcification agent) and either 20 µl ex-tem® reagent (Rabbit brain thromboplastin) or in-tem® reagent (contact activator ellagic acid) to each cup. For fib-tem® analysis, 20 µl of ex-tem® reagent followed by 20 µl of fib-tem® reagent (platelet inhibitor cytochalasin D) was used. This was followed by the addition of 300 µl of whole blood to each cup, and immediate analysis was started and followed for 2 hours

using the ROTEM-delta system. A typical trace generated from a ROTEM assay can be seen in Figure 12. Each sample was analysed in duplicate. Parameters measured in this study included: Lag time, which is the time from the start of the measurement until the initiation of clotting, and maximum clot firmness (MCF), which reflects the absolute strength of the fibrin and platelet clot.

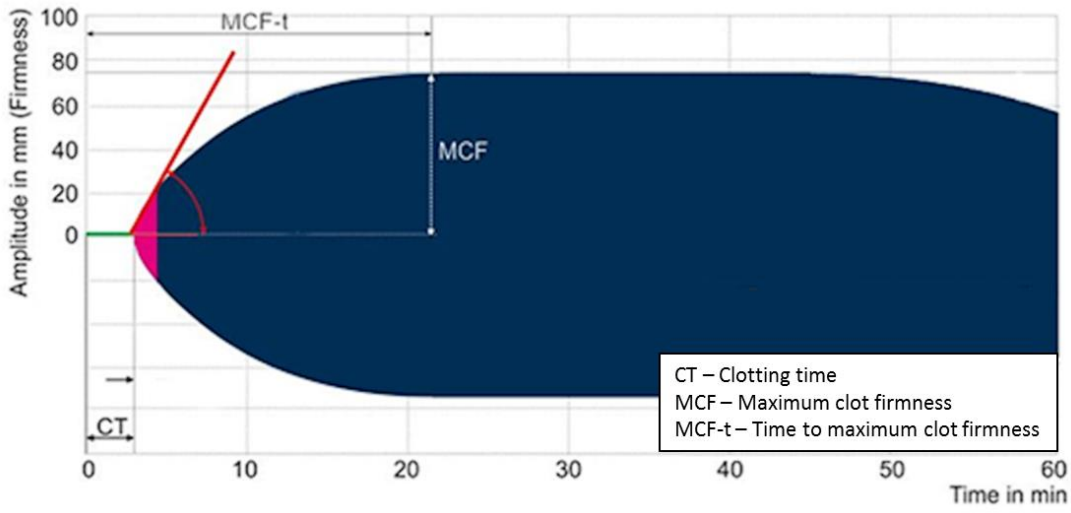

Figure 12 ROTEM trace. Typical curve generated by a ROTEM® (adapted from Rotem.de).

2.1.10 Clot permeation

Clots for permeation measurements were generated by mixing 10 µL of activation mixture (human thrombin (0.5 $U.mL^{-1}$) and $CaCl_2$ (10 mM)) with 100 µL of plasma. Immediately after mixing, 100 µL of the clotting mixture was carefully transferred to a 4.5 cm plastic tip with a roughened interior surface, which was cut off from a 1 ml Costar pipette tip. The clot was left to consolidate in a humidified chamber at room temperature for 2 hours. The plastic tip was connected through a silicon tube to a syringe containing TBS with a 4 cm pressure drop. Upon connection, TBS was left to permeate

through the fibrin clot network for 1.5 hours to wash away other plasma proteins (Figure 13). Measurements were performed in duplicate by collecting drops passing through the clot in a pre-weighed Eppendorf tube and weighing the total volume of liquid in the tube every 30 minutes for two hours. Clot permeability was determined by calculating Darcy's constant (Ks), which is a measure of the average pore size of the fibrin network (Woodhead et al., 1996).

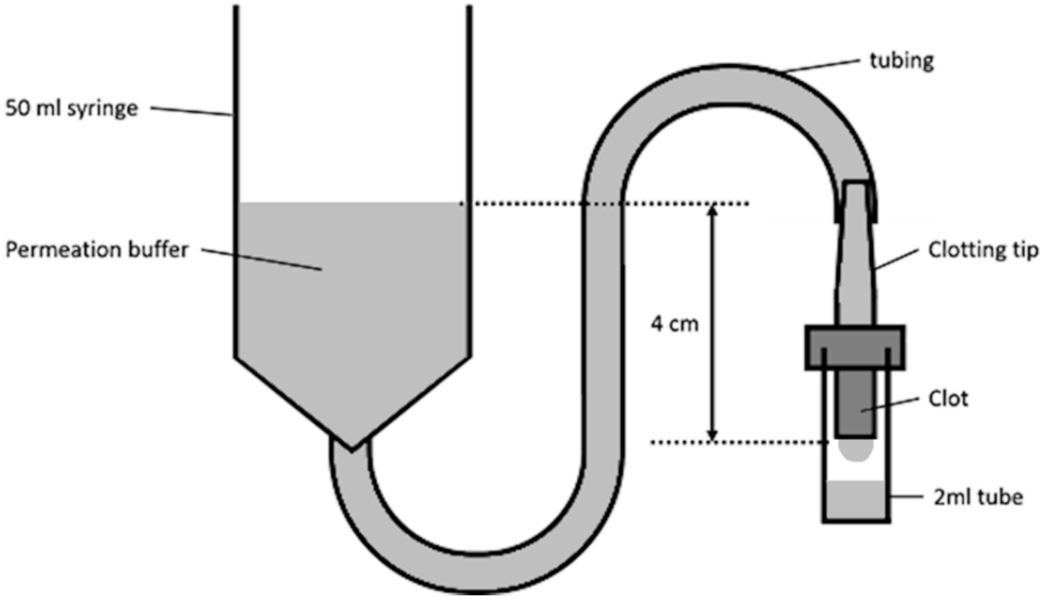

Figure 13 Permeation set-up. Diagrammatic representation of the permeation set-up.

2.2 The role of fibrinogen γ' in clot structure

Given the previous evidence of the role of fibrinogen γ' in clot structure in purified protein systems, a series of experiments were designed to establish if fibrinogen γ' played a role in clot structure at physiological levels and in

patient plasma samples. The role of fibrinogen γ' was also investigated in whole blood samples and under flow conditions.

2.2.1 Measurement of fibrinogen γ' levels in patients by ELISA

Fibrinogen γ' concentrations were measured in 1168 patient plasma samples by ELISA as previously described in chapter 2.1.6. From the 1168 patients measured, all patients who possessed a low (1-7 % (~3 %), n = 41), normal (9-11 % (~10 %), n = 45) and high (22-40 % (~30 %), n = 33) fibrinogen γ' levels, with fibrinogen levels between 2.3-4.0 $mg.ml^{-1}$ were selected for further analysis on the effects of fibrinogen γ' on clot structure.

2.2.2 Fluorescent labelling of fibrinogen γA/γA and γA/γ'

To analyse the effects of fibrinogen γ' on clot structure by LSCM fibrinogen γA/γA and γA/γ' were fluorescently labelled. Purified fibrinogen γA/γA and γA/γ' were fluorescently labelled with Alexa Fluor-488 using the Alexa Fluor protein labelling kit (Thermo Fisher Scientific, UK). In brief, fibrinogen γA/γA and γA/γ' were dialysed into 0.01 M phosphate buffered saline, pH 7.4 (PBS, 5 PBS tablets dissolved in 1 litre of ddH_2O, Sigma-Aldrich, UK). The fibrinogens were diluted down to 1 $mg.ml^{-1}$ and 9 µl of 1 M sodium bicarbonate was added to 90 µl (to raise the pH of the reaction mixture). This was then added to the appropriate fluorescent dye and incubated for 1 hour at room temperature. The fibrinogen γA/γA and γA/γ' was then purified to remove unbound dye from the solutions using a resin purification spin column provided in the kit. The degree of labelling and fibrinogen concentration was determined by spectrophotometry using a Nanodrop (ND-1000 Spectrophotometer, LabTech International) to check the fibrinogens had been labelled sufficiently.

2.2.3 Fibrinogen γ' clot structure by confocal microscopy

Previous research has shown that fibrinogen γ' contributes to changes in clot structure (Macrae et al., 2016). To assess if changes to fibrinogen γA/γA and γA/γ' concentrations at physiological levels and ratios played a role in clot structure, LSCM was carried out on purified fibrinogens, repleted plasma and plasma clots as previously described in chapter 2.1.7, but with some differences.

For purified samples, purified fibrinogen γA/γA and γA/γ' were combined at 3, 10 and 30 %, with or without FXIII (3.7 $\mu g.ml^{-1}$), and spiked with fluorescently labelled γA/γA and γA/γ' at 2.5 % of the respective fibrinogen concentration, with a final total fibrinogen concentration of 0.5 $mg.ml^{-1}$. For repleted plasma samples, fibrinogen deficient plasma (ERL, UK) diluted by half was repleted with purified fibrinogen γA/γA and γA/γ' at above ratios and spiked with 25 $\mu g.ml^{-1}$ of the fluorescently labelled γA/γA and γA/γ, with a final total fibrinogen concentration of 1 $mg.ml^{-1}$. Patient plasma samples were carried out as described previously.

2.2.4 Role of fibrinogen γ' in clot formation and breakdown using the turbidity and lysis assay

Previous research has shown that fibrinogen γ' plays a role in clot formation and breakdown (Macrae et al., 2016). In order to establish if physiological levels of fibrinogen γ' played a role in clot formation and breakdown, turbidity and lysis experiments were performed as previously described (chapter 2.1.8) using purified fibrinogen, repleted plasma and patient plasma with some changes.

For purified samples, purified fibrinogen γA/γA and γA/γ' were combined at 3, 10 and 30 %, with or without FXIII (3.7 $\mu g.ml^{-1}$) with a final total fibrinogen concentration of 0.5 $mg.ml^{-1}$. For repleted plasma samples, fibrinogen deficient plasma (Merck Millipore, Darmstadt, Germany) diluted by half was repleted with purified fibrinogen γA/γA and γA/γ' at above ratios, with a final total fibrinogen concentration of 0.5 $mg.ml^{-1}$. Patient plasma samples were carried out as described previously.

2.2.5 Roles of fibrinogen γ' in clot viscoelasticity by whole blood ROTEM

The effects of fibrinogen γ' on clot viscoelasticity in whole blood was examined using ROTEM as previously described in chapter 2.1.9. It was performed on the whole blood of a sub population of 78 patients who were the most recent recruits to the pool of 1168 patients that had both fibrinogen and fibrinogen γ' levels measured. These most recent patients had ROTEM analysis carried out on their blood samples after the acquisition of a ROTEM machine, allowing for whole blood analysis.

2.2.6 Effects of fibrinogen γ' under flow

The effects of fibrinogen γ' under flow were investigated, in collaboration with Prof. Johan Heemskerk, Dr Frauke Swieringa and Dr Constance Baaten at the University of Maastricht. Whole blood was obtained after medical ethical approval from healthy volunteers after full informed consent, according to the declaration of Helsinki. Blood donors were free from antithrombotic medication for at least 2 weeks. Free flowing blood was taken by venepuncture of the median cubital vein into 1/10 volume of 3.2 % trisodium citrate and 40 $\mu g.ml^{-1}$ corn trypsin inhibitor (CTI).

Glass coverslips were cleaned with 1 M hydrochloric acid (HCL) in 50 % ethanol and then coated with two consecutive 2 µl microspots of Horm type I collagen (50 $\mu g.ml^{-1}$) at least 0.7 cm apart and left in a humidity chamber for 1 hour (Van Kruchten et al., 2012). After rinsing with saline and drying under nitrogen gas, 2 µL of 500 pM TF (Innovin, Siemens, Marburg, Germany) or saline solution were applied on each microspot and incubated for 1 hour in a humidity chamber. The Collagen/TF-coated coverslips were blocked for 1 hour with 1 % BSA in HEPES buffer pH 7.45 (136 mM NaCl, 10 mM HEPES, 2.7 mM KCl, 2 mM MgCl2, 1 $mg.ml^{-1}$ glucose). Assuming homogeneous TF distribution, a coating with 2.0 µL of 500 pM (microspots of 6.75 mm^2) gave a calculated applied TF density of 89×10^6 molecules TF per mm^2. Collagen was coated at a density of 14.8 $ng.mm^{-2}$.

To investigate thrombus formation in fibrinogen γA/γA and γA/γ' under flow, a two-step model was used. Anticoagulated whole blood, with 3.6 mM $MgCl_2$ but no re-calcification, was perfused through a parallel-plate flow chamber with collagen/TF microspots at a wall shear rate of 1,000 s^{-1} for 5 minutes. Platelet thrombi were formed on the microspots, after which the channel was rinsed with saline solution.

Fibrinogen deficient plasma was repleted with 0.5 $mg.ml^{-1}$ purified fibrinogen γA/γA or γA/γ' and spiked with 5 $\mu g.ml^{-1}$ of the appropriate Alexa fluor-488 labelled fibrinogen variant. The plasma was then recalcified and immediately perfused over the preformed thrombi at 150 s^{-1} or 500 s^{-1}. Fibrin formation was assessed by time series confocal fluorescence imaging with a camera-containing line-scanning Live-7 microscopic system (Carl Zeiss, Oberkochen, Germany) and a 63 × /1.4 numerical aperture oil immersion

objective every second. The assay was stopped when fibrin accumulation stopped or the channel was occluded. A number of endpoint Z-stack images (0.5 µm per slice) were then taken in random locations across the microspot to assess differences in endpoint clot formation

For time series analysis, accumulation of fluorescence was measured from the images every 5 seconds and a number of parameters were compared including: Lag time, Maximum fluorescence and rate of accumulation. Endpoint Z-stacks were depth coded, with cross sections and views from above analysed. Maximum heights and volumes were compared.

2.3 Formation of the fibrin film

A number of experiments were designed to explore the exterior face of blood clots found at the blood air-interface to examine the structures present and to explore the fibrin fibre network at this border.

2.3.1 Mutant fibrinogen expression

Recombinant human fibrinogen expression and purification was carried out by Dr Cedric Duval and Helen McPherson as previously described (Standeven et al., 2007, Duval et al., 2014). Briefly, truncations at fibrinogen αSer220 and αAsp390, and γ-chain mutations Q398N/Q399N/K406R referred to as γ3x, were established through the use of QuikChange II Site-Directed Mutagenesis Kit (Agilent Technologies; Stockport, UK). The expression vector pMLP encoded the entire cDNA for either the α- or γ-chain. Primers were designed to change residues at desired locations (γ398, 399, 406) or to create a stop codon at α221 and α391. Mutations and truncations were confirmed by sequencing (MRC PPU DNA Sequencing and

Services; University of Dundee, Scotland). Plasmids were transfected into Chinese hamster ovarian (CHO) cells containing the remaining fibrinogen chains. A second plasmid was transfected for selection (pMSV-his). Recombinant fibrinogen wildtype (WT), γ3x and α-truncations were produced in roller bottles containing microcarrier beads. DMEM/F12 medium (Thermo Fisher Scientific; Paisley, UK) was supplemented with aprotinin, 5 $\mu g.ml^{-1}$ insulin, 5 $\mu g.ml^{-1}$ transferrin and 5 $ng.ml^{-1}$ sodium selenite (Roche; Welwyn Garden City, UK). Medium was collected and replaced every 48 hours and stored at -40 °C with the addition of 150 µM phenylmethylsulfonyl fluoride (PMSF), and harvested for 8 weeks. The fibrinogen was precipitated overnight with 40 % saturated ammonium sulphate (VWR International, Leicestershire, UK) and a mixture of protein inhibitors (MES hydrate 20 mM pH 5.6, 6-Aminihexanoic acid 5 mM, benzamidine 5 mM, PMSF 100 µM, pepstatin 1 µM, leupeptin 1 µM). The precipitated medium was centrifuged at 14,500 g for 45 minutes without brakes at 4°C in an Avanti J-265 XPI (Beckman Coulter, High Wycombe, UK). The pellet was re-suspended in a protein cocktail (NaCl 333 mM, Tris 222 mM, PMSF 111 µM, pepstatin 5 µM, leupeptin 5 µM, EDTA 1 mM, trypsin inhibitor 11 $U.mL^{-1}$, benzamidine 5 mM, 6-Aminihexanoic acid 5 mM), incubated for 30 min at 4 °C and centrifuged at 43,000 g for 30 minutes. Supernatant was collected and kept at -80 °C. Samples were purified by immunoaffinity chromatography (IF-1 mAb, 10 mg; Kamiya Biomedical; Seattle, USA) as previously described (Duval et al., 2014). Fractions containing fibrinogen were pooled and stored at –80°C. Fibrinogen was concentrated and dialysed in 50 mM Tris-HCl and 100 mM NaCl pH 7.4. Protein integrity was assessed by SDS-PAGE.

2.3.2 Scanning electron microscopy – whole blood, plasma, purified, thrombin/tissue factor

Clots for scanning electron microscopy (SEM) were prepared by adding 10 µl of activation mixture (Whole blood/plasma – human thrombin 0.5 $U.ml^{-1}$ or tissue factor 5 pM (Diagnostica Stago; Theale, UK), $CaCl_2$ 5 mM, Purified fibrinogen – human thrombin 0.5 $U.ml^{-1}$, $CaCl_2$ 5 mM final concentrations, in TBS) to 100 µl of whole blood, plasma or purified fibrinogens ± FXIII (final concentrations: Fibrinogen – 1 $mg.ml^{-1}$, FXIII – 3.7 $\mu g.ml^{-1}$). The clotting mixture was immediately transferred to pierced Eppendorf lids (for subsequent perfusion). Clots were left to form in a humidified chamber at room temperature for 2 hours. Clots were washed with saline solution to remove excess salt and prepared for microscopy by fixation in 2 % glutaraldehyde solution for at least 120 minutes. Clots were further washed with sodium cacodylate buffer (67 mM $C_2H_6AsNaO_2$, pH 7.4) and dehydrated in a series of increasing acetone concentrations (30–100 %). Clots were critical-point dried with carbon dioxide (CO_2), mounted onto stubs and sputter-coated with platinum using a Cressington 208 HR (Cressington Scientific Instruments, Watford, UK). Each clot was formed in duplicate and imaged in five areas, at different magnifications (2500, 5000, 10000, 20000, 25000 and 50000 x) using a Hitachi SU8230 high performance cold field emission (CFE) SEM (Chiyoda, Tokyo, Japan).

2.3.3 Laser scanning confocal microscopy – whole blood, plasma and purified

Whole blood or plasma samples were prepared for laser scanning confocal microscopy by diluting 1/2 with saline or TBS respectively, and spiked with

25 μg.ml^{-1} AlexaFluor-594 or -488 fibrinogen respectively and 5 mM $CaCl_2$. 0.5 U.ml^{-1} of human thrombin or 5 pM tissue factor was added to initiate clotting. Purified fibrinogen (1 mg.ml^{-1}) was spiked with 25 μg.ml^{-1} AlexaFluor-488 fibrinogen, with or without FXIII (3.7 μg.ml^{-1}) and 5 mM $CaCl_2$. 0.5 U.ml^{-1} of human thrombin was added to initiate clotting. Immediately after the initiation of clotting a 30 μl drop of the mixture was transferred to the centre of the well of an uncoated 8-well Ibidi slide (Ibidi GmbH, Munich, Germany) and the slide was transferred to a dark humidity chamber for 4 hours at room temperature. Imaging was performed using an inverted Zeiss LSM880 microscope (Carl Zeiss; Welwyn Garden City, UK) with a 40×/1.4 numerical aperture oil immersion objective lens. Fibrin clots were prepared in duplicate and four images were taken at the air-liquid interface for each clot, Z-stacks (20 μm, 30 slices) were combined to form 3D images (ZEN 2.1 black, Carl Zeiss, Cambridge, UK).

2.3.4 Conditions - thrombin, calcium, fibrinogen concentration, reptilase, temperature, platelets, fibrinogen variants.

LSCM and SEM were carried out as above, but with some differences between the conditions. Experiments were carried out where clotting was initiated with different thrombin concentrations (final concentrations: 0.1, 0.5, 1, 10 U.ml^{-1}), $CaCl_2$ concentrations (0, 5, 10, 20 mM) and fibrinogen concentrations (0.05, 0.5, 1, 2.5 mg.ml^{-1}) in a purified system. In some experiments clotting was initiated with reptilase (2.4 U.ml^{-1}; Diagnostica Stago; Theale, UK) to investigate the effects of only cleaving FpA when compared to thrombin (0.5 U.ml^{-1}). The effects of temperature were investigated by incubating the reaction mix at different temperatures (room

temperature - 21 °C, skin temperature - 31.5 °C, core body temperature - 37 °C) before and throughout clotting. Average skin temperature was determined as 31.5 °C using a contact thermometer on the fore-arm and hand. Immediately after clotting initiation, a 30 µl drop of the reaction mixture was transferred into the centre of the well of an uncoated 8 well Ibidi slide (Ibidi GmbH, Martinsried, Germany) and the slide was transferred to a dark humidity chamber in an incubator at the appropriate temperature for 4 hours. The effects of platelets on film formation were studied by comparing film formation between platelet poor plasma and platelet rich plasma from 6 healthy volunteers. Reaction mixtures were prepared by diluting PPP or PRP by half with saline, and spiked with 25 $\mu g.ml^{-1}$ AlexaFluor-594 fibrinogen and 5 mM $CaCl_2$. 5 pM TF was added to initiate clotting. The effects of fibrinogen variants were investigated with purified γA/γA or γA/γ', γ3x mutant, α220 or α390 mutants (each at 2.94 µM).

2.3.5 Fibrin(ogen)-binding Affimers for imaging the film in dys- and afibrinogeneamia

Free-flowing blood was taken from the antecubital vein of 2 dysfibrinogenemia patients (FGA c.112A>G - p.R38G, FGG c.901C>T - p.R301C) and 3 afibrinogenemia patients (FGA c.635T>G - p.L212X, FGA c.635T>G - p.L212X, FGA c.635T>G - p.L212X) and spun down to PPP and stored as described above (chapter 2.1.2). Dysfibrinogenemia and afibrinogenemia patient plasma samples were provided by Dr Alessandro Casini (Geneva University). To image the plasma samples a fibrin(ogen) specific Affimer, was isolated from an Affimer phage display library by Katherine Kearney using a previously described screening process (Tiede et

al., 2017). This Affimer was fluorescently labelled using an Alexa Fluor-488 protein labelling kit (Invitrogen, Carlsbad, California, United States) according to manufacturer's instructions. Fluorescently labelled Affimer was then added to normal pool plasma or patient plasma at 17.6 μM and incubated for 30 mins. Clotting was initiated with 5 mM $CaCl_2$ and 0.5 $U.ml^{-1}$ of human thrombin and a 30 μl drop of the mixture was immediately transferred to the centre of the well of an uncoated 8-well Ibidi slide (Ibidi GmbH, Munich, Germany). Clots were incubated for 4 hours in a humidity chamber and were then imaged by LSCM as previously described.

2.3.6 Confocal time series formation/lysis

To investigate film formation by LSCM, the reaction mixture was produced as described in chapter 2.3.3 for both plasma and purified protein reactions. A 27 μl drop of this mixture was placed into the centre of a well of an uncoated 8-well Ibidi slide and 2 μl of thrombin (0.5 $U.ml^{-1}$) or tissue factor (5 pM) was added to the drop, and film formation was immediately followed over time by LSCM using a 40x oil immersion objective lens with 29 x 0.7 μm Z-stacks every 60 seconds. The effects of preventing polymerization on film formation were investigated by pre-incubating fibrinogen (1 $mg.ml^{-1}$) or plasma with Gly-Pro-Arg-Pro (GPRP, 5 mM) for 20 minutes. Three microliters of thrombin (0.5 $U.ml^{-1}$) was then added to the drop, which was immediately observed by LSCM as above.

To investigate fibrinolysis, clots were formed as described above. After film formation (1 hour), 5 μl of tPA (85 $ng.ml^{-1}$) was added to plasma clots, and 5 μl of plasminogen (25 $\mu g.ml^{-1}$) and tPA (85 $ng.ml^{-1}$) was added to purified clots. Film breakdown was immediately observed by LSCM using the same

set up as described for film formation. 3D videos were created from the Z-stacks using ZEN 2.1 black.

2.3.7 Preventing film formation – oil, tween-20, petroleum jelly

Reaction mixtures for plasma were produced as described above (chapter 2.3.3). For oil experiments, a 27 µl drop of this mixture was placed into the centre of a well of an uncoated 8-well Ibidi slide. Mineral oil was then carefully placed around the drop to fill the well before clotting, to eliminate the air-liquid interface. For petroleum jelly experiments, 27 µl of reaction mixture was injected into the centre of a small ball of petroleum jelly that had been placed in the middle of the well of a slide. For reactions with tween-20, the reaction mix was incubated with 0.1 % tween-20 before being placed in the bottom of a well of a slide. Two microliters of thrombin (0.5 $U.ml^{-1}$) was added to the reaction mixture to initiate clotting. The slide was then transferred to a humidity chamber for 4 hours at room temperature. Imaging was performed as described above (chapter 2.3.3). Each fibrin clot was prepared in duplicate and four images were taken of each sample, Z-stacks were combined to form 3D images.

2.3.8 Film thickness

The thickness of the film was calculated using confocal images. The width of the film was measured at 60 points per image along the film perpendicular to the air liquid interface using Image J (v2.0, NIH), and the average thickness for each image was used to compare between conditions.

2.3.9 Fluorescence measurements

To quantify film fluorescence, an outline was drawn around the film on each focal plane. Area, integrated density and three adjacent background readings were made using ImageJ (v2.0, NIH). Fluorescence was calculated using the equation below:

$$\begin{matrix} Corrected \\ film\ fluorescence \end{matrix} = integrated\ density - \left(\begin{matrix} region \\ of\ interest \end{matrix} \times \begin{matrix} mean \\ fluorescence\ background \end{matrix} \right)$$

This was calculated for each focal plane and then the mean of corrected film fluorescence from each focal plane was calculated and was divided by 10,000 arbitrarily to simplify. This was called Mean Sheet Fluorescence (MSF). To validate this method, measurements of average film thickness was taken from 72 confocal images of separate samples. Average thickness for each image was correlated with MSF taken from the same image (Figure 14).

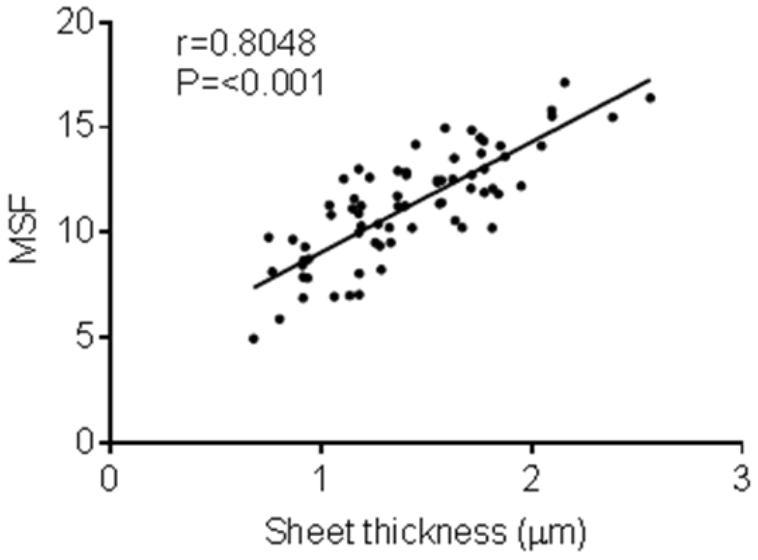

Figure 14 Mean sheet fluorescence v sheet thickness. Mean sheet fluorescence was validated by plotting MSF against sheet thickness, Pearson correlation, n = 72 experiments. MSF – Mean Sheet Fluorescence.

2.3.10 Film peel

Clots were generated by spreading 100 µl of plasma ± 1,3,4,5-Tetramethyl-2-[(2-oxopropyl)thio]imidazolium chloride (T101, transglutaminase inhibitor, 1 mM; Zedira; Darmstadt, Germany) or purified fibrinogen (1 $mg.ml^{-1}$) ± FXIII (3.7 $\mu g.ml^{-1}$) into an approximately 2x2 cm square on a coverslip. Ten microliters of activation mixture (human thrombin, 0.5 $U.ml^{-1}$ and $CaCl_2$ 5 mM) was added to initiate clotting. After 4 hours a hypodermic needle was used to peel the film away from the surface of the clot (Figure 15). The film was either, reduced and run on SDS-PAGE, or it was stretched over a coverslip exposing either the interior surface or exterior surface of the film and was prepped for SEM.

Figure 15 Film peel. The film was peeled from clots using a needle.

2.3.11 SDS-PAGE and western blot

All SDS-page and western blot experiments in Chapter 4 were carried out by Katherine Kearney. Clots were made using plasma by the addition of thrombin (0.5 $U.ml^{-1}$) and $CaCl_2$ (5 mM), with and without FXIII inhibitor T101

(1 mM). The fibrin film was removed from each clot and reduced by the addition of NuPAGE sample reducing agent (100 mM Dithiothreitol (DTT)) and heating at 95 °C for 15 minutes. A fibrin sample was prepared by forming a clot with IF-1 fibrinogen (1 $mg.ml^{-1}$), thrombin (0.5 $U.ml^{-1}$) and $CaCl_2$ (5 mM), and then reducing it as described above. Samples of FXIII, BSA and IF-1 purified fibrinogen were reduced in a similar way, and run alongside the films to help identify bands in the gel, and as controls for the blots. Protein concentrations were determined using Nanodrop, to load 2 µg of each protein sample on two identical 4-12 % NuPAGE bis-tris gels. After running, one gel was stained using GelCode Blue Safe Protein Stain (Thermo Scientific, Paisley, UK) and one was transferred to a Polyvinylidene fluoride (PVDF) membrane (Thermo Scientific). The membrane was blocked overnight using 4 % skimmed milk in 50 mM Tris, 150 mM NaCl, 0.1 % tween-20. A polyclonal rabbit anti-human fibrinogen antibody (A0080; Dako, Ely, UK) was added to the blot in blocking buffer, and detected using a goat anti-rabbit-HRP secondary antibody (P0448; Dako). Signal was detected using Supersignal West Pico Chemiluminescent Substrate (Thermo Scientific).

2.3.12 Atomic Force Microscopy sample preparation

All atomic force microscopy (AFM) experiments were carried out by Dr Stephen Baker. Samples for AFM mechanical measurements and imaging were prepared from normal pool plasma with a one in two final dilution. Plasma was mixed with an activation mix of $CaCl_2$ (5 mM) and thrombin (0.5 $U.ml^{-1}$) and placed onto 34 mm diameter tissue culture dish (TPP, Trasadingen, Switzerland) with the plasma mixture covering a 10x10 mm

square. For samples with T101, a final concentration of 1 mM was added to the mixture. Samples were then placed into a humidity chamber and allowed to clot for 1 hour. Samples were hydrated with 3-5 ml of 50 mM Tris, 100 mM NaCl and placed on the AFM sample stage. Imaging and force measurements were performed on a JPK NanoWizard 4 and a Zeiss AxioObserver D1 in qi mode with 10 nm radius AFM probes (CB3, qp-BioAC, Nanosensors, Neuchâtel, Switzerland). All measurements were done in triplicate over a 15 x 15 µm square. Young's modulus was calculated for plasma samples with and without transglutaminase inhibitor T101 by fitting a Sneddon model for conical tips to all force curves found over the entire area that was imaged. The equation for the Sneddon model used was as follows:

$$F = \frac{2}{\pi}\frac{E}{(1-\nu^2)}\,tan(\alpha)\delta^2$$

Where F is the force from the force curve, E is Young's modulus, v is Poisson's ratio (0.5), α is the half angle for the indenter (15 degrees for our tips), and δ is the indentation. Note that this equation is only accurate with a half angle of 15 degrees for the first 200nm of indentation.

2.3.13 Langmuir-Blodgett trough

Surface tension measurements were used to determine fibrinogen and fibrin adsorption at the air-liquid interface. Measurements were performed with an extra small KSV NIMA (Biolin Scientific, Manchester, UK) double barrier Langmuir-Blodgett trough (203 x 50 x 1.2 mm) with surface pressure sensor, based on the Wilhelmy method, with a Whatman CHR1 chromatography paper plate (perimeter 20.6 mm; accuracy in surface pressure - 0.01 $\mu N.m^{-1}$; KSV NIMA, Biolin Scientific, Manchester, UK). Because adsorption

measurements are sensitive to the presence of impurities, extreme care was taken to ensure that all materials and instruments used in this study were clean. The trough and barriers were cleaned with methanol and rinsed with deionized water before each run. A new Wilhelmy plate was used for each run. Due to the duration of the experiment, the trough was maintained in a dust and draught exclusion cabinet throughout the measurements to minimise the presence of impurities from the atmosphere. A humid atmosphere was maintained by putting a trough of water in the enclosing box. The sub-phase was composed of 30 ml of 0.2 µm filtered TBS pH 7.4 at room temperature. The surface was checked prior to each measurement to ensure that it was clean by moving the barriers to the centre and confirm that the surface pressure was below 0.3 $mN.m^{-1}$. The system was set to record surface pressure every second for 18 hours. The desired final protein concentrations (fibrinogen – 1, 5, 20, 30, 100, 5312 $x10^{13}$ molecules (final concentrations - 0.00018 – 1 $mg.ml^{-1}$); fibrin 1, 5, 20, 30, 100 $x10^{13}$ molecules (final concentrations - 0.00018 - 0.019 $mg.ml^{-1}$)) were achieved by pre diluting fibrinogen or fibrin into TBS, and then injecting this into the 30 ml sub-phase of the trough in one 50 µl injection with a Hamilton gastight syringe (Thermo Scientific). The accumulation of protein at the surface and was then followed for 18 hours. Fibrin monomers were formed by pre-incubating fibrinogen with GPRP (5mM) overnight at 4 °C, followed by incubation with thrombin (0.5 $U.ml^{-1}$) for 2 hours prior to each experiment. As a control a 50 µl mixture of thrombin (0.5 $U.ml^{-1}$) and GPRP (5 mM) was run on the trough to show that the thrombin and GPRP did not cover enough of the surface to register an increase in surface pressure.

2.4 Roles of the fibrin film

After demonstrating a hitherto undisclosed structure of fibrin that forms a film at the air-liquid interface, experiments were designed to elucidate its physiological role at the clot surface.

2.4.1 Bacteria migration assay

To investigate bacteria migration, an assay was set up using a Boyden chamber (VWR, Lutterworth, UK) shown in Figure 16. Three types of bacteria, Escherichia coli (ATCC #13706), Staphylococcus epidermidis (ATCC #12228) and Staphylococcus aureus (ATCC #29247), commonly found in the natural skin flora were transformed with pSELECT-Zeo plasmid (Invivogen, Toulouse, France) to provide resistance to antibiotic Zeocin. A single colony was picked for each bacterium and was grown up overnight (3.6-8.5 $x10^8$ cells.ml^{-1}) in nutrient broth containing Zeocin (25 µg.ml^{-1}, Sigma-Aldrich). Three clots for each strain of bacteria were formed in a Boyden chamber (0.8 µm pores, Millipore, Billerica, MA), two normal (Fibrinogen – 1 mg.ml^{-1}, $CaCl_2$ – 5 mM, Thrombin – 0.5 U.ml^{-1}) and one in the presence of tween-20 (0.1 %) and left overnight in a humidity chamber at room temperature. The next day the film on one of the normal clots for each bacterium was perforated by running a hypodermic needle across the surface of the clot. Each bacterium was fluorescently labelled with BacLight green following manufacturer's instructions (ThermoFischer Scientific, Ulm, Germany). The bacteria were then spun down and re-suspended in 50 % nutrient broth to remove any unused label, and were checked for fluorescence levels. Zeocin (25 µg.ml^{-1}) was added to super optimal broth with catabolite repression (SOC) media (Thermo Fisher), and 1 ml was

added to each well of the plate. Each clot was placed in the well and 300 µl of labelled bacteria was added in the chamber on top of each clot. Fifty microliters of SOC media was taken from each well and replaced with fresh SOC media every 2 hours for 48 hours and measured for fluorescence using a Bio-Tek Synergy H1 hybrid plate reader. The time to the first bacteria breaking through the clots into the second, lower chamber was defined as when fluorescence became greater than 2 % of the fluorescent bacteria added to the top chamber.

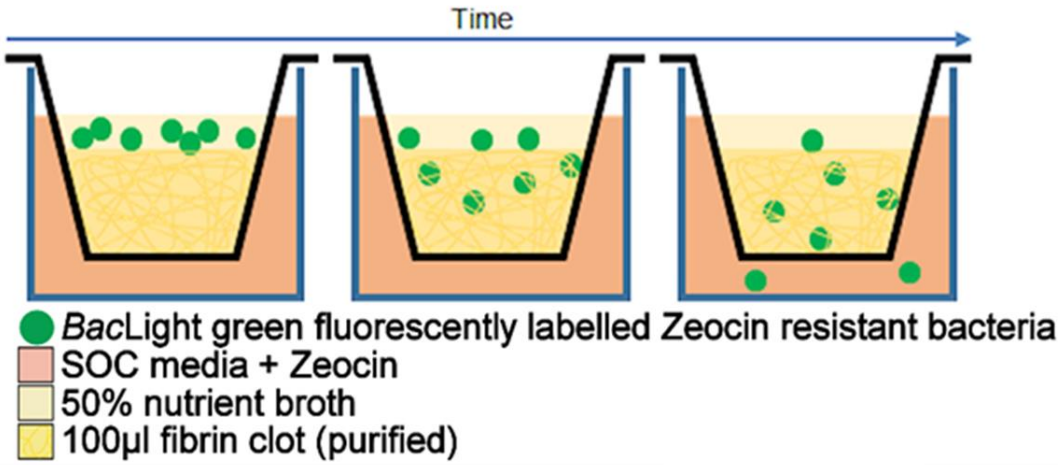

Figure 16 Method for assessing the role of the film in bacterial migration. Diagrammatic representation of the bacteria clot migration assay in the Boyden chamber. Bacteria moved from the 50 % nutrient broth through the fibrin film (if present), into the fibrin clot and then into the super-optimal broth with 20 mM glucose (SOC) medium. Quantity of bacteria moving through the clot over time was analysed by fluorescence in the SOC media.

2.4.2 *Ex vivo* wildtype and fibrinogen deficient mouse clots

C57BL/6 and fibrinogen-deficient mice (C57BL/6 background; in house) (Suh et al., 1995), aged nine- to fourteen-week old and weighing 19-30 g were used for all experiments (n = 4). Male and female mice were used in equal numbers. The mice were anaesthetized with isoflurane and bled through the inferior vena cava (IVC) on 0.109 M sodium citrate before being

euthanized (*in vivo* work was carried out by Dr Cedric Duval and Dr Nadira Yuldasheva). Whole blood clots from WT and fibrinogen-deficient mice were prepared for and imaged by SEM as described in chapter 2.3.260, but clotting was initiated with mouse thrombin (0.5 $U.ml^{-1}$).

2.4.3 In vivo mouse dermal punctures

C57BL/6 (in house) or BALB/cJRj (Janvier Labs; Le Genest-Saint-Isle, France), aged nine- to fourteen-week old and weighing 19-30 g were used for all experiments. Male and female mice were used in equal numbers. The mice were anaesthetized with isoflurane, the abdomen was shaved and waxed. Six puncture wounds were created using a 2 mm biopsy punch (World Precision Instruments Ltd, Hitchin, UK), and were filled with blood from a tail vein. The injury was either left clear or immediately covered with a thin layer of oil to remove the air-liquid interface. After 60 minutes the animals were euthanized by cervical dislocation, the area around the wound together with the clot for each condition was surgically removed and fixed in 4 % paraformaldehyde, for histology or immunohistochemistry (IHC) (n = 4) or 2 % glutaraldehyde, for SEM (n = 4) (*in vivo* work was carried out by Dr Cedric Duval and Dr Nadira Yuldasheva).

The fixed tissues for histology or IHC were dehydrated and embedded in paraffin. Consecutive 5 µm sections were cut and mounted. Sections were then stained with Martius, Scarlet and Blue (MSB) to observe the sectioned wound, collagen appears in blue, erythrocytes in yellow and fibrin in pink. Slides were observed under an Olympus BX40 Dual View microscope, and photographs were taken using Image Pro-Plus 8.0 software (Histology work was carried out by Dr Nadira Yuldasheva). For IHC an EXPOSE rabbit

specific HRP/DAB detection IHC kit (ab80437, Abcam, Cambridge, UK) was used following manufacturer's instructions. Slides were stained with mouse anti-fibrin antibody (59D8, 1:1000, antibody provided by Charles Esmon, Oklahoma Medical Research Foundation, Oklahoma City, Oklahoma, USA), which detects mouse fibrin (Hui et al., 1983) for 1 hour at room temperature in a humidity controlled chamber. The sections were washed and incubated with HRP-conjugated anti-mouse secondary antibody. Negative controls were stained simultaneously in the absence of primary antibody. Alternatively after fixing, samples were prepared for and imaged by SEM as described in chapter 2.3.2.

2.4.4 Red blood cell retention assay

Red blood cell retention was measured by analysing the quantity of haemoglobin released from different types of whole blood clots. Whole blood clots were formed in a well of an uncoated 8-well Ibidi slide in the presence of $CaCl_2$ (5 mM), with the addition of 1 pM tissue factor and incubated in a humidity chamber for 2 hours at room temperature. Clots were either formed with no intervention, in the presence of tween-20 (0.1 %) or with the film being perforated after 1 hour. After 2 hours saline solution was added to the clot surface and the clots were placed on an orbital shaker (400 rpm) for 30 minutes. A sample of the solution above the clot surface was carefully taken and was diluted by 50 % in distilled water and left for 30 minutes for haemolysis to occur. The samples were then analysed for haemoglobin levels using the Harboe method and a spectrophotometer (Cookson et al., 2004). The Harboe method measures the optical density of oxyhaemoglobin in a sample at 415 nm, and corrects for background by incorporating optical

densities of non-specific plasma components that interfered at 380 nm and bilirubin/albumin complexes at 450 nm (Harboe, 1959, Malinauskas, 1997). Conversion of absorbance values to haemoglobin (Hb) concentrations was made using the following equation:

$$Hb\ (g.L^{-1}) = \frac{(k[167.2 \times A_{415} - 83.6 \times A_{380} - 83.6 \times A_{450}])}{1000}$$

Where the calibration coefficient (*k*) was 1.

2.4.5 Wound infection model

Wound infection models were carried out by Dr Cedric Duval and Dr Praveen Papareddy. Bioluminescent *Pseudomonas aeruginosa* (strain Xen 41, derived from the parental pleural isolate PAO1; PerkinElmer, Waltham, MA), possessing a copy of the luxCDABE operon of *Pseudomonas luminescens*, integrated at a single site on the chromosome, were aerobically grown in Todd Hewitt (TH) broth at 37 °C to logarithmic phase (OD_{620}~0.5). Bacteria were harvested, washed in phosphate buffered saline (PBS), and diluted in the same buffer to 2 x10^8 colony forming units CFU ml^{-1}. BALB/cJRj mice (8 weeks of age; Janvier Labs; Le Genest-Saint-Isle, France) were maintained under specific-pathogen-free conditions and had free access to commercial chow and water. Male and female mice were used in equal numbers. For the experimental procedures, animals were anaesthetised with isoflurane, and one puncture wound was created using a 2 mm biopsy punch (World Precision Instruments Ltd, Hitchin, UK) on the back of each mouse. The puncture wound was filled with blood, from a BALB/cJRj donor mouse, and the wound was either left to clot while exposed to the air for 30 minutes (experimental group 1, n = 8), or

immediately covered with mineral oil and left to clot for 30 minutes, before the oil was washed off the clot with saline (experimental group 2, n = 8). As a control to investigate the effect of oil on bacterial proliferation, blood was not added to the puncture wounds on some mice, and these were either left untreated (control group 1, n = 4) or covered with mineral oil (control group 2, n = 4). All animals were subsequently infected with 2 µl of bioluminescent *Pseudomonas aeruginosa* suspension carefully deposited on top of the clots. Mice were then anaesthetized and imaged to check that the same amount of bacteria was added to each mouse and then anaesthetized again at 4, 8, 12 hours after bacterial infection to allow for data acquisition using a three-dimensional IVIS Spectrum In vivo Imaging System (PerkinElmer), and analysis using the Living Image® software (PerkinElmer). Differences in appearance between mice +film and –film in Figure 56 are due to the oil used to prevent film formation being transferred to the fur of the mice.

2.4.6 Determination of bacterial colony forming units

Bacterial growth and dissemination experiments were carried out by Dr Cedric Duval and Dr Praveen Papareddy. In order to study bacterial growth and dissemination, the skin around the wound was harvested from sacrificed animals at the end of the experiment (12 hours). The tissues were mechanically homogenized using 1.4 mm ceramic beads (Qiagen; Sollentuna, Sweden) and a MagNA Lyser (Roche; Bromma, Sweden), and serial dilutions were subsequently plated on TH agar plates overnight at 37 °C in order to enumerate the bacterial CFU present in the samples. The quantity of bacteria on the plates was also measured by bioluminescence and the three-dimensional IVIS Spectrum In vivo Imaging System.

2.5 Clotting in AAA

Fibrin clot structure plays a role in the development and progression of AAA. Patients with AAA produce fibrin clots that are denser and more resistant to proteolytic degradation. This contributes to the development of an ILT that is more stable and therefore increases the proteolytic and hypoxic burden in the AAA. In view of the central role of FXIII and fibrinogen in thrombus formation and the complications of ILT in AAA, a series of experiments were designed to investigate 1) links between genetic sequence variants of FXIII and fibrinogen and AAA, to identify high risk genotypes and potential disease mechanisms and 2) the relationship between fibrinogen and fibrinogen γ' levels with AAA.

2.5.1 Blood sampling and DNA extraction for genotyping

Whole blood was collected by Mrs Anne Johnson from five hundred and twenty (n = 520) AAA patients and four hundred and ninety nine (n = 499) age-matched control subjects that were enrolled as part of the LEADS as previously described (chapter 2.1.2). DNA was extracted from whole blood taken into K_2EDTA tubes using a QIAamp DNA Blood Maxi Kit (QIAGEN, Manchester, UK) following manufacturer's instructions. A full protocol can be found in Appendices 6. The DNA samples were diluted to 10 $ng.ml^{-1}$ using DNA- and RNA- free Tris Buffered Saline, and stored at 4°C until genotyping. DNA concentration was measured using the 260/280 nm optical density ratio using a Nanodrop ND-1000 spectrophotometer (LabTech International, Uckfield, UK).

2.5.2 Real Time Polymerase Chain Reaction

TaqMan single nucleotide polymorphism (SNP) Genotyping Assays (Life Technologies, Paisley, UK) were used to identify each of the genetic sequence variants (FXIII A Val34Leu (rs5985), FXIII B His95Arg (rs6003), Splice Variant (intron K nt29576C-G) (rs12134960), Fib-b Arg448Lys (rs4220), Fib-a Thr312Ala (rs6050), Fib-γ 10034C>T (rs2066865). Real-time polymerase chain reaction (PCR) was set up in 384 well PCR plates with 2.2 µl of 10 ng/ml DNA in each well, 2.50 µl of Master Mix and 0.25 µl of probe. The TaqMan universal PCR master mix is a premix of all the components, except primers and probe, necessary to perform a 5' nuclease assay. Two no template controls (containing only MasterProbe) were included on each plate. A Roche LightCycler480 (Roche Diagnostics, Burgess Hill, UK) was used for programming the real time polymerase chain reaction, with final PCR conditions being: 95°C for ten minutes, 95°C for 15 seconds, and 60°C for one minute 30 seconds for 50 cycles. End-point genotyping was used to determine genotype frequencies. Genotyping was called with an accuracy of 96–100 %; samples which were not called successfully were repeated. In addition to the no template controls, random samples were repeated on each plate to ensure reproducibility of the results. Only samples that had all six genotypes successfully determined were included in the analysis.

2.5.3 Fibrinogen γ' and total fibrinogen levels

Fibrinogen γ' (chapter 2.1.6) and fibrinogen levels (chapter 2.1.4) were measured in plasma collected as previously described (chapter 2.1.2) from 608 AAA patients and 560 age and sex matched controls (same total patient population as the 1168 patients in chapter 2.1.6).

2.6 Clotting in PNH and the effects of eculizumab

To assess the clotting characteristics of patients with PNH and to determine the role of eculizumab in thrombosis reduction, 104 patients selected from the PNH National Service Clinic at St James University Hospital, Leeds were enrolled into the study. Participation in the study was voluntary with patients recruited by routine clinic appointments. 22 patients were removed from the analysis due to them being on anticoagulant therapy or having missing data.

2.6.1 Blood samples

Blood was taken and stored by members of the PNH Clinic led by Dr Anita Hill as previously described (chapter 2.1.2) when patients attended routine clinical appointments.

2.6.2 PNH Diagnosis, granulocyte clone size and LDH levels

Diagnosis of PNH was determined by GPI deficiency. GPI deficient cells were identified using flow cytometry carried out by members of the PNH Clinic. Detection of PNH granulocytes and/or monocytes in peripheral blood was carried out as follows. 100 µL of whole blood was labelled with 45 µL of a combination of fluorochrome conjugated monoclonal antibodies and probes in a single six colour test. These included fluorescent aerolysin (FLAER) reagent alexa 488 (Protox biotech, Pinewood Scientific Services Inc, Victoria BC, Canada), CD24 PE (Becton Dickinson Pharmingen, Oxford, UK), CD16 PerCP:Cy5.5 (Becton Dickinson Biosciences, Oxford, UK (BDB)), CD33 PE:Cy7 (BDB), CD15 APC (Becton Dickinson Pharmingen, Oxford UK) and CD14 APC:Cy7 (BDB). The whole blood was left to stain for 20 minutes and then the RBCs were removed by adding 2 mL of

FACSLysing solution (BDB). After two washes to remove excess unbound antibody and cellular debris, samples were analysed on a FACSCanto II flow cytometer (BDB) using FACSDiVa software (BDB). Granulocytes were identified by CD15 expression and light scatter characteristics as described previously (Richards and Barnett, 2007) and monocytes were identified by bright CD33 expression and low/ intermediate light scatter. Granulocyte PNH clones were identified by the lack of GPI-anchored antigens CD16 and CD24 and, in a small (less than 5 %) populations, by deficiency of FLAER (a pan-GPI-anchor marker). The percentage of granulocyte PNH clones was calculated and used as a scale of disease severity.

Serum lactate dehydrogenase (LDH) levels were measured as a marker of cell damage and lysis, using a Bayer Advia 1650 or 2400 (Siemens Healthcare, Surrey, UK). The adult reference range is 160–430 $IU.L^{-1}$ for serum or plasma. LDH levels in patients in this study ranged from 279-6568 $IU.L^{-1}$.

2.6.3 PNH Clot permeability

Permeability of clots formed from plasma of PNH patients were measured as previously described (chapter 2.1.10).

2.6.4 PNH confocal microscopy

Confocal microscopy was carried out on clots formed from patient plasma as previously described in chapter 2.1.7.

2.6.5 PNH turbidity and lysis

Clot formation and breakdown in patients with PNH was analysed using the previously described turbidity and lysis assay (chapter 2.1.8).

2.6.6 PNH fibrinogen levels

Fibrinogen levels in patients with PNH were measured as previously described in chapter 2.1.4.

2.6.7 PNH thrombin generation

Thrombin generation was measured in patients with PNH using the Calibrated Automated Thrombogram (CAT) method (Thrombinoscope BV, The Netherlands). Measurements were taken following the manufacturer's instructions. In brief, for each patient 80 µl of plasma was added to 6 wells of an "Immulon 2HB transparent U-bottom 96-well plate". To the first 3 wells 20 µl of thrombin calibrator (citrate buffered saline, bovine proteins and saccharides) was added to the patient plasma. The thrombin calibrator is a thrombin-like enzyme at a known activity that is not inhibited by plasmatic inhibitors and does not react with any substrates in plasma. This allows for quantification of thrombin concentration in the plasma. To the second 3 wells, 20 µl of PPP-Reagent (phospholipids 4 µM and tissue factor 5 pM) was added to the patient plasma. The plate was immediately placed in a Fluoroskan™ Microplate Fluorometer (Thermo Fisher Scientific, Massachusetts USA), where 20 µl of FluCa solution (20 µM of HEPES, 60 $mg.ml^{-1}$ BSA and $CaCl_2$) was added at time zero that initiates clotting due to the addition of calcium. Fluorescence using a 390/460 nm filter pair was measured every 20 seconds for 120 minutes at 37^0C. The data was collected using the thrombinoscope software (Thrombinoscope BV, The Netherlands) and curves were automatically calculated by the analysis software correcting for inner filter effect, substrate consumption and α2-macroglobulin-thrombin activity.

2.6.8 PNH ROTEM

ROTEM in patients with PNH was carried out as previously described in chapter 2.1.9. It was performed on the whole blood of a sub population of a selection of 15 patients who were the most recent recruits from the study population of 82 patients. These most recent patients had ROTEM carried on their blood samples after the acquisition of a ROTEM machine allowing for whole blood analysis.

2.7 Data analysis

All raw data was initially collected into Microsoft Excel. GraphPad Prism v7 (La Jolla, CA, USA) was used to represent the data graphically. Statistical tests were performed using GraphPad Prism v7 or IBM SPSS Statistics v20 (SPSS Inc. Chicago, Illinois, USA). Statistically significant results were taken as $p < 0.05$. Distribution of data was tested using the D'Agostino and Pearson normality test. Continuous parametric data was presented as mean ± standard deviation and continuous non-parametric data was presented as median and interquartile range. For patient demographics, continuous data is presented as mean ± standard deviation (parametric) or median and inter-quartile range (non-parametric) and categorical data as number of subjects (% of total), with differences between the groups initially analysed using 2 tailed t-tests or Mann-Whitney U test for continuous data and Pearson's Chi-Squared for categorical data, before carrying out binary logistic regression analysis. 2-tailed unpaired t-tests for comparison of two groups, Paired t-tests for paired groups, one-way ANOVA followed by Tukey's multiple comparisons test or two-way ANOVA followed by a Sidak's multiple

comparisons test for comparison of multiple groups were used for parametric data. Mann-Whitney U test for the comparison of two groups, Wilcoxon matched pairs singed-rank test for paired groups and Kruskal-Wallis test followed by Dunn's multiple comparisons test for the comparison of multiple groups was used for non-parametric data.

For genetic sequence variants data, genotype distributions were tested for concordance with the Hardy-Weinberg equilibrium. The difference in the distribution of genotypes between groups was analysed using Pearson's Chi-Squared testing.

2.8 Study approvals

Ethical approval for blood taking was obtained from the Leeds East National Research Ethics Committee (approval number 03/142), Maastricht medical ethics committee (METC 10-3-023) or the University Hospitals of Geneva and Faculty of Medicine review board. Written informed consent was received from all patients and volunteers prior to inclusion in a study in accordance with the Declaration of Helsinki. All mouse experiments were conducted according to institutional guidelines and were authorized by either the University of Leeds Ethics Committee, in accordance with Home Office UK Animals (Scientific Procedures) Act 1986 (PPL 70/8115), or the Malmö-Lund Animal Care Ethics Committee, Sweden (entry no. M89-16).

Chapter 3 - Fibrinogen γ' and its role in clot structure

Fibrinogen γ’ is one of the most common mutations in fibrinogen. It results in a bulky negatively charged extension being formed at the c-terminus of the γ-chain of about 10-12 % of all fibrinogen molecules, although this can vary quite drastically. This variant has been shown to modulate thrombin via binding to exosite II and influence clot architecture, forming clots with increased branching, smaller pores and thinner fibres. It has also been shown to play a role in fibrin clot breakdown, making clots more resistant to lysis. Increases in fibrinogen γ’ have been associated with arterial thrombosis and decreases with venous thrombosis suggesting that fibrinogen γ’ induced changes in clot structure may play a role in the pathophysiology of thrombosis. So far this variant has been found in all human individuals, with many studies investigating its role in pathophysiology. The majority of previous studies have investigated the roles of fibrinogen γ’ using purified proteins, comparing 100 % γ’ to 100 % of the WT fibrinogen (γA) in static conditions. In this chapter the role of γ’ in clot formation and breakdown is investigated at physiological levels, in plasma and whole blood. This will help to demonstrate if previously described effects of γ’ on fibrin clot formation and breakdown play a role when both variants of fibrinogen are present at physiological concentrations. Furthermore, very little research has been carried out on fibrinogen γ’ under flow conditions. Therefore, initial experiments into the role of fibrinogen γ’ under flow are also discussed in this chapter. These will help to uncover how fibrinogen γ’ modulates clot structure at different flow rates.

3.1 Fibrinogen γ’ and fibrinogen γ’ percentage

A splice variant of the fibrinogen γ-chain leads to a negatively charged extension at the C-terminus, known as fibrinogen γ’ (Macrae et al., 2016). This variant has been shown to influence clot architecture. The majority of clot structure studies have been performed using purified proteins, comparing 100 % γA/γ’ to 100 % γA/γA. In view of this we went on to investigate the effects of physiological levels of fibrinogen γ’ on clot formation and breakdown, and if these effects were similar to those seen in previous studies.

3.1.1 The effects of physiological plasma fibrinogen γ’ levels

Fibrinogen γ’ levels were measured in 1164 plasma samples, provided by patients recruited into LEADS (chapter 2.1.2), using the γ’ ELISA described in chapter 2.1.6 (Figure 17A). The demographic and clinical characteristics of this group can be seen in Table 3. Fibrinogen levels were also measured in the same patients (Figure 17B) and from this fibrinogen γ’ % was calculated (Figure 17C). Levels of γ’ in the whole group covered a large range from 0.8-39.5 %.

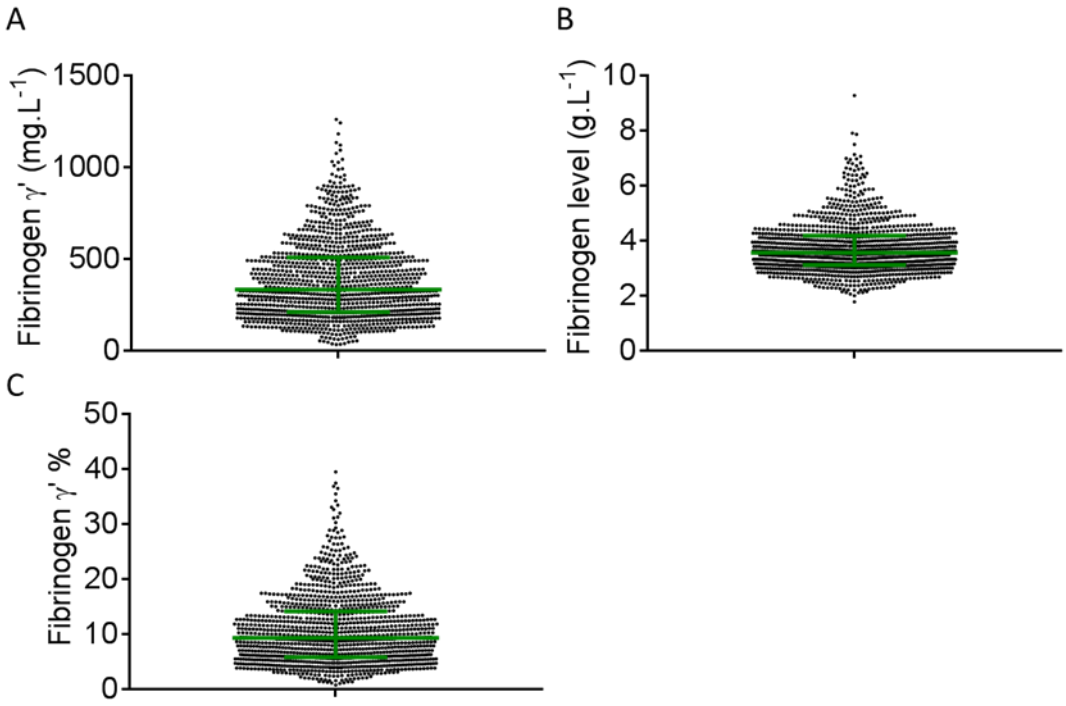

Figure 17 Fibrinogen γ' and total fibrinogen levels. Fibrinogen γ', total fibrinogen levels and fibrinogen γ' % were measured in 1164 patients plasma samples. **A,** Fibrinogen γ' levels measured in patient plasma by ELISA. **B,** Fibrinogen levels measured by Clauss method. **C,** Fibrinogen γ' % calculated from total fibrinogen and fibrinogen γ' levels. n = 1164.Data presented as median and IQR.

Table 3 Demographic and clinical characteristics of all patients with γ' levels measured.

	(n = 1164)
Age (years) §	71 (66, 77)
BMI, Kg.m^{-2} §	27.46 (24.38, 30.15)
Female ¥	245 (21.0%)
MI ¥	218 (18.7%)
PVD ¥	281 (24.1%)
CVA/TIA ¥	174 (14.9%)
DVT ¥	46 (4.0%)
PE ¥	11 (0.9%)
DM ¥	166 (14.2%)
Current smoker ¥	222 (19.1%)
Ever smokers ¥	948 (81.4%)
Statins ¥	750 (64.4%)
Aspirin ¥	668 (57.4%)
Warfarin ¥	12 (1.0%)

BMI – body mass index, MI - Myocardial infarction, PVD - peripheral vascular disease, CVA/TIA - cerebro-vascular accident/ transient ischemic attack, DVT- deep vein thrombosis, PE – pulmonary embolism, DM - Diabetes mellitus.

§ - Nonparametric data expressed as median (25th, 75th quartiles).
¥ - Categorical data expressed as No. (%).

From this large cohort of patients three groups of patients that represented a low level, a normal or average level and a high level of γ' were selected: all patients who possessed low (1-7 % (~3 %), n = 41), normal (9-11 % (~10 %), n = 45) and high (22-40 % (~30 %), n = 33) fibrinogen γ' levels, all with fibrinogen levels between 2.3-4.0 $g.L^{-1}$ were chosen (Table 4, Figure 18A-C). These samples were then analysed by confocal microscopy and turbidity and lysis assays.

Table 4 Fibrinogen γ' level groups.

	Low (n=41)		Normal (n=45)		High (n=33)	
Fibrinogen γ' ($mg.L^{-1}$)	110	(26)	327	(45)	940	(117)
Total fibrinogen ($g.L^{-1}$)	3.3	(0.2)	3.3	(0.4)	3.2	(0.4)
Fibrinogen γ' %	3.4	(0.8)	10.0	(0.6)	28.7	(5.0)

Data shown as mean (SD)

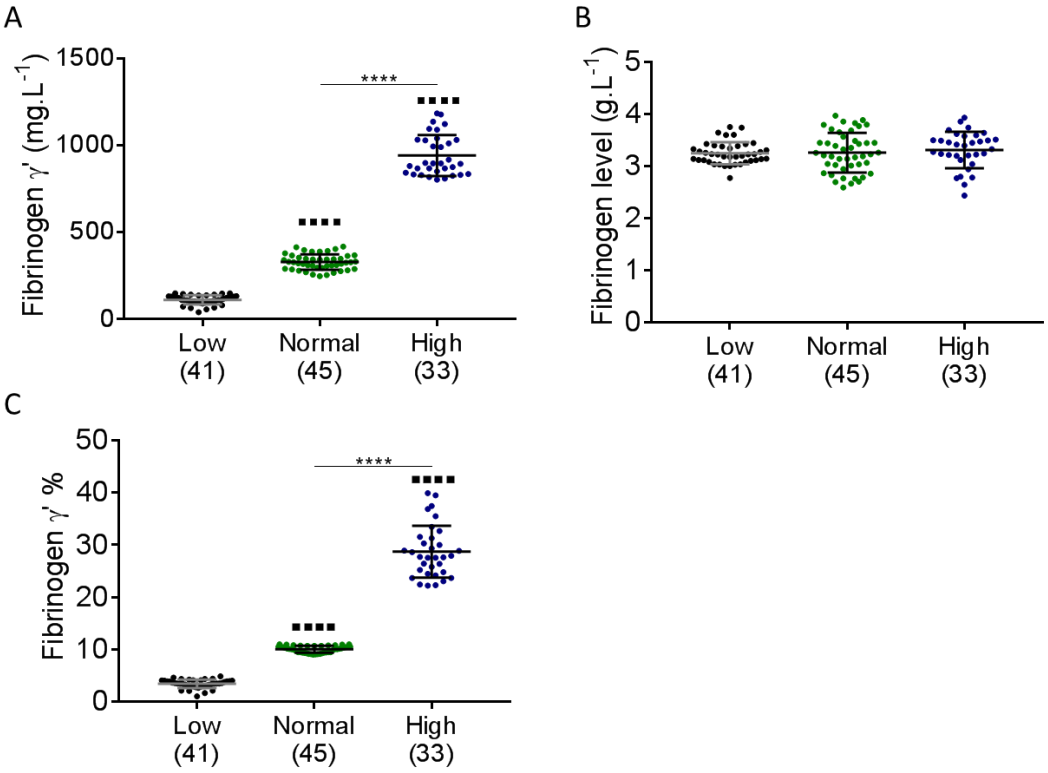

Figure 18 Selection of fibrinogen γ' level groups. Three groups of patient samples were selected with low, normal and high fibrinogen γ' levels. **A,** Fibrinogen γ' levels. **B,** Total fibrinogen levels. **C,** Fibrinogen γ' %. n = 1164. ▪ represents difference from 1st column, * represents difference between other columns. **** or ▪▪▪▪ $p < 0.0001$. Data presented as mean ± SD.

The demographic and clinical characteristics of the three groups are represented in Table 5. No statistically significant differences were found in any of the basic demographical or clinical characteristics between the three groups.

Table 5 Demographic and clinical characteristics of the low, normal and high fibrinogen γ' level groups.

	Low (n=41)	Normal (n=45)	High (n=33)	p value
Age (years)†	72.6 (8.0)	68.9 (7.9)	70.2 (7.4)	0.085
BMI ($Kg.m^{-2}$) †	27.5 (3.6)	28.6 (4.1)	27.4 (3.9)	0.341
Female§	3 (7.3 %)	4 (8.9 %)	8 (24.2 %)	0.059
MI§	7 (17.1 %)	10 (22.2 %)	6 (18.2 %)	0.817
PVD§	7 (17.1 %)	10 (22.2 %)	6 (18.2 %)	0.817
CVA/TIA§	5 (12.2 %)	3 (6.7 %)	8 (24.2 %)	0.077
DVT§	2 (4.9 %)	2 (4.4 %)	1 (3.0 %)	0.920
PE§	1 (2.4 %)	2 (4.4 %)	0 (0.0 %)	0.465
DM§	6 (14.6 %)	5 (11.1 %)	3 (9.1 %)	0.752
Current smoker§	7 (17.1 %)	10 (23.3 %)	7 (21.2 %)	0.777
Ever smoker§	31 (77.5 %)	36 (80.0 %)	26 (78.8 %)	0.961
Aspirin§	24 (58.5 %)	27 (60.0 %)	17 (51.5 %)	0.737
Statins§	27 (65.9 %)	27 (60.0 %)	19 (57.6 %)	0.747
Warfarin§	1 (2.4 %)	0 (0.0 %)	0 (0.0 %)	0.383

BMI – Body mass index, MI – Myocardial infarction, PVD – Peripheral vascular disease, CVA/TIA – Cerebrovascular accident/transient ischemic attack, DVT – Deep vein thrombosis, PE – Pulmonary embolism, DM – Diabetes mellitus

† - Mean (± standard deviation)

§ - n (%)

The clot structure of the three patient groups were then compared to the clot structure of clots produced with purified fibrinogens with and without FXIII, and a repleted plasma system with the same fibrinogen γ' ratios. Differences in clot structure were analysed by confocal microscopy. Clots were produced in the presence of fluorescently labelled fibrinogen and the density of clots was calculated. No differences in clot structure or density were found between different fibrinogen γ' % in a purified system in the absence of FXIII (Figure 19A-B). However, when FXIII was added there was a significant increase in clot density as γ' % increased (Low – 5.86 ± 0.51, Normal – 9.69 ± 0.71, High – 12.01 ± 0.98 fibres/100 μm). This pattern was also seen in the repleted plasma (Low – 39.00 ± 2.45, Normal – 41.53 ± 1.76, High – 44.20 ± 2.10 fibres/100 μm, $p = 0.0027$) and the patient plasma (Low –33.48 ± 4.57, Normal – 35.41 ± 4.11, High –38.21 ± 3.22 fibres/100 μm, $p < 0.0001$) (Figure 19A-B). These data show that the ratio of γA/γ' to γA/γA fibrinogen plays an important role in clot structure, and that an increase in γA/γ' % in patient plasma may lead to the formation of a denser clot in the presence of FXIII. These findings agree with previous studies that showed that clots produced with 100 % fibrinogen γA/γ' were denser than those made with 100 % γA/γA (Cooper et al., 2003, Siebenlist et al., 2005), even though these earlier studies were performed in the absence of FXIII. The findings were backed up by permeation assays performed on the patient plasma, showing a similar trend, with permeability decreasing as the percentage of fibrinogen γ' increased ($p = 0.0022$, Figure 19C).

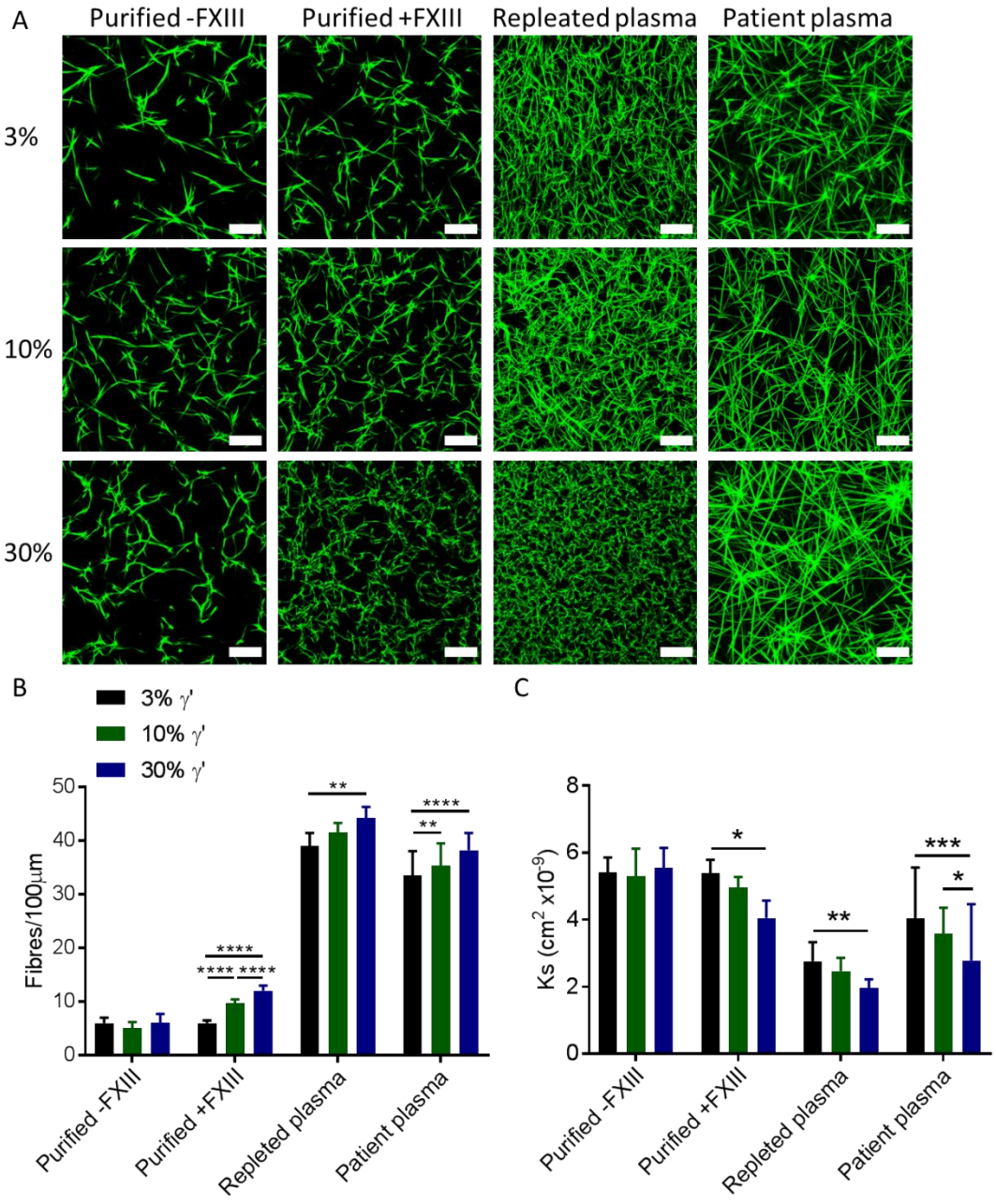

Figure 19 Changes in clot structure with increasing fibrinogen γ' %. A, Clots were formed with 3, 10 and 30 % fibrinogen γ' in a purified system with (n = 3) or without FXIII (n = 3), in repleted plasma (n = 9) or in patient samples (Low n = 41, Normal n = 45, High n = 33) with these fibrinogen γ' percentages. Clots were spiked with fluorescently labelled γA/γA and γA/γ' and viewed by LSCM. Scale bar - 25μm. **B,** Clot density was quantified by calculating the number of fibres per 100μm. **C,** Permeation assays were carried out to calculate porosity of clots (Ks cm^2 $x10^{-9}$). * $p < 0.05$, ** $p < 0.01$, *** $p < 0.001$, **** $p < 0.0001$. Data presented as mean ± SD. One way ANOVA.

The effects of fibrinogen γ' percentage on clot formation were further explored using turbidity assays. Clots were produced in wells of a 96-well plate with 3, 10 or 30 % fibrinogen γ' in a purified system with or without FXIII, in repleted plasma or in patient plasmas. Clot formation was initiated with 0.5 $U.ml^{-1}$ thrombin, and clot formation was followed by measuring the absorbance of the clot at 340 nm wavelength (Figure 20A-D).

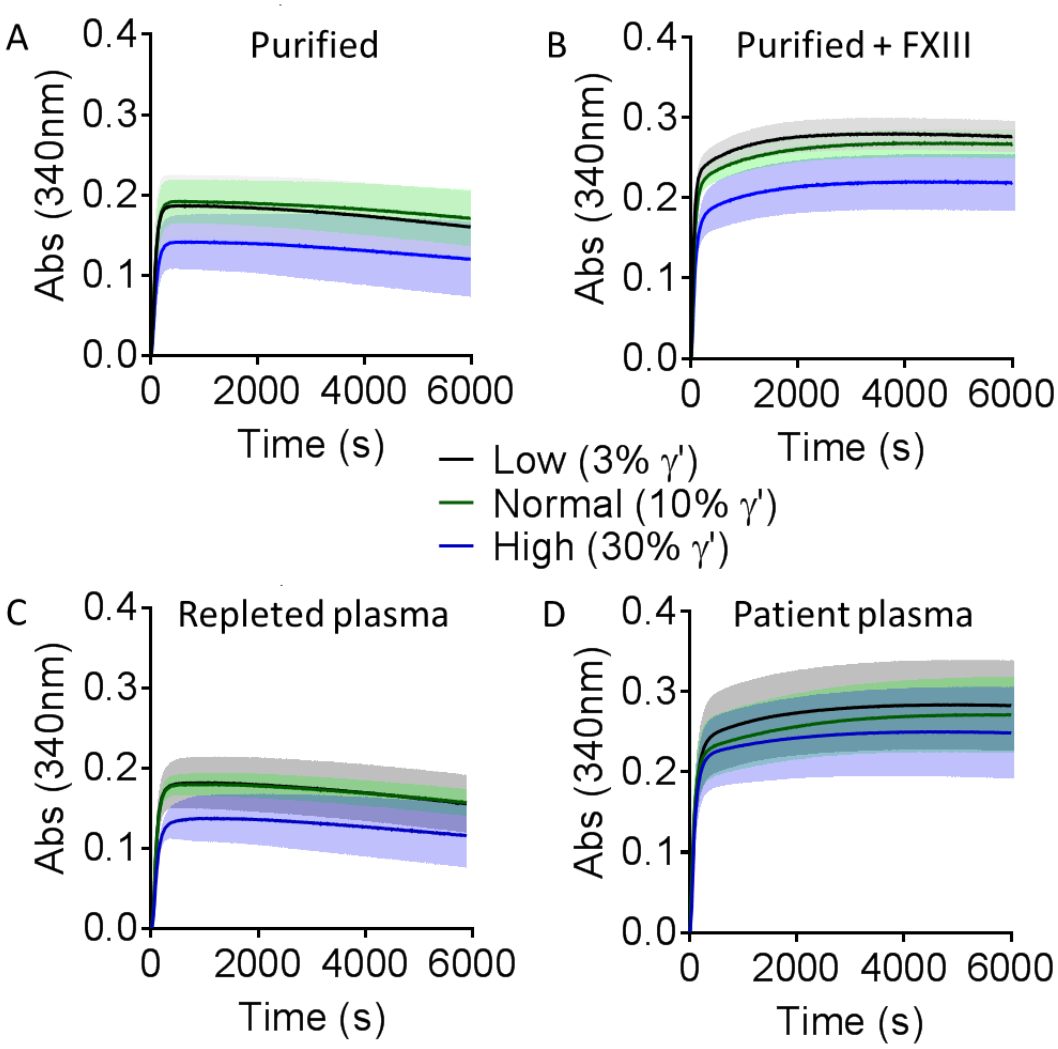

Figure 20 Clot formation curves with increasing fibrinogen γ' %. Clot formation was followed over time in clots formed with 3, 10 and 30 % fibrinogen γ' in a purified system with or without FXIII, in repleted plasma or in patient samples with these fibrinogen γ' percentages using the turbidity assay. The effects of γ' % on clot formation was followed in **A,** a purified system, n = 3, **B,** a purified system in the presence of FXIII, n = 3, **C,** repleted plasma, n = 9 **D,** patient plasma, Low n = 41, Normal n = 45, High n = 33. Abs – absorbance.

From these curves a number of clot formation parameters were calculated. In a purified system Max OD was found to decrease with increasing fibrinogen γ' percentage both with and without FXIII. This was also seen in repleted plasma and in the patient samples (Figure 21A, Table 6). These data suggest that an increase in fibrinogen γ' percentage leads to clots with thinner fibres, which is in agreement with previous studies that have shown clots made with 100 % fibrinogen γA/γ' have thinner fibres than clots formed from 100 % γA/γA (Cooper et al., 2003, Siebenlist et al., 2005). No differences in time to Max OD were seen in the purified, repleted plasma or patient plasma experiments (Figure 21B, Table 6). Time to Max OD was much shorter with experiments in purified fibrinogen without FXIII and the repleted plasma experiments. In the graphs in Figure 20A and Figure 20C the curves can be seen to rapidly increase up to a maximum but then begin to gradually decrease relatively early in comparison to the curves in Figure 20B and Figure 20D. This could be due to the lack of FXIII in the purified experiments, and lower FXIII levels in the fibrinogen depleted plasma as some FXIII will have been lost bound to fibrinogen in the depletion process. This decrease or lack of FXIII would lead to a less stable clot being formed. A decrease in the maximum rate of clotting (turbidity Vmax) with an increase in fibrinogen γ' percentage was found in purified experiments with and without FXIII. This was not the case in repleted plasma and patient samples where no difference in maximum clotting rate was seen as the fibrinogen γ' percentage increased (Figure 21C, Table 6). This may be due to other factors in the plasma playing a role in clot formation, negating the effect of the increase in fibrinogen γ' percentage. There was a decrease in average rate of clotting as fibrinogen γ' percentage increased in the purified

experiments with and without FXIII. However, this was not seen in repleted plasma or patient sample experiments, again further suggesting that other components of plasma negate the effects of fibrinogen γ' on clotting rate (Figure 21D, Table 6). Together, these results show that increases in fibrinogen γ' percentage effect clot structure, forming clots with thinner fibres, but in plasma there is no effect on the rate of clot formation.

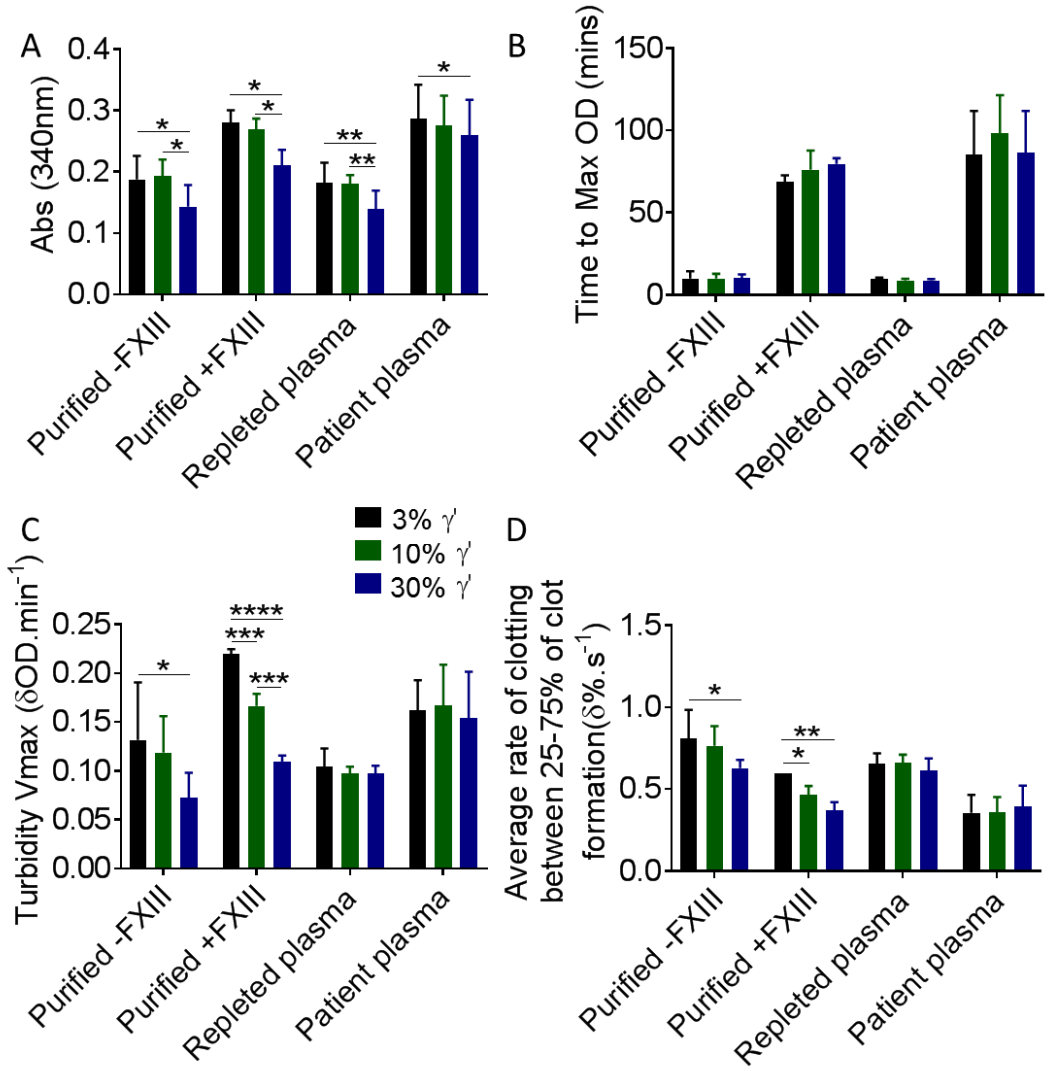

Figure 21 The effects of fibrinogen γ' % on clot formation. The effects of fibrinogen γ' % on clot formation parameters in purified system with (n = 3) and without (n = 3) FXIII, in repleted plasma (n = 9) and patient plasma samples (Low n = 41, Normal n = 45, High n = 33) using the turbidity assay. **A,** Max OD, **B,** time to Max OD, **C,** Turbidity Vmax, **D,** Average rate of clotting between 25-75 % of clot formation. * $p < 0.05$, ** $p < 0.01$, *** $p < 0.001$, **** $p < 0.0001$. Data presented as mean ± SD. One way ANOVA. Abs – absorbance.

Table **6 The effects of fibrinogen γ' % on clot formation.**

	Max OD (Abs 340nm)		p	Time to Max OD (mins)		p	Turbidity Vmax (δOD.min^{-1})		p	Average rate of clotting (δ%.s^{-1})		p
Purified –FXIII												
3% γ'	0.187	(0.039)	0.0096	9.90	(4.45)	0.9962	0.132	(0.059)	0.0188	0.810	(0.174)	0.0140
10% γ'	0.193	(0.028)		9.96	(2.91)		0.119	(0.037)		0.764	(0.120)	
30% γ'	0.143	(0.035)		10.04	(2.41)		0.073	(0.026)		0.628	(0.050)	
Purified +FXIII												
3% γ'	0.280	(0.020)	0.0149	68.57	(4.13)	0.2503	0.219	(0.005)	<0.0001	0.595	(0.014)	0.0017
10% γ'	0.269	(0.018)		76.12	(11.57)		0.166	(0.012)		0.467	(0.052)	
30% γ'	0.211	(0.025)		79.60	(3.41)		0.109	(0.007)		0.372	(0.048)	
Repleted plasma												
3% γ'	0.183	(0.033)	0.0031	9.80	(0.81)	0.0579	0.104	(0.019)	0.4063	0.653	(0.066)	0.2579
10% γ'	0.181	(0.014)		8.73	(1.06)		0.098	(0.007)		0.661	(0.050)	
30% γ'	0.140	(0.030)		8.79	(0.90)		0.097	(0.008)		0.614	(0.074)	
Patient plasma												
3% γ'	0.286	(0.056)	0.0203	85.31	(26.47)	0.0560	0.162	(0.031)	0.4067	0.355	(0.111)	0.2075
10% γ'	0.276	(0.048)		98.08	(23.36)		0.167	(0.042)		0.356	(0.095)	
30% γ'	0.259	(0.058)		86.20	(25.57)		0.154	(0.047)		0.396	(0.126)	

Abs – absorbance, OD – optical density. Data presented as Mean (± standard deviation)

The effects of fibrinogen γ' percentage on clot breakdown were also explored using the turbidity assay. Clots were produced in the same way as described for clot formation assays. In the purified experiments, both tPA (85 ng.ml^{-1}) and plasminogen (25μg.ml^{-1}) were added to the clotting mixture, while in repleted plasma or patient plasma experiments just tPA (85 ng.ml^{-1}) was added at the beginning of the experiments to induce lysis. Clot formation was initiated with 0.5 U.ml^{-1} thrombin, and clot formation and breakdown was followed by measuring the absorbance of the clot at 340 nm (Figure 22A-D).

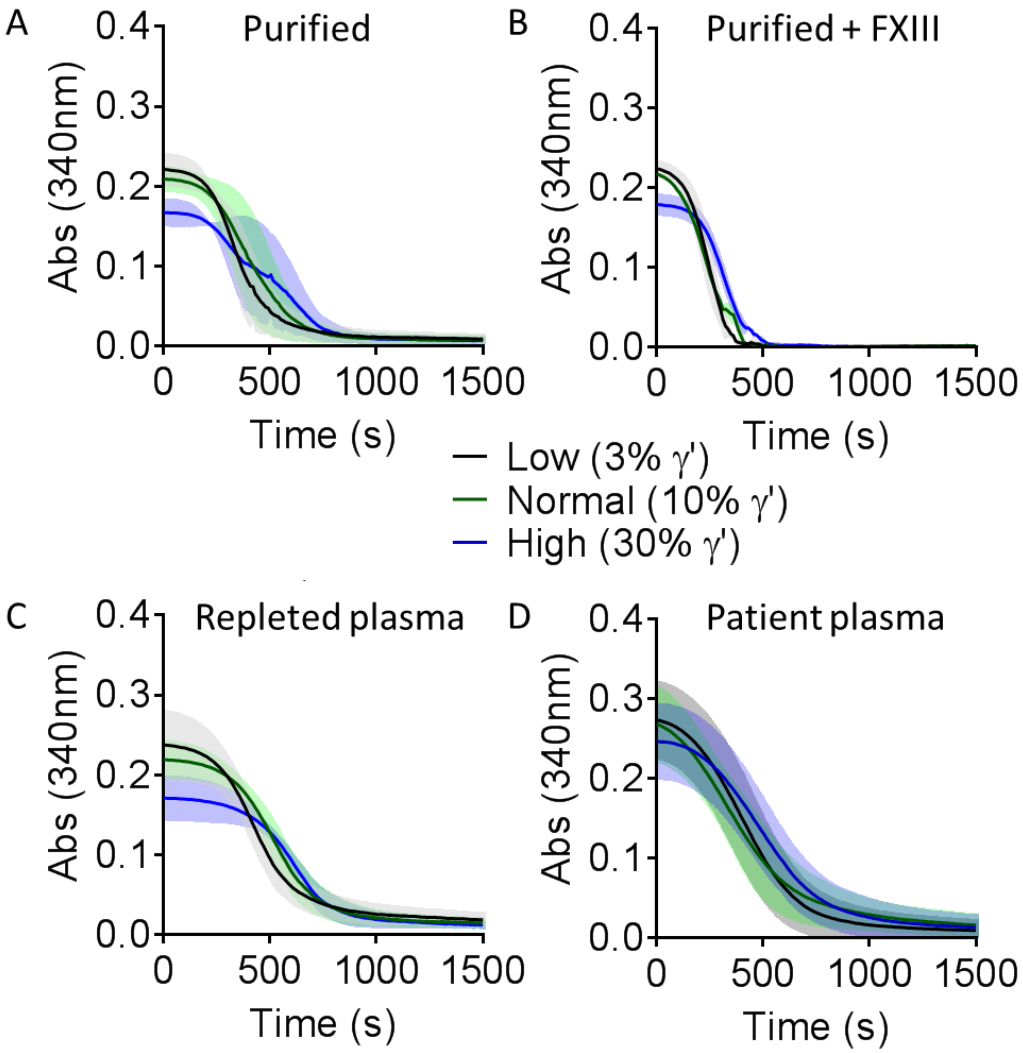

Figure 22 Clot breakdown curves with increasing fibrinogen γ' %. Clot breakdown was followed over time in clots formed with 3, 10 and 30 % fibrinogen γ' in a purified system with or without FXIII, in repleted plasma or in patient samples with these fibrinogen γ' percentages using the turbidity assay. The effects of γ' % on clot breakdown was followed in **A,** a purified system, n = 3, **B,** a purified system in the presence of FXIII, n = 3, **C,** repleted plasma, n = 9 **D,** patient plasma, Low n = 41, Normal n = 45, High n = 33. Abs – absorbance.

A number of clot breakdown parameters were calculated from the lysis curves. Both time to 50 % lysis and 75 % lysis were found to increase with increasing γ' percentage in a purified system with and without FXIII and repleted plasma experiments. In the patient samples as γ' percentage increased there appeared to be no difference in time to 50 % lysis, while time to 75 % lysis was increased (Figure 23A, Table 7). These data suggest

that an increase in fibrinogen γ' percentage leads to an increase in lysis time, in agreement with previous studies that show fibrinogen γA/γ' has longer lysis times than γA/γA, and that an increase in fibrinogen γA/γ' levels caused a delay in clot lysis (Siebenlist et al., 2005, Kim et al., 2014, Falls and Farrell, 1997, Pieters et al., 2013). No significant differences in maximum lysis rate or average lysis rate were seen in purified experiments without FXIII, reflecting the lack of change in clot structure in the absence of FXIII. A significant decrease in maximum lysis rate and average lysis rate were seen in purified experiments with FXIII and repleted plasma. However, only maximum lysis rate was effected in patient samples as γ' percentage increased (Figure 23C-D, Table 7). These data suggest that other factors (thrombin concentration, FXIII levels etc.) within the plasma may negate or lessen some of the effects of increasing γ' levels.

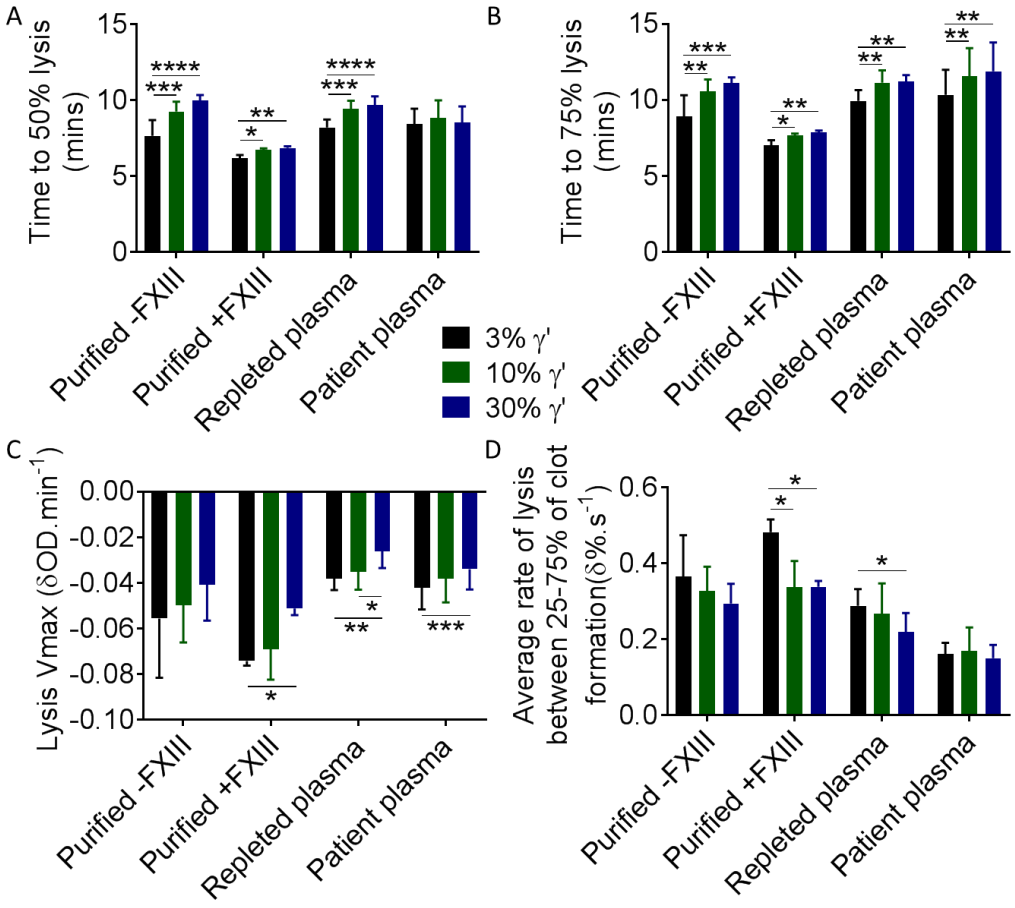

Figure 23 The effects of fibrinogen γ' % on clot breakdown. The effects of fibrinogen γ' % on clot breakdown parameters in purified system with (n = 3) and without (n = 3) FXIII, in repleted plasma (n = 9) and patient plasma samples (Low n = 41, Normal n = 45, High n = 33) using the turbidity and lysis assay. **A,** Time to 50 % lysis, **B,** time to 75 % lysis, **C,** Lysis Vmax, **D,** Average rate of lysis between 25-75 % of clot formation. * $p < 0.05$, ** $p < 0.01$, *** $p < 0.001$, **** $p < 0.0001$. Data presented as mean ± SD. One way ANOVA.

Table 7 The effects of fibrinogen γ' % on clot breakdown.

	Time to 50% lysis (mins)	p	Time to 75% lysis (mins)	p	Lysis Vmax (δOD.min-1)	p	Average rate of lysis (δ%.s-1)	p
Purified -FXIII								
3% γ'	7.67 (1.04)	<0.0001	8.91 (1.39)	0.0001	-0.056 (0.026)	0.2985	0.365 (0.109)	0.1869
10% γ'	9.27 (0.66)		10.56 (0.79)		-0.050 (0.016)		0.328 (0.064)	
30% γ'	10.00 (0.36)		11.11 (0.38)		-0.041 (0.016)		0.294 (0.052)	
Purified +FXIII								
3% γ'	6.20 (0.20)	0.0035	7.47 (0.23)	0.0351	-0.074 (0.002)	0.0288	0.482 (0.033)	0.0115
10% γ'	6.73 (0.12)		7.67 (0.16)		-0.069 (0.014)		0.337 (0.069)	
30% γ'	6.87 (0.15)		7.87 (0.12)		-0.051 (0.003)		0.338 (0.015)	
Repleted plasma								
3% γ'	8.22 (0.52)	<0.0001	9.93 (0.72)	0.0005	-0.038 (0.005)	0.0029	0.288 (0.044)	0.0188
10% γ'	9.44 (0.54)		11.13 (0.81)		-0.035 (0.008)		0.267 (0.080)	
30% γ'	9.69 (0.58)		11.22 (0.41)		-0.026 (0.007)		0.208 (0.041)	
Patient plasma								
3% γ'	8.43 (1.02)	0.1814	10.33 (1.65)	0.0006	-0.042 (0.010)	0.0003	0.162 (0.029)	0.1786
10% γ'	8.85 (1.16)		11.54 (1.86)		-0.038 (0.011)		0.170 (0.061)	
30% γ'	8.55 (1.05)		11.88 (1.89)		-0.034 (0.009)		0.150 (0.035)	

OD – optical density. Data presented as Mean (± standard deviation)

3.1.2 The effects of γ' in whole blood clot viscoelasticity

From the 1164 patients that had γ' levels measured, a subset of 78 patients had ROTEM analysis carried out on their whole blood and the relationship between γ' levels and ROTEM outputs were investigated. The demographic for this group of patients can be seen below in Table 8.

Table 8 Demographic of ROTEM analysed patients.

	Patient samples (n = 78)
Age (years) †	69.69 (6.68)
Female ¥	5 (6.4%)
BMI ($Kg.m^{-2}$) †	28.7 (4.2)
Waist:hip ratio §	0.96 (0.92-1.01)
Current smoker ¥	22 (28.2%)
Ever smokers ¥	64 (82.1%)
Alcohol, units/week §	10 (1-25)
Angina ¥	17 (21.8%)
MI ¥	14 (17.9%)
CVA/TIA ¥	11 (14.1%)
Hypertension ¥	55 (70.5%)
Statins ¥	68 (87.2%)
Aspirin ¥	63 (80.8%)
Fibrinogen ($g.L^{-1}$) §	3.45 (3.14-4.01)
Fibrinogen γ' ($mg.L^{-1}$) §	290 (180-410)
Fibrinogen γ' (%) §	7.01 (4.81-11.77)

BMI – Body mass index
† - Mean (±SD), § - Median (IQR), ¥ - n (%)

Three hundred microliters of whole blood from each patient was combined with 20 µl of either ex-tem or in-tem reagent (tissue factor) and 20 µl of star-tem reagent (calcium) and the viscoelastic properties of clot formation were followed over time using the ROTEM delta. Parameters from these measurements were correlated with fibrinogen level, fibrinogen γ' level and fibrinogen γ' % (Table 9).

Table 9 Correlation of ROTEM parameters with γ' levels and γ' %.

	Ex-tem		In-tem	
	r	p value	r	p value
Fibrinogen level (g.L^{-1})				
Lag time (s)	0.1916	0.0929	0.1860	0.1054
CR between end of lag time and 25% clotting (%.s^{-1})	0.1621	0.1562	-0.0328	0.7768
CR between 25 and 50% clotting (%.s^{-1})	0.0919	0.4234	0.0107	0.9267
MCF (mm)	**0.2772**	**0.0140**	**0.2314**	**0.0473**
Time to MCF (s)	-0.0905	0.4308	0.0928	0.4219
Maximum rate of clotting (mm.min^{-1})	0.2100	0.0650	0.0877	0.4482
Time to maximum rate of clotting (s)	-0.0565	0.6234	0.1279	0.2676
Average rate of clotting (%.s^{-1})	0.1681	0.1414	0.0145	0.9006
Fibrinogen γ' levels (mg.L^{-1})				
Lag time (s)	**-0.2306**	**0.0423**	0.0570	0.6223
CR between end of lag time and 25% clotting (%.s^{-1})	**0.2705**	**0.0166**	-0.1857	0.1058
CR between 25 and 50% clotting (%.s^{-1})	0.1650	0.1489	-0.2081	0.0693
MCF (mm)	0.2225	0.0502	0.1078	0.3505
Time to MCF (s)	-0.1104	0.3358	-0.1166	0.3124
Maximum rate of clotting (mm.min^{-1})	**0.3197**	**0.0043**	0.1939	0.0911
Time to maximum rate of clotting (s)	**-0.2721**	**0.0160**	0.0789	0.4954
Average rate of clotting (%.s^{-1})	0.1587	0.1652	-0.1849	0.1074
Fibrinogen γ' %				
Lag time (s)	**-0.2539**	**0.0249**	0.0015	0.9896
CR between end of lag time and 25% clotting (%.s^{-1})	**0.2294**	**0.0433**	-0.1921	0.0942
CR between 25 and 50% clotting (%.s^{-1})	0.1486	0.1941	-0.2203	0.0542
MCF (mm)	0.1247	0.2768	0.1122	0.3313
Time to MCF (s)	-0.1332	0.2451	-0.1582	0.1695
Maximum rate of clotting (mm.min^{-1})	**0.2476**	**0.0289**	0.1879	0.1017
Time to maximum rate of clotting (s)	**-0.2667**	**0.0183**	0.0375	0.7459
Average rate of clotting (%.min^{-1})	0.1324	0.2480	-0.1987	0.0832

MCF – maximum clot firmness, CR – clotting rate, Spearman correlation

Fibrinogen levels correlated with MCF when clotting was initiated with ex-tem (r = 0.2772, p = 0.014) or in-tem (r = 0.2314, p = 0.0473). This was expected as previous studies have shown that an increase in fibrinogen levels leads to an increase in clot strength (Harr et al., 2013, Rourke et al., 2012). When clotting was initiated with the ex-tem reagent fibrinogen γ' levels and γ' % were both found to negatively correlate with lag time (Figure 24A-B) and positively correlate with the clotting rate between end of lag time and 25 % clotting (Figure 24C-D), but not with the clotting rate between 25

and 50 % clotting (Figure 24E-F). This indicates that in whole blood higher levels of γ' fibrinogen may lead to a faster onset of clotting and more rapid clot formation in the early stages, but this increase in rate does not propagate through to later points of clot formation as there was no change in the time to MCF as γ' levels increased (Table 9). Fibrinogen γ' levels and γ' % were also found to positively correlate with the maximum clotting rates (Figure 25A-B) and negatively with the time taken to reach the maximum clotting rate (Figure 25C-D), but not with the average rate of clotting (Figure 25E-F). This further suggests that γ' is playing a role in the early stages of clotting, with increasing levels of γ' leading to higher maximum clotting rates and these maximum rates being reached more quickly. However, this increase in clotting rate does not continue as there was no relationship between average clotting rates and γ' levels.

When clotting was initiated with the in-tem reagent no correlations were seen apart from with MCF with fibrinogen levels. This suggests that in whole blood fibrinogen γ' is only having an effect on the extrinsic pathway and not on the intrinsic pathway.

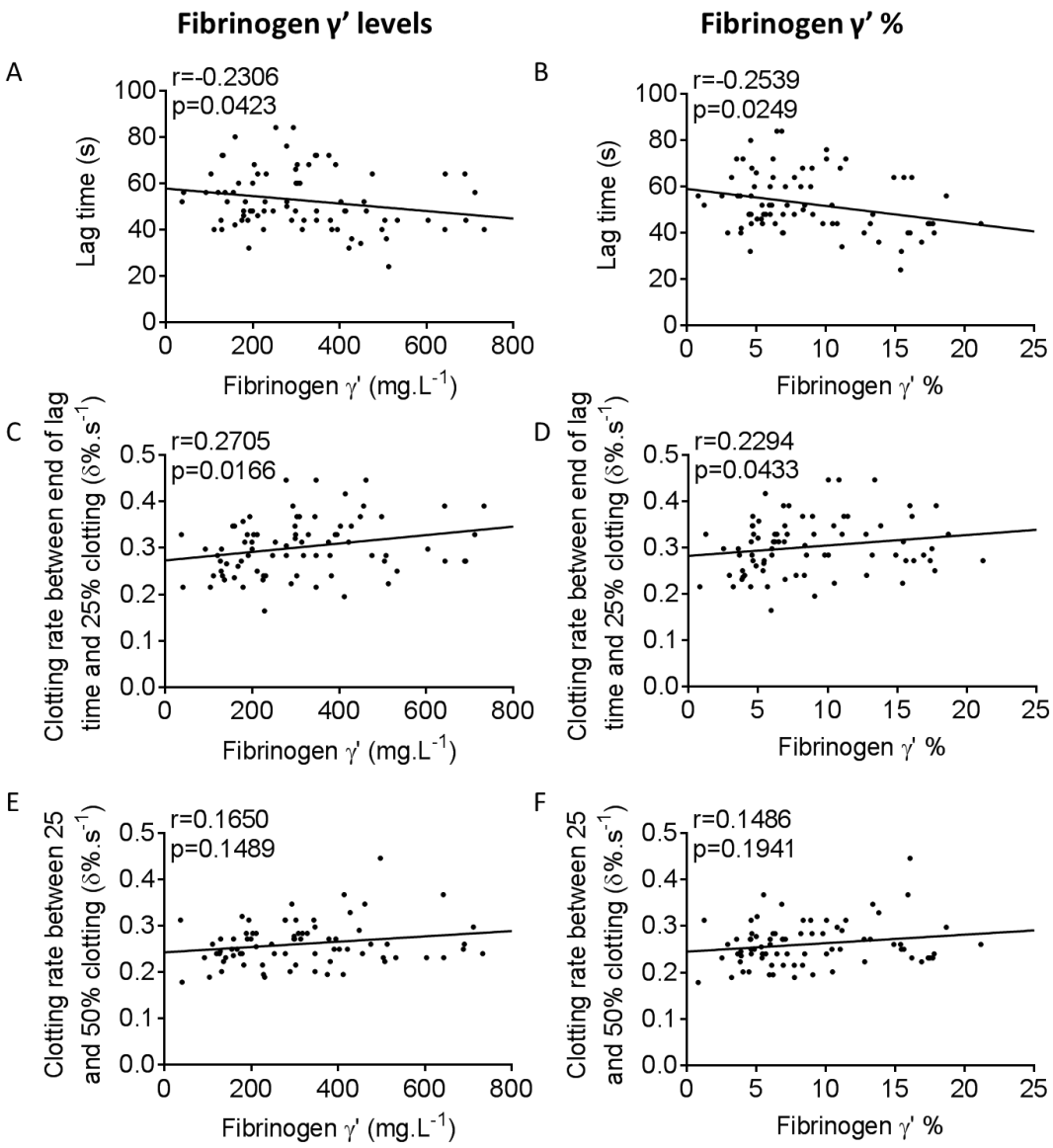

Figure 24 Ex-tem ROTEM analysis of the effects of fibrinogen γ' levels and γ' % on early clotting. The effects of fibrinogen γ' level and γ' % on the initial stages of clotting were assessed when clotting was initiated with EXTEM using ROTEM (n = 78). **A,C,E** Fibrinogen γ' levels correlated with **A,** lag time, **C,** Clotting rate between end of lag time and 25 % clotting **E,** Clotting rate between 25 and 50 % clotting. **B, D, F** Fibrinogen γ' % correlated with **B,** lag time, **D,** Clotting rate between end of lag time and 25 % clotting **F,** Clotting rate between 25 and 50 % clotting. Spearman's rank correlation.

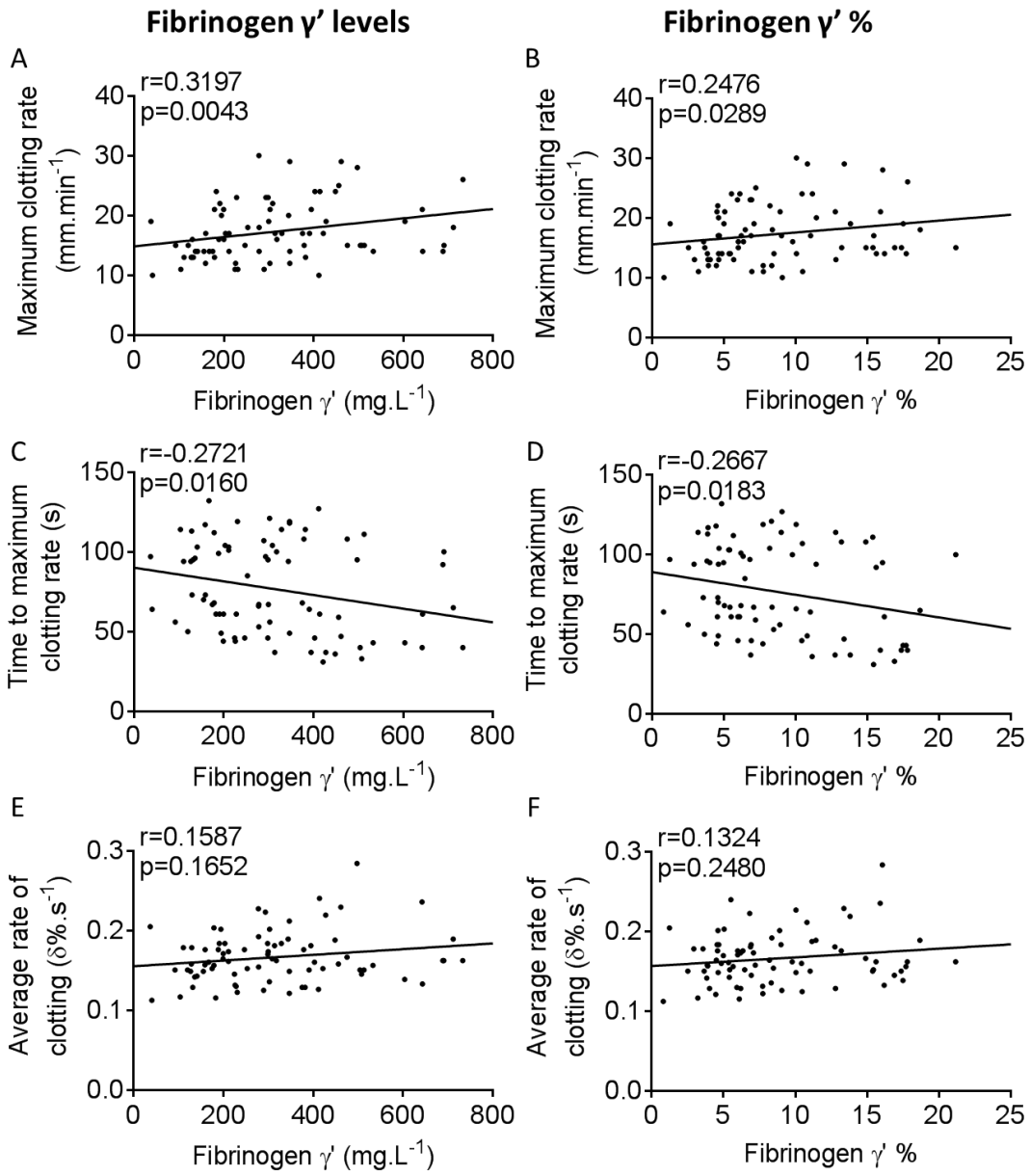

Figure 25 Ex-tem ROTEM analysis of the effects of fibrinogen γ' levels and γ' % on clotting rates. The effects of fibrinogen γ' level and γ' % on clotting rates were assessed when clotting was initiated with EXTEM using ROTEM. (n = 78). **A,C,E** Fibrinogen γ' levels correlated with **A,** Maximum clotting rate, **C,** Time to maximum clotting rate **E,** Average clotting rate. **B, D, F** Fibrinogen γ' % correlated with **B,** Maximum clotting rate, **D,** Time to maximum clotting rate **F,** Average clotting rate. Spearman's rank correlation.

3.2 Fibrinogen γ' under flow

The majority of research into the effects of fibrinogen γ' on clot structure have been done in static conditions, with only a couple of papers investigating the role of γ' and its thrombin binding abilities under flow conditions (Muthard et al., 2015, Zhu et al., 2018). Due to previous links of fibrinogen γ' levels with both venous and arterial thrombosis, its effects on clot structure under flow conditions could help to explain this link and provide a mechanism for its role in thrombosis.

3.2.1 Fibrinogen γ' under venous and arterial flow rates

The effects of venous and arterial flow rates on clot formation with γA/γA and γA/γ' fibrinogen was investigated using a two-step model in a microfluidic chamber in collaboration with Prof. Johan Heemskerk, Dr Frauke Swieringa and Dr Constance Baaten at the University of Maastricht. Initially, anticoagulated whole blood was perfused through a flow chamber that contained microspots of collagen and tissue factor at a shear rate of 1000 s^{-1}. This led to the formation of platelet thrombi on the microspots. Fibrinogen deficient plasma was repleted with purified and fluorescent γA/γA or γA/γ', re-calcified, and then immediately perfused over the preformed thrombi at either 150 s^{-1} or 500 s^{-1}. Fibrin formation around the platelet thrombi was followed by time series confocal fluorescent imaging and quantified by fluorescence accumulation (Figure 26).

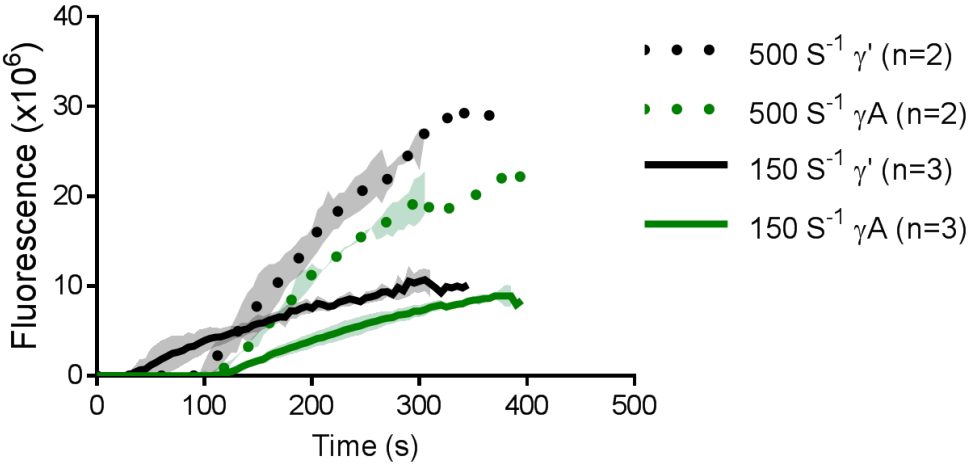

Figure 26 The effects of γA/γA and γA/γ' on fibrin accumulation under venous and arterial flow. γA/γA or γA/γ' fibrinogen repleted plasma was perfused over platelet thrombi at 150 s^{-1} 500 s^{-1}, and fibrin accumulation was quantified by fluorescence over time.

The time to the first fibrin deposition, or lag time, of fibrinogen γA/γ' at a flow rate of 150 s^{-1} was found to be significantly shorter than γA/γA at 150 s^{-1} and 500 s^{-1} and γA/γ' at 500 s^{-1}. Fibrin deposition was seen after just 42 s ±14 with γA/γ' at 150 s^{-1}, but not until 118 s ± 10 and 101 s ± 16 with γA/γA at 150 s^{-1} and 500 s^{-1} respectively, and 100 s ± 8 with γA/γ' at 500 s^{-1} ($p = 0.0013$) (Figure 27A). The average rate of fibrin deposition was significantly slower at 500 s^{-1} than 150 s^{-1}, but no difference in the average rate of fibrin deposition was seen between γA/γA and γA/γ' at either flow rate (Figure 27B). Maximum fibrin deposition, or maximum fluorescence, was significantly higher at 500 s^{-1} than at 150 s^{-1}, and at both 150 s^{-1} and 500 s^{-1}, maximum fibrin deposition was found to be significantly higher with γA/γ' (150 s^{-1} - 11.5 ± 1.1 x10^6, 500 s^{-1} - 28.8 ± 1.4 x10^6) than γA/γA (150 s^{-1} - 9.2 ± 0.8 x10^6, 500 s^{-1} - 22.8 ± 0.7 x10^6, $p < 0.0001$)(Figure 27C). At 150 s^{-1}, γA/γ' reached maximum fluorescence more quickly than γA/γA fibrinogen (γA/γ' – 4.62 ± 0.82 mins, γA/γA – 6.68 ± 0.66 mins, $p = 0.0274$), but no

difference in the time taken to reach maximum fibrin deposition was seen at 500 s^{-1} (Figure 27D). These data suggest that at venous flow rates γA/γ' fibrinogen may lead to faster deposition of fibrin, and at both venous and arterial flow rates γA/γ' fibrinogen leads to a greater deposition of fibrin around platelet thrombi.

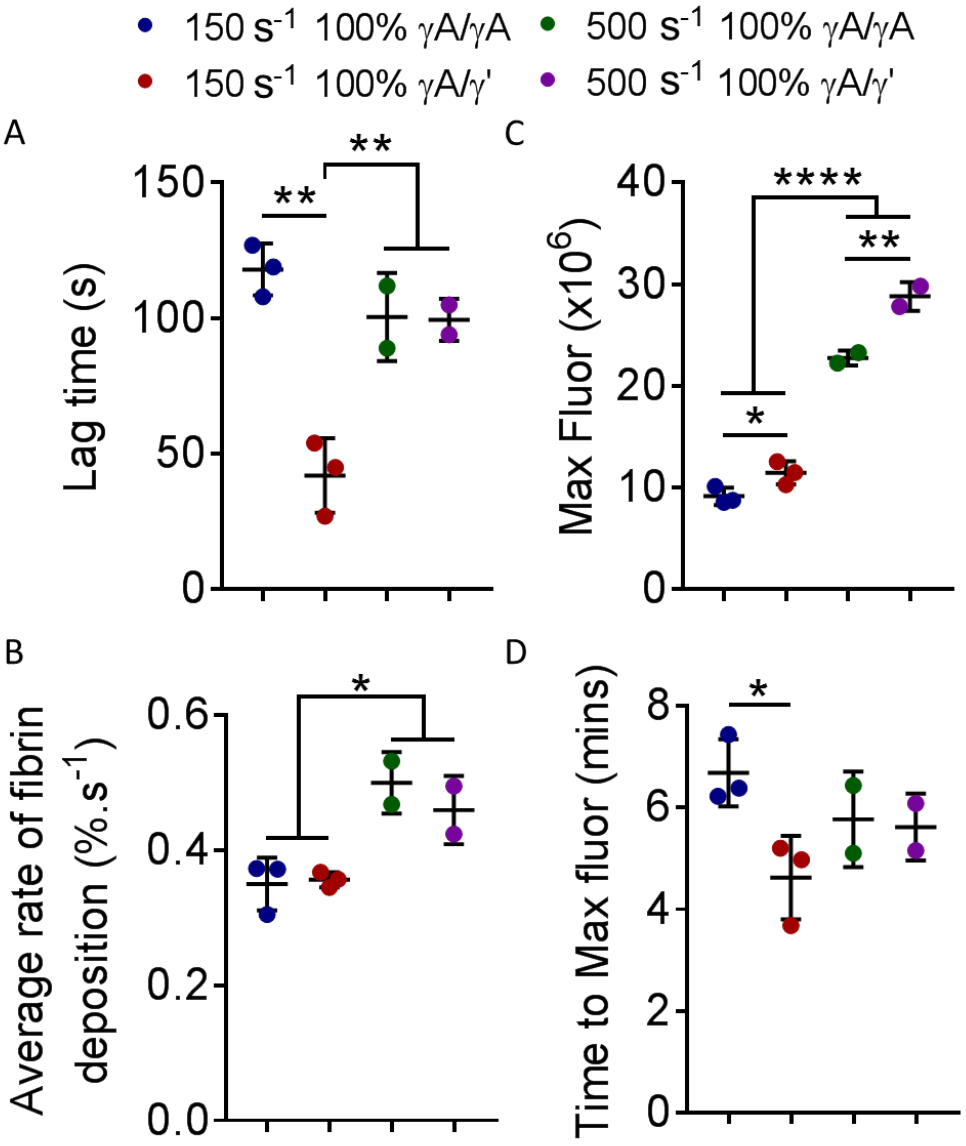

Figure 27 Differences in fibrin deposition between γA/γA and γA/γ' fibrinogen at arterial and venous flow rates. From the accumulation of fluorescence data a number of parameters were compared between γA/γA and γA/γ' fibrinogen. **A,** lag time, **B,** Average rate of fibrin deposition, **C,** Maximum fluorescence, **D,** Time to maximum fluorescence. * $p < 0.05$, ** $p < 0.01$. Data presented as mean ± SD. One-way ANOVA. Fluor – fluorescence.

At the end of each experiment, a number of endpoint Z-stacks were taken at random points around each microspot to assess differences in endpoint clot formation. Volume and height of the clots were measured and images were depth coded for visual representation.

When the clots were visualised by depth coding clear differences were observed between γA/γ' and γA/γA clots. The γA/γ' clots were much taller (Figure 28A) and appeared to have a greater volume at 150 s^{-1} than clots formed from γA/γA fibrinogen, with γA/γA clots appearing more fibrous (Figure 29A). Similar differences were seen at 500 s^{-1}, but with both forms of fibrinogen producing clots with less height and volume (Figure 28B and Figure 29B).

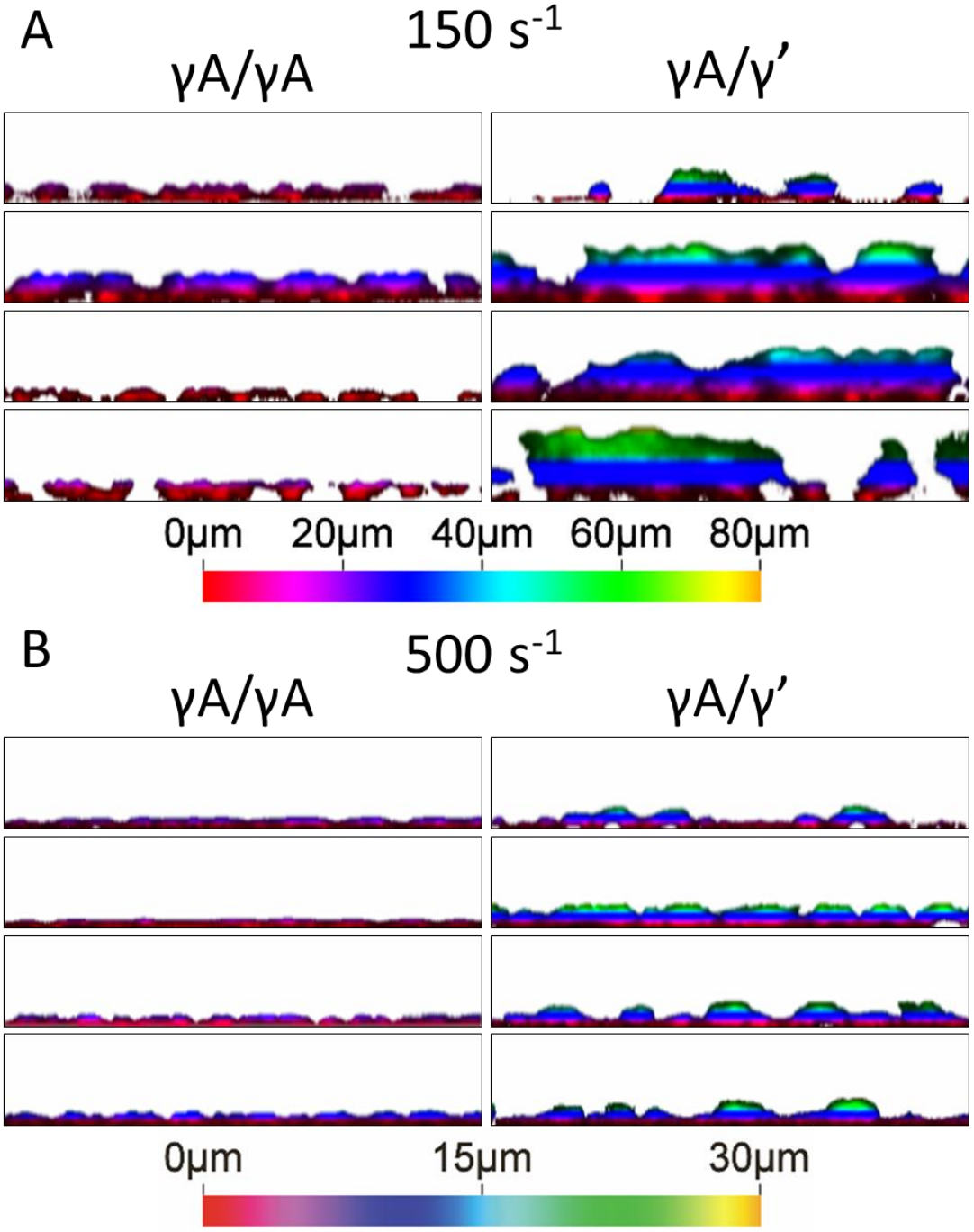

Figure 28 End-point cross-sectional view of depth coded clots formed from γA/γA or γA/γ' at venous and arterial flow rates. Cross sections of depth coded endpoint Z-stacks of clots formed from γA/γA or γA/γ' fibrinogen repleted plasma perfused over platelet thrombi at **A,** 150 s^{-1} and **B,** 500 s^{-1}. Images 90 x 213 μm.

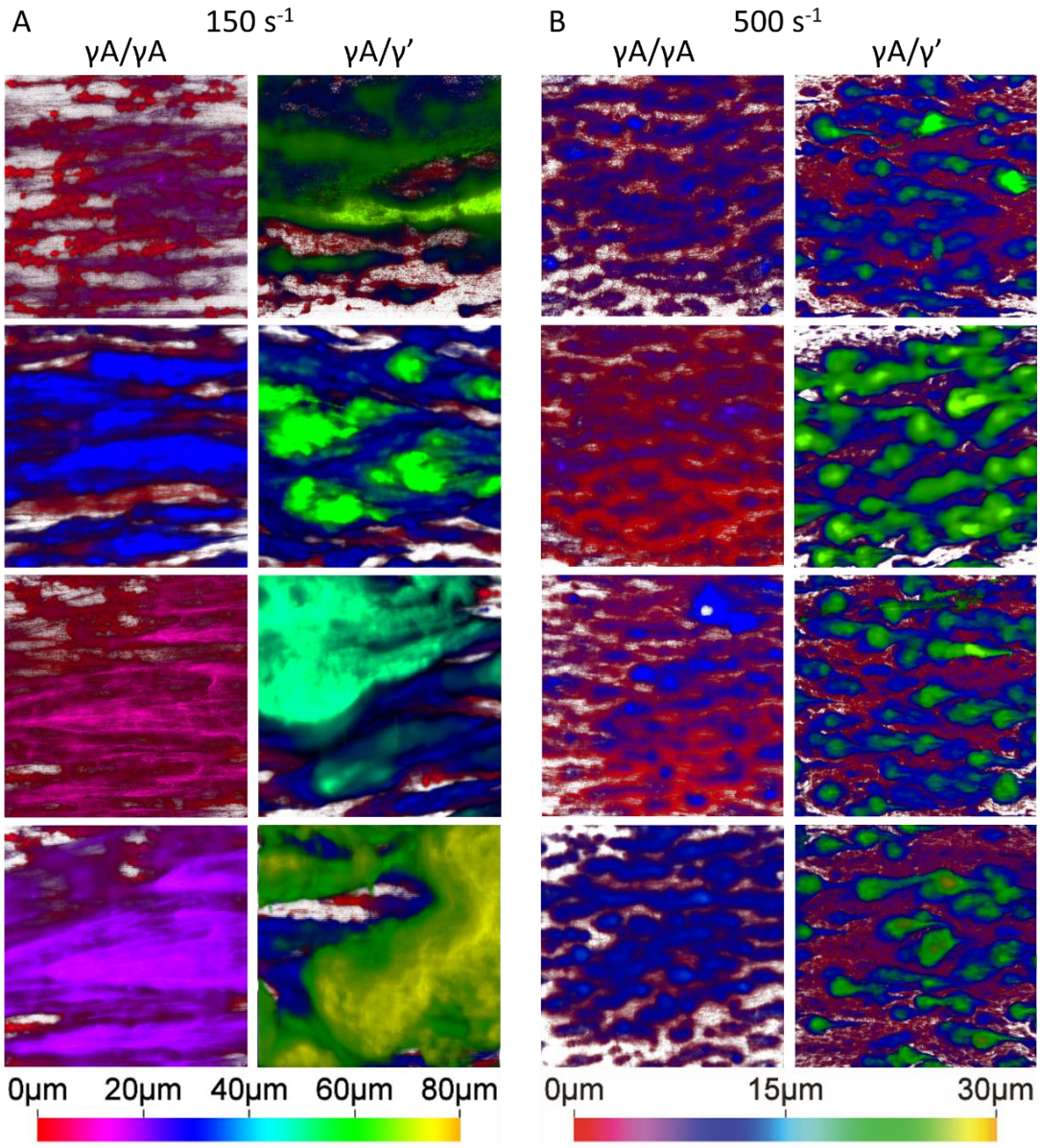

Figure 29 End-point depth coded clots formed from γA/γA or γA/γ' at venous and arterial flow rates from above. Depth coded endpoint Z-stacks of clots formed from γA/γA or γA/γ' fibrinogen repleted plasma perfused over platelet thrombi viewed from above at **A,** 150 s^{-1} and **B,** 500 s^{-1}. Images 213 x 213 μm.

Quantitative analysis of these images confirmed the differences between γA/γA and γA/γ' fibrinogen. The volume of the fibrin clots formed with γA/γ' fibrinogen were found to be greater than clots formed with γA/γA at both 150 s^{-1} (70.21 ± 23.19 μm^3 vs 28.51 ± 10.89 μm^3, $p < 0.0001$) and at 500 s^{-1} (26.64 ± 2.30 vs 17.69 ± 5.07 μm^3, $p < 0.0001$) (Figure 30A). The maximum height of clots formed from γA/γ' were also found to be significantly higher than clots formed with γA/γA at 150 s^{-1} (52.91 ± 14.09 μm^3 vs 26.77 ± 8.96 μm^3) and at 500 s^{-1} (20.95 ± 2.31 vs 11.55 ± 2.43 μm^3, $p < 0.0001$)(Figure 30B). When the volume of fibrin in each slice of the Z-stacks was plotted against the distance of the slice from the slide, the differences between the distribution of fibrin and the heights of the clots can clearly be seen (Figure 30C). Clots formed at 150 s^{-1} are tall and the largest area per slice of fibrin is away from the surface, with a small area of contact with the platelets and the surface. However, clots formed at 500 s^{-1} are more compact with the largest area per slice of fibrin on, or close to the surface, with a larger area of fibrin in contact with the slide. This helps to explain why there is an increase in maximum fluorescence at 500 s^{-1} compared to 150 s^{-1} in time series experiments (Figure 27C), when endpoint images appear to show much greater volumes of fibrin at 150 s^{-1}. Time series experiments were imaged close to the surface, and so analysis of time series experiments were picking up the increased deposition of fibrin on the slide surface at 500 s^{-1}. At 150 s^{-1} γA/γ' appears to increase the height and the distance of the largest area per slice of fibrin from the slide when compared to γA/γA, but at 500 s^{-1} γA/γ' only appears to effect the height of the clots.

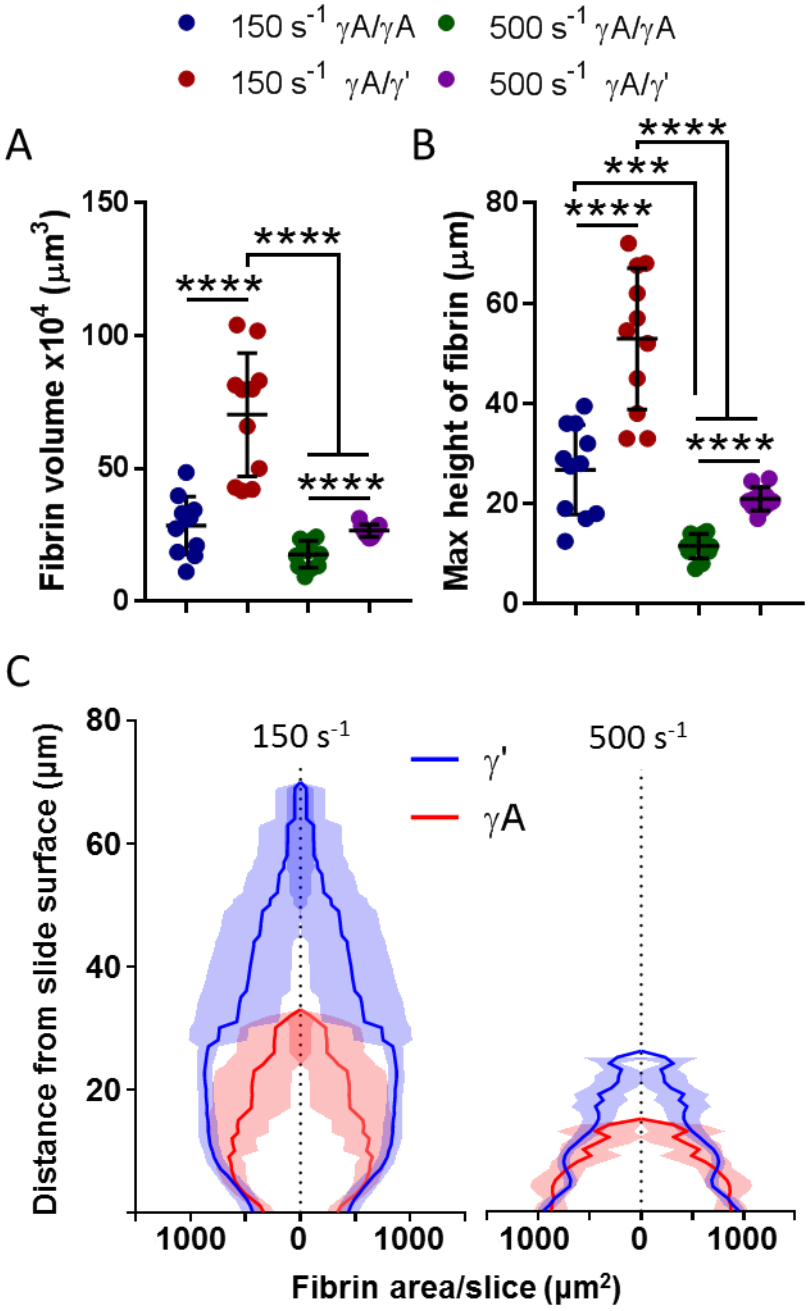

Figure 30 The effects of γA/γ' on clot height and volume at venous and arterial flow rates. Height and total volume of fibrin was calculated from endpoint Z-stacks of clots formed from γA/γA or γA/γ' fibrinogen repleted plasma perfused over platelet thrombi at 150 s^{-1} and 500 s^{-1}. **A,** Total volume of fibrin, **B,** Maximum height of fibrin clot, **C,** Area of fibrin per slice vs distance from the clotting surface.

3.3 Discussion

There is a plethora of studies investigating the role of fibrinogen γ' in clot structure, but the majority of these have used purified proteins, comparing 100 % γA/γ' to 100 % of the wildtype fibrinogen (γA/γA) in static conditions. In this chapter the effects of physiological levels of fibrinogen γ' in plasma and whole blood on clot structure were examined, and how fibrinogen γ' impacts clot structure under flow. Fibrinogen γ' influenced clotting and clot structure in plasma even at physiological levels, with clot density increasing as the level of γ' increased, but only in the presence of FXIII. Clot formation rates appeared to decrease as γ' levels increased, but this was not seen in clots made with plasma samples from patients with cardiovascular diseases. Fibrinolysis was also effected by γ', with increased levels prolonging lysis times and slowing fibrinolysis rates. In whole blood analysis increasing γ' levels led to shorter clotting times and an increased rate of clotting in the early stages of clot formation, but this did not propagate to the later stages of clot formation, with no change in average rate of clotting or time to MCF. Fibrinogen γ' also influenced clot formation under flow conditions, shortening the lag times at slower flow rates, and increasing amounts of fibrinogen being deposited around the platelet aggregates at both low and high flow rates. Analysis of end-point clots showed that clots formed with 100 % γA/γ' lead to clots with greater height and volume. Than clots formed from 100 % γA/γA.

Changes seen in clot structure at physiological levels of γ' fibrinogen mostly agreed with previous studies. An increase in clot density was seen as the percentage of γ' increased in a purified system, repleted fibrinogen deficient

plasma and in patient plasma samples. This was in agreement with previous studies showing that fibrinogen γ' forms denser clots (Cooper et al., 2003, Siebenlist et al., 2005). In addition, using a combination of purified and plasma based systems, this study now indicates that the changes in clot structure appeared to be FXIII dependent. The same trend was seen in permeation assays, with increases in γ' leading to decreases in clot permeability, but in the absence of FXIII porosity was not affected. In this study IF-1 fibrinogen purification was used to eliminate all FXIII from fibrinogen preparations, before fibrinogen variants γA/γ' and γA/γA were produced using anion-exchange chromatography. Previous studies that have shown changes in clot structure due to fibrinogen γ' did not do this (Cooper et al., 2003, Siebenlist et al., 2005, Allan et al., 2012), and so they were potentially all carried out in the presence of some FXIII as it has been found to copurifiy with fibrinogen γ' on anion-exchange chromatography (Mosesson and Finlayson, 1963). Therefore, further studies using FXIII inhibitors should be carried out to confirm the FXIII dependent clot changes caused by fibrinogen γ'.

There were similarities and differences in clot formation and breakdown data to previous studies. As fibrinogen γ' levels increased, there was a decrease in Max OD, indicative of the formation of thinner fibres, and a decrease in clotting rates, both in agreement with previous data (Cooper et al., 2003, Siebenlist et al., 2005). Interestingly, the effects of fibrinogen γ' on clotting rates were not seen in the repleted plasma or patient plasma samples, suggesting that other factors within the plasma may negate or lessen the effects of the changes in fibrinogen γ' levels. Changes in clot breakdown followed a similar trend, with increasing fibrinogen γ' levels leading to

prolonged lysis times and decreased lysis rates, mirroring previous findings (Falls and Farrell, 1997, Siebenlist et al., 2005, Kim et al., 2014, Pieters et al., 2013), but in patient samples lysis was only found to be prolonged at 75 % lysis and no change in average lysis rates were found. This suggests that although fibrinogen γ' levels influence fibrinolysis, the effects are reduced in patient plasma samples, and this may be due to other contributing factors in the plasma (FXIII levels, α2AP levels).

In a novel approach, the effects of fibrinogen γ' levels on the mechanical properties of whole blood clots were investigated by ROTEM (n = 78). As fibrinogen γ' levels increased there was a decrease in lag time and an increase in the rate of early clot formation and maximum rate of clot formation. However, this increase in rate did not propagate to the later stages of clot formation, with no changes seen in average rate of clot formation or time to MCF. Finally, no differences were seen in MCF as fibrinogen γ' levels increased. These data suggest that in whole blood, increases in fibrinogen γ' may in fact lead to an increase in early clotting rates, which is in agreement with Allan et al., who reported earlier gelling of fibrinogen γ' clots (Allan et al., 2012). No effect of increasing fibrinogen γ' was seen on the stiffness of whole blood clots. This was unexpected as differences in stiffness between γA/γ' and γA/γA have previously been reported in purified and plasma systems, with γA/γ' being significantly more viscous (Allan et al., 2012, Domingues et al., 2016). This might be explained by two possible reasons, either the effect of fibrinogen γ' on clot stiffness is annulled in whole blood by the presence of other blood cells, or another possibility is that the ROTEM is not sensitive enough to pick up the small differences in clot stiffness induced by fibrinogen γ' in whole blood. To

further investigate this, a more sensitive system may be required like the magnetic tweezers used in the paper of Allan et al. This could be modified to investigate clot stiffness in whole blood clots using fluorescently labelled magnetic beads (Allan et al., 2012). The increase in the early rates of clotting and maximum rates of clotting with increasing fibrinogen γ' levels in whole blood clots differs from many studies that have demonstrated a reduction in clotting rates with fibrinogen γA/γ' (Cooper et al., 2003, Siebenlist et al., 2005, Lovely et al., 2007, Allan et al., 2012). This suggests that the effects of fibrinogen γ' in whole blood may be reduced with average clot formation rates normalised, and at the same time its effects on faster clot gelation and increased early clotting rates dominating. Further studies are needed to confirm this, using other whole blood clotting techniques.

In ROTEM experiments changes in fibrinogen γ' only appeared to induce effects on clot formation when clotting was triggered via the extrinsic pathway. When clotting was initiated with the in-tem reagent no differences were seen as fibrinogen γ' levels increased. This suggests the effects of fibrinogen γ' in whole blood are produced via the extrinsic pathway. This was somewhat unexpected as previous studies have linked fibrinogen γ' to the intrinsic pathway, showing that the fibrinogen γ' C-terminal peptide (410-427) inhibits the intrinsic pathway via FVIII (Lovely et al., 2007). These studies were carried out at very high concentrations of peptide, and so physiological levels of fibrinogen γ' may have little to no effect on the intrinsic system. This may suggest that in whole blood fibrinogen γ' may impart its effects through the extrinsic pathway or the thrombin feedback loop. Whole blood thrombin generation in patients with a range of fibrinogen concentrations could be used to further study this (Ninivaggi et al., 2012).

In collaboration with Prof Johan Heemskerk's lab at the University of Maastricht the effects of venous and arterial flow rates on clot formation with γA/γA and γA/γ' fibrinogen was investigated using a two-step model in a microfluidic chamber. Fibrinogen deficient plasma repleted with fluorescent γA/γA or γA/γ' fibrinogen was perfused over preformed platelet thrombi, and the accumulation of fluorescent fibrin around the platelet thrombi was quantified. Fibrin deposition occurred much more rapidly with γA/γ' fibrinogen at venous flow rates than γA/γA fibrinogen, but this effect was abolished at arterial flow rates. This fits with the decrease in lag time and increase in initial clotting rates with increasing γ' levels seen in ROTEM analysis, and with previous findings that demonstrate faster gelling of γ' fibrinogen clots (Allan et al., 2012). Clots in the ROTEM analysis and in previous studies were all formed in static conditions, so combining this with the flow data puts forward the idea that in static or reduced flow rate conditions γ' fibrinogen leads to an increase in early clot formation, but at higher flow rates this effect is nullified. At both flow rates more fibrin was deposited around the platelet thrombi with γA/γ' than γA/γA fibrinogen at the end of the experiment, and this supports the idea of γ' fibrinogen being more prothrombotic and a cardiovascular risk factor (Pieters et al., 2013). At arterial flow rates more fibrin was laid down around the platelet thrombi, and at a faster rate, with both fibrinogen variants. γA/γ' fibrinogen appeared to reach maximum fluorescence more quickly than γA/γA at venous flow rates, but this may be reflective of the shorter lag times.

When end-point clot images were analysed, there were clear differences in clot morphology between the flow rates and fibrinogen variants. Clots formed at arterial flow rates were much shorter and smaller than clots formed at

venous flow rates. This was expected as the pressure is much higher at arterial flow rates and this would prevent growth of the clots away from the surface. γA/γ' fibrinogen led to significantly taller and more voluminous clots at both venous and arterial flow rates. This mirrored the results from the kinetic experiments, with γA/γ' fibrinogen leading to a greater maximum fluorescence, indicating more fibrin being deposited around the platelet thrombi. When the volume of each slice was plotted against the distance from the slide the distribution of fibrin in these clots was remarkably different between the different flow rates and the two fibrinogen splice variants. At venous flow rates, the majority of the fibrin clot forms away from the slide surface and the platelet thrombi, with only a small area of contact, and this was exaggerated greatly in the γA/γ' clots with more height and volume. At higher flow rates clots were much lower in height and the largest area of fibrin was on the surface around the platelet thrombi. This was reflected in the results from the kinetic experiments, which showed significantly more fibrin deposited around platelet thrombi with both fibrinogen variants at higher flow rates. γA/γ' fibrinogen had less of an effect on the volume of the clot at higher flow rates, but still resulted in significantly taller clots. These data clearly indicate γA/γ' fibrinogen leads to the formation of much larger clots at both venous and arterial flow rates, much more so at venous flow rates. Interestingly, even though γA/γ' led to the formation of much larger clots at venous flow rates, most previous studies have linked venous thrombosis with a decrease in γ' fibrinogen levels (Uitte de Willige et al., 2005, Mosesson et al., 2007, Nowak-Gottl et al., 2009). This raises questions about the properties of these larger γA/γ' clots at venous flow rates. These clots appeared to be made up of voluminous clouds of fibrin

when compared to the more familiar fibrous clots formed with γA/γA fibrinogen, with very small points of contact with the platelet thrombi. This could result in these clots being much weaker than the more fibrous γA/γA clots, leading to clots that embolize more easily or clots that are more easily broken down. This could help to explain the association of decreasing levels of fibrinogen γ' with venous thrombosis, as lower levels of fibrinogen γ' in clots formed at venous flow rates may lead to clots that are more difficult to breakdown forming a more stable clot, and this may create conditions where venous thrombosis is more likely. At higher flow rates the clots formed with both fibrinogen splice variants were much shorter, with a wider base. This would suggest that these clots would be much more stable. γA/γ' clots, in these more stable conditions, were still significantly larger than clots formed from γA/γA, and this could be important in conditions involving obstructive clots. Previous studies have already associated increased γ' levels with ischemic stroke (Cheung et al., 2008, van den Herik et al., 2011) and myocardial infarction (Mannila et al., 2007), and this may be due to the increased clot size with increasing levels of fibrinogen γ' that are more likely to obstruct blood flow. Further studies will be required to see if the size of clots under flow are effected at physiological fibrinogen γ' levels, and if increases in these levels lead to increases in volume. Another area of interest is how these clots break down under flow, and if fibrinogen γ' plays a role in fibrinolysis under flow.

All together the data from this chapter indicate that γ' fibrinogen may play an important role in thrombosis. At physiological concentrations it increases clot density and prolongs lysis, and in whole blood and under flow it appears to speed up the initial stages of clot formation. Under flow γ' fibrinogen also

resulted in the formation of much larger clots. All of these changes in clot structure suggest γ' fibrinogen may play a significant role in thrombosis, and highlight the need for more work to be carried out to understand the mechanisms involved.

3.4 Future work

This chapter has highlighted that γ' fibrinogen may play an important role in the pathogenesis of thrombosis and that more work is required to uncover the significance of this clinically, and if the mechanisms underlying this role in thrombosis can be targeted. Due to the apparent role of FXIII in fibrinogen γ' induced changes in clot structure, more research is required to confirm this and uncover its mechanisms. By Inhibiting FXIII in plasma with T101 or another FXIII inhibitor, it would be possible to see if the effects of γ' on clot structure could be reversed. This would add to the evidence that the changes are indeed FXIII dependent. More flow experiments need to be carried out, with more repeats of the clot formation experiments under venous and arterial flow needed. Following on from these experiments with different ratios of γA/γ' to γA/γA fibrinogen are required to examine how physiological levels of γ' fibrinogen influence clot formation and structure at venous and arterial flow rates. The relationship between fibrinogen binding receptors on platelets and γ' fibrinogen could be assessed under flow by introducing different receptor inhibitors. The role of γ' in fibrinolysis needs to be investigated in more detail. Whole blood ROTEM fibrinolysis and lysis under flow could be explored to elucidate if γ' prolongs lysis in whole blood and under flow conditions. Experiments of lysis under flow have already begun, but more repeats are required. One step flow experiments using

patient whole blood samples with measured γ’ levels could also be carried out. This would be more physiologically relevant as clot formation would proceed in one step, as opposed to platelet thrombi formation first followed by fibrin deposition, and it would also eliminate the need to use fibrinogen deficient plasma.

Together these studies would take this investigation forward taking a more in-depth look at the role of γ’ in thrombosis, uncovering the significance of its impact and potentially creating a new therapeutic target in the treatment of thrombosis.

Chapter 4 - Clot structure at the air-blood interface

Haemostasis is a pivotal mechanism to prevent life-threatening blood loss from sites of injury and involves close interplay between coagulation and platelets. The resulting blood clot contains activated platelets, RBCs, and fibrin polymer, which holds the clot together. Fibrin is formed by limited proteolysis of fibrinogen by thrombin. Thrombin cleaves small peptidic sequences from the N-termini of the Aα- and Bβ-polypeptides, exposing interaction sites for binding pockets in the C-terminal domains of the β- and γ-chains, respectively (Weisel, 2005). Fibrin then polymerizes into protofibrils, which aggregate laterally into fibres. The fibres branch and produce a 3D network with remarkable elastic properties (Liu et al., 2006). The structure of the fibrin network is determined by fibre diameter, protofibril packing, and pore size, the latter of which is sufficient for the incorporation of cells. Dense networks with thin fibres and increased rigidity are associated with increased risk of thrombosis, while loose clot networks with thick fibres and reduced rigidity are associated with bleeding (Weisel, 2005, Undas and Ariens, 2011, Wolberg, 2010).

A major conundrum after decades of fibrin polymer research is that fibrin fibres in blood clots appear endless, with little or no evidence of fibre ends (Figure 31). Thus, the mechanisms and structures that determine the external boundary of an extravascular (haemostatic) blood clot are unknown. What happens to the fibrin network and fibres when they reach the peripheral, exposed surface of the clot? Do the fibres just stop, flatten, or bend, or is the surface lined by platelets, RBCs, or other cells? The architecture of this interface is important because it forms a distinction between host and the environment. To explore this, the structural characteristics of the exterior face of the blood clot were investigated.

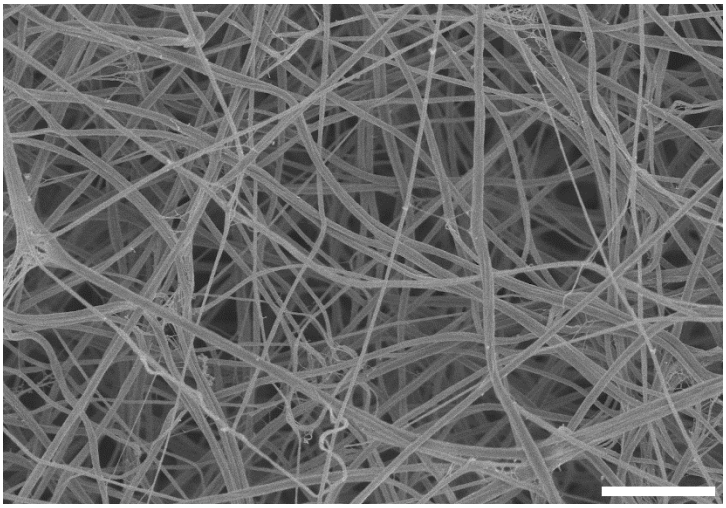

Figure 31 Fibrin clot network. SEM image of a three-dimensional fibrin fibre network from the inside of a clot. Fibrin fibres in this image appear limitless and without fibre ends. Scale bar -2 µm. Image from Macrae et al. (2018).

4.1 Film forms at air-liquid interface

Scanning electron microscopy and laser scanning confocal microscopy were used to investigate the liquid-air interface of clots (Figure 32 and Figure 33). In dehydrated conditions used in SEM, a thin film was found to form at the liquid-air interface of clots formed from whole blood or PPP, when clotting was initiated with either thrombin (0.5 $U.ml^{-1}$, Figure 32A-B) or tissue factor (5 pM, Figure 32C-D). This film was also seen in clots formed in fully hydrated conditions using LSCM, in both whole blood (thrombin - 0.5 $U.ml^{-1}$, TF – 5 pM, Figure 33A-B) and PPP (thrombin - 0.5 $U.ml^{-1}$, tissue factor – 5 pM, Figure 33C-D). The film was found to be continuous, covering the entire air-liquid interface, when single slices of clots were examined in the Z-plane using LSCM (Figure 33E).

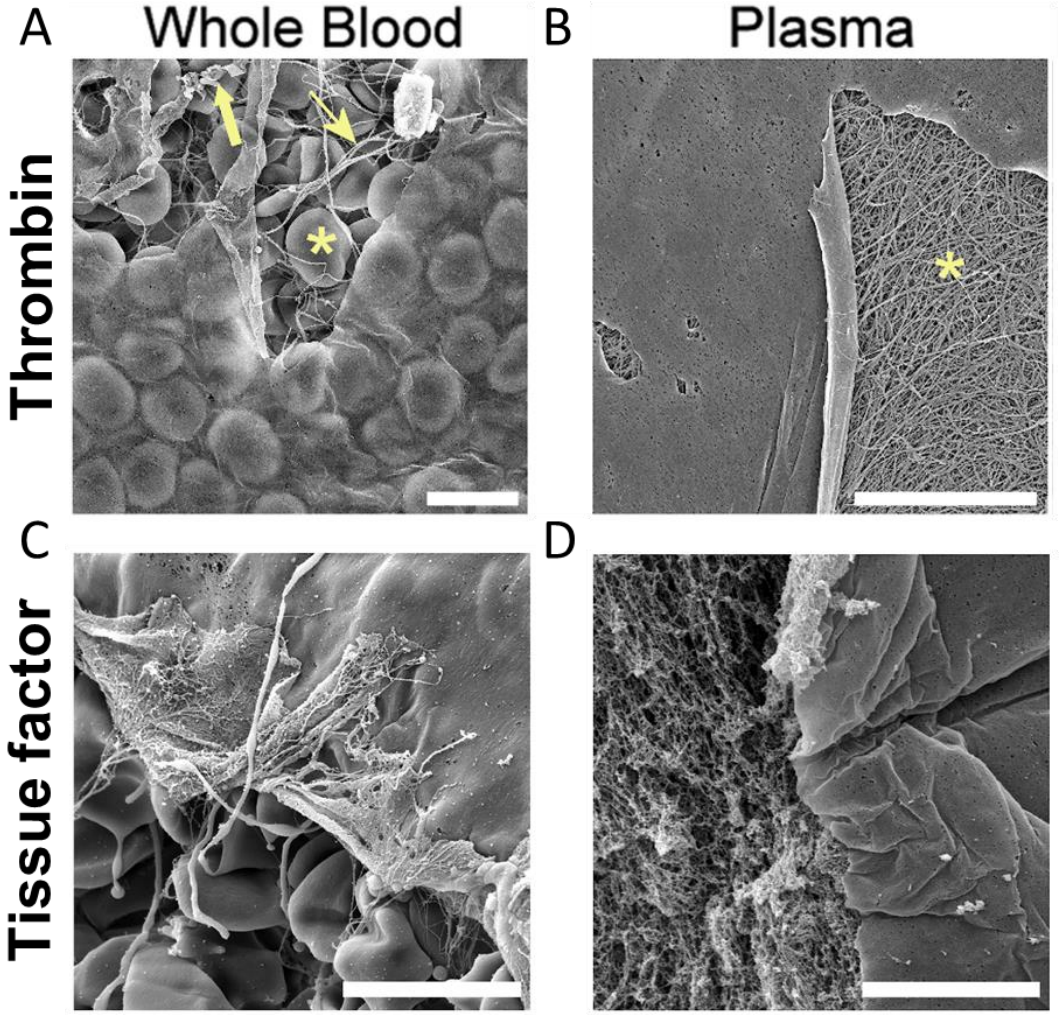

Figure 32 Film forms on clot surface at the air-liquid interface. SEM of film formed at the air-liquid interface in whole blood and plasma clots. **A, B,** clotting was initiated with thrombin. **C, D,** clotting was initiated with tissue factor. At places where the film is torn (due to SEM sample processing procedures), red blood cells (asterisk), platelets (thick arrow) and fibrin (thin arrow) are observed in whole blood clots, and fibrin in plasma clots. Red blood cells are also seen shining through the film in whole blood clots. Images represent findings reproduced in at least n = 3 experiments. Scale bars: A, B – 10 μm, C, D – 20 μm. Data from Macrae et al. (2018).

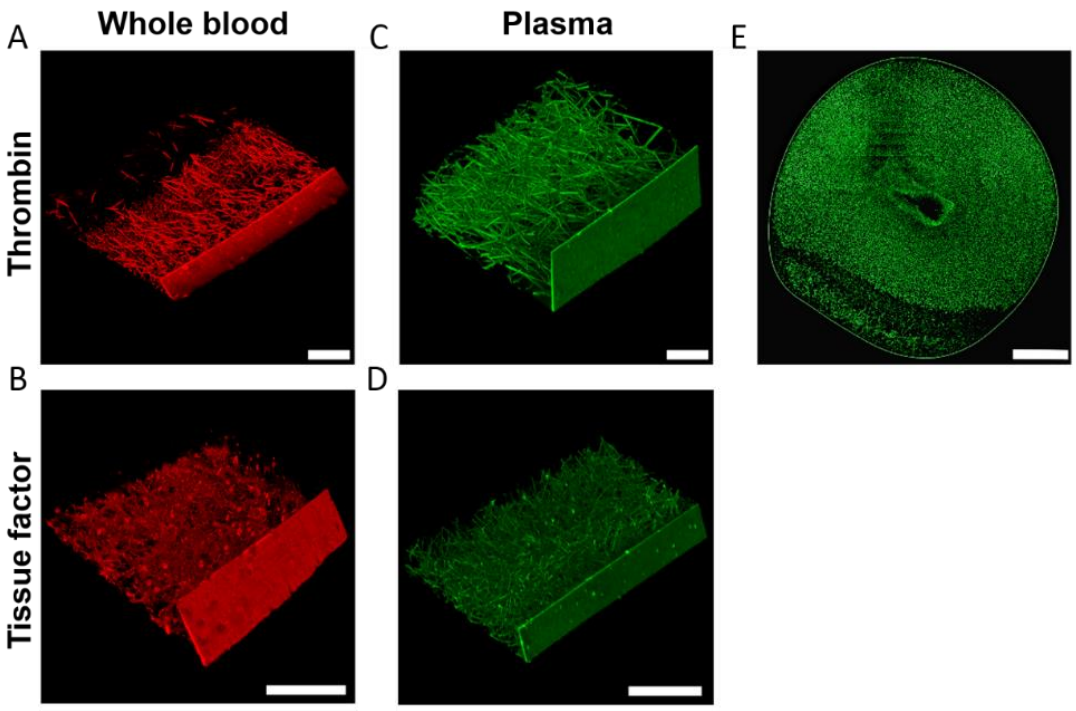

Figure 33 Film is present in hydrated conditions. LSCM of film formed at the air-liquid interface in whole blood and plasma clots**. A, C,** clotting was initiated with thrombin. **B, D,** clotting was initiated with tissue factor. Fibrinogen was fluorescently labelled with Alexa Fluor-488 (green) or -594 (red). Under fully hydrated conditions of LSCM, tears in the film were not observed. E, LSCM of a single Z-plane slice of a plasma clot showing continuous film around the clot. The central gap in the clot image is where the pipette was introduced into the plasma drop to inject thrombin. Images represent findings reproduced in at least n = 3 experiments. Scale bars: A-D – 50 µm, E – 1 mm. Data from Macrae et al. (2018).

4.2 Film is composed of fibrin

Fluorescence encountered within the film in LSCM images indicated fibrinogen or fibrin was present (Figure 33). To elucidate the components of the film, it was peeled away from the surface of plasma clots (Figure 34A) formed with or without T101 (transglutaminase inhibitor). The films were reduced and subjected to SDS-PAGE (Figure 34B). The film was found to mainly contain fibrin and this was confirmed by western blotting with a polyclonal antibody against fibrinogen (Figure 34C).

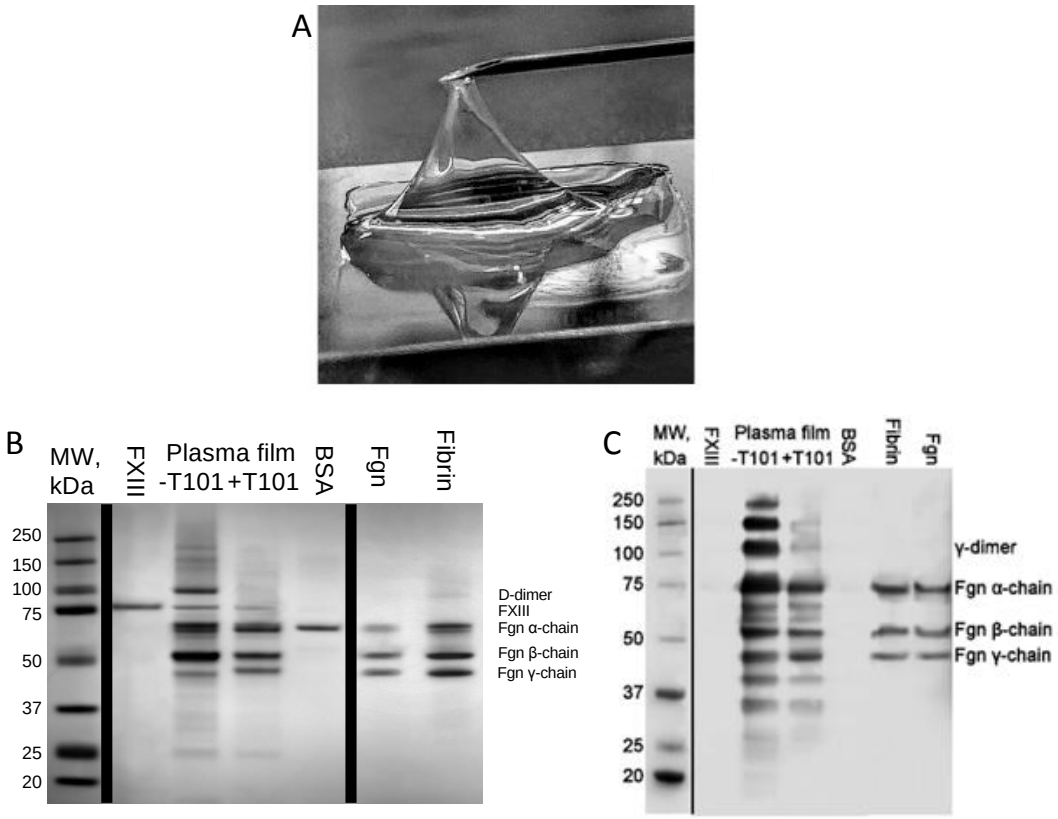

Figure 34 Film contains fibrin.

A, The film was peeled from clots using a needle. **B,** Films removed from clots produced ± T101 were run alongside FXIII, BSA, purified fibrin and purified fibrinogen (Fgn), on reducing SDS-PAGE. MW – molecular weight marker. **C,** films removed from clots formed with or without T101, and run alongside FXIII, BSA, a reduced purified fibrin clot and purified fibrinogen on reducing SDS-PAGE and analysed by western blotting with a polyclonal antibody against fibrinogen. Fgn – purified fibrinogen, BSA – bovine serum albumin, MW –molecular weight marker. Representative gel and blot of n = 3 experiments. Data from Macrae et al. (2018).

To ascertain whether the film could be formed from fibrin alone, clots were produced using purified fibrinogen (1 mg.ml^{-1}) and thrombin (0.5 U.ml^{-1}) and were examined using SEM and LSCM. Films that mimicked those formed on whole blood and plasma clots were observed (Figure 35A-B). Films were also found to transition from film to fibres in places (Figure 35C), and connected to the fibrin network through tethering fibres (Figure 35D). These observations show that fibrin(ogen) alone is capable of producing a film at the clot surface.

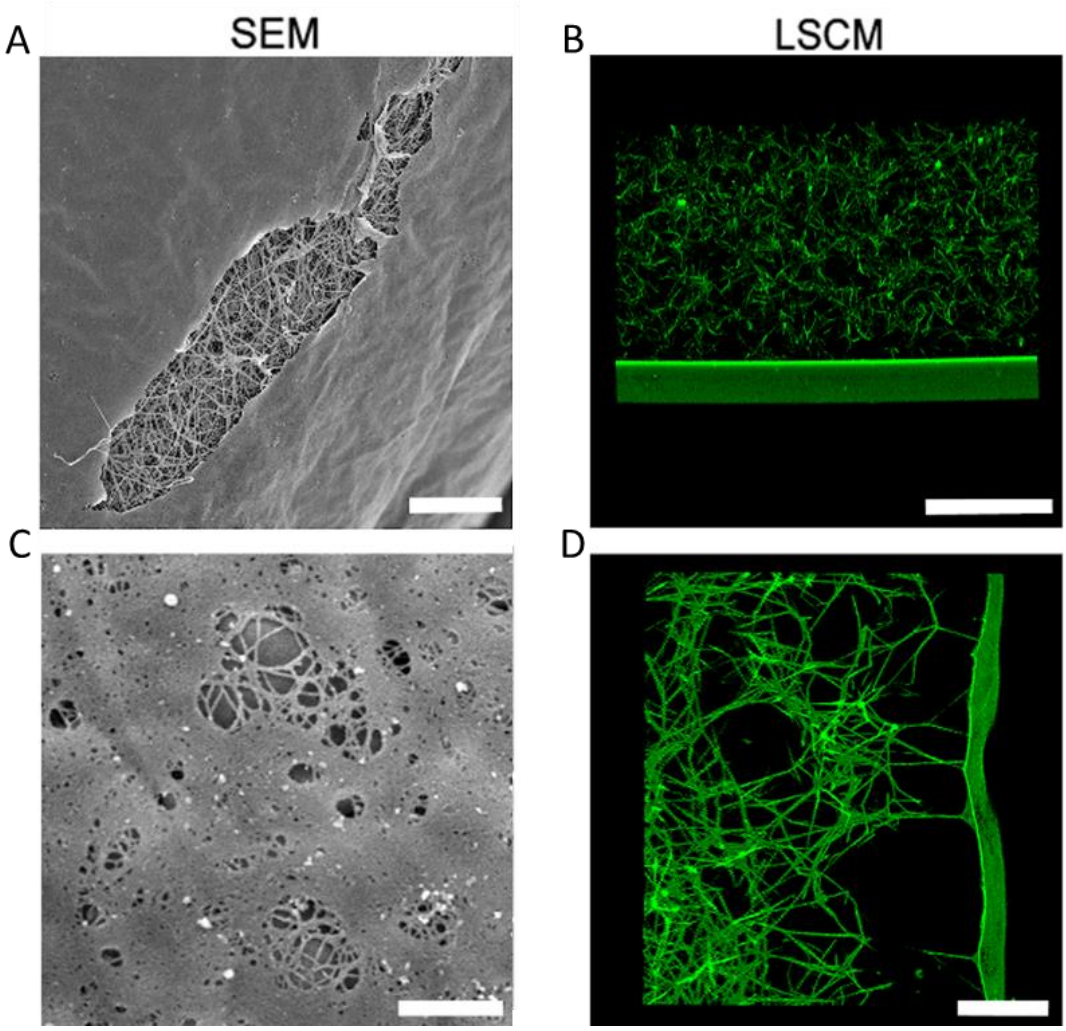

Figure 35 Only fibrin is required for film formation. A, SEM of the film in a clot produced from purified fibrinogen. A tear in the film exposes the underlying clot as often observed in SEM. Scale bar – 10 µm. **B,** LSCM of the film at the air-liquid interface of a clot produced from purified fibrinogen, without breaks in fully hydrated conditions. Fibrinogen fluorescently labelled with Alexa Fluor-488. Scale bar – 50 µm. **C,** SEM image of areas of film transitioning into fibres. Scale bar – 1 µm. **D,** LSCM of tethering fibres connected to the film. Scale bar – 50 µm. Images A-D representative of n = 3 experiments. Data from Macrae et al. (2018).

To investigate if plasma components influenced film formation different clotting conditions were used and their influence on film density and thickness was assessed. Purified fibrinogen was spiked with Alexa Fluor-488 fibrinogen (25 $\mu g.ml^{-1}$) and different clotting conditions were tested. Film MSF, as a measure of fibrinogen density, and film thickness were measured to quantify changes (Table 10).

Table 10 Mean sheet fluorescence and film thickness of fibrin films in different conditions. Table from Macrae et al. (2018).

	Mean Sheet fluorescence					Estimated film thickness				
Condition	Mean	SD	p value	F/t	df	Mean (µm)	SD	p value	F/t	df
Thrombin (U.ml^{-1})										
0.1	15.28	0.89	< 0.0001	193.3	3	2.15	0.40	<0.0001	29.11	3
0.5	10.54	0.97				1.72	0.11			
1.0	7.57	0.68				1.16	0.11			
10	2.57	0.38				1.18	0.03			
Calcium (mM)										
0	6.24	1.02	0.003	8.58	3	0.87	0.24	0.0010	10.7	3
5	12.69	3.45				1.54	0.28			
10	14.68	3.10				1.92	0.19			
20	11.83	1.33				1.3	0.51			
Fibrinogen (mg.ml^{-1})										
0.05	9.34	0.83	<0.0001	23.69	3	1.85	0.17	<0.0001	15.81	3
0.5	7.59	1.03				1.70	0.19			
1.0	4.72	1.30				1.25	0.16			
2.5	5.05	1.19				1.41	0.14			
Normal pool	10.00	1.57				1.75	0.11			
Dysfibrinogenemia	13.24	0.71				1.99	0.14			
Afibrinogenemia	0.22	0.24				0.00	0.00			
Thrombin (0.5 U.ml-1)	12.3	0.94	0.057	2.36	6	1.75	0.17	0.8	0.27	6
Reptilase (2.4 U.ml-1)	14.06	1.16				1.84	0.51			
21°C	10.23	0.73	< 0.0001	34.96	2	1.19	0.28	0.0007	18.02	2
31.5°C	12.67	0.75				1.54	0.15			
37°C	8.54	0.63				0.88	0.10			
-FXIII	13.14	1.25	0.82	0.24	6	1.56	0.33	0.65	0.5	6
+FXIII (3.7 µg.ml-1)	12.69	3.45				1.71	0.41			
PPP	13.51	2.35	0.26	1.19	10	1.58	0.29	0.27	1.18	10
PRP	12.06	1.81				1.42	0.16			
γA/γA	10.61	1.29	0.49	0.72	6	1.17	0.11	0.54	0.68	6
γA/γ'	11.23	1.66				1.12	0.07			
WT	9.21	1.83	0.007	6.49	3	0.92	0.01	<0.0001	51.05	3
WT + FXIII	9.08	2.44				1.1	0.16			
γ3x	12.69	1.04				1.51	0.09			
γ3x + FXIII	13.05	1.04				1.51	0.09			
WT	9.08	1.25	< 0.0001	28.78	2	1.1	0.16	<0.0001	26.96	2
α220	16.24	1.99				1.73	0.37			
α390	11.74	1.63				1.21	0.09			

df – degrees of freedom, F/t – F or t value for ANOVA or t-test, FXIII – factor XIII, MSF – mean sheet fluorescence, SD – standard deviation, WT – wildtype

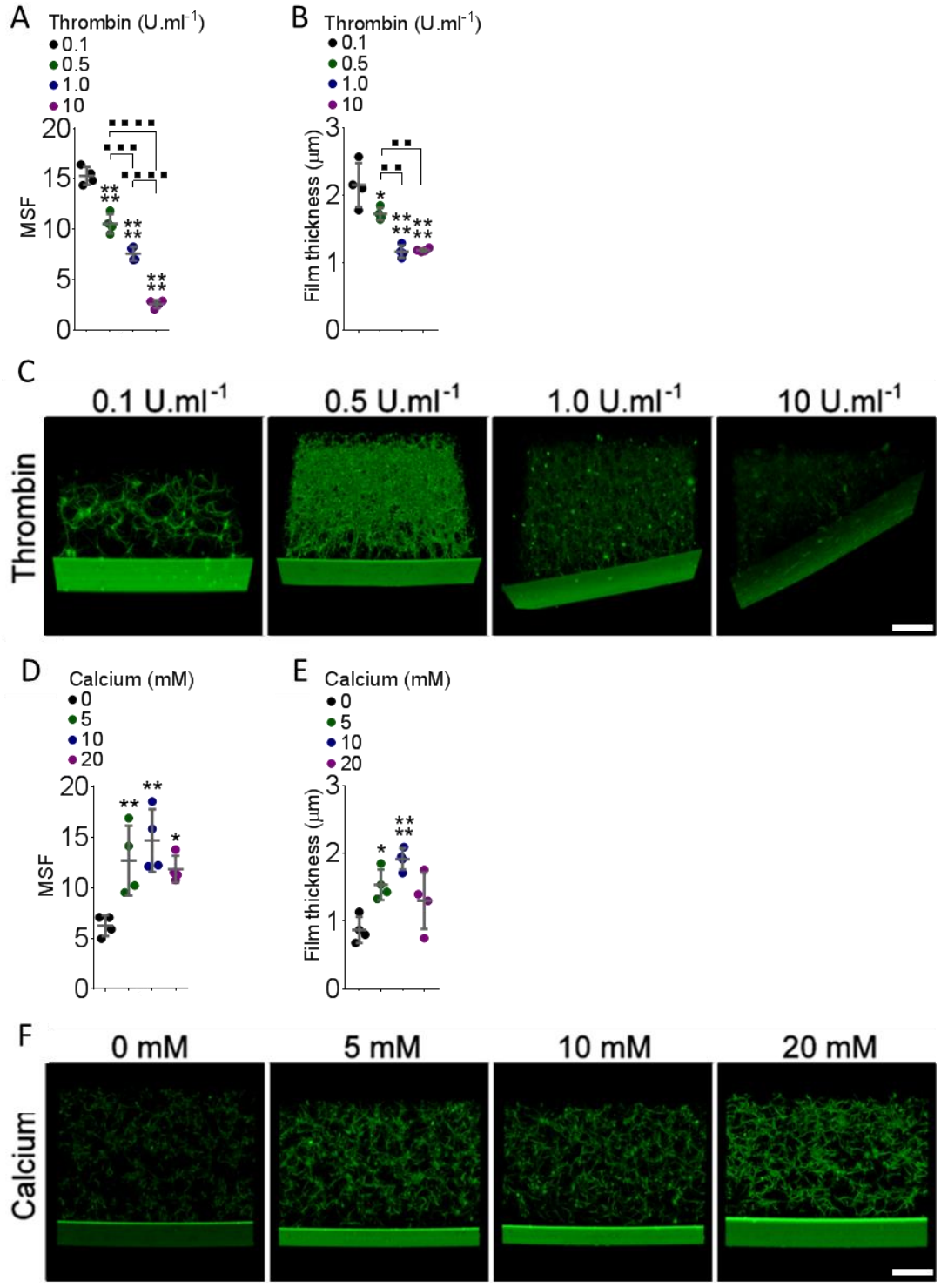

Figure 36 Thrombin and calcium effect on film formation. A, Mean sheet fluorescence (MSF) measurements of the film at different thrombin concentrations, n = 4, **B,** Film thickness at different thrombin concentrations, n = 4. **C,** Representative images (n = 4) of 3D Z-stack images obtained with LSCM of clots produced with purified fibrinogen initiated with different thrombin concentrations, **D,** MSF of the film at different $CaCl_2$ concentrations, n = 4, **E,** Film thickness at different $CaCl_2$ concentrations, n = 4, **F,** Representative images (n = 4) of 3D Z-stack images obtained with LSCM of clots produced with different $CaCl_2$ concentrations. * represents difference from 1st column, ▪ represents difference between other columns. * $p < 0.05$, ** or ▪▪ $p < 0.01$, *** or ▪▪▪ $p < 0.001$, **** or ▪▪▪▪ $p < 0.0001$. Mean ± SD. One-way ANOVA (multiple groups). Scale bars -50 µm. Data from Macrae et al. (2018).

The role of thrombin concentration on film formation was studied first. The film was found to form at all thrombin concentrations tested (0.1, 0.5, 1, 10 $U.ml^{-1}$, Figure 36A-C). However, film thickness and density decreased in a stepwise matter as the thrombin concentration increased, indicating a reduction in the quantity of fibrin present in the film. Thrombin generation triggered by tissue factor in plasma starts slowly after a short lag-phase, and then its concentration rapidly increases to a maximum of several hundred nM (tens of $U.ml^{-1}$) (Hemker and Beguin, 1995, Hemker et al., 2003). However, fibrin formation occurs at just 2-3 nM thrombin (0.2-0.3 $U.ml^{-1}$), before the vast majority of thrombin has been generated (Brummel et al., 2002). Film formation appeared to be optimal at lower thrombin concentrations, when clotting times are longer, allowing more fibrin to accumulate at the surface before the underlying network has formed. Previous data from our lab has shown that lower thrombin concentrations are optimal for maximum protofibril packing in fibrin fibres (Domingues et al., 2016).

Changes in $CaCl_2$ concentration (5, 10, 20 mM) had no effect on film density or thickness (Figure 36D-F), but the absence of $CaCl_2$ resulted in at least a 1.9x decrease in MSF and 1.5x decrease in film thickness. This indicates that film formation is not influenced by fluctuations in $CaCl_2$ concentration, but the absence of $CaCl_2$ dramatically reduces its formation.

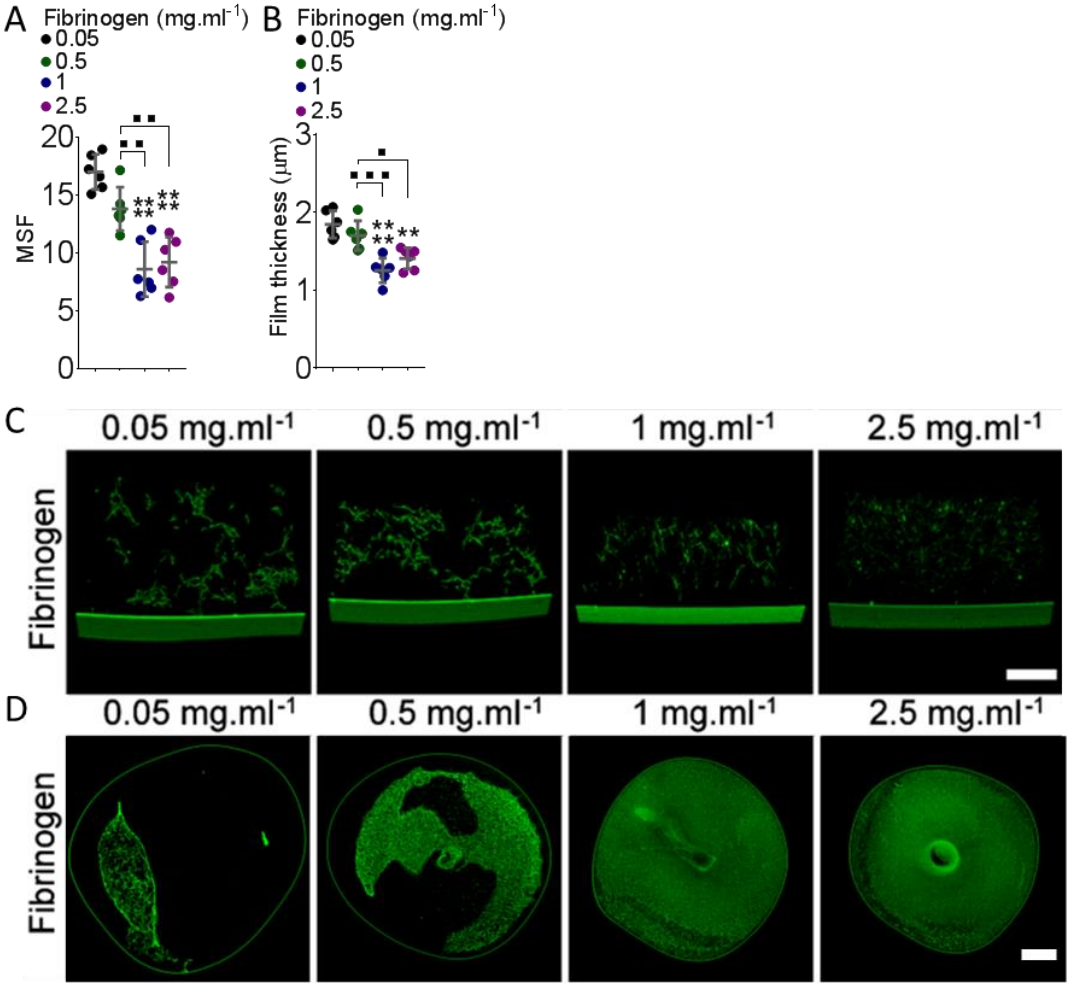

Figure 37 Influence of fibrinogen concentration on film formation. A, Mean sheet fluorescence (MSF) measurements of the film at different fibrinogen concentrations, n = 6, **B,** Film thickness at different fibrinogen concentrations, n=6. **C,** Representative images (n = 6) of 3D Z-stack images obtained with LSCM of clots produced with purified fibrinogen initiated with different thrombin concentrations, **D,** single Z-plane slices of plasma clots with different fibrinogen concentrations showing a continuous film around the whole clot even when there is insufficient fibrinogen to fill the whole droplet. * represents difference from 1st column, ▪ represents difference between other columns. * $p < 0.05$, ** or ▪▪ $p < 0.01$, *** or ▪▪▪ $p < 0.001$, **** or ▪▪▪▪ $p < 0.0001$. Mean ± SD, One-way ANOVA (multiple groups). Scale bars -50 μm. Data from Macrae et al. (2018).

Film formation occurred at all fibrinogen concentrations tested (0.05, 0.5, 1, 2.5 $mg.ml^{-1}$, Figure 37A-D), even when the fibrinogen levels were not sufficient to form a clot that filled the whole volume of the liquid (Figure 37D). Surprisingly, as fibrinogen levels increased up to 1 $mg.ml^{-1}$ the MSF and film thickness decreased in a stepwise manner signifying a reduction in film

formation. Increases in fibrinogen concentration have been shown to lead to shorter lag times and faster clotting rates (Weisel and Nagaswami, 1992). So in a similar fashion to thrombin concentrations, shorter lag times led to less fibrin accumulating at the air-liquid interface leading to thinner films.

Film formation was assessed in patients with dysfibrinogenemia and afibrinogenemia (patient plasma provided by Dr Alessandro Casini). To prevent changes in the clot or film structure with the addition of normal fluorescently labelled fibrinogen, a non-antibody binding protein (Affimer) (Tiede et al., 2017) specific to fibrinogen was fluorescently labelled with Alexa fluor 488. This was added to the patient plasma before a clot was formed, where it bound to any fibrinogen within the plasma. Clotting was then initiated, and once a clot had formed it was imaged using LSCM. Patients with dysfibrinogenemia formed a film that had a slightly higher MSF and thickness than clots formed from normal pool plasma. As expected patients with afibrinogenemia did not form a fibrin clot or film (Figure 38A-C).

No difference in MSF of film thickness was found in clots produced with reptilase (2.4 $U.ml^{-1}$), which only cleaves FpA (and not FpB) from fibrinogen, and thrombin (0.5 $U.ml^{-1}$, Figure 38D-F). This demonstrates that film formation only requires fibrinogen to fibrin conversion, regardless of the activating protease and independent of FpB release.

The effects of temperature on film formation was investigated (21°C – room temperature, 31.5°C – skin temperature, 37°C – core body temperature). Films were found to form at all three temperatures, but film formation increased at least 20-30 % at 31.5°C compared to room temperature or core body temperature (Figure 38G-I). Enhanced film formation at skin

temperature supports a physiological role for fibrin films in cutaneous wounds and dermal injuries.

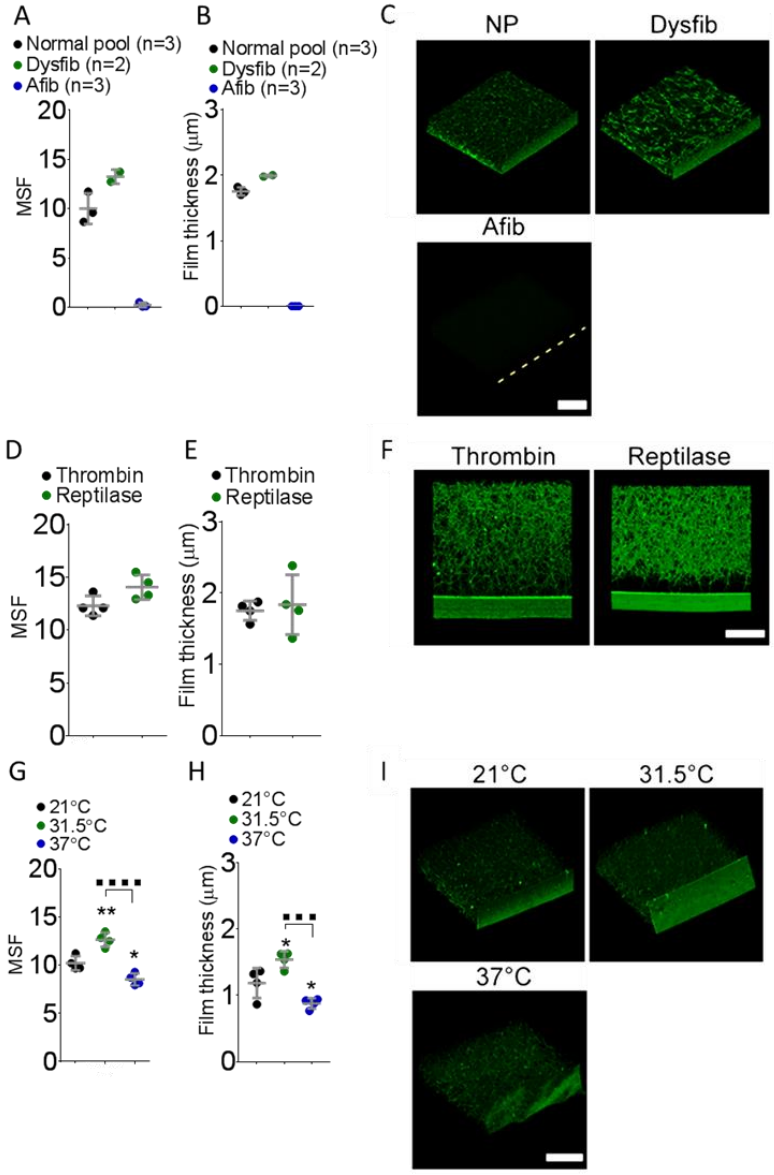

Figure 38 The role of other factors in film formation. A, MSF in normal pool plasma (NP) v Dysfibrinogenemia (Dysfib)/Afibrinogenemia (Afib) plasma, **B,** Film thickness in NP v Dysfib/Afib plasma, **C,** Representative LSCM images of 3D Z-stack images of clots produced from NP v Dysfib/Afib plasma. **D,** MSF with thrombin v reptilase, n = 4, **E,** Film thickness with thrombin v reptilase, n = 4, **F,** Representative LSCM images (n = 4) of 3D Z-stack images of clots produced with thrombin v reptilase, n = 4, **G,** MSF with different temperatures, n=4, **H,** Film thickness with different temperatures, n = 4, **I,** Representative LSCM images (n = 4) of 3D Z-stack images of clots produced at different temperatures, n = 4. * represents difference from 1st column, ▪ represents difference between other columns. * $p < 0.05$, ** or ▪▪ $p < 0.01$, *** or ▪▪▪ $p < 0.001$, **** or ▪▪▪▪ $p < 0.0001$. Mean ± SD, Unpaired student's t-test for pairwise comparisons (two groups); One-way ANOVA (multiple groups). Scale bars - 50 µm. Data from Macrae et al. (2018).

There were no differences in film MSF or thickness with or without FXIII (3.7 μg.ml^{-1}; Figure 39A-C), showing that the presence of FXIII is not a necessity for film formation.

The role of platelets in film formation was investigated by comparing film formation in PPP and PRP. No difference in MSF and film thickness between PPP and PRP indicated that platelets did not influence film formation (Figure 39D-F).

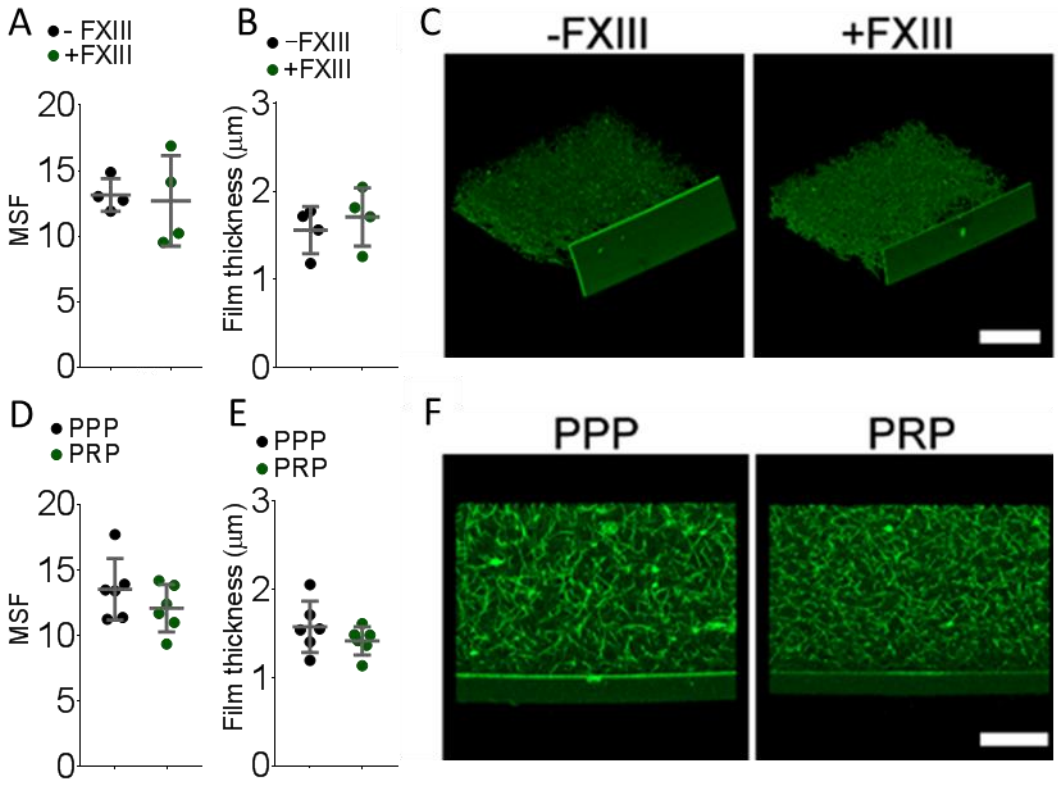

Figure 39 Role of FXIII and platelets in film formation. A, MSF with and without Factor XIII (FXIII), n = 4, **B,** Film thickness with and without FXIII, n = 4, **C,** Representative LSCM images of 3D Z-stack images of clots produced with and without FXIII, n = 4, **D,** MSF in platelet poor plasma (PPP) v platelet rich plasma (PRP), n = 6, **E,** Film thickness in PPP v PRP, n = 6, **F,** Representative LSCM images (n = 6) of 3D Z-stack images of clots produced with in PPP v PRP, n = 6. Mean ± SD, Unpaired student's t-test for pairwise comparisons (two groups), Scale bars -50 μm. Data from Macrae et al. (2018).

The impact of fibrinogen structural elements on film formation was explored, by assessing natural and recombinant fibrinogen variants: γA/γA, the common fibrinogen isoform; γA/γ', a heterodimeric splice variant which adds negative charge to the C-terminus of the γ-chain (Macrae et al., 2016); γ3x, a triple γ-chain mutant that eliminates all γ-chain crosslinking (Standeven et al., 2007), which was produced by Dr Cedric Duval; α220, in which the α-chain is truncated after residue Ser220 removing the connector and C-terminal globular domain of the αC-region; and α390, in which the α-chain is truncated after residue Asp 390 removing the C-terminal globular domain, which were both produced by Helen McPherson. Clots formed with γA/γA or γ A/γ' both formed films with no differences in MSF or sheet thickness (Figure 40A-C). Clots formed with 3xγ, α390 or α220 were all found to form films with an increased MSF, with 3xγ and α220 also forming thicker film (Figure 40D-I). These differences in MSF are likely attributable to differences in polymerization rates of the mutants, which lead to longer lag times.(McPherson et al., 2017) These data indicate that neither the C-terminal domain of the γ-chain, the α-chain C-terminal connector region, nor the α-chain C-terminal globular domain are required for film formation, but they do play a role in its rate of formation and final thickness.

Collectively, these findings show that fibrin produces a film that covers the blood clot at the air-liquid interface, and although other factors modulate film thickness or the amount of fibrin in the film, only fibrin is required.

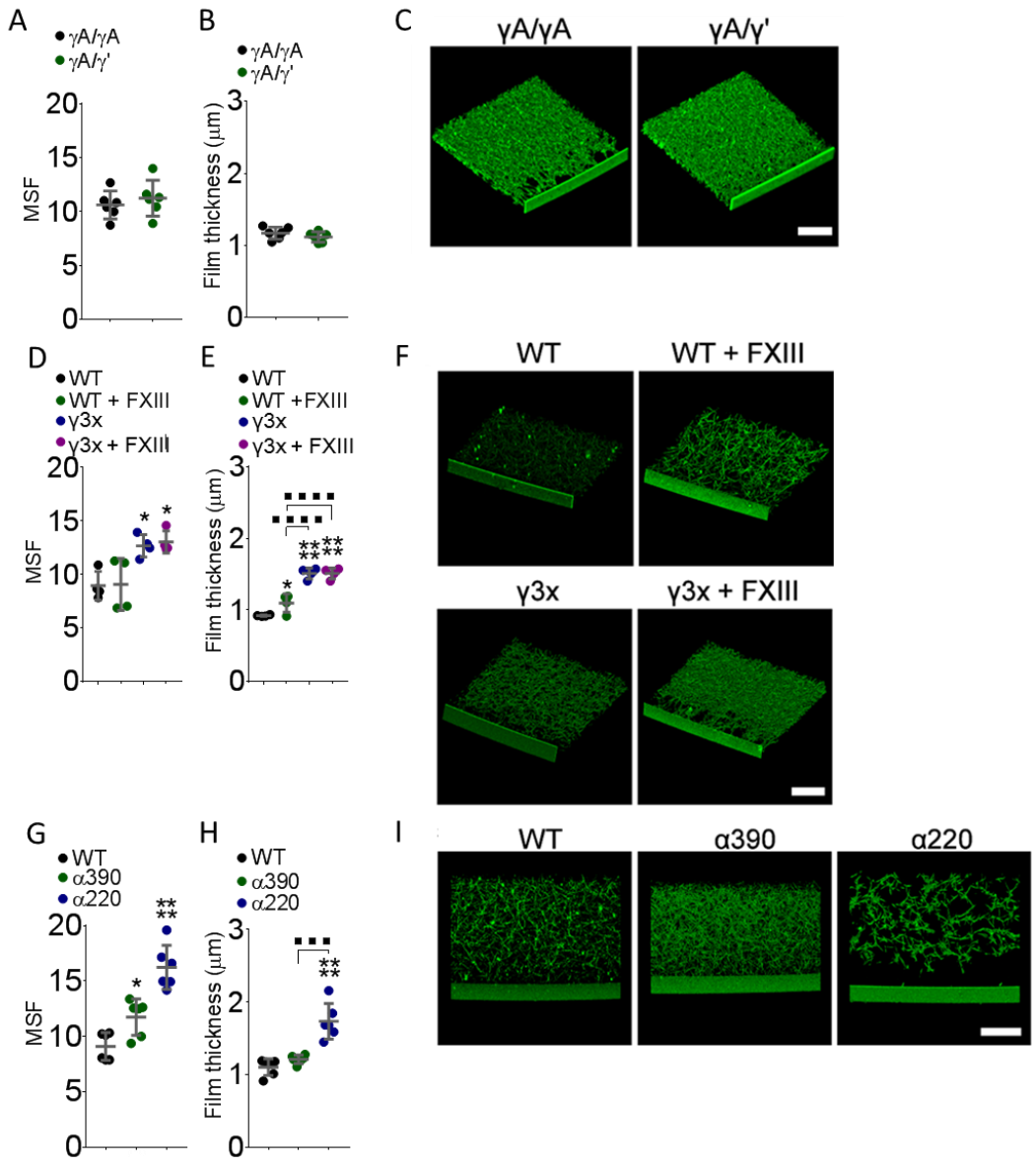

Figure 40 Effect of fibrinogen structural elements on film formation. A, MSF of γA/γA fibrinogen v γA/γ' fibrinogen, n = 6, **B,** Film thickness of γA/γA fibrinogen v γA/γ' fibrinogen, n = 6, **C,** Representative LSCM images of 3D Z-stack images of clots produced with γA/γA fibrinogen v γA/γ' fibrinogen, n = 6, **D,** MSF of fibrinogen triple γ-chain crosslinking mutant v wildtype fibrinogen, n = 6, **E,** Film thickness of fibrinogen triple γ-chain crosslinking mutant v wildtype fibrinogen, n = 6,**F,** Representative LSCM images of 3D Z-stack images of clots produced with fibrinogen triple γ-chain crosslinking mutant v wildtype fibrinogen, n = 6, **G,** MSF of fibrinogen α-chain deletion mutants v wildtype fibrinogen, n = 6, **H,** Film thickness of fibrinogen α-chain deletion mutants v wildtype fibrinogen, n = 6, **I,** Representative LSCM images of 3D Z-stack images of clots produced with fibrinogen α-chain deletion mutants v wildtype fibrinogen, n = 6, * represents difference from 1st column, ▪ represents difference between other columns. * $p < 0.05$, ** or ▪▪ $p < 0.01$, *** or ▪▪▪ $p < 0.001$, **** or ▪▪▪▪ $p < 0.0001$. Mean ± SD. Unpaired student's t-test for pairwise comparisons (two groups); One-way ANOVA (multiple groups). FXIII – factor XIII, WT – Wildtype. Scale bars - 50 μm. Data from Macrae et al. (2018).

4.3 Mechanism of formation

The transitioning of film to fibres (Figure 35C) and connections of the film to the clot network via tethering fibres (Figure 35D) indicated that a specific biophysical mechanism governs fibrin film formation. To identify this mechanism, LSCM was used to visualise film formation and breakdown in plasma and purified fibrinogen solutions over time. Clot formation was initiated with thrombin (0.5 $U.ml^{-1}$) in plasma (Figure 41A) or purified fibrinogen (Figure 41B), and with TF (5 pM) in plasma (Figure 41C). Fibrin accumulated at the surface forming a film before, or at a similar rate as the earliest fibrin fibres that constitute the clot network underneath.

Once the clot was fully formed, clot breakdown was initiated with tPA (85 $ng.ml^{-1}$) in plasma clots (Figure 42A), or tPA and plasminogen (25 $\mu g.ml^{-1}$) in purified systems (Figure 42B), and observed over time. In both cases, the films lysed at the same rate as the underlying network of fibrin fibres.

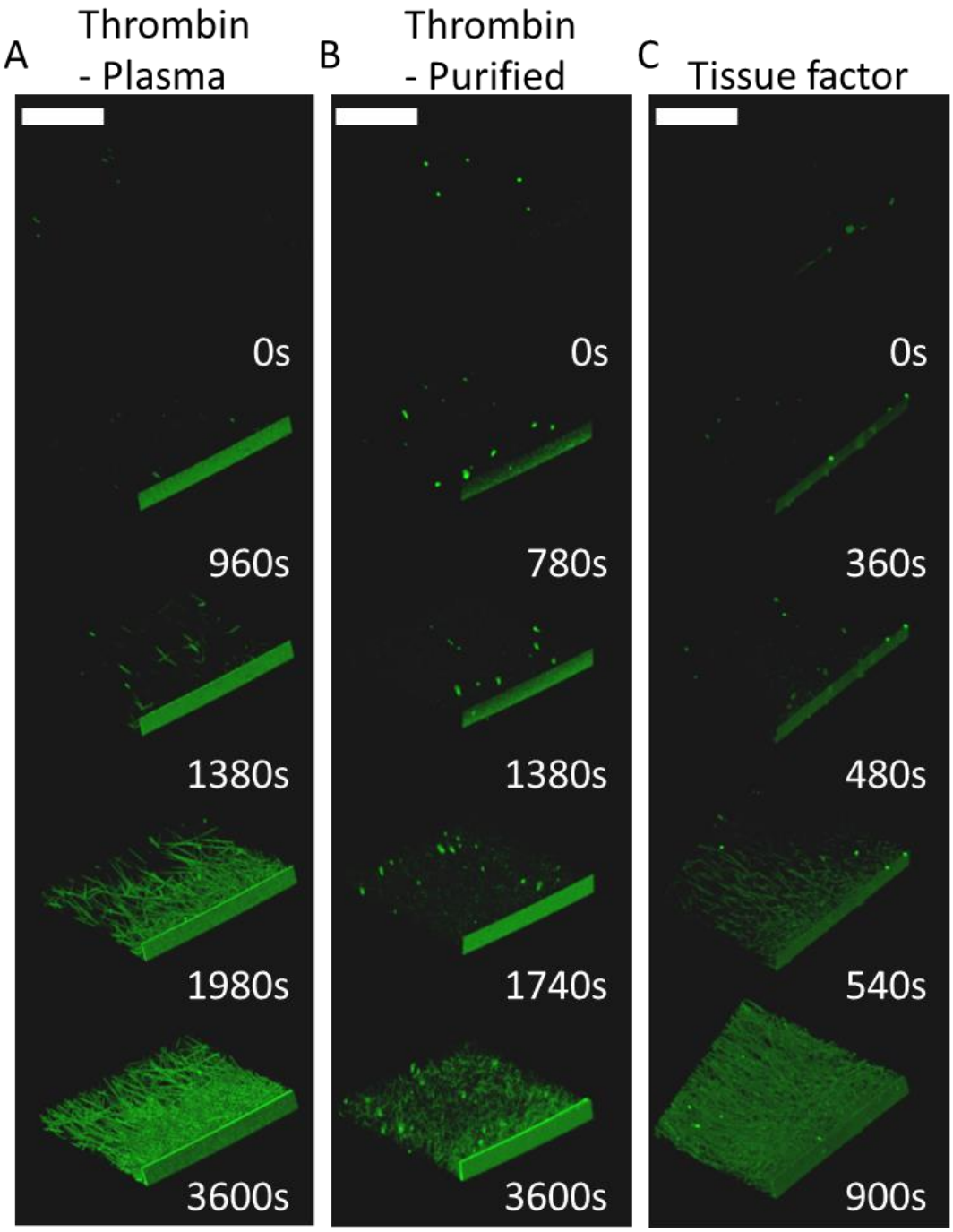

Figure 41 Film formation over time. A-C, Stills from movies of fibrin film formation over time. **A,** In plasma when clotting was initiated with thrombin. **B,** with purified fibrinogen when clotting was initiated with thrombin **C,** in plasma when clotting was initiated with tissue factor. n = 3 experiments, Scale bars – 50 μm. Data from Macrae et al. (2018).

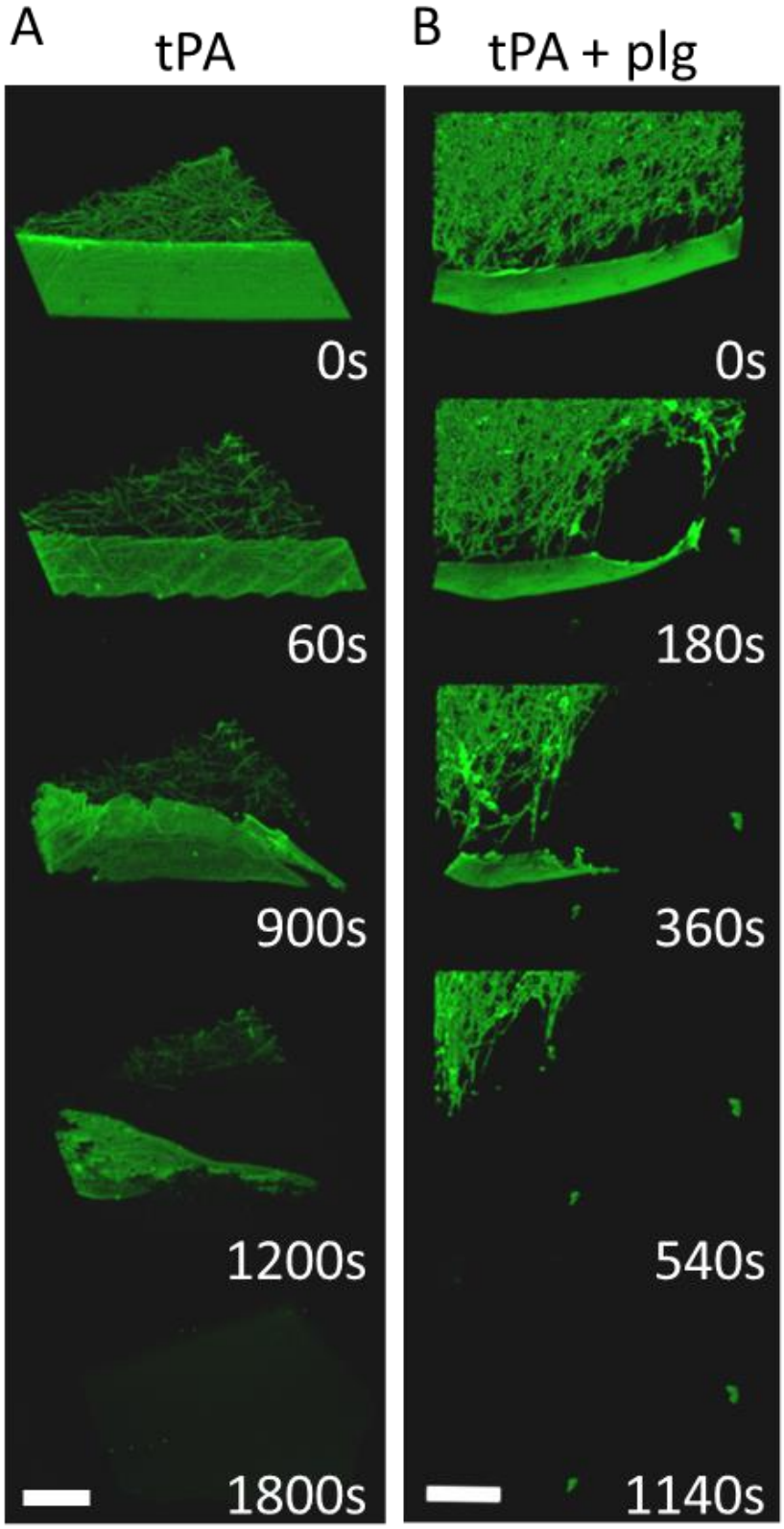

Figure 42 Film lysis over time. A-B, Stills from movies of fibrin film lysis over time. **A,** Film lysis by tPA in plasma clots. **B,** Film lysis by tPA and plasminogen in purified fibrinogen clots. n = 3 experiments, Scale bar – 50 μm. plg – plasminogen. Data from Macrae et al. (2018).

The behaviour of fibrinogen and fibrin at the air-liquid interface was subsequently investigated by following their accumulation at the air-liquid interface using a Langmuir-Blodgett trough, which analyses monolayer film formation of amphiphilic molecules at the air-liquid interface (Hann, 1990, Langmuir, 1917). A small number of previous studies have investigated the behaviour of fibrinogen at the air-liquid interface (Hernandez and Franses, 2003, Razumovsky and Damodaran, 1999, Werb et al., 1992, Sankaranarayanan et al., 2010), but none thus far had examined fibrin. Purified fibrinogen or fibrin monomers (fibrinogen ± 1 $U.ml^{-1}$ thrombin and 5 mM GPRP) were injected into the sub-phase of the trough at increasing quantities (1 $x10^{13}$ – 100 $x10^{13}$ molecules of fibrinogen/fibrin) and surface pressure measurements were recorded over time. As protein accumulated at the surface over time, surface pressure increased and then plateaued, resulting in a maximum pressure (Figure 43A). At 1 $x10^{13}$ molecules, neither fibrin nor fibrinogen covered the surface so there was no increase in surface pressure. At 5 and 20 $x10^{13}$ molecules of fibrinogen/fibrin there was a delay before fibrinogen or fibrin resulted in an increase in surface pressure. However, higher quantities (30 and 100 $x10^{13}$ molecules) of fibrinogen and fibrin caused an increase in surface pressure almost instantaneously (Figure 43B, Table 11).

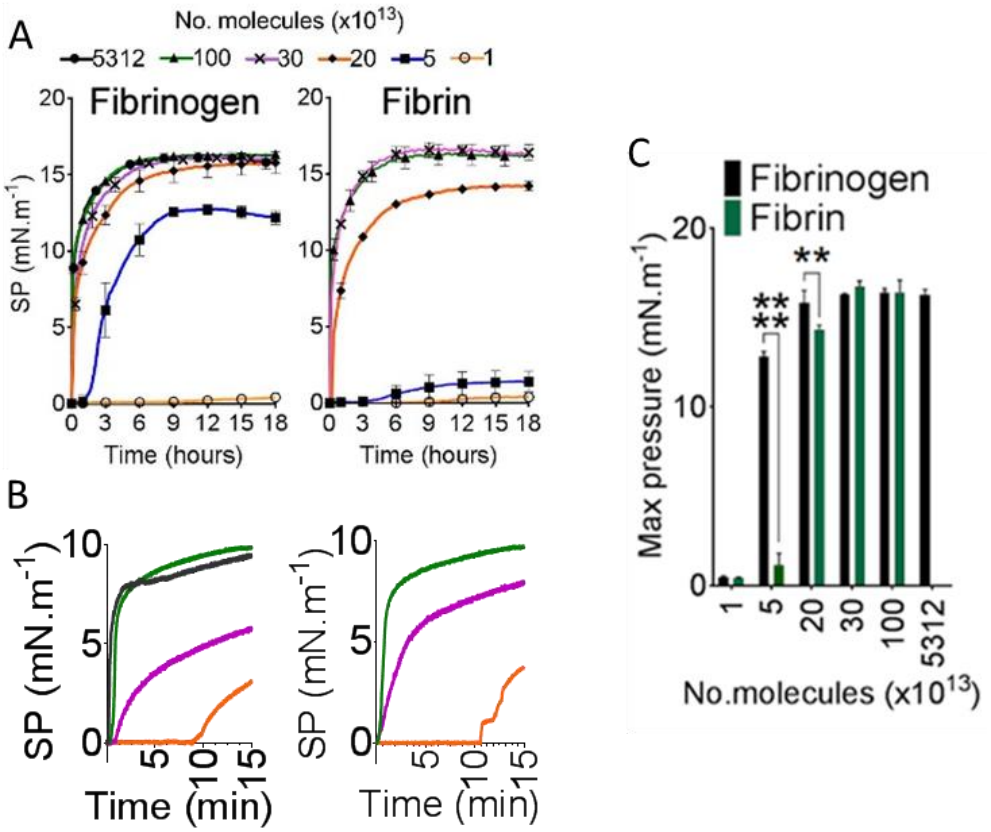

Figure 43 Fibrin(ogen) behaviour at the air-liquid interface. A, Changes in surface pressure in the Langmuir-Blodgett trough with different fibrinogen or fibrin concentrations over time. Data shown as mean ± SD, n = 3 experiments. **B,** Early time points of surface pressure in the Langmuir-Blodgett trough (0-15 min), n = 3 experiments, SP – Surface pressure. **C,** Maximum Langmuir-Blodgett trough surface pressure of fibrinogen and fibrin with increasing concentrations, data shown as mean ± SD, ** $p < 0.01$, **** $p < 0.0001$, n = 3 experiments. Two-way ANOVA, F = 293.5, df = 1, p = < 0.0001. Data from Macrae et al. (2018).

Table 11 Effect of fibrinogen or fibrin quantity on time to first increase in surface pressure. Table from Macrae et al. (2018).

No. of molecules ($x10^{13}$)	Fibrinogen		Fibrin	
	Time (s)	SD	Time (s)	SD
1	N/A		N/A	
5	918.0	140.3	1018.0	31.0
20	519.3	22.2	647.0	60.2
30	32.3	19.9	34.0	18.0
100	24.0	5.2	24.0	5.0
5312	9.0	0.0		

N/A – not applicable (surface pressure did not increase), SD – standard deviation

Maximum surface pressure was found to escalate with increasing amounts of fibrinogen and fibrin (Figure 43C, Table 12). Fibrin presented with significantly lower surface pressures than fibrinogen at 5 and 20 $x10^{13}$ molecules, but as the quantity of fibrinogen/fibrin increased, these differences were no longer seen. The addition of more than 30 $x10^{13}$ molecules of fibrinogen did not lead to a further increase maximum pressure (100 $x10^{13}$ and 5312 $x10^{13}$ molecules (1 $mg.ml^{-1}$)), signifying that 30 $x10^{13}$ (0.006 $mg.ml^{-1}$) is the maximum amount of fibrin/fibrinogen that can be accommodated at the surface. The concentration of fibrinogen or fibrin in the subphase (0,006 $mg.ml^{-1}$) required for this was much lower than physiological circulating fibrinogen levels (2-4 $mg.ml^{-1}$).

Table **12 Maximum surface pressure.** Table from Macrae et al. (2018).

	Fibrinogen		Fibrin				
No. of molecules ($x10^{13}$)	Max surface pressure ($mN.m^{-1}$)	SD	Max surface pressure ($mN.m^{-1}$)	SD	p value	t-value	df
1	0.48	0.05	0.43	0.02	>0.99	0.14	20
5	12.84	0.25	1.15	0.65	<0.0001	35.07	20
20	15.83	0.71	14.34	0.24	0.001	4.47	20
30	16.30	0.04	16.74	0.32	0.68	1.32	20
100	16.39	0.23	16.41	0.69	>0.99	0.06	20
5312	16.28	0.29					

Two way ANOVA, df – degrees of freedom, SD – standard deviation

From this it was possible to calculate that at 30 x 10^{13} molecules there would be ~30-34 nm^2 per fibrin/fibrinogen molecule at the air liquid interface. Assuming previously described fibrin(ogen) D-region (~6.5-6.7 nm) and E-region (~5-5.3 nm) diameters, (Wilgus et al., 2013, Hall and Slayter, 1959) and implementing the half-staggered fibrin model,(Fowler et al., 1981) it was possible to create a model that would allow for ~28-31 nm^2 per

fibrin/fibrinogen molecule (Figure 44). This was in close agreement with our experimental data. These data indicates that fibrin/fibrinogen molecules are tightly packed and are positioned perpendicularly to the air-liquid interface.

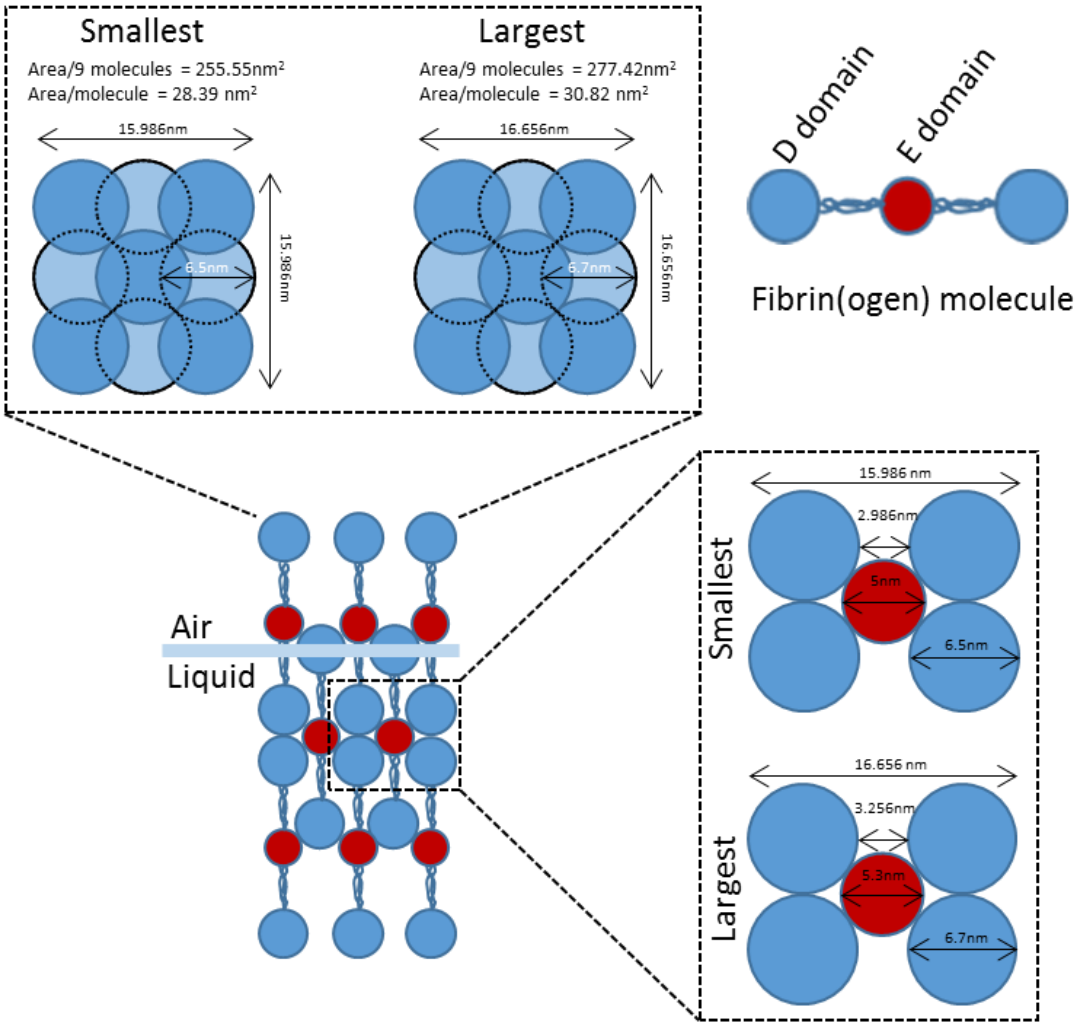

Figure 44 Fibrin(ogen) molecule packing at the air-liquid interface. Calculations carried out to estimate the area/molecule of fibrin(ogen) in the film at the smallest and largest described domain sizes. D domains are represented by blue circles and E domains by red circles.

In order to investigate the morphology of the film below the surface, the interior and the exterior surfaces were compared using SEM. The film was peeled away from the exterior of the clot and stretched over a coverslip with either the interior or exterior surface exposed (Figure 45). The exterior surface was smooth, sometimes with very small pores (~24.8 ± 8.8 nm

pores, yellow arrows) or with small nodes (~6.4 ± 0.9 nm domains, yellow circles). In contrast, the interior surface was rough with holes, pores and a fibrous structure, more closely resembling the clot network. In agreement with the Langmuir-Blodgett trough data, these data imply that fibrin films have an ordered, dense structure at the surface, but deeper into the film it becomes less ordered, where the film transitions into more fibrous structures.

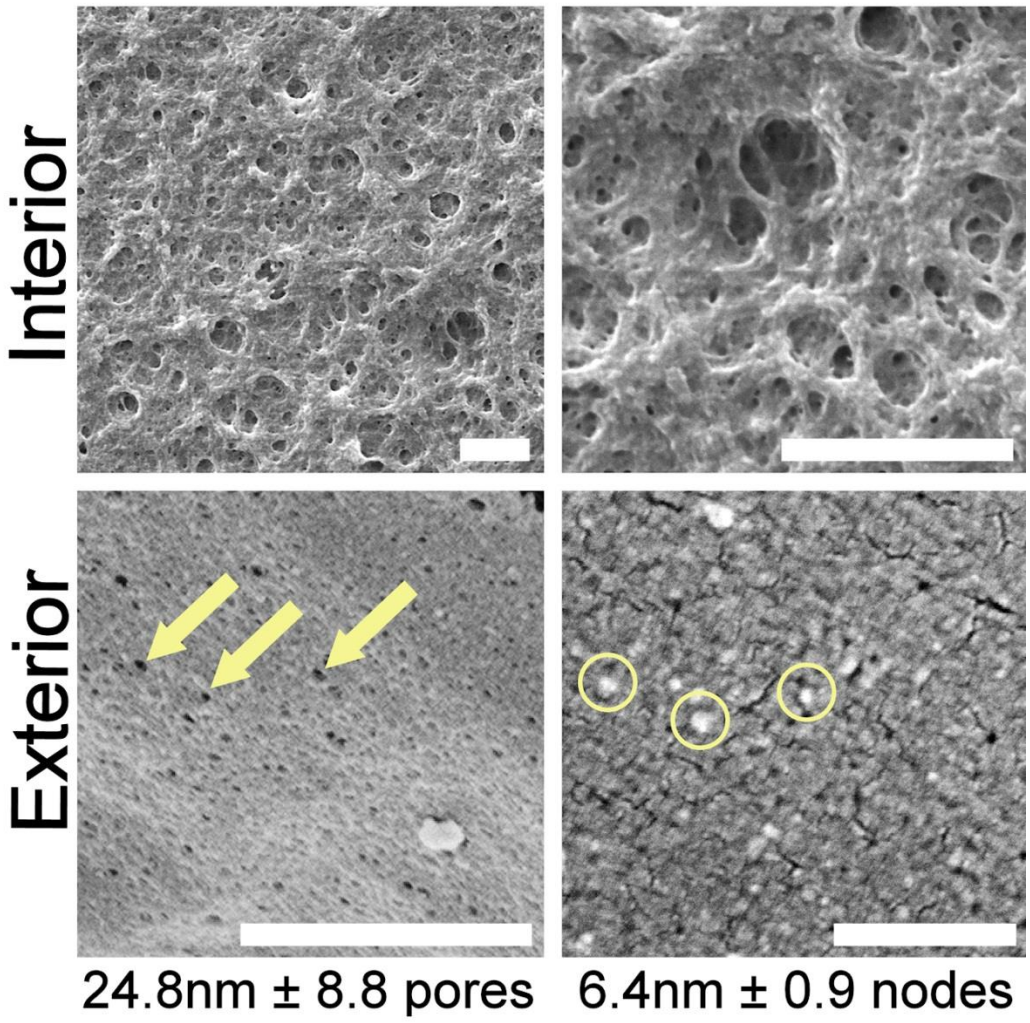

Figure 45 Comparing the interior and exterior of the film. SEM images of the interior and exterior surfaces of films peeled away from plasma clots. Note differences in scale bars – Interior 3 μm, Exterior left 500 nm, right 50 nm. Data from Macrae et al. (2018).

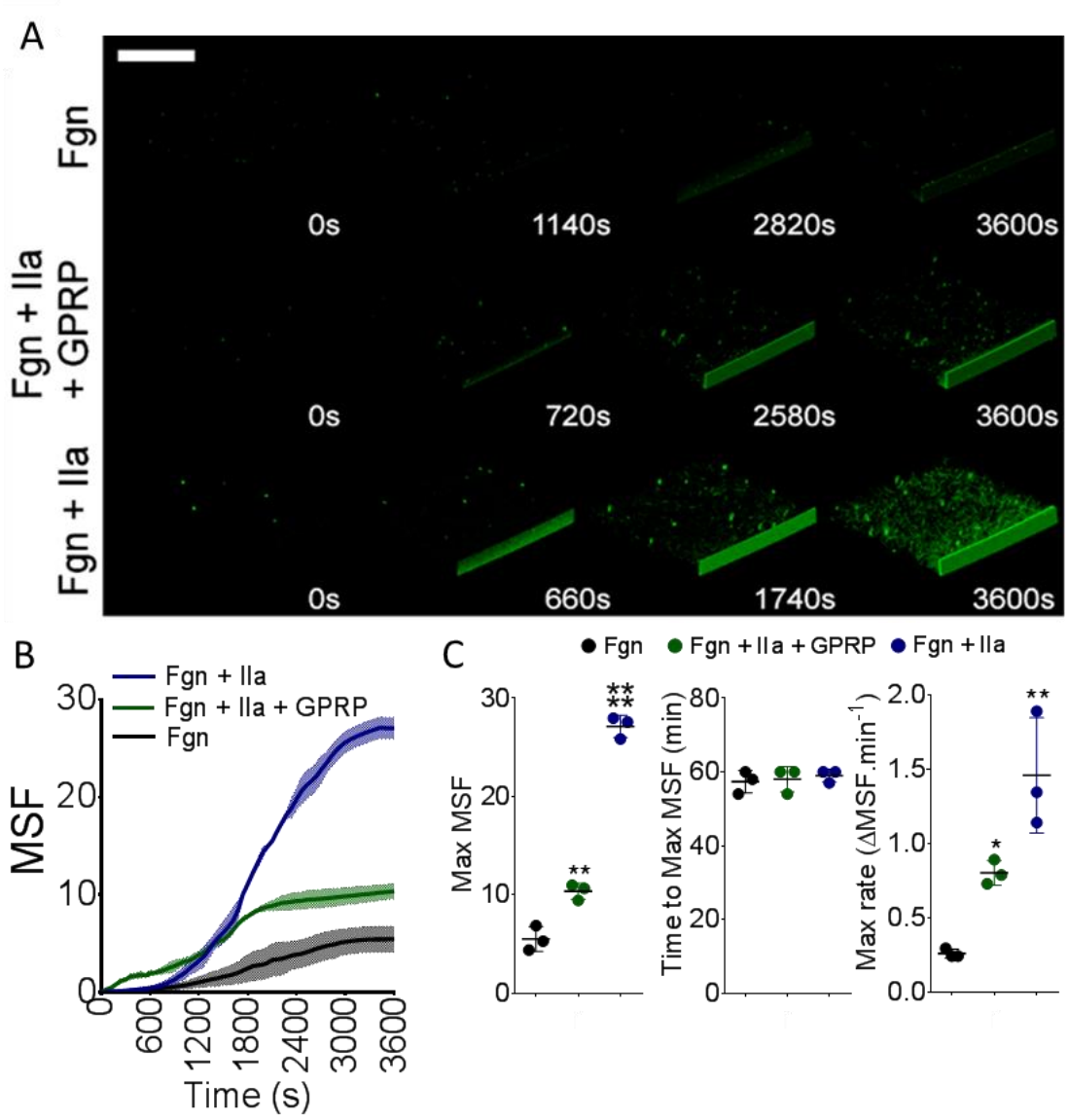

Figure 46 The effect of fibrin(ogen) polymerization of film formation in a purified system. A, Accumulation of fibrinogen, fibrin monomers (fibrinogen + IIa + GPRP) or polymerizing fibrinogen at the air-liquid interface in a purified system over time, imaged by LSCM. Images representative of n = 3 experiments. **B,** Accumulation of MSF of clots from purified fibrinogen over time, data shown as mean ± SD. **C,** Maximum MSF, n = 3 experiments, F = 330.7, df = 2, p < 0.0001, time to maximum MSF, n = 3 experiments, F=0.1875, df = 2, p = 0.8337, maximum rate of MSF increase, n = 3 experiments, F = 20.55, df = 2, p = 0.0021 as analysed by LSCM, data shown as mean ± SD. * represents difference from fibrinogen (black dots), * p < 0.05, ** p < 0.01, **** p < 0.0001. MSF –mean sheet fluorescence, IIa – thrombin, GPRP -Gly-Pro-Arg-Pro peptide, Fgn –fibrinogen. Scale bars - 50 μm. Data from Macrae et al. (2018).

With the interior surface looking so similar to a fibrous clot network, it was hypothesised that fibrin polymerisation may play a role in film formation. To assess this, accumulation of fibrin/fibrinogen below the surface of the air-liquid interface was followed over time by LSCM and the impact of polymerization on film formation was analysed. Time courses of polymerizing fibrin, fibrin monomers or fibrinogen alone spiked with Alexa Fluor-488 fibrinogen were followed in a purified system (1 $mg.ml^{-1}$ fibrinogen/fibrin) (Figure 46A).

Accumulation was quantified by MSF (Figure 46B). Purified fibrinogen accumulated at the air-liquid interface with a maximum rate of 0.26 ± 0.03 $MSF.min^{-1}$, reaching maximum fluorescence (5.5 ± 1.3 MSF) after 57.3 ± 2.1 min. Fibrin monomers had a maximum rate ~3-fold faster than that of fibrinogen (0.8 ± 0.8 $MSF.min^{-1}$), with twice as much protein accumulating at the surface (Max MSF – 10.4 ± 0.8) after 58 ± 1.5 min. Polymerizing fibrin accumulated at the surface at the greatest rate, with a maximum increase in fluorescence of 1.46 ± 0.39 min^{-1}, over 5-fold the rate of fibrinogen. It reached a maximum fluorescence (27.1 ± 1.1 MSF) after 59 ± 0.7 min (Figure 46C, Table 13).

Table 13 Mean sheet fluorescence of fibrin(ogen) accumulation at air-liquid interface. Table from Macrae et al., 2018.

Condition	Max MSF	SD	Time to Max MSF (s)	SD	Max rate of MSF increase (δMSF.min^{-1})	SD
Fibrinogen	5.5	1.3	3540	60	0.33	0.03
Fibrinogen + IIa + GPRP	10.4	0.8	3480	208	0.61	0.11
Fibrinogen + IIa	27.1	1.1	3540	104	1.46	0.39
Plasma	3.3	0.2	3560	69	0.19	0.04
Plasma + IIa + GPRP	8.4	0.8	3380	330	0.59	0.16
Plasma + IIa	20.2	1.1	3520	139	0.87	0.04

GPRP – Gly-Pro-Arg-Pro peptide, IIa – thrombin, MSF – mean sheet fluorescence, SD – standard deviation

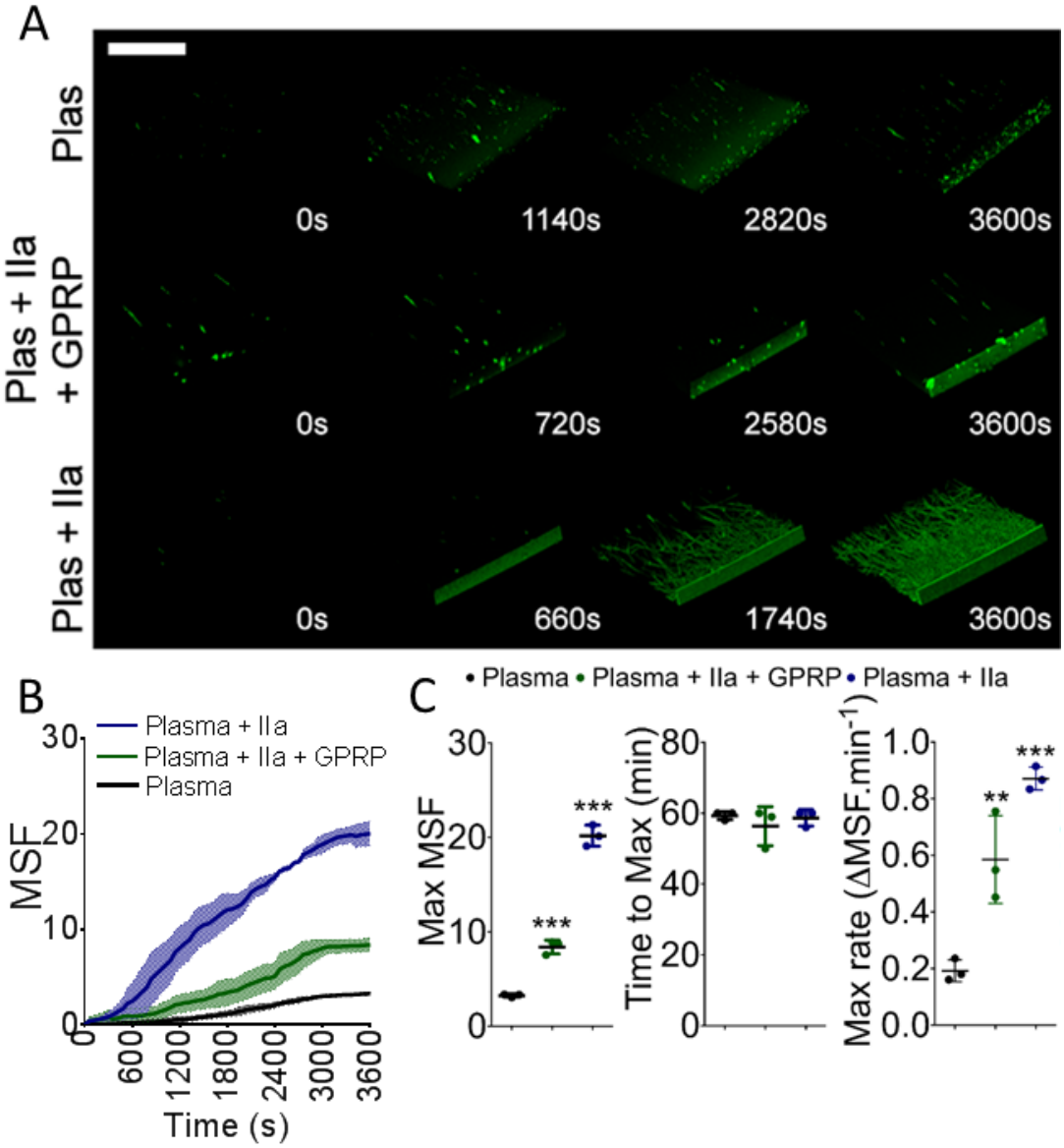

Figure 47 The effect of fibrin(ogen) polymerization of film formation in plasma. A, Accumulation of fibrinogen, fibrin monomers (plasma + IIa + GPRP) or polymerizing fibrinogen at the air-liquid interface in a plasma system over time, imaged by LSCM. Images representative of n = 3 experiments. **B,** Accumulation of MSF of plasma clots over time, data shown as mean ± SD. (n = 3 experiments) **C,** Max MSF, F = 370.2, df = 2, p < 0.0001, time to max MSF, F = 0.6036, df = 2, p = 0.5770 and maximum rate of MSF increase, F = 38.51, df = 2, p = 0.0004, data shown as mean ± SD, n = 3 experiments. * represents difference from fibrinogen (black spots), ** p < 0.01, *** p < 0.001. MSF – mean sheet fluorescence, IIa – thrombin, GPRP - Gly-Pro-Arg-Pro peptide, Plas – Plasma. Scale bars - 50 μm. Data from Macrae et al. (2018).

A similar pattern was seen in plasma with polymerizing fibrin accumulating at the surface quicker than fibrin monomers and fibrinogen (Figure 47A-C, Table 13). This indicates that fibrin polymerization contributes to film formation by enhancing the accumulation of fibrin at the air-liquid interface. This effect is likely due to a combination of stronger interactions between the molecules of fibrin versus fibrinogen, and an increase in hydrophobicity of fibrin (van Oss, 1990, Weisel, 2005), both of which retain it at the surface.

The strength of the film was quantified using AFM, carried out by Dr Stephen Baker. Young's Modulus was calculated for plasma samples with and without transglutaminase inhibitor T101 by fitting a Sneddon model for conical tips to all force curves found over the entire area that was imaged (Figure 48A-B). Fibrin fibres were visible under the film surface and these areas presented with much stiffer Young's modulus than places suspended between fibres. To find the stiffness of the film alone, Young's Modulus was determined by measuring areas between the underlying fibres of clots formed from plasma. The average Young's Modulus of the film was ~3-fold lower than regions supported by fibres (suspended- 7.65 ± 0.24 kPa vs fibre - 21.79 ± 2.79 kPa, $p = 0.0001$). Inhibition of cross-linking with T101 decreased the modulus of the suspended film further by just over 10-fold to 0.72 ± 0.14 kPa, which is slightly more than the decrease in fibrin stiffness previously reported in whole clots and single fibres (2-8.5x) (Collet et al., 2005, Koh and DiPietro, 2011, Liu et al., 2010, Shen and Lorand, 1983). Areas supported by fibrin fibres decreased just over 4-fold to 5.1 ± 0.75 kPa in the absence of cross-linking (Figure 48C). As a consequence, although fibrin crosslinking is not required for film formation (Figure 39B), it increases film elastic modulus.

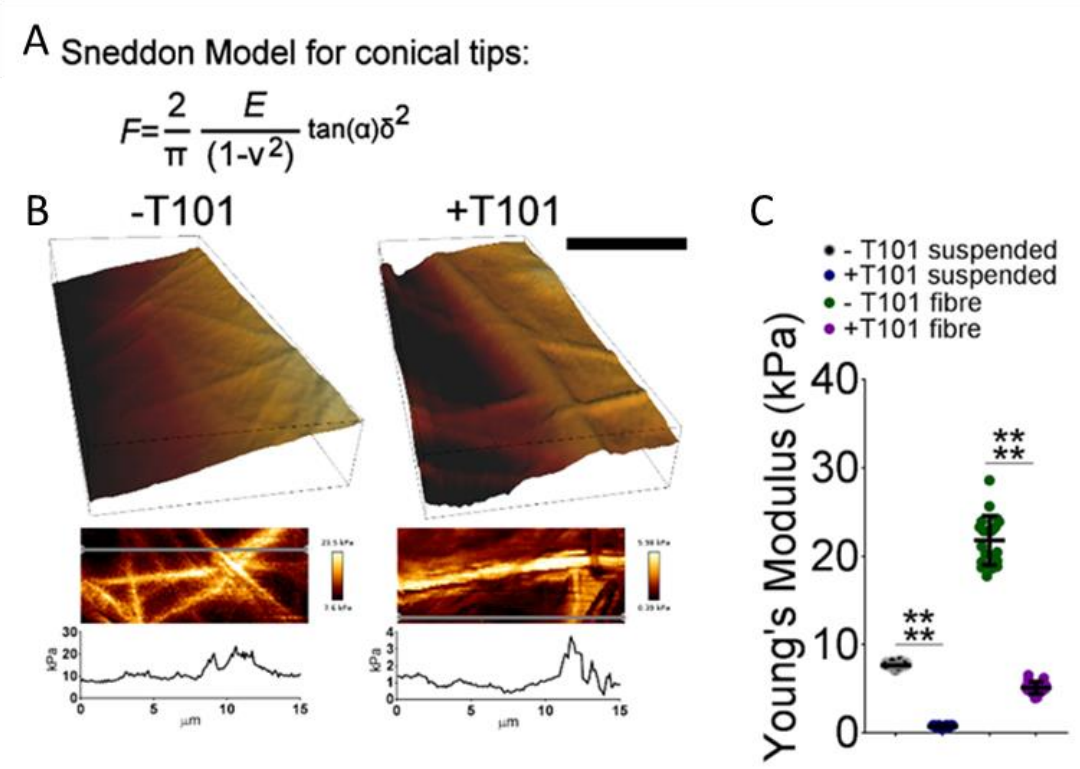

Figure 48 Investigating the strength of the film. A, Sneddon model used to calculate Young's Modulus, where F is the force from the force curve, E is Young's modulus, *v* is Poisson's ratio (0.5), α is the half angle for the indenter (15 degrees for our tips), and δ is the indentation. Note that this equation is only accurate with a half angle of 15 degrees for the first 200 nm of indentation. **B,** Strength of the fibrin film in clots produced with plasma and thrombin with or without T101 (FXIII inhibitor) investigated using atomic force microscopy (AFM). Fibrin fibres were visible under the film surface and these areas presented with stiffer Young's modulus than fibrin film suspended between fibres. Grey lines in the zoomed-in images represent Young's modulus scan area represented in the line force graphs. Scale bar -2 μm. **C,** Young's Modulus was calculated for the suspended film and the film supported by fibres with and without T101 by fitting a Sneddon model to all AFM force curves found over the entire area that was imaged. 20 measurements were taken for each condition. **** $p < 0.0001$. Data from Macrae et al. (2018).

Given that fibrin accumulates at the air-liquid interface, it was hypothesised that film formation should be preventable by blocking the air interface with surfactant molecules. In agreement with this, the addition of tween-20 (0.1 %) prevented film formation and resulted in a dense, partly collapsed clot, probably due to the loss of surface tension (Figure 49A). Furthermore, blocking the air-liquid interface using mineral oil or petroleum jelly also prevented film formation (Figure 49B-C).

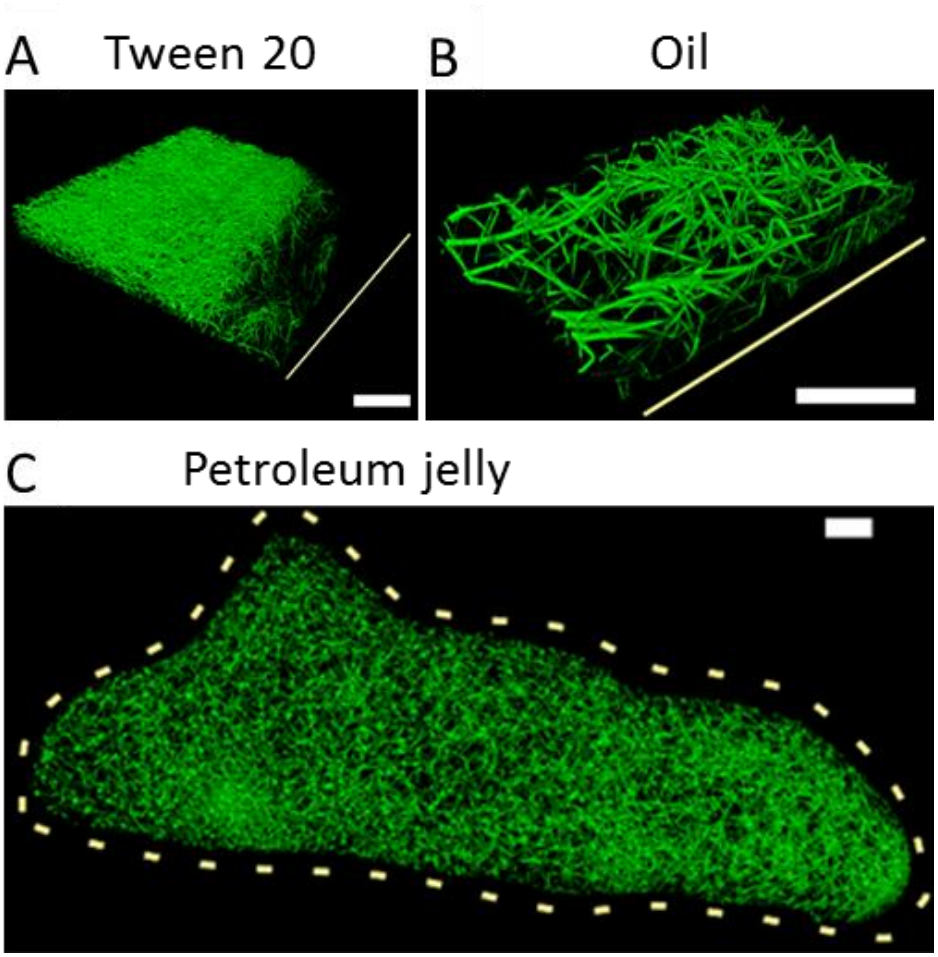

Figure 49 Blocking the air-liquid interface prevents film formation. Clots produced from plasma with thrombin in the presence of different surfactants and imaged by LSCM. **A,** tween-20 (0.1 %). **B,** Oil. **C,** Petroleum jelly. Yellow line represents the location of the air-liquid interface. Images representative of n = 3 experiments. Scale bars – 50 μm. Data from Macrae et al. (2018).

Based on the Langmuir-Blodgett data (Figure 43) and accumulation data (Figure 46 and Figure 47) a model of film formation is proposed (Figure 50A) where, upon injury and exposure to air, fibrinogen molecules in the blood are rapidly adsorbed to the air exposed surface, forming an organized monolayer at the air-liquid interface. Simultaneously, tissue factor stimulates fibrinogen cleavage via thrombin, leading to fibrin formation. Fibrin(ogen) continues to rise and accumulate at the air-liquid interface, packing in more molecules. At the same time fibrin begins to fit together in a half-staggered

formation, allowing for the build-up of multiple layers of fibrin through A:a and B:b knob-hole interactions, and the formation of tethering fibres (Figure 50A-C). This leads to a dense layer of fibrin across the surface of the clot.

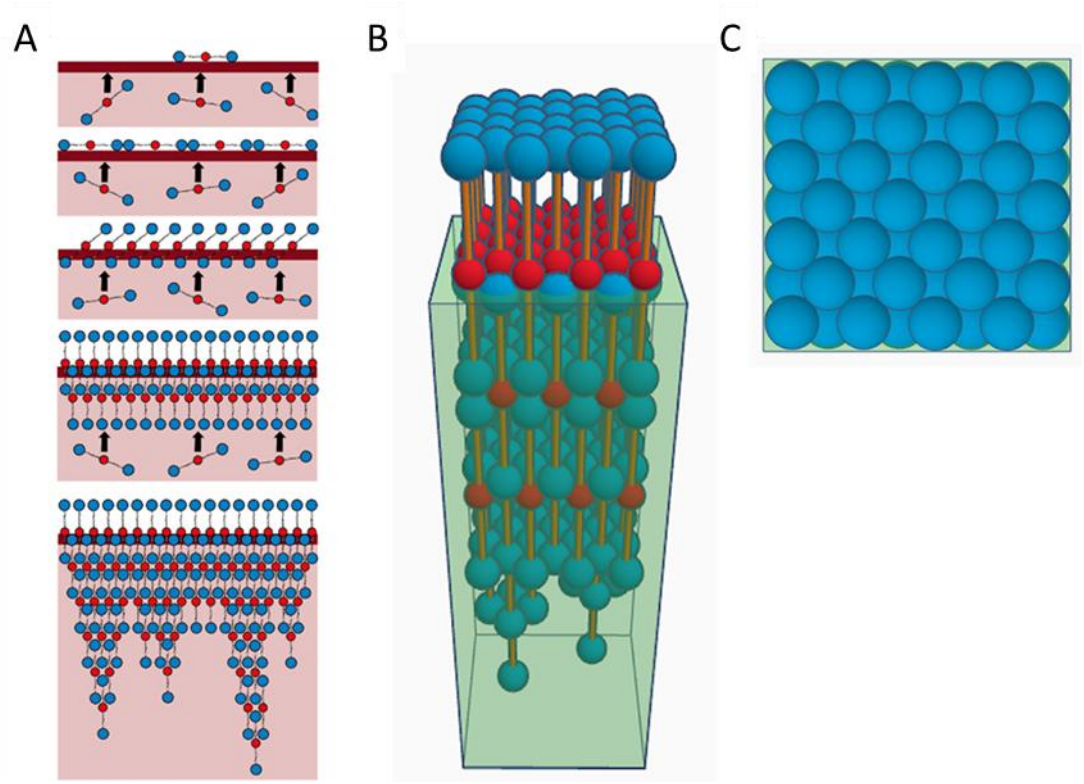

Figure 50 A model of fibrin film forming at the clot surface. A, Proposed 2D model of fibrin(ogen) rising to the air-liquid interface and accumulating into a multi-layer film with half-staggered fibrin molecules and tethering protofibrils (beginning of fibrin fibres). **B,** A side-on view of a 3D model of the fibrin film with half-staggered fibrin molecules. D-regions are represented by 6.7 nm diameter blue spheres, E-regions are represented by 5.3 nm diameter red spheres and the connecting α-, β- and γ-chains are represented by an orange cylinder. The translucent box represents the liquid at the air-liquid interface **C,** Top view of the 3D fibrin film model. Data from Macrae et al. (2018).

4.3 Discussion

This chapter demonstrates that fibrin produces a continuous film at the interface between the clotting blood and the air that encapsulates the clot. The structural characteristics of this fibrin film are completely different from those of the fibrin fibre network. Rather than forming a porous network of fibres, these films are made up of tightly packed molecules arranged perpendicular to the liquid-air interface. The film only requires fibrin to form, producing a continuous layer of fibrin that is connected to the fibrous fibrin network through tethering fibres. Film formation is initiated by the exposure of blood to the air interface and accumulates due to the conversion of fibrinogen to fibrin, and the resultant increase in hydrophobicity of the fibrin molecule (Weisel, 2005, van Oss, 1990). The unique fibrin polymerization mechanisms, which involve knob-hole interactions, lead to fibrin being able to produce both films and fibres (O'Brien et al., 2008), and this culminates in a remarkable integrated clot structure that includes a fibrin film covering a network of fibres. The thickness of the film was modulated by multiple conditions, such as thrombin concentration, [Ca^{2+}], fibrinogen concentration, fibrinogen variants and temperature, and it was shown to be digested by plasmin, which typically is responsible for fibrinolysis of fibrin clots. The internal and external surfaces of the film have been characterized using SEM, showing a very smooth external face and a more porous and fibrous internal face. Mechanisms of film formation were elucidated with the use of a Langmuir-Blodgett trough, using changes in surface pressure to quantify the maximum amount of protein that could fit at the air-liquid interface. This was followed by calculations of molecular dimensions of the film and the

orientation of molecules. Formation of the film was followed as a function of time using confocal microscopy, showing that fibrin accumulates at a much faster rate than fibrinogen. Strength of the film was tested using atomic force microscopy in the presence and absence of FXIIIa activity. FXIII was found to stabilize the film highlighting the contribution of crosslinked fibrin in the structural integrity of films. The formation of the film was shown to be prevented by blocking or disrupting the blood-air interface with surfactants or oils, indicating the importance of the alignment of fibrin at the air-liquid interface in film formation. This finding transforms our understanding of blood clots at injury sites and sheds new light on a major enigma — how the clot ends at the air-blood interface — that has troubled the field for a long time.

This study was originally motivated by observations from SEM revealing thin film-like structures on the surface of blood clots. This film has previously been observed in our laboratory and those of others in SEM images of blood, plasma, or fibrin clots for more than two decades. However, until now, it has been overlooked, as it was alleged to be an artefact of sample preparation. The close association of fibrin clot structure with thrombosis risk (Undas and Ariens, 2011, Ariens, 2016, Bridge et al., 2014) has led researchers to focus on areas of the clot not covered by the fibrin film, i.e., away from the clot-air interface, or in areas where the film may have ruptured during sample processing. Previous studies have also shown that fibrin is able to produce sheet-like structures, across gaps in a striated substrate, for example (O'Brien et al., 2008), or in blood clots (Pretorius et al., 2012). However, researchers have failed to highlight the physiological relevance of these structures and the mechanism of formation were not

explored. In addition to the previous sightings of these film-like structures, Langmuir film formation has been recognized for over 100 years as a common phenomenon with most or all protein solutions forming monolayers at air-liquid interfaces (Langmuir, 1917). However, fibrin film formation appears to expand on this mechanism, resulting in the accumulation of multiple layers of protein at the surface, due to the conversion of fibrinogen to fibrin and its subsequent polymerisation.

So far only a model of film formation can be proposed. The model puts forward the idea that upon cutaneous injury fibrinogen molecules in the blood are rapidly adsorped to the air liquid interface, forming an organized monolayer through a biophysical mechanism similar to Langmuir film formation (Zasadzinski et al., 1994). Simultaneously, haemostatic pathways are activated and thrombin cleaves fibrinogen to fibrin. More fibrin continues to move to and pack together at the surface, forcing the molecules perpendicular to the air-liquid interface, forming a dense and tightly packed sheet. At the same time fibrin molecules begin to fit together in a half-staggered formation, allowing for the build-up of multiple layers through knob-hole interactions. These interactions also allow for the film to connect to the underlying network through tethering fibres. More information is required on the precise structure of these films. The orientation of the molecules at the air liquid interface was deduced from Langmuir-Blodgett trough data. Attempts to take high definition images of the surface of the film were attempted using AFM, hoping to demonstrate the presence of fibrin D domains which would fit with our model. Unfortunately problems were encountered due to the stickiness of the films, preventing high definition imaging with the AFM tip. Other structural data that should be obtained

would include more precise thicknesses of the films, possibly obtained using transmission electron microscopy, AFM imaging with functionalised (E- or D-region, GPRP) tips, information on the contribution of other proteins to the films arrangement and finally the contribution of the film to clot contraction.

Naming of these structures as fibrin biofilms may result in some potential confusion. The term “fibrin films” in the past has been used to describe fibrin clots that have been compressed and have been used as a sealant for wound healing and other surgical procedures (Matras, 1985). On top of this the term “biofilms” in the past has been used to refer to colonies of bacteria that form a thick layer on many surfaces and provide protection to the bacteria. Therefore the name fibrin biofilm is perhaps not ideal, but it was chosen to be used until a better proposal is made.

The findings in this chapter raise many questions about what this film is for and if it plays a role in haemostasis, and this will be discussed in the next chapter.

Chapter 5 - The physiological roles of the fibrin film

The obvious questions that arose after finding the fibrin film (described in Chapter 4) that covers the external surfaces of haemostatic clots is, what is its physiological function? Many characteristics of the film described in the previous chapter lend themselves towards having some form of physiological role. Its rapid formation, before the underlying network, and changes in film thickness instigated by changes in clotting conditions all point to it playing a part in the early stages of clotting. Furthermore, the organised nature of the fibrin molecules, the density of protein at the surface, and the smoothness of the film with very small pores also suggest that the film may contribute to cell and fluid containment or as a protective covering. In this chapter the reasons for film formation are explored highlighting how it provides a natural limit to clot growth, prevents blood cell loss, and protects from bacterial infection.

5.1 Film protects against microbes

In view of the rapid formation of the fibrin film after exposure of blood to an air-liquid interface, it was theorised that the film may play an important physiological role, forming an immediate barrier across an injury to protect the vascular breach against microbial invasion, until white blood cells are recruited to the wound site (Velnar et al., 2009). To investigate this hypothesis, a bacterial migration assay in a Boyden chamber was used to study migration of three types of bacteria commonly found in the natural skin flora (*Escherichia coli*, *Staphylococcus epidermidis and Staphylococcus aureus*) through clots (chapter 2.4.1 and Figure 16). Bacteria were grown to 3.6-8.5 $x10^8$ $cells.ml^{-1}$, fluorescently-labelled with BacLight green, and applied to the external surface of three types of clots: 1) clots formed with

0.1 % tween-20 to prevent film formation, 2) clots where the surface was perforated with a needle to make holes in the film and 3) normal clots with intact film.

Fluorescent bacteria that moved through the clots were quantified over 48 hours (Figure 51A). The time taken for the first bacteria to break through the clots was defined as when fluorescence became greater than 2 % of the total added fluorescent bacteria. No fluorescent bacteria migrated through the clots within the first 8 hours. *E.coli* migrated through the perforated (11.3 ± 1.2 hours, $p = 0.0005$) and tween-20 treated clots (25.3 ± 1.2 hours, $p = 0.0193$) significantly faster than the normal clots (38.0 ± 7.2 hours) (Figure 51B). A similar trend was seen with *S. epidermidis* (perforated - $p = 0.0022$, tween-20 - $p = 0.0075$) and *S. aureus* (perforated - $p = 0.0076$, tween-20 - $p = 0.0401$, Figure 51B), with bacteria moving through perforated and tween-20 treated clots much quicker than in clots with an intact film. After the initial breakthrough, the rate of bacteria migration was comparable between clot types. This suggests that the film plays a role in preventing bacterial infiltration into the site of injury for at least 12-27 hours, allowing time for white blood cell recruitment and the underlying clot to fully form.

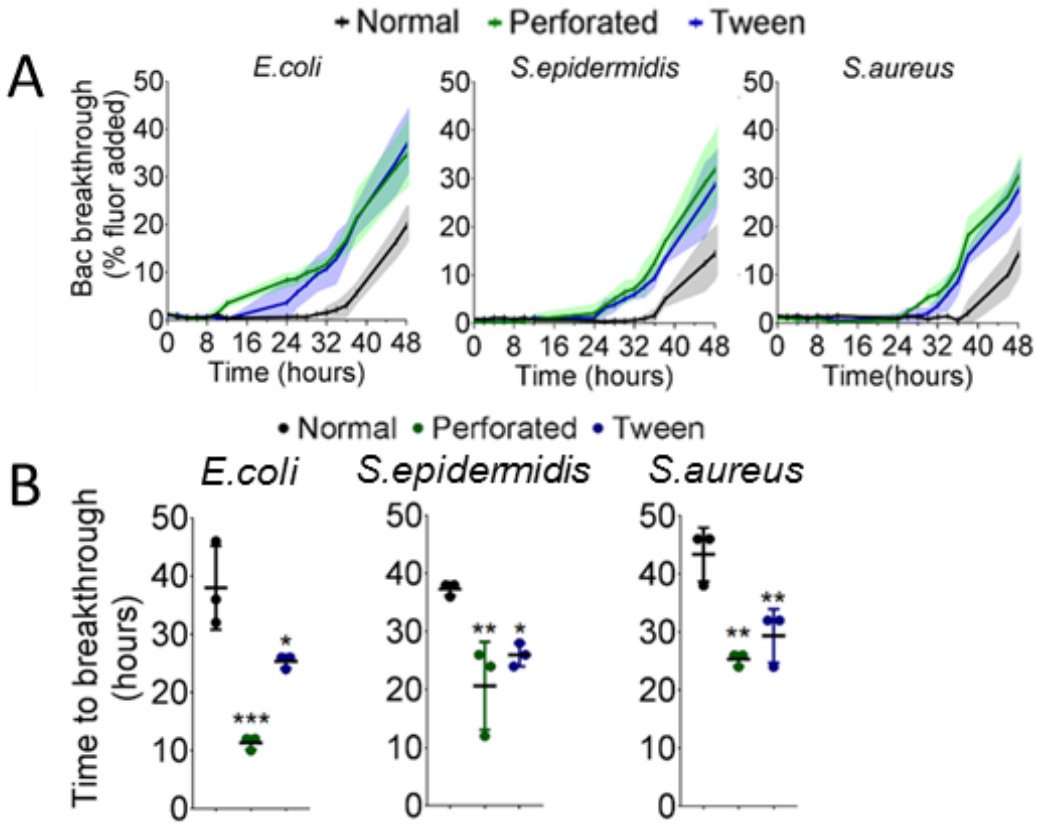

Figure 51 Film slows bacterial migration. A, Movement of fluorescently labelled *E. coli*, *S. epidermidis* and *S.aureus* bacteria through three types of clot, (displayed as quantity of fluorescent bacteria breaking through the clot as a percentage of fluorescent bacteria added) with three different film conditions; normal, perforated or removal with tween-20. **B,** Time taken for the first fluorescently labelled *E. coli, S. epidermidis* or *S. aureus* bacteria to break through the clot. * represents difference from normal clot. * $p < 0.05$, *** $p < 0.001$, n = 3 experiments, one-way ANOVA. Bac – Bacteria. Data from Macrae et al. (2018).

5.2 Fibrin film formation and its role in blood cell retention

To investigate the function of the film *in vivo*, a novel murine dermal injury model was established. Initially, the formation of the fibrin film *ex vivo* in mouse blood was investigated. Clots were formed with whole blood from WT or fibrinogen-deficient mice and were prepared for SEM. Blood from WT mice formed a fibrin film at the air-liquid interface, whereas blood from fibrinogen-deficient mice did not (Figure 52).

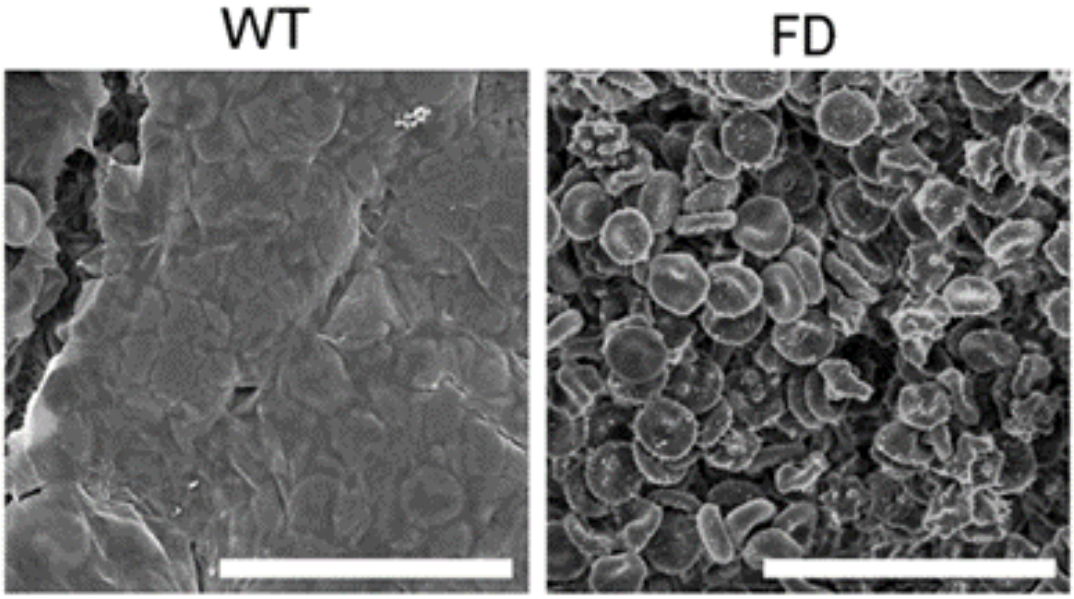

Figure 52 *Ex vivo* film formation in wildtype and fibrinogen deficient mice. Clots formed using whole blood and murine thrombin from wildtype and fibrinogen-deficient mice were imaged by SEM. Images representative of n = 4 mice. Scale bars – 20 μm. FD – fibrinogen deficient mice. Data from Macrae et al. (2018).

A murine dermal injury model was established next, in which a 2 mm puncture was created in the skin on the back or abdomen of anaesthetised mice. The *in vivo* work was carried out by Dr Cedric Duval. The injury was either left clear to clot exposed to the air or immediately covered with a thin layer of oil to remove the air-liquid interface, which was washed off with saline once the clot had formed. After 60 minutes, clots and surrounding skin were surgically removed, processed, and imaged by SEM (Figure 53A). In the untreated control sections, clots possessed a film on the exterior surface. Consistent with the *in vitro* experiments, oil treatment prevented film formation, leaving the underlying fibrous fibrin network exposed and clearly visible. Some of these clots were embedded in paraffin, sectioned, and were either stained using MSB or probed with a fibrin specific antibody (59D8). In the untreated control sections stained with MSB the film can be seen along the surface of the clot, as a thin pink layer (Figure 53B), or as a thin brown

layer with 59D8 staining, confirming that fibrin makes up the film *in vivo* (Figure 53C). In clots treated with oil, the film is not present. This showed that the oil prevented film formation *in vivo* and could be used to assess bacterial migration and proliferation in clots without a film.

During the establishment of the *in vivo* model, regions of loose cells that were not retained within the clot were found in histology sections of clots formed in the presence of oil, and therefore lacking the film (Figure 54A). In micrographs of the control clots we found erythrocytes pushed against the inside of the film (Figure 54B). These findings suggested the fibrin film helps to prevent leakage of blood cells from dermal lesions. To investigate this, clots from whole blood were formed either with no intervention, in the presence of tween-20 (0.1 %) or with the film being perforated after 1 hour. After two hours, the quantity of RBCs released from the clot was assessed by measuring haemoglobin levels. The quantity of haemoglobin released was more than 12-fold higher in the tween-20 (4.37 ± 0.38 $g.L^{-1}$) and perforated clots (4.14 ± 0.85 $g.L^{-1}$), with almost no haemoglobin being released from the normal clot (0.32 ± 0.18 $g.L^{-1}$, $p = 0.0002$, Figure 35C). This data shows that the film plays a role in the retention of RBCs within the clot.

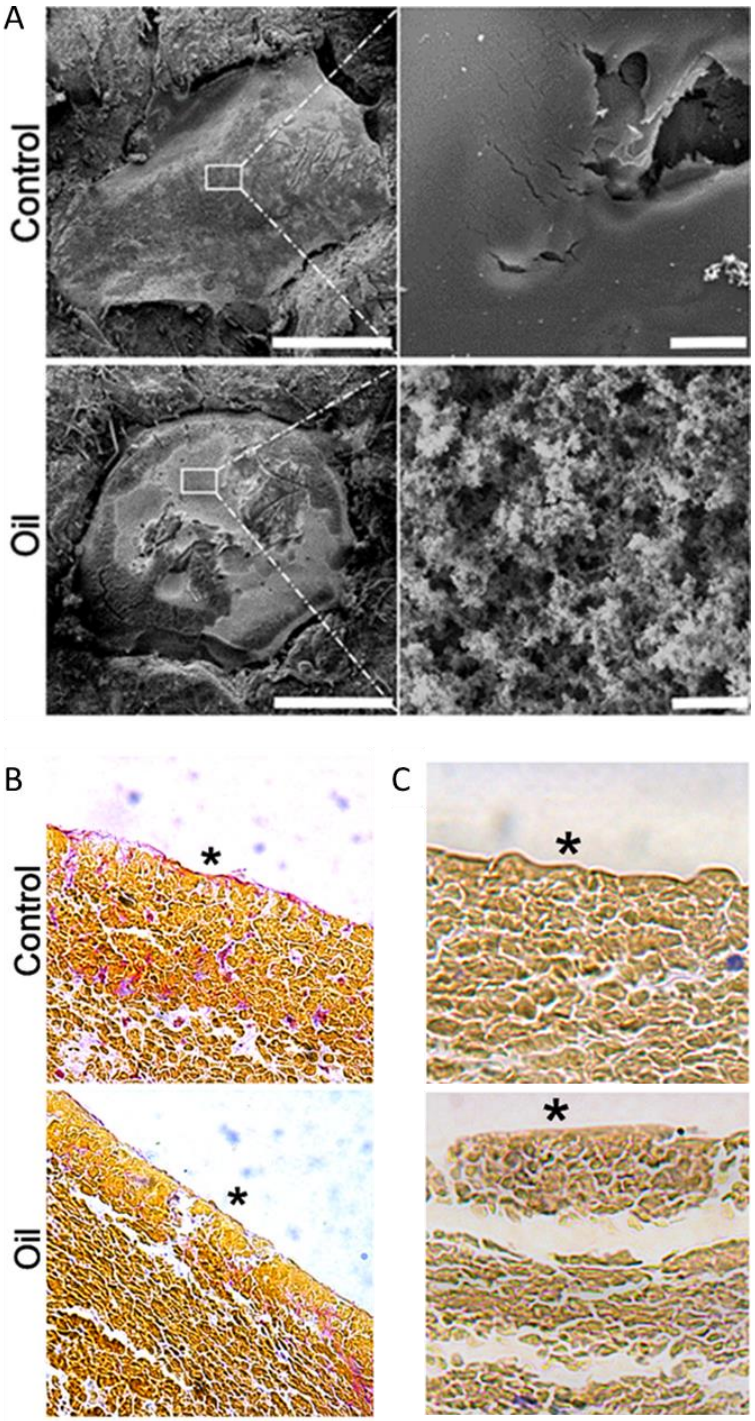

Figure 53 Fibrin film forms *in vivo*. A, Clots were formed in a ventral or dermal puncture injury model in mice and left clear or covered with a thin layer of mineral oil, fixed, dehydrated and imaged by SEM. The white box represents the area of magnification for the image to the right. Images are representative of n = 4 mice. Scale bars – left 1 mm, right 2 µm. **B,C,** Clots left clear or with a layer of oil covering the surface from the dermal puncture model were surgically removed, and cross-sections were stained with: **B,** Martius, Scarlet and Blue (MSB; erythrocytes in yellow, and fibrin in pink). Fibrin film shows as continuous pink layer, clot appears yellow interspersed with pink. Or **C,** stained with mouse anti-fibrin antibody (59D8). In the absence of oil, a brown layer can be seen along the surface of the clot, showing fibrin is present in the film. This layer was absent in clots formed with oil. * highlights air liquid interface. Images representative of n = 4 mice. Data from Macrae et al. (2018).

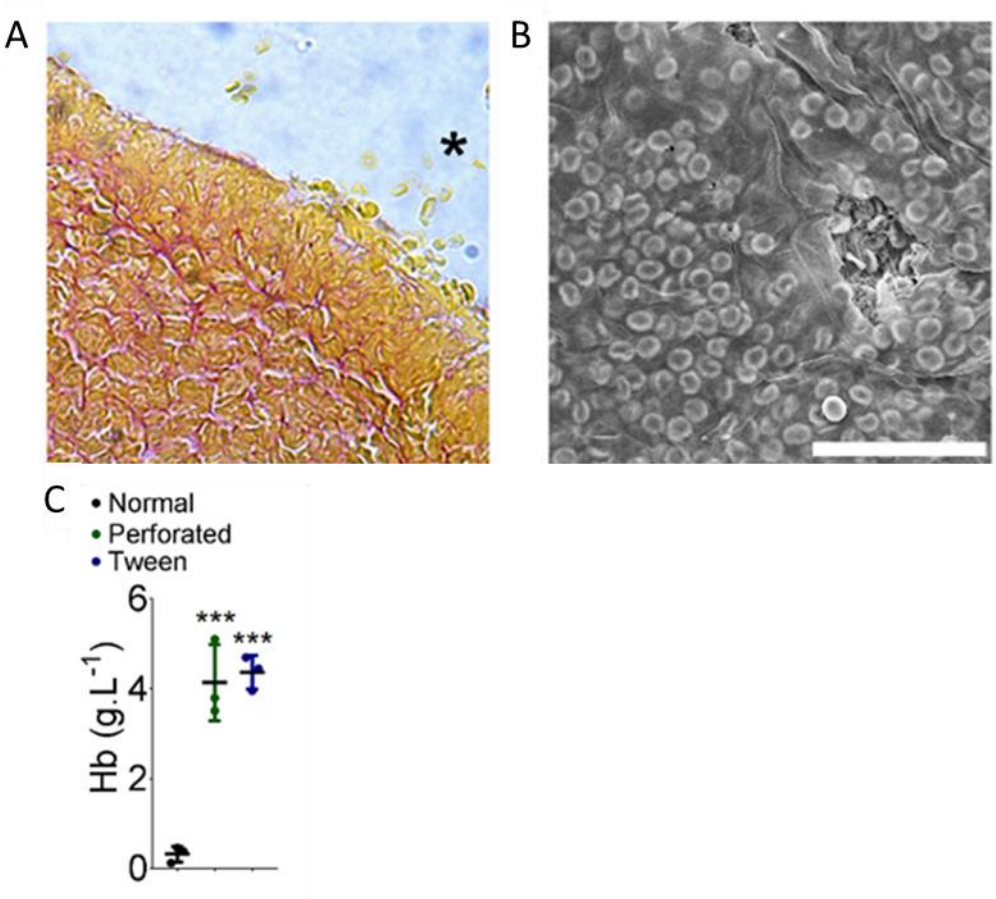

Figure 54 Fibrin film helps retain blood cells within the clot. A, Clots from the murine dermal puncture model covered with oil showed extrusion of red blood cells from the clot in the absence of a fibrin film. * highlights extrusion of red blood cells from the clot. Images representative of n = 4 mice. **B,** Clots produced with human whole blood and thrombin, and imaged by SEM demonstrated containment red blood cells by the fibrin film. Images representative of n = 3 individuals. Scale bar – 40 µm. **C,** Haemoglobin retention assay in normal, perforated and tween-20 treated clots. * represents difference from normal clot. *** $p < 0.001$, n = 3 individuals, one-way ANOVA, $F = 52.14$, $df = 2$, $p = 0.0002$. Hb – haemoglobin. Data from Macrae et al. (2018).

5.3 Protective role of fibrin film in a murine dermal injury model

The role of the fibrin film in protection against bacterial proliferation and dissemination *in vivo* was investigated next. This work was carried out by Dr Cedric Duval and Dr Praveen Papareddy at the University of Lund. After the clots were formed as described above (with or without a layer of oil), 2 µl of

bioluminescent *Pseudomonas aeruginosa* (4 x10^5 CFU), a Gram-negative flagellated bacterium associated with severe hospital-acquired infections and significant resistance to antibiotics, were carefully deposited on the surface of the clots covering the dermal punctures. Mice were imaged every 4 hours using a three-dimensional IVIS spectrum *in vivo* imaging system to assess bacterial proliferation. Control experiments were run in parallel where wounds with no clots were subjected to a layer of oil or were left clear to demonstrate oil had no effect on bacterial proliferation. In the absence of a clot, the oil had no effect on the levels of bacteria present in the wound over 12 hours (Figure 55A-B).

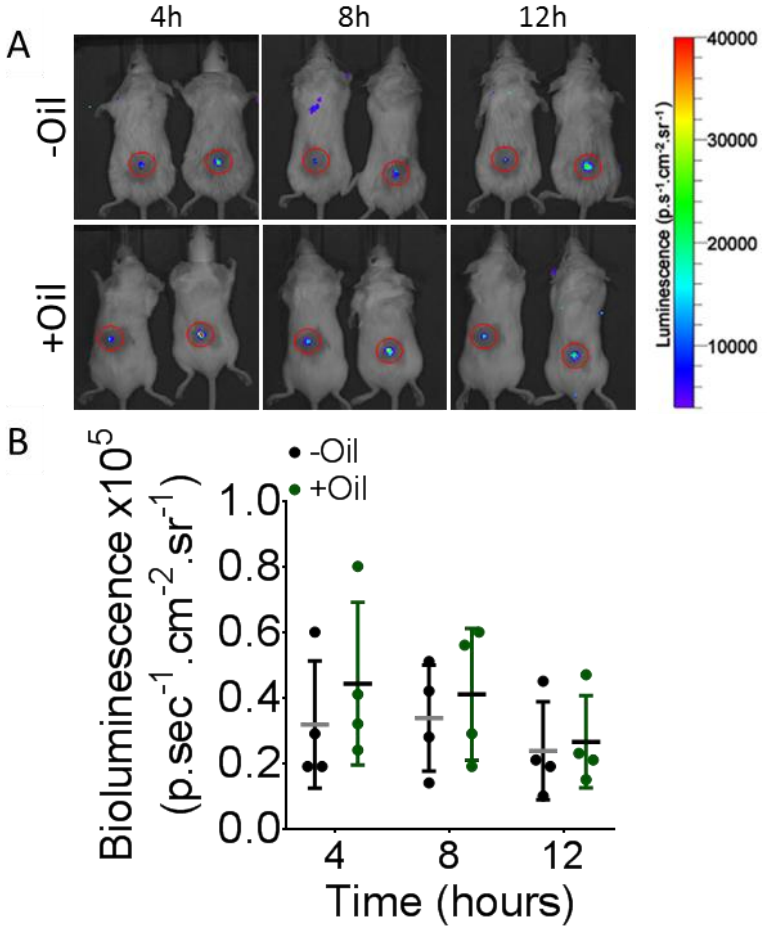

Figure 55 In the absence of a blood clot oil has no effect on bacteria number. **A,** Measurement of bioluminescent bacteria proliferation with no clot present with or without oil in a murine dermal injury model over time. Images representative of n = 4 mice. **B,** Quantification of bioluminescent bacteria in this model, n = 4 mice.

Once it was established that the oil had no effect on bacteria proliferation, experiments on mice with blood clots in their wounds were carried out. In the mice with an intact fibrin film, the bioluminescence did not increase over 12 hours, showing that the bacteria did not proliferate over this period in these mice. This also suggests the bacteria did not disseminate into the clot because, in mice without a fibrin film the bioluminescence was significantly higher after 4 hours and increased over time up to 1.03 $x10^5$ $p.sec^{-1}.cm^{-2}.sr^{-1}$ (IQR – 0.470, 0.359), compared to 0.15 $x10^5$ $p.sec^{-1}.cm^{-2}.sr^{-1}$ (IQR - 0.107, 0.371, $p = 0.0005$) in the mice with films (Figure 56A-B, Table 14). These data show that the bacteria had moved into the clot and were proliferating within the wound in the absence of the film. To confirm the difference in bacteria numbers, the clots and surrounding skin were harvested from sacrificed animals after 12 hours and mechanically homogenised. Serial dilutions of the homogenates were plated on agar to analyse bioluminescence and bacterial CFUs (Figure 56C-D). In agreement with the bioluminescence data, the mice that had no film on their clot showed a much greater number of bacteria (2.53 ± 0.298 $x10^6$ $CFU.ml^{-1}$) within the wound and skin than the mice that had an intact clot film (0.064 ± 0.014 $x10^6$ $CFU.ml^{-1}$). These data demonstrate that the film has a protective role, slowing or preventing the proliferation of bacteria and reducing the movement of bacteria into wounds and skin for at least 12 hours after injury.

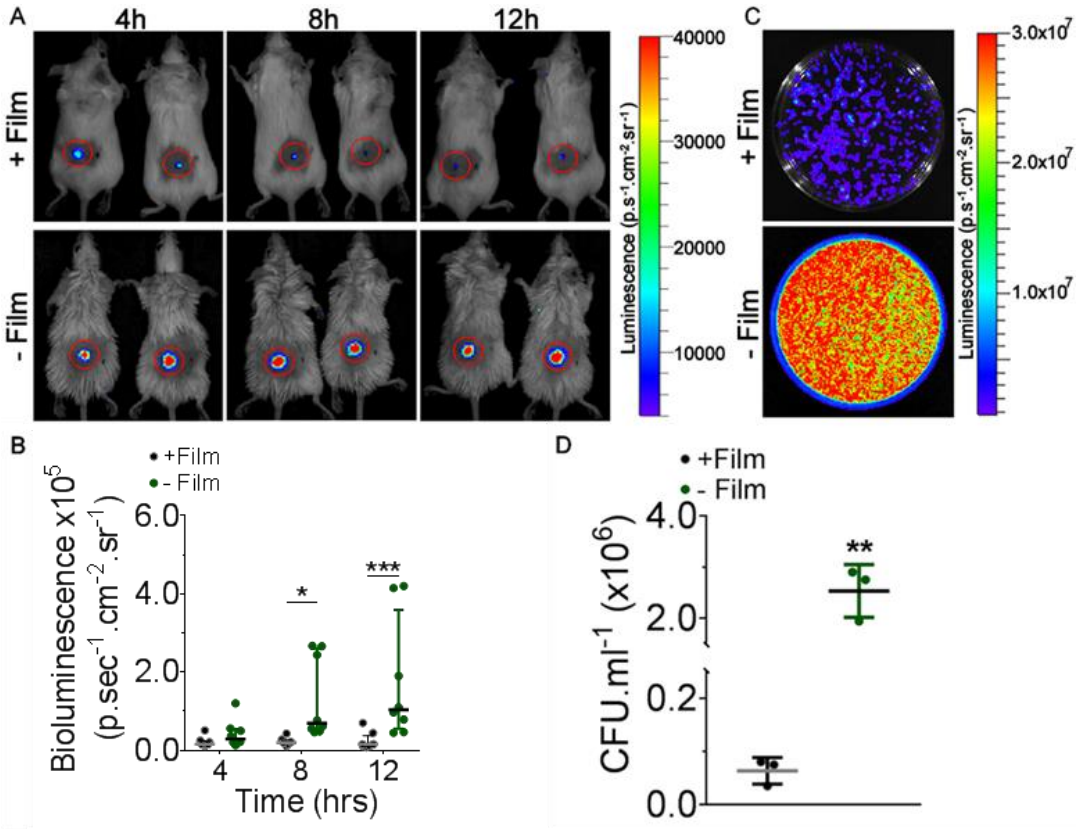

Figure 56 Fibrin film slows bacteria proliferation and dissemination *in vivo*. A, Measurement of bioluminescent bacteria proliferation with or without film in a murine dermal injury model over time. Images representative of n = 8 mice **B,** Quantification of bioluminescent bacteria in this model. * $p < 0.05$, *** $p < 0.001$, n = 8 mice, Kruskal-Wallis test, Kruskal-Wallis statistic = 36.55, 6 groups, $p < 0.0001$. **C,** Measurement of bioluminescent bacteria from wound and surrounding skin with and without film after 12h spread on agar plates. Images representative of n = 3 mice **D,** CFU/ml of bacteria from wound and surrounding skin with or without film after 12h. ** $p < 0.01$, n = 3 mice, Unpaired student's t-test for pairwise comparisons, t = 8.26, df = 4, p = 0.0012. CFU – colony forming unit. Data from Macrae et al. (2018).

Table 14 Bacterial proliferation measured by bioluminescence. Table from Macrae et al. (2018).

Condition	Biolumiescence x10^5 p.sec^{-1}.cm^{-2}.sr^{-1}	IQR (25,75%)	p value	Kruskal-Wallis statistic	Number of groups
4 hours					
+ film	0.152	0.147, 0.236	>0.999	28.11	6
- film	0.285	0.196, 0.541			
8 hours					
+ film	0.193	0.165, 0.259	0.046		
- film	0.690	0.500, 2.605			
12 hours					
+ film	0.151	0.107, 0.371	0.002		
- film	1.034	0.470, 4.200			

Data shown as median, IQR – Interquartile range

5.4 Discussion

This chapter shows that fibrin films form *in vivo* and play an unexpected role in haemostasis, producing a film that not only encapsulates the clot and thereby retains cells, but also functions as a protective layer at the interface between the clotting blood and the air, preventing microbial infection.

There have been many previous links between haemostasis and innate immunity due to their common evolutionary ancestry as a rapid response system in the event of a physical injury (Krem and Di Cera, 2002). Extensive crosstalk between the coagulation cascade and the complement cascade allows for an arrangement where the host responses can be amplified or dampened in both systems, coordinating blood coagulation with infection control (Esmon, 2004, Foley and Conway, 2016). The outcome of this relationship between the two cascades has been termed "immunothrombosis"; and this involves the formation of the fibrin clot and activation of white blood cells and platelets, which all come together to recognize, compartmentalize and trap pathogens (Engelmann and Massberg, 2013). The importance of the fibrin clot in this process was highlighted in previous studies with mice lacking fibrinogen, and mice that possessed a mutant fibrinogen that could not polymerize to form fibrin clots. These mice had decreased survival due to impaired bacterial clearance (Prasad et al., 2015, Degen et al., 2007). The fibrin network appears to act through two mechanisms: 1) as a physical barrier to bacterial invasion; and 2) fibrin(ogen) can activate a number of immune and inflammatory cells, such as neutrophils at a site of injury (Foley and Conway, 2016). In opposition to this, some bacteria have developed the ability to specifically

bind fibrin to evade innate immune surveillance and form resistant bacterial biofilms (Degen et al., 2007).

The previously overlooked fibrin film structures in this thesis present another mechanism for antimicrobial protection and suggests a novel mechanism of collaboration between the haemostatic and immune systems. In response to external injury, the fibrin film forms an almost instant barrier that provides an initial line of defence against microbial invasion, allowing the formation of an underlying clot and activation of immune system. This is supported by the formation of thicker films at lower thrombin concentrations which are present in the early stages of haemostasis. To show these films function as bioprotective barriers, a bacterial migration assay was set up using Boyden chambers and different types of bacteria commonly found in skin flora (*Escherichia coli, Staphylococcus epidermidis, and Staphylococcus aureus*). Intact fibrin films prevented bacterial infiltration for the first 36 hours, but when film formation was disrupted with surfactants, or the film was damaged, bacterial invasion occurred much sooner (12-24 hours). Disruption of the fibrin film also resulted in the leakage of RBCs, highlighting the role of the film in cell retention. Cell retention could also play a role in infection control via two mechanisms: 1) retention of white cells within the clot would help fight infection, and 2) a clot with a higher RBC content would be less porous, slowing the movement of bacteria through the clot. Importantly this antimicrobial protection was also confirmed in a murine model of dermal infection with *P. aeruginosa.* This model indicated that the films not only prevented infiltration of bacteria, but that they may also play a role in preventing bacterial proliferation. Bacteria in mice that possessed an

intact film appeared not to proliferate over time suggesting that the film may play an active role in preventing bacterial growth.

The finding of this film and its physiological roles in host defence begins to raise important questions about its potential clinical implications. The role of the films in controlling infections is supported by the prevalence of dermal infections in some afibrinogenemia patients (Figure 57). However, many immune mechanisms already exist that help limit microbial invasion, and the importance of the films in this are currently unknown. Does this structure play an important pathophysiological process? There is no current research into the effects of current wound treatments and their effects on the film, and if this would increase infection and related morbidity. One area of required research would be to address the question of whether the application of petroleum jelly to help stem bleeds from injuries in contact sports or to a wound after minor surgery wound actually increase the risk of infection.

Figure 57 Dermal infection in a patient with afibrinogenemia.

Another research question to be addressed is the possibility of these films occurring in intravascular clots or thrombi, or on other surfaces such as stents or medical devices. There is some previous evidence that this may be the case, with film like structures found on the outer faces of thrombi (Autar et al., 2018, van Es et al., 2017). These films could play a role as a site for the initiation of intravascular fibrin fibre formation in thrombotic conditions. They could also play a part in the clot stability of old and new thrombi, and may influence perfusion through clots, which in turn may alter the rate of fibrinolysis or thrombolysis.

The findings of the extraordinary formation of a protective fibrin film on the blood clot exterior reveal a mechanism in haemostasis that helps retain blood cells and control microbial infection. More research is required to reveal the structure of these biofilms and their pathophysiological roles. Clot film formation appears an important physiological process that should be exploited in the future to improve recovery and healing from minor and major injuries.

5.5 Future work

Chapter 4 and Chapter 5 have discussed the discovery of novel, previously unexplored fibrin biofilms and how they have physiological roles, retaining cells within the clot and preventing the proliferation and dissemination of bacteria into a site of injury. However, there are still many questions to be answered relating to the biofilm structure and its pathophysiological roles.

We currently do not accurately know how the fibrin molecules interact within the biofilms. Langmuir trough data indicate that fibrin monomers aligned at

the air-liquid interface occupy roughly the same area as the diameter of a single fibrin monomer positioned perpendicularly to the air-liquid interface. Future atomic force microscopy experiments could be used to create more detailed images of the surface revealing nanometer definition, and also to probe the film surface with GPRP peptide and fibrin D-region to test for the presence of D- and E-region in the film. By embedding clots with films and taking cross-sections of the film, transmission electron microscopy could be used to help elucidate the molecular packing arrangement of the films and better characterise the transition from films to fibres. Together, these approaches should elucidate how the fibrin units are packed in the biofilm and a more detailed understanding of the molecular arrangements in the films could help to engineer ways to alter the film to improve its ability to resist bacterial invasion.

Another direction for further research in this field is alternative locations of film formation. Previous studies have presented extracted thrombi from patients that possess similar structures to the fibrin biofilms and also the formation of films on other surfaces such as stents (Autar et al., 2018, van Es et al., 2017). We also already have persuasive pilot evidence for the formation of intravascular biofilm structures in thrombi. Biofilms are consistently observed in thrombi extracted from patients with abdominal aortic aneurysms. We also observe films in clots from mice after $FeCl_3$ induced thrombosis, also after *in vivo* fixation before retrieval of the thrombi. Formation of fibrinogen films on phosphatidylcholine coated surfaces further contributes to the possibility of intravascular films (Sankaranarayanan et al., 2010). These films could play an important role in determining the physical limit of thrombi and their stability. Established models of murine femoral vein

thrombosis could be used to investigate the make-up of *in vivo* thrombi and assess intravascular fibrin biofilm formation. Further studies into film formation on different surfaces could also be carried out using the Langmuir-Blodgett trough and flow chambers.

The role of the films in infection control also needs to be investigated further. In this chapter, fibrin biofilms have been shown to protect against bacterial proliferation and dissemination for at least 12 hours, but for how long do these films provide protection? Bacterial proliferation on wounds in the presence and absence of films could be followed over longer periods of time (24-72 hours), and the dissemination of bacteria to organs (liver, spleen and kidneys) could be monitored to assess if these films can deter systemic infection and sepsis. On top of this, the effects of infection prevention by the film could be analysed by assessing the effects on complement activation, inflammation and neutrophil and macrophage recruitment.

Infection at injury sites is known to impair the wound healing process, and is a major contributor in chronic wound formation. With this in mind, the protective role of the film against infection in the initial stages of tissue repair could benefit wound healing. To investigate this, tissue repair in the presence and absence of film formation and bacterial infection could be followed, with levels of growth factors being monitored in tissue samples over the healing period. The Infiltration of neutrophils, macrophages and contractile myofibroblasts into wounds could be monitored and the rates and quantity of angiogenesis within the wound could be quantified. The replacement of the film with extracellular matrix, epithelial cells or fibroblasts could be followed as the wound heals by IHC and SEM. Finally, the

proliferation and migration of primary dermal fibroblasts, epithelial and endothelial cells on the film could be explored *in vitro* using cell culture.

Chapter 6 - Common FXIII and Fibrinogen Polymorphisms in Abdominal Aortic Aneurysms

In this chapter the link between fibrinogen and FXIII with AAA is investigated by analysing associations between known sequence variants and disease. Also discussed in this chapter is the association of fibrinogen and fibrinogen γ' levels with AAAs. About 75 % of all larger aneurysms are characterized by the presence of an ILT, which forms over many years, and persists even after endovascular repair when it remains present between the stent and the aneurysmal wall (Vorp et al., 2001, Harter et al., 1982). The ILT is composed of a three dimensional (3D), FXIII crosslinked, fibrin network structure that incorporates red and white blood cells, platelets, other blood proteins, and cellular debris. Many studies have shown that the ILT accelerates the dilatation of an AAA due to hypoxia and biochemical stress. In addition to the effects of the ILT, it has been found that patients with AAA demonstrate abnormal coagulation and clot structure profiles (Parry et al., 2009). The main proteins involved in thrombus formation are coagulation factors fibrinogen, thrombin and FXIII, and functional common genetic sequence variants have been identified in both FXIII and fibrinogen. Variants FXIII-A Val34Leu, Fib-α Thr312Ala, Fib-β Arg448Lys and Fib-γ 10034C>T have all previously been linked to alterations in clot structure. The sequence variant FXIII-A 34Leu occurs in the activation peptide of FXIII and has been shown to accelerate FXIII activation. Clotting in the presence of this variant occurs more quickly resulting in clots with thinner fibres and smaller pores (Ariens et al., 2000). This variant has also been suggested to have a protective effect against venous thromboembolism and MI (Wells et al., 2006, Franco et al., 2000). The Fib-α 312Ala sequence variant occurs in close proximity to the FXIIIa crosslinking site at position Aα 328 (Muszbek et al., 1996) It has been shown to form clots with thicker fibres and increased α-chain cross-

linking,(Standeven et al., 2003) and has been suggested to result in increased embolization (Carter et al., 2000). Clots formed from fibrinogen-β 448Lys have been shown to be stiffer with thinner fibres and smaller pores and have increased resistance to lysis (Ajjan et al., 2008). Fib-γ 10034T has indirectly been linked to changes in fibrin clot structure via the alteration of fibrinogen γ' levels (Uitte de Willige et al., 2007) and has been linked to venous thrombosis (Grunbacher et al., 2007). In view of the central role of FXIII and fibrinogen in thrombus formation and the complications of ILT in AAA, the relationship between these genetic sequence variants and AAA was explored.

Both sequence variants FXIII-B His95Arg and FXIII-B splice variant (Intron K nt29577C-G) show considerable geographic differentiation, with FXIII-B His95Arg being most common in populations of African descent, whereas the FXIII-B splice variant is most common in populations of Asian descent (Ryan et al., 2009). AAA incidence has been reported to be decreased in both these populations (Costa and Robbs, 1986, Li et al., 2013). Therefore, the association of these polymorphisms with AAA was explored.

Finally, fibrinogen γ' levels have previously been linked to a number of arterial and venous thrombotic disorders and may also play a role in the pathophysiology of AAAs. To explore this, the levels of fibrinogen and fibrinogen γ' were investigated in AAA patients to determine if the splice variant influences AAA development.

6.1 Common factor XIII and fibrinogen sequence variants in abdominal aortic aneurysms

In total 969 participants, comprising 520 AAA patients and 449 controls, recruited into LEADS provided samples of plasma and whole blood for the study. DNA was extracted from the whole blood, and TaqMan genotyping assays were used to analyse six sequence variants: FXIII-A Val34Leu, FXIII-B His95Arg, FXIII-B splice variant (Intron K nt29577C-G), Fib-α Thr312Ala, Fib-β Arg448Lys and Fib-γ 10034C>T. Fibrinogen levels were measured in plasma using the Fibri-prest automate assay. These methods are described in full in chapter 2.5.1, 2.5.2 and 2.5.3. The demographic and clinical characteristics of the two groups are represented in Table 15. As expected, the AAA group had larger aortic diameters compared with controls. There were higher rates of CVD, including angina, CVA/TIA, hypertension and MI at recruitment, in agreement with previous studies (Alcorn et al., 1996). There was a greater prevalence of current and ever smokers in the AAA group, in agreement with previous studies showing that smokers have a higher risk of developing an AAA compared with non-smokers (Singh et al., 2001). A higher proportion of AAA patients were taking statins and aspirin, likely a reflection of the increased number of subjects with CVD in this group, and there was no major difference in alcohol consumption between the two groups. However, fibrinogen levels were found to be higher in patients with AAA compared with control subjects ($p = 0.0003$), in agreement with previous findings (Al-Barjas et al., 2006). After binary logistic regression analysis, only aortic diameter remained significantly different between the two groups ($p < 0.0001$).

Table 15 Demographic and clinical characteristics of the AAA and Control groups from the LEADS study. Adapted from Macrae et al. (2014).

	AAA (n = 520)	Control (n = 449)	Corrected p value
Age (years) †	74.4 (7.5)	70.1 (7.3)	0.198
Weight, Kg §	78.9 (68.9, 89.0)	78.2 (70.0, 88.7)	0.301
Height, m §	1.72 (1.67, 1.77)	1.70 (1.63, 1.75)	0.274
BMI**, $Kg.m^{-2}$ †	27.1 (4.5)	27.6 (4.1)	0.360
Waist: hip ratio §	0.95 (0.90, 1.00)	0.93 (0.88, 0.97)	0.478
Aortic Diameter, cm §	5.4 (4.0, 6.2)	1.9 (1.7, 2.3)	< 0.0001
Current smoker, % ¥	118 (27.8%)	73 (16.3%)	0.102
Ever smokers, % ¥	473 (91.3%)	320 (71.3%)	0.397
Alcohol, units/week §	10 (4, 21)	10 (4, 18.5)	0.563
CVD* ¥	299 (57.5%)	207 (46.1%)	0.413
Angina ¥	140 (26.9%)	82 (18.3%)	0.794
MI ¥	149 (28.7%)	50 (11.1%)	0.619
CVA/TIA ¥	96 (18.46%)	60 (13.4%)	0.684
Hypertension ¥	324 (62.6%)	199 (44.3%)	0.267
Statins ¥	370 (71.2%)	222 (49.4%)	0.207
Aspirin ¥	230 (44.2%)	137 (30.5%)	0.509
Fibrinogen, $g.L^{-1}$ §	3.72 (3.19, 4.39)	3.51 (3.08, 3.51)	0.522

*Cardiovascular disease (CVD) = ischaemic heart disease (angina, MI or abnormal ECG) + peripheral arterial disease (PAD) + cerebro-vascular disease (TIA, stroke or known asymptomatic carotid disease). **BMI – body mass index.
† - Parametric data expressed as mean (standard deviation).
§ - Nonparametric data expressed as median (25th, 75th quartiles).
¥ - Categorical data expressed as No. (%).

All genotype distributions for each sequence variant were consistent with the Hardy-Weinberg equilibrium (Table 16), and overall allele frequencies for each sequence variant were consistent with those reported by SeattleSNPs and other previously published studies on these sequence variants in different cardiovascular diseases (Nickerson, 2003, Rasmussen-Torvik et al., 2007, Ryan et al., 2009, Ruigrok et al., 2010, Suntharalingam et al., 2008). An example of the output generated using PCR and end-point genotyping is shown in Figure 58.

Table 16 Genotype distributions for each sequence variant were consistent with the Hardy-Weinberg. Adapted from Macrae et al. (2014).

	Total population		
	Rare Allele Frequency	X^2	p
FXIII-A Val34Leu	0.26	2.20	0.14
FXIII-B His95Arg	0.11	1.26	0.26
FXIII-B splice variant	0.17	0.34	0.56
Fib-α Thr312Ala	0.25	2.89	0.09
Fib-β Arg448Lys	0.18	0.01	0.92
Fib-γ 10034C>T	0.20	1.63	0.20

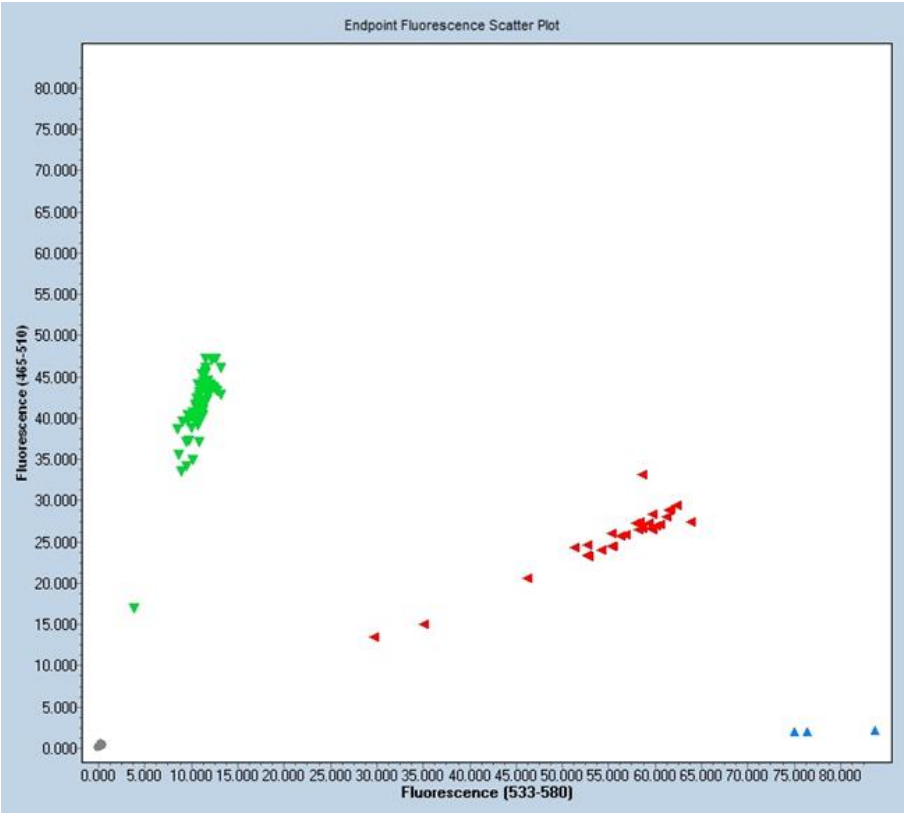

Figure 58 Example output of end-point genotyping assay. Genotyping was carried out using TaqMan genotyping assays. The relative amount of the two reporter dyes can be used to determine the genotype. This can be plotted on a graph as shown above. The example shown is for FXIII His95Arg; blue triangles represent His/His homozygotes, red triangles represent His/Arg heterozygotes, and green triangles represent Arg/Arg homozygotes. Grey circles represent blanks.

6.1.1 Polymorphic allele distribution in AAA vs Controls

The distribution of the FXIII-B 95Arg allele was significantly different between AAA patients and controls, with a significantly higher percentage of AAA patients presenting as heterozygous (1.45x higher) and homozygous (2.33x higher) for the Arg variant when compared with controls ($p = 0.006$; $p = 0.03$ after Bonferroni adjustment for multiple testing) (Table 17). When combining the heterozygote and homozygote carriers of the rare Arg allele, the relative risk of developing an AAA with the FXIII-B 95Arg allele was 1.240 (CI 1.093–1.407) indicating a small increase in the risk of developing an AAA when in possession of an Arg allele. The distribution of the Fib-γ 10034C>T sequence variant was also significantly different between AAA patients and controls, with a significantly higher percentage of AAA patients presenting as homozygous for the C allele (CC, 1.14x higher) than controls ($p = 0.028$, Table 17), although this was not significant after Bonferoni adjustment. When comparing the homozygote carriers of the C allele to the carriers of the sequence variant T allele, the relative risk of developing an AAA with at least one T allele was 0.830 (CI 0.725-0.950) suggesting that the possession of one T allele may have a small protective effect against developing an AAA. There were no associations between the rare alleles of FXIII-A Val34Leu, FXIII-B Splice variant, Fib-α Thr312Ala or Fib-β Arg448Lys sequence variants and AAA (Table 17).

Table 17 Sequence variant distribution in AAA vs Controls. Adapted from Macrae et al. (2014).

Polymorphisms		AAA (n=520)	Control (n=449)	p
FXIII-A Val34Leu	Val/Val	56.3% (293)	57.9% (260)	0.713
	Val/Leu	35.8% (186)	33.4% (150)	
	Leu/Leu	7.9% (41)	8.7% (39)	
FXIII-B His95Arg	His/His	76.0% (395)	84.0% (377)	**0.006**
	His/Arg	21.9% (114)	15.1% (68)	
	Arg/Arg	2.1% (11)	0.9% (4)	
FXIII-B Splice Variant	Wt/Wt	68.3% (355)	69.7% (313)	0.890
	Wt/SV	28.5% (148)	27.2% (122)	
	SV/SV	3.3% (17)	3.1% (14)	
Fib-α Thr312Ala	Thr/Thr	56.7% (295)	53.2% (239)	0.331
	Thr/Ala	38.8% (202)	40.5% (182)	
	Ala/Ala	4.4% (23)	6.2% (28)	
Fib-β Arg448Lys	Arg/Arg	65.2% (339)	68.6% (308)	0.355
	Arg/Lys	30.8% (160)	28.7% (129)	
	Lys/Lys	4.0% (21)	2.7% (12)	
Fib-γ 10034C>T	C/C	67.4% (333)	59.0% (261)	**0.028**
	C/T	29.1% (164)	32.6% (144)	
	T/T	3.4% (17)	3.8% (17)	

Data expressed as percentage (No.), analysed by X^2, Wt – wildtype, SV – splice variant

6.1.2 Association of sequence variants with fibrinogen levels

The effect of the possession of at least one rare allele, for each sequence variant, on fibrinogen levels was investigated in the total study population. Patients who possessed at least one Fib-β 448Lys allele (3.81 $g.L^{-1}$) were found to have significantly higher fibrinogen levels than patients homozygous for the Arg allele (3.55 $g.L^{-1}$) in the whole study population ($p = 0.001$) (Table 18). Fibrinogen levels were found to increase step wise with

an increase in the number of Lys alleles, Arg/Arg 3.55 $g.L^{-1}$ (3.08,4.13), Arg/Lys 3.74 $g.L^{-1}$ (3.22, 4.44) and Lys/Lys 4.18 $g.L^{-1}$ (3.41, 4.53) (p = 0.0009). There was no association of fibrinogen levels with FXIII-A Val34Leu, FXIII-B His95Arg, FXIII-B Splice variant, Fib-a Thr312Ala and Fib-γ 10034C>T sequence variants (Table 18, Figure 59A-F).

Table 18 Association of sequence variants with fibrinogen levels in total study population. Adapted from Macrae et al. (2014).

Polymorphisms		Fibrinogen levels $g.L^{-1}$	p
FXIII-A Val34Leu	Leu -	3.56 (3.11, 4.23)	0.313
	Leu +	3.67 (3.19, 4.24)	
FXIII-B His95Arg	Arg -	3.59 (3.12, 4.24)	0.136
	Arg +	3.76 (3.26, 4.25)	
FXIII-B Splice Variant	SV -	3.66 (3.16, 4.26)	0.318
	SV +	3.55 (3.10, 4.19)	
Fib-α Thr312Ala	Ala -	3.62 (3.19, 4.22)	0.526
	Ala +	3.62 (3.06, 4.27)	
Fib-β Arg448Lys	Lys -	3.55 (3.08, 4.13)	**0.001**
	Lys +	3.81 (3.23, 4.46)	
Fib-γ 10034C>T	T -	3.74 (3.14, 4.19)	0.722
	T+	3.80 (3.15, 4.33)	

Data expressed as Median (25^{th}, 75^{th} quartiles), analysed by Mann-Whitney U. SV – splice variant

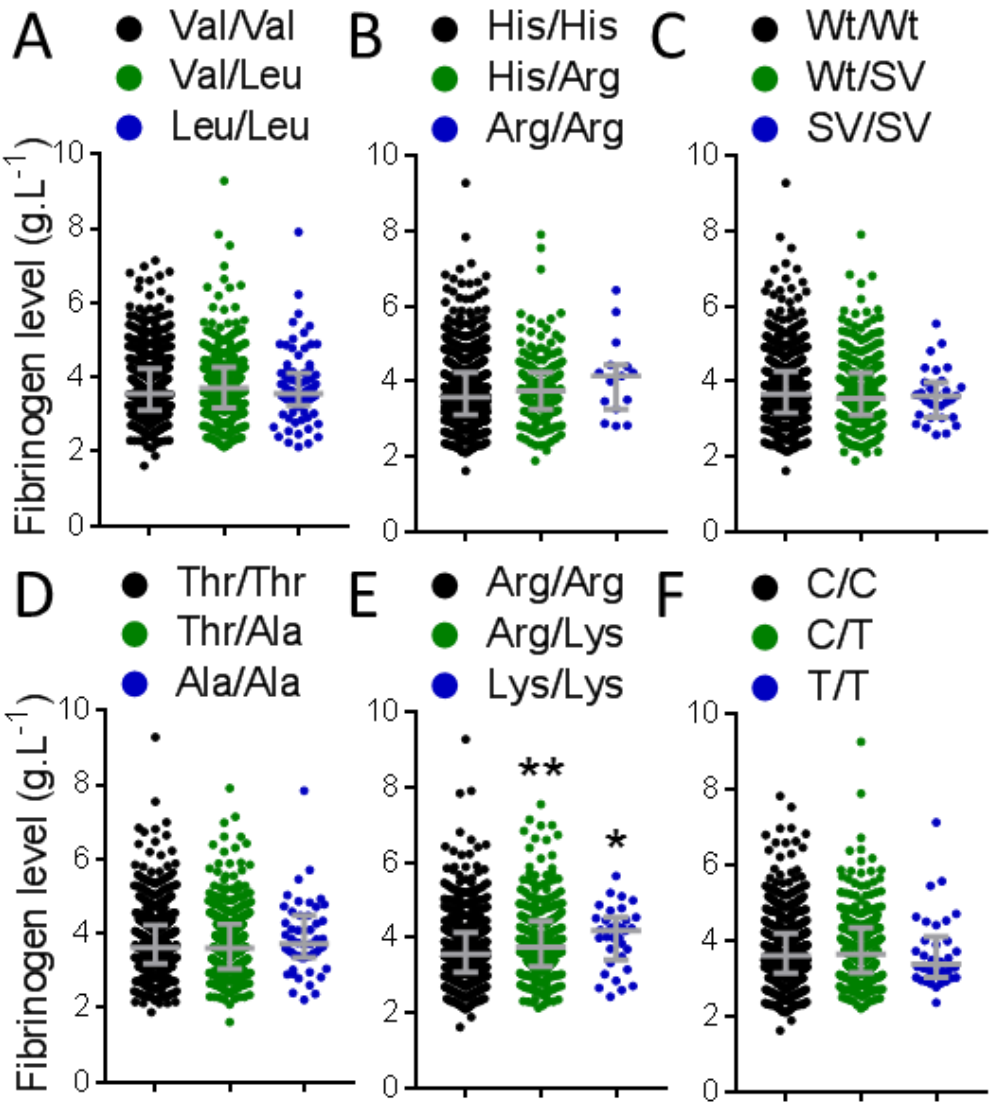

Figure 59 Association of genotypes with fibrinogen levels. Comparison of fibrinogen levels across different genotypes for each sequence variant: **A,** FXIII-A Val34Leu, **B,** FXIII-B His95Arg, **C,** FXIII-B splice variant (Intron K nt29577C-G), **D,** Fib-α Thr312Ala, **E,** Fib-β Arg448Lys and **F,** Fib-γ 10034C>T. Data shown as median and IQR. * represents significant difference from first bar. * $p < 0.05$, ** $p < 0.01$. Kruskal-Wallis test.

6.1.3 Association of alleles

The association of alleles was investigated to assess for relationships between sequence variants (Table 19). In the total study population there was evidence of negative linkage disequilibrium between the His95Arg and Splice Variant sequence variants (D' = -0.609, p = 0.011) (Table 20). In the

control subjects the sequence variants were found to be close to complete negative disequilibrium (D' = -1.0, p = 0.018). The association of His95Arg with AAA was still significant if subjects with the Splice Variant were excluded from the analysis (p = 0.016).

Table 19 The association between sequence variants.

Associated polymorphisms		D'	p
FXIII-A Val34Leu	FXIII-B His95Arg	0.060	0.333
	FXIII-B splice variant	-0.053	0.881
	Fib-α Thr312Ala	0.020	0.213
	Fib-β Arg488Lys	0.330	0.765
	Fib-γ 10034C>T	-0.066	0.857
FXIII-B His95Arg	FXIII-B splice variant	**-0.609**	**0.008**
	Fib-α Thr312Ala	-0.387	0.062
	Fib-β Arg488Lys	0.026	0.486
	Fib-γ 10034C>T	0.011	0.120
FXIII-B splice variant	Fib-α Thr312Ala	0.047	0.192
	Fib-β Arg488Lys	0.005	0.954
	Fib-γ 10034C>T	0.017	0.976
Fib-α Thr312Ala	Fib-β Arg488Lys	-0.387	0.010
	Fib-γ 10034C>T	0.049	0.745
Fib-β Arg488Lys	Fib-γ 10034C>T	0.334	0.995

Table 20 The association between the FXIII-B His95Arg and Splice Variant sequence variants in the total study population. Adapted from Macrae et al., 2014.

		FXIII-B Splice Variant				
		Wt/Wt	Wt/SV	SV/SV	Total	p
FXIII-B His95Arg	His/His	511 (52.7)	233 (24)	28 (2.9)	772	0.011
	His/Arg	145 (15)	34 (3.5)	3 (0.3)	182	
	Arg/Arg	12 (1.2)	3 (0.3)	0 (0)	15	
	Total	669	270	31	969	

Wt – wild type, SV – splice variant, Data expressed as No. (%), analysed by X^2

6.2 Fibrinogen-γ' levels in AAA

After finding a difference in the distribution of the Fib-γ 10034C>T, a sequence variant associated with fibrinogen γ' levels, between AAA patients and controls, fibrinogen levels and fibrinogen γ' levels were next analysed in 608 AAA patients and 560 control subjects. The basic demographic for these groups can be seen in Table 21. As expected, the AAA group had larger aortic diameters compared with controls. The two groups were compared for compounding risk factors. There were some differences in the incidence of cardiovascular disease, in agreement with previous studies (Alcorn et al., 1996). There were more current and ever smokers in the AAA group, once again in agreement with previous studies with smokers having a greater risk of developing an AAA (Singh et al., 2001). There was a greater number of AAA patients being on medication, reflecting the increased cardiovascular disease burden in this group of patients. After binary logistic regression analysis, only aortic diameter remained significantly different between the two groups ($p < 0.0001$).

Table 21 Demographic and clinical characteristics of the AAA and Control groups from the LEADS study.

	AAA (n = 608)	Control (n = 560)
Age (years) †	73.4 (7.4)	69.6 (7.4)
Female ¥	97 (16.0%)	130 (23.3%)
Weight, Kg §	79.5 (69.3, 89.0)	79.0 (70.2, 89.6)
Height, m §	1.71 (1.65, 1.76)	1.70 (1.64, 1.75)
BMI*, $Kg.m^{-2}$ †	27.3 (4.6)	27.7 (4.3)
Waist:hip ratio §	0.95 (0.90, 1.00)	0.93 (0.88, 0.97)
Aortic Diameter, cm §	4.6 (3.7, 5.8)	1.9 (1.7, 2.1)
Current smoker, % ¥	141 (23.3%)	81 (14.5%)
Ever smokers, % ¥	544 (89.8%)	384 (68.8%)
Alcohol, units/week §	5 (1, 16)	7 (1, 15)
Angina ¥	135 (22.3%)	80 (14.3%)
MI ¥	161 (26.6%)	56 (10.0%)
CVA/TIA ¥	106 (17.5%)	67 (12.0%)
Hypertension ¥	362 (62.6%)	237 (44.3%)
Statins ¥	460 (75.9%)	276 (49.4%)
Aspirin ¥	413 (68.2%)	247 (44.3%)

*BMI – body mass index.
† - Parametric data expressed as mean (standard deviation).
§ - Nonparametric data expressed as median (25th, 75th quartiles).
¥ - Categorical data expressed as No. (%).

The plasma levels of fibrinogen γ' in the AAA and control groups were measured by an in-house ELISA described in chapter 2.1.6. All samples were diluted to two different concentrations and run in duplicate to ensure accuracy of results. Intra-assay variability was measured by comparing the same sample on each plate (Figure 60A). Any plates containing a control sample that fell outside two standard deviations (red dots) were repeated. The plasma fibrinogen levels were measured by the Fibri-prest automate assay as described in chapter 2.1.4. All samples were run in duplicate, if the duplicate variability was greater than 5 % the sample was repeated. To ensure repeatability between days, controls (Control N and P) supplied in the kit were monitored between days (Figure 60B). On days where controls

were outside the suggested range, all samples on that day were repeated (red points).

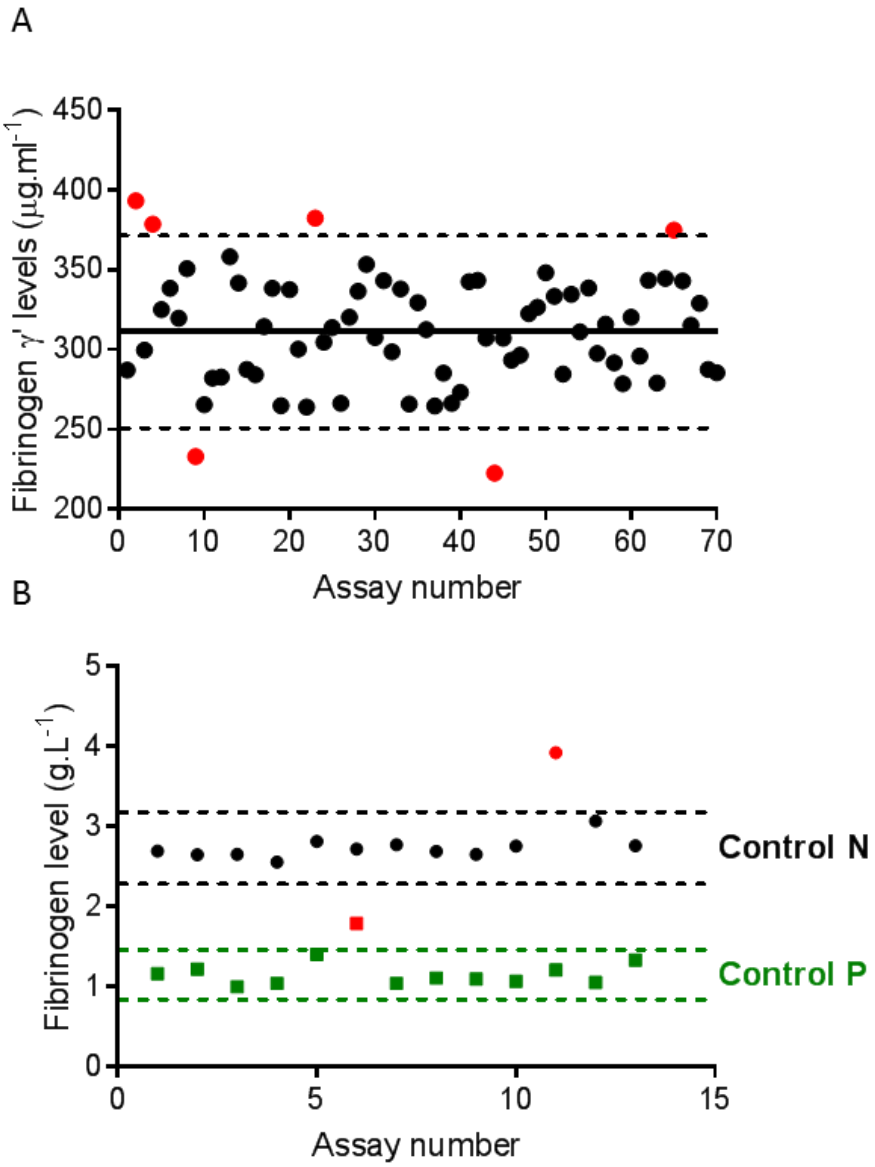

Figure 60 Intra-assay variability. A, Fibrinogen γ' ELISA variability, each dot represents the average fibrinogen γ' concentration, from four wells on each plate, of a control plasma sample. The solid black line represents the mean value and the black dotted lines represent 2 standard deviations from the mean. All plates containing a control sample outside 2 standard deviations were repeated (red dots). Coefficient of variation = 9.68 %. **B,** Fibrinogen level assay variability, each point represents the fibrinogen level of either Control N or Control P each day the assay was carried out. The dotted lines represent the range of acceptable fibrinogen levels for Control P (green) or Control N (black). On days where either Control P or Control N were outside these ranges (red points), all samples on that day were re-measured.

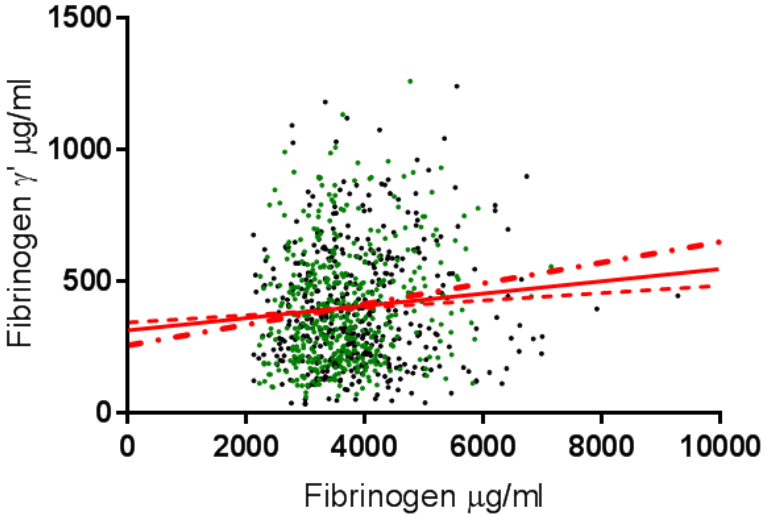

Figure 61 Association between total fibrinogen levels and fibrinogen γ'. The association of fibrinogen and fibrinogen γ' levels were analysed in **A,** the whole study population (solid line, r = 0.080, p = 0.027). **B,** AAA patients (Black dots, dashed line, r = 0.038, p = 0.428). **C,** Control subjects (Green dots, dash/dot line, r = 0.1281, p = 0.008).

The levels of fibrinogen and fibrinogen γ' were measured in 606 AAA patients and 558 control patients. No association was found between fibrinogen and fibrinogen γ' levels in AAA patients (r = 0.038). However, there was a very weak but significant positive correlation within the whole study population (r = 0.080, p = 0.027) and control patients (r = 0.1281, p = 0.008) (Figure 61). This is similar to previous studies that have found at most a weak correlation between fibrinogen and fibrinogen γ' levels (Pieters et al., 2013, Appiah et al., 2016, Appiah et al., 2015, Uitte de Willige et al., 2005).

AAA patients were found to have significantly increased plasma levels of fibrinogen (3.68 (3.19 - 4.32) $g.L^{-1}$) compared with control subjects (3.50 (3.09 - 4.08) $g.L^{-1}$, p = 0.0012) (Figure 62A). This is in line with a much smaller previous study that showed increased fibrinogen levels in AAA patients (Al-Barjas et al., 2006). There was no difference in fibrinogen γ'

levels between the AAA patients and control subjects (334.5 (212.2 - 508.0) $\mu g.ml^{-1}$ vs 334.4 (211.3 - 511.0) $\mu g.ml^{-1}$ respectively, p = 0.734) (Figure 62B). There was no difference in fibrinogen γ' % in the controls (9.4 (6.0 - 14.9) %) compared with the AAA patients (9.3 (5.6 - 13.7) %, p = 0.17) (Figure 62C). There was a very large range of gamma prime levels ranging from 1200 $\mu g.ml^{-1}$ down to 35 $\mu g.ml^{-1}$ resulting in gamma prime ratios that ranged from 40 % down to 1 %.

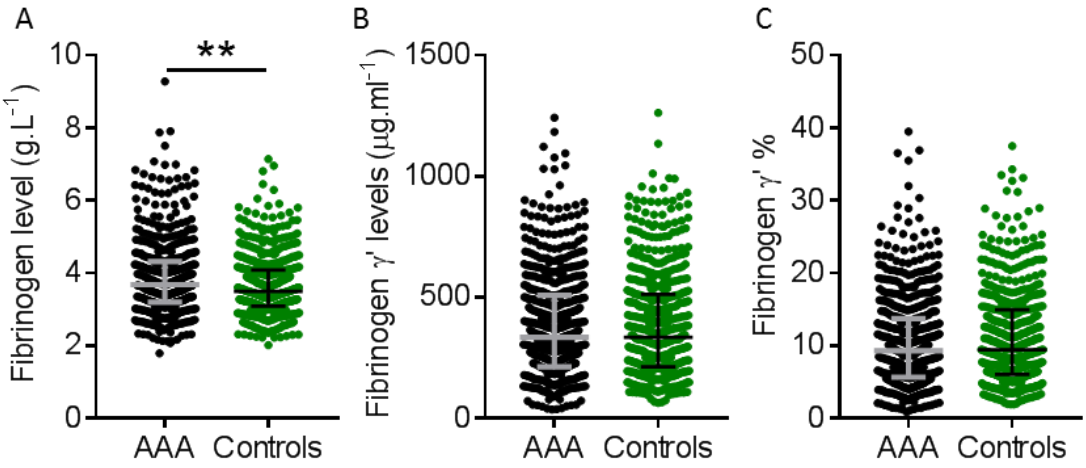

Figure 62 Increased fibrinogen but not fibrinogen γ' levels in AAA patients. A, Total fibrinogen levels were measured in 609 AAA patients and 558 controls using the Clauss method. **B,** Fibrinogen γ' levels were measured by ELISA in 609 AAA and 558 control patients. **C,** Fibrinogen γ' % was calculated by dividing the fibrinogen γ' level by the total fibrinogen level. Data shown as median and IQR. ** p < 0.01. Mann-Whitney U test for pairwise comparisons.

After finding no differences in fibrinogen γ' levels between AAA patients and control subjects, the association of the Fib-γ 10034C>T sequence variant with fibrinogen γ' levels within this cohort of patients was assessed (Figure 63). Fib-γ 10034C>T has previously been linked to a reduction in fibrinogen γ' levels in a number of studies (Uitte de Willige et al., 2005), so this was assessed in this group of patients to see if they followed a similar trend. No differences in fibrinogen, fibrinogen γ' levels or fibrinogen γ' % were

observed in patients in possession of the Fib-γ 10034C>T allele in the whole study group, or within the AAA patients or control subjects (Table 22, Figure 63).

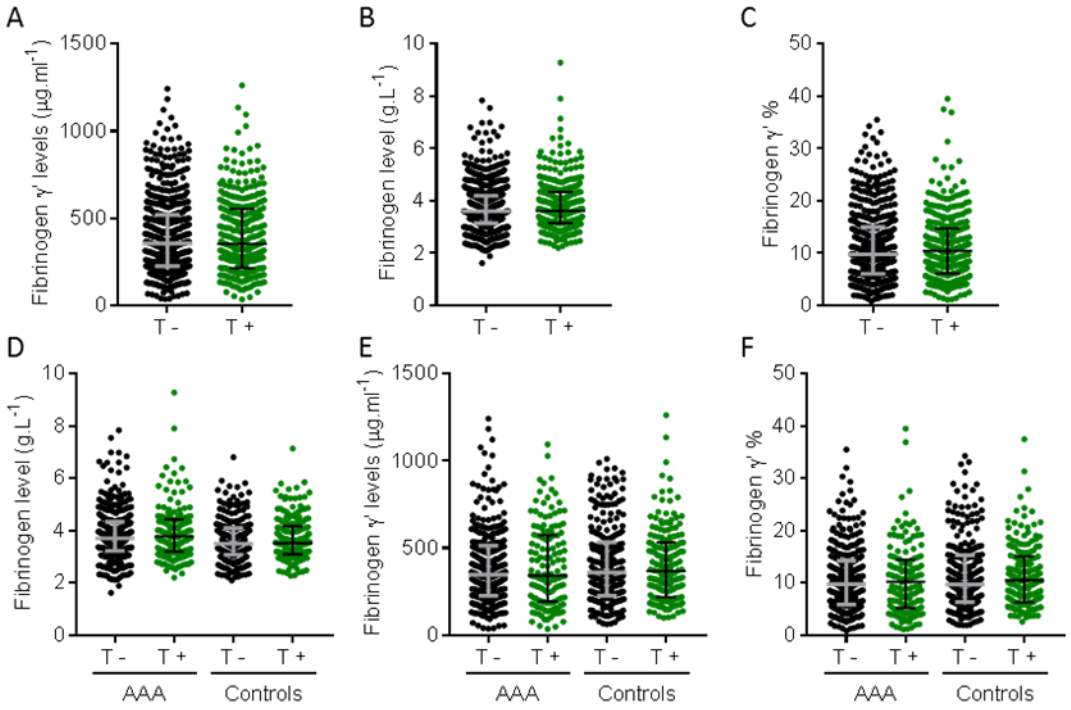

Figure 63 The association of Fib-γ 10034C>T with fibrinogen and fibrinogen γ' levels. A, Total fibrinogen levels, **B,** Fibrinogen γ' levels and **C,** Fibrinogen γ' % were compared between patients with or without the Fib-γ 10034C>T sequence variant (± Thr allele). **D,** Total fibrinogen levels, **E,** Fibrinogen γ' levels and **F,** Fibrinogen γ' % were compared between patients with or without the Fib-γ 10034C>T sequence variant (± T allele) within AAA patients or control subjects. Data shown as median and IQR. * $p < 0.05$, ** $p < 0.01$. Mann-Whitney U test for pairwise comparisons.

Table 22 Association of Fib-γ 10034C>T with fibrinogen and fibrinogen γ' levels.

	Fibrinogen	Fibrinogen γ'	Fibrinogen γ' %
Whole group			
T -	3.60 (3.14-4.19)	354.8 (225.4-520.6)	9.74 (6.08-14.97)
T +	3.62 (3.15-4.33)	352.8 (213.6-553.0)	10.40 (6.10-14.70)
AAA patients			
T -	3.70 (3.22-4.34)	346.4 (224.8-513.3)	9.76 (5.85-14.22)
T +	3.78 (3.19-4.43)	341.5 (193.5-573.3)	10.24 (5.17-14.43)
Control subjects			
T -	3.51 (3.08-4.10)	359.6 (225.9-532.3)	9.69 (6.32-15.28)
T +	3.52 (3.10-4.17)	368.1 (218.0-531.4)	10.45 (6.32-15.02)

6.3 Discussion

In this chapter the links between five previously described sequence variants in the FXIII and fibrinogen genes and AAAs were investigated. In addition, the levels of fibrinogen and fibrinogen γ' in AAA patients were assessed. The sequence variants investigated were FXIII-A Val34Leu, FXIII-B His95Arg, FXIII-B Splice Variant (intron K nt29576C-G), Fib-α Thr312Ala, Fib-β Arg448Lys and Fib-γ 10034C>T. An association between the Arg allele at position 95 of FXIII-B and the occurrence of AAA was found. There was a small association between the possession of a Fib-γ 10034T allele and control patients suggesting a small protective effect of the sequence variant against the development of an AAA, but this was not significant after Bonferoni adjustment. FXIII-B His95Arg and FXIII-B splice variant were found to be in negative linkage disequilibrium. Finally, fibrinogen levels, but not fibrinogen γ' levels, were found to be associated with the development of an AAA.

An over-representation of the Arg allele in patients with AAA suggested that FXIII-B Arg allele is a potential risk factor for the development or progression of an AAA. The FXIII-B His95Arg sequence variant has previously been linked to a 50 % increased risk of venous thrombosis and has been shown to increase subunit dissociation of the FXIII-A and -B subunits in plasma (Komanasin et al., 2005). It has previously been shown that in the N-terminal region of FXIII-B, within the peptide YGCASGYK spanning positions 96–103 in the second sushi domain, there is an interaction site for FXIII-B with FXIII-A2 (Katona et al., 2014). FXIII-B His95Arg occurs in the amino acid position immediately before the start of this interaction site and may play a role in

FXIII-A2 and FXIII-B interactions. Substitution of His to Arg at position 95 could therefore have an effect on FXIII activation which could result in altered cross-linking activity, potentially influencing the stability of the ILT. An increase in fibrin clot stability likely leads to a more stable, lysis resistant ILT, which in turn may enhance the inflammatory and proteolytic insult on the underlying aortic wall, resulting in AAA progression. Although the B-subunit has no enzymatic activity, it has been suggested that FXIII-B may help to stabilize FXIII-A in plasma and also be important in the secretion of the FXIII-A subunit from its site of synthesis in the bone marrow (Iwata et al., 2009). In addition, there may be hitherto unknown functional roles for FXIII-B after it has dissociated from FXIII-A. As FXIII-B may bind to fibrinogen (de Willige et al., 2009, Byrnes et al., 2016), FXIII-B may also play an important role directing FXIII transglutaminase activity towards its main substrate fibrin. These findings indicate that further studies are warranted to fully investigate the role of FXIII in AAA. Alternatively, the FXIII His95Arg sequence variant could be affecting the role of FXIII in tissue repair of the diseased aortic wall. The FXIII A-subunit belongs to the transglutaminase family of enzymes, which are known to cross-link various matrix proteins and are involved in tissue repair (Dardik et al., 2006). Indeed, FXIII may crosslink collagen and fibronectin for example, two proteins involved in the extracellular matrix of the vascular wall. Due to its effect on increased subunit dissociation, the FXIII-B His95Arg sequence variant could increase FXIII activation at the site of fibrin deposition and within the ILT, reducing the amount of FXIII available for diffusion into the aortic wall. An increase in the stability of the ILT would result in a thicker ILT, so that local hypoxia of the underlying wall would be more marked, and there would also be a larger distance between the lumen

and the wall, so repair proteins would have further to travel. This could negatively affect the role of FXIII in repairing the tissue damage that occurs in the aortic wall, resulting in an increased level of AAA development. In support of a systemic role of FXIII in arterial wall repair, FXIII Val34Leu has been previously associated with arachnoid aneurysms (Ladenvall et al., 2009).

Genetic association studies on multiple SNPs can result in type I errors, when the null hypothesis is rejected due to multiple testing, but there is no true association between the sequence variant and the phenotype (Lunetta, 2008). To correct for this, we used the Bonferroni adjustment for multiple testing. After multiplication of the P values by the total number of SNP's tested, the P value for the association of FXIII-B His95Arg and AAA was 0.03 so should still be considered significant. However, our findings will need to be confirmed in other, large studies of FXIII in AAA.

There is an ongoing debate in previous literature whether Fib-β Arg448Lys is associated with a change in fibrinogen levels. Some studies found no effect on fibrinogen concentrations (Lim et al., 2003) and some have found that Fib-β 448Lys was associated with an increase in fibrinogen concentrations (Kain et al., 2002). In this study increased fibrinogen levels were found in patients possessing the Fib-β 448Lys allele, and the association appeared to be related to the number of Lys alleles which is largely in agreement with the observations by Kain et al, 2002 (Kain et al., 2002). Fib-β Arg448Lys has been shown to be in linkage disequilibrium with Fib-β -455 G/A (Suntharalingam et al., 2008, Kain et al., 2002), and Fib-β -455 G/A has also been associated with an increase in fibrinogen levels (van der Bom et al.,

1998). The inconsistency of the relationship between Fib-β Arg448Lys and fibrinogen levels is likely a reflection of complex gene environment interactions including several genetic and environmental factors. FXIII-B His95Arg was not found to be associated with fibrinogen levels, so it can be assumed that the association with AAA is not due to fibrinogen levels.

A strong negative linkage disequilibrium was found between the His95Arg and Splice Variant sequence variants (D' = -0.609) of FXIII, and in the control subjects the sequence variants were found to be closer to complete negative disequilibrium (D' = -1.0). This should be interpreted cautiously, as this relationship may be due to low numbers of heterozygotes for both sequence variants. These findings indicate that the minor allele at one locus is associated with the major allele at the other locus. Both of these sequence variants have previously been reported to show considerable geographic differentiation, with FXIII-B His95Arg being most common in populations of African descent, whereas the FXIII-B splice variant is most common in populations of Asian descent (Ryan et al., 2009). This could help to explain the low numbers of heterozygotes and homozygotes for the rare allele for both sequence variants. Although the two factor XIII polymorphisms were in strong negative linkage disequilibrium, the association of His96Arg with AAA was not observed with the Splice Variant. The association of His95Arg with AAA was still observed when only subjects who did not possess the splice variant were included in the analysis. This further corroborates that the FXIII His95Arg substitution plays a role in AAA and that its effects do not appear to occur through linkage disequilibrium with the FXIII-B splice variant. However, linkage disequilibrium with other potentially functional variants

cannot be excluded with these data, and future studies, including genome wide association studies, are required to confirm these findings.

A weak positive correlation was found between fibrinogen and fibrinogen γ' levels in control patients, and this is in agreement with previous studies (Pieters et al., 2013, Appiah et al., 2016, Uitte de Willige et al., 2005). This correlation was not seen in the AAA group. This suggests that although levels of fibrinogen γ' do fluctuate due to changes in fibrinogen level, other factors appear to have a greater influence on γ' levels. Fibrinogen levels were found to be increased in AAA patients, as previously described in a much smaller study (Al-Barjas et al., 2006). This maybe be due to the relationship between fibrinogen expression and IL-6 (Heinrich et al., 1990) with elevated IL-6 levels being previously reported in AAA patients (Juvonen et al., 1997), and recent meta-analysis of GWAS studies in AAA indicating IL-6 receptor as a major risk factor for AAA (Jones et al., 2017). No difference in γ' levels or γ' percentage was seen, and this was slightly different to previous studies that have shown a link between increased γ' levels and arterial thrombosis (Cheung et al., 2009, van den Herik et al., 2011, Pieters et al., 2013). Nonetheless, these studies supported the idea that other factors modulate γ' levels. Another result that supports this is the huge range of γ' levels found in the study group ranging from 1200 $\mu g.ml^{-1}$ down to 35 $\mu g.ml^{-1}$ resulting in gamma prime ratios that ranged from 40 % down to 1 %. With only a weak correlation between fibrinogen and fibrinogen γ' levels within this group, other stronger modulators must be causing the vast changes in γ' levels.

In conclusion, FXIII-B Arg95 was found to be associated with an increased risk of developing AAA. FXIII-B His95Arg was shown to be in negative disequilibrium with the FXIII-B Splice Variant. Finally, fibrinogen, but not fibrinogen γ' levels were increased in AAA patients. Further studies are warranted to elucidate the role of FXIII and fibrinogen in AAA pathogenesis using *in vitro* and *in vivo* models to clarify the underlying mechanisms and provide potential avenues in the development of new therapeutic agents.

6.4 Future work

This chapter has discussed the association of the sequence variant FXIII-B His95Arg with AAAs. The next step in this research would be to assess the downstream effects of this sequence variant, and if the changes in FXIII caused by this sequence variant play a direct role in AAA development or progression. This could be initially examined by examining the FXIII A_2B_2 95Arg variant more closely, investigating its role in cross-linking fibrin and other matrix proteins. A previous study has shown that the Arg variant leads to an increase in subunit dissociation (Komanasin et al., 2005), but the study failed to look at the downstream effects of this change. Another approach would be to develop a FXIII-B 96Arg mouse model, or inject FXIII-B 96Arg into a FXIII deficient mouse, and explore its effects on AAA by using the $CaCl_2$ or elastase model of AAA formation (Tsui, 2010).

To investigate the role of fibrinogen in AAA development, models of murine AAA could be carried out in fibrinogen deficient mice. By infusing fibrinogen into these mice, the role of fibrinogen in the slowing or progression of

dilatation could be investigated. The use of recombinant fibrinogen variants could also be investigated in this setting.

These studies would help to identify if the FXIII-B His95Arg sequence variant and fibrinogen play a functional role in the development and progression of AAA. They will also help to identify new therapeutic targets for the prevention and treatment of AAA.

Chapter 7 - The relationship between PNH clone size, eculizumab treatment and fibrin clot structure

PNH is a rare acquired hematologic disorder, the most serious complication of which is thrombosis. The increased incidence of thrombosis in PNH is still poorly understood, which unlike many other thrombotic disorders, predominantly involves complement-mediated mechanisms. This chapter explores the link between thrombosis in patients with PNH and changes in clot structure, and also the effects of treatment with eculizumab on clot formation. These areas of research are of interest because they may help uncover new factors that contribute to the increased risk of thrombosis in PNH. Many previous studies have demonstrated links between altered clot structure and thrombosis (Bridge et al., 2014). In view of this, clot structure was examined in patients with PNH to determine if altered clot structure contributes to the increased thrombotic risk in PNH. Pathological effects of platelet activation, intravascular haemolysis and neutrophil/monocyte activation have already been reported to increase thrombotic risk. While impaired fibrinolysis has also been observed and may be caused by several mechanisms involving interactions between complement activation, coagulation and fibrinolysis. In this chapter, *in vitro* analysis has been carried out on plasma and whole blood samples taken from patients with PNH, in an attempt to uncover mechanisms that contribute to thrombosis and impaired fibrinolysis in PNH.

7.1 Patient demographics

Previous studies on patients with PNH have shown that an increase in granulocyte clone size leads to a greater risk of thrombosis (Moyo et al., 2004), and that patients with different thrombotic disorders show altered clot structure (Bridge et al., 2014). Therefore, clot structure was analysed in

patients with PNH to investigate if abnormal clot structure could be an additional mechanism by which the risk of thrombosis is increased in PNH patients. Furthermore, the effects of eculizumab (treatment for patients with PNH targeting complement activation) on clot structure was also assessed. The demographics and clinical characteristics of the whole group (n = 82) of patients, and the distribution of patients on (n = 53) and off (n = 31) treatment are presented in Table 23. A significant difference was found in granulocyte size and LDH between patients on and off eculizumab. This was expected as patients with a high clone size are at increased risk of thrombosis, and so are more likely to be on treatment. Eculizumab prevents complement activation by preventing C5 activation and this leads to reduced inflammation. LDH is a marker of intravascular haemolysis and tissue damage, and so a decrease of LDH in patients treated with eculizumab is expected (Hillmen et al., 2013, Parker et al., 2005).

Table 23 Demographics and clinical characteristics of all PNH patients and the distribution of patients on and off treatment.

	Whole group (n=82)	No Eculizumab (n=51)	Eculizumab (n=31)	p value
Age (years)†	47.89 (31.2,63.3)	46.7 (28.9, 64.0)	48.7 (35.7, 62.4)	0.559
Weight (Kg)†	80.6 (69.9, 93.7)	81.9 (66.2, 94.1)	74.9 (69.9, 87.3)	0.735
Average Granulocyte clone size (%)†	56.7 (18.8, 85.8)	34.4 (5.3, 69.8)	97.6 (73.3, 99.7)	<0.0001
LDH†	510 (425, 813)	712 (435, 1315)	482 (411, 418)	<0.0001
Systolic blood pressure (mmHg)§	132.5 (21.6)	134.8 (21.6)	128.2 (21.4)	0.221
Diastolic blood pressure (mmHg)§	76.4 (12.4)	77.5 (13.1)	74.3 (10.8)	0.347
On Eculizumab¥	28 (34%)	0 (0%)	31 (100%)	<0.0001
Smoker¥	12 (15%)	10 (20%)	2 (6%)	0.202

† = median (IQR)
§ = mean (SD)
¥ = n (%)

7.2 Analysis by clone size

Due to the effects of eculizumab treatment on inflammation levels and prevention of complement activation, the relationship of granulocyte clone size with clot formation, structure and breakdown was analysed in patients not on treatment. A strong positive correlation was found between increasing granulocyte clone size and LDH levels ($r = 0.8598$, $p < 0.0001$, Figure 64). This indicated that as granulocyte clone size increased, disease severity was increasing, indicated by increasing LDH levels. This was in agreement with previous studies that have shown that a higher clone size leads to an increase in LDH (Schrezenmeier et al., 2014), indicating an increase in intravascular haemolysis and inflammation.

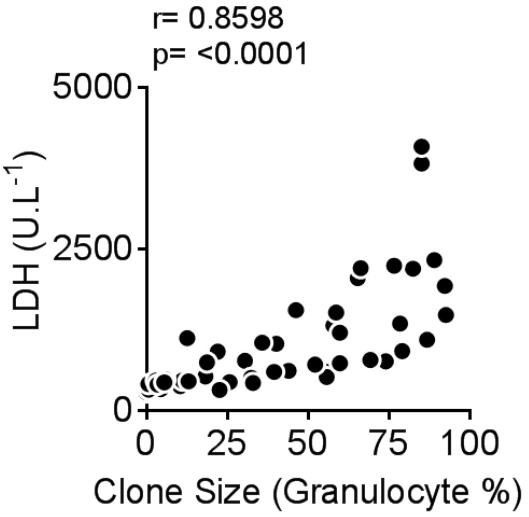

Figure 64 The relationship between clone size and LDH levels. The effects of increasing granulocyte clone size on LDH levels were assessed in patients not on treatment. Spearman's rank correlation. LDH - lactate dehydrogenase.

The relationship of granulocyte clone size with clot structure was investigated using confocal microscopy and permeation assays to assess

clot density. Changes in granulocyte size appeared to have no link to clot density, with confocal images showing no clear differences in clot structure between patients with different clone sizes (Figure 65A-B). Permeation assays supported this, showing no relationship between clone size and the porosity of clots (Figure 65C).

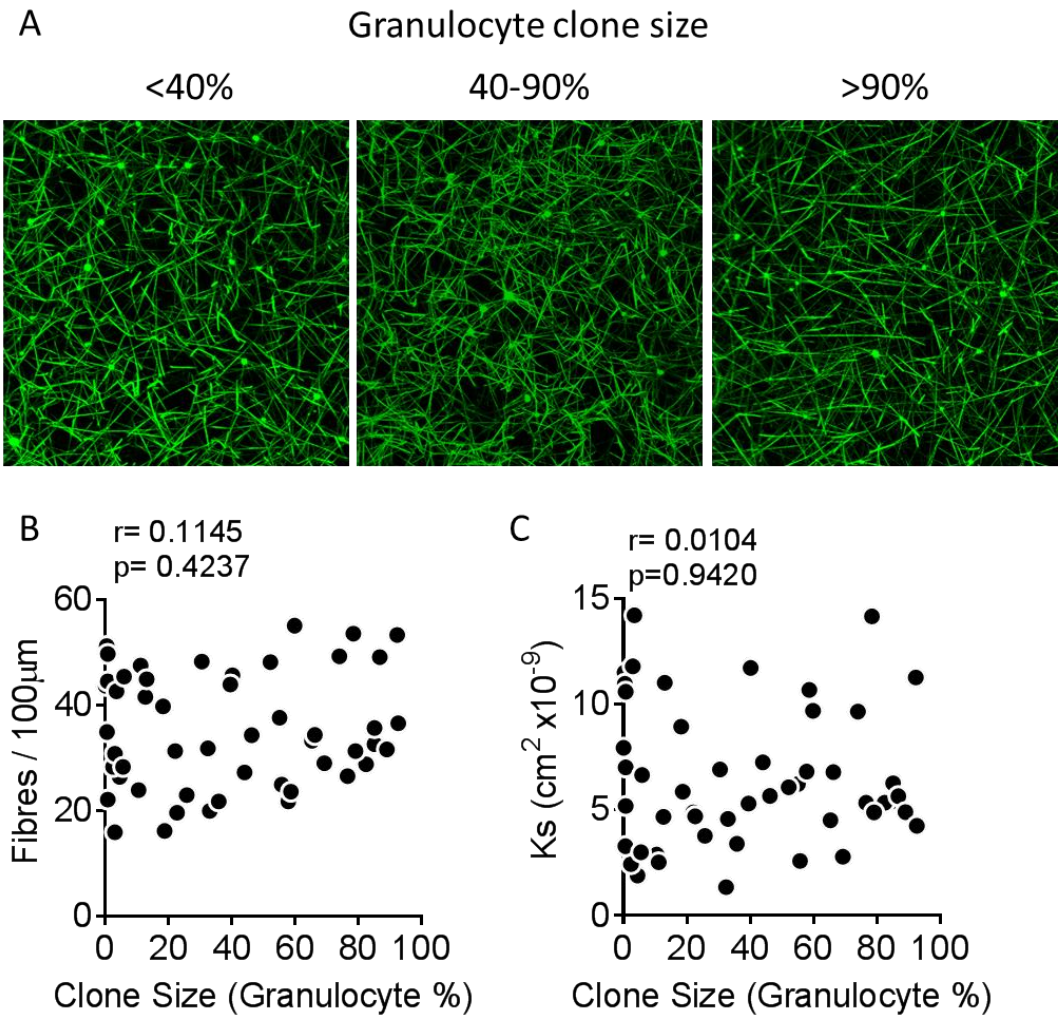

Figure 65 The relationship of clone size with clot structure. The relationship of increasing granulocyte clone size with clot structure and porosity was assessed in patients not on treatment. **A,** Representative confocal microscopy images of plasma clots from patients with a < 40 %, 40-90 % or > 90 % granulocyte clone size. **B,** Correlation of clone size with fibres/100 µm. Spearman's rank correlation. **C,** Correlation of clone size with Ks (cm^2 $x10^{-9}$, permeation constant). Spearman's rank correlation.

The relationship of granulocyte clone size with clot formation and breakdown was investigated using a turbidity and lysis assays. Changes in granulocyte

clone size appeared to have no link to clot formation, with no correlation found between clone size and lag time, Max OD, time to Max OD, time from 25-75 % clotting or turbidity Vmax (Figure 66A-E).

Similarly, changes in granulocyte clone size appeared to have no effect on clot breakdown either, with no correlation found between clone size and time to 50 % lysis, time from 25-75 % lysis and lysis Vmax (Figure 66F-H).

Previous studies have shown correlations between increased thrombotic risk and increased fibrinogen levels and thrombin production (Bridge et al., 2014). Therefore, the relationship of granulocyte clone size with fibrinogen levels and thrombin generation were investigated. No correlation was found between clone size and fibrinogen levels, endogenous thrombin potential (ETP) or peak thrombin generation (Figure 66I-K).

Together, these data suggest that there are no links between granulocyte clone size and clot formation, structure and breakdown or fibrinogen levels.

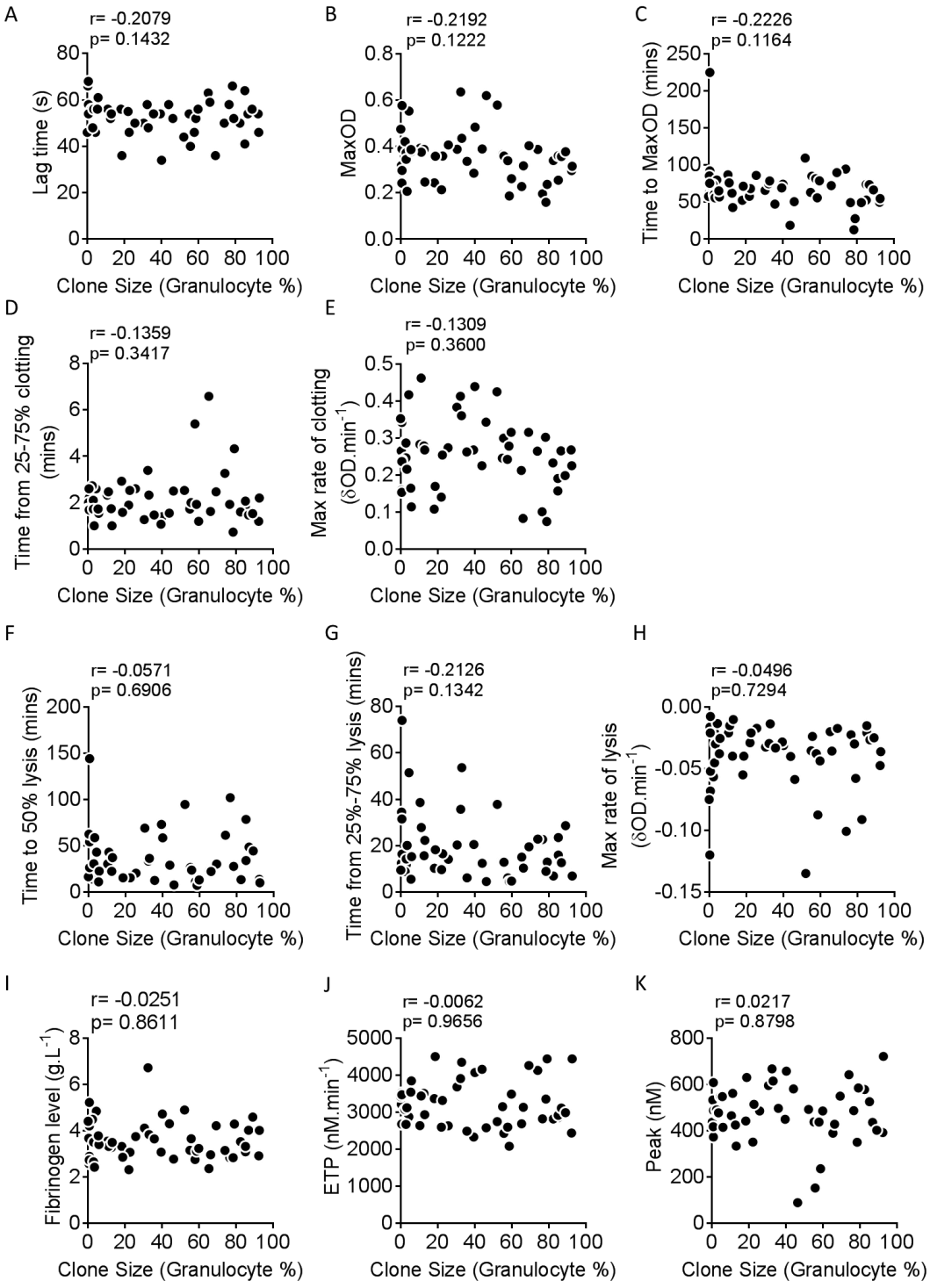

Figure 66 The relationship of clone size with clot formation and breakdown, fibrinogen levels and thrombin generation. The relationship of increasing granulocyte clone size with different parameters of clot formation and breakdown, fibrinogen levels and thrombin generation were assessed in patients not on treatment. **A,** Lag time (s). **B,** MaxOD. **C,** Time to MaxOD (mins). **D,** Time from 25-75 % clotting (mins). **E,** Max rate of clotting (δOD.min^{-1}). **F,** Time to 50 % lysis (mins). **G,** Time from 25-75 % lysis (mins). **H,** Max rate of lysis (δOD.min^{-1}). **I,** Fibrinogen levels (g.L^{-1}). **J,** ETP (nM.min^{-1}). **K,** Peak thrombin generation (nM). OD – optical density, ETP – Endogenous thrombin potential. Spearman's rank correlation.

7.3 Analysis by treatment

Treatment of PNH patients with eculizumab has been shown to drastically decrease thrombotic risk. To assess if changes in the clotting process may play a role in this reduction of thrombotic risk, the effects of treatment with eculizumab on clot formation and breakdown were investigated. Patients on eculizumab had a larger clone size of 90.1 % (IQR 71.6-99.7) than patients not on treatment with 33.0 % (IQR 5.6-66.2, $p < 0.0001$, Figure 67A). This was expected as studies have shown that an increase in clone size leads to a greater thrombotic risk, and therefore a greater need for treatment. Treatment with eculizumab prevents complement C5 cleavage, thereby inhibiting terminal complement activation. So patients on eculizumab presented with much lower levels of LDH, 482 $U.L^{-1}$ (IQR 409-524), than patients not on eculizumab, 615 $U.L^{-1}$ (IQR 435-1315), indicating a decrease in intravascular haemolysis and inflammation ($p = 0.0051$, Figure 67B).

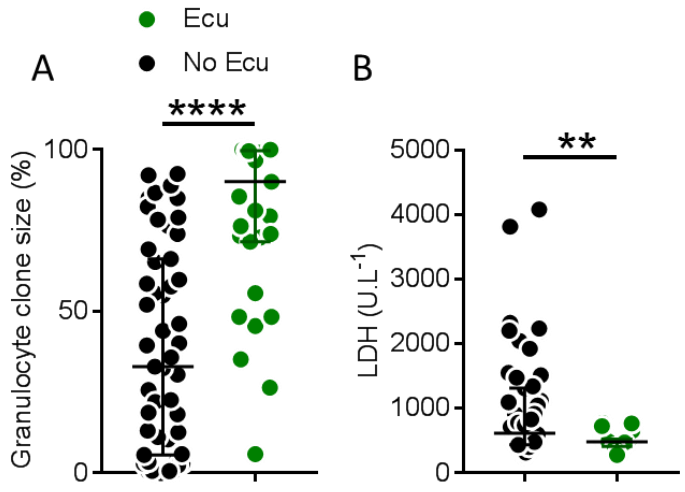

Figure 67 Granulocyte clone size and LDH levels between treatment groups. Granulocyte clone size and LDH levels were compared between patients on and off eculizumab. **A,** Granulocyte clone size in patients on or off eculizumab. **B,** LDH levels in patients on or off eculizumab. Mann-Whitney U test for pairwise comparisons. Ecu - eculizumab, LDH - lactate dehydrogenase.

The effects of eculizumab treatment on clot structure were explored using confocal and permeation assays. Patients on eculizumab treatment presented with clots that were less dense (Figure 68A). Clot density was quantified by counting the number of fibres/100 μm, and patients on eculizumab had significantly less dense clots (22.2 fibres/100 μm (IQR 19.7-32.2)) than patients not on treatment (33.2 fibres/100 μm (IQR 26.4-44.9), p = 0.0003, Figure 68B). There was a trend towards a higher porosity of clot (Ks) in patients on eculizumab, 7.6 cm^2 $x10^{-9}$ (IQR 3.7-11.5), compared to those not on eculizumab, 5.66 cm^2 $x10^{-9}$ (IQR 4.3-9.0), but this did not reach significance (p = 0.2763, Figure 68C).

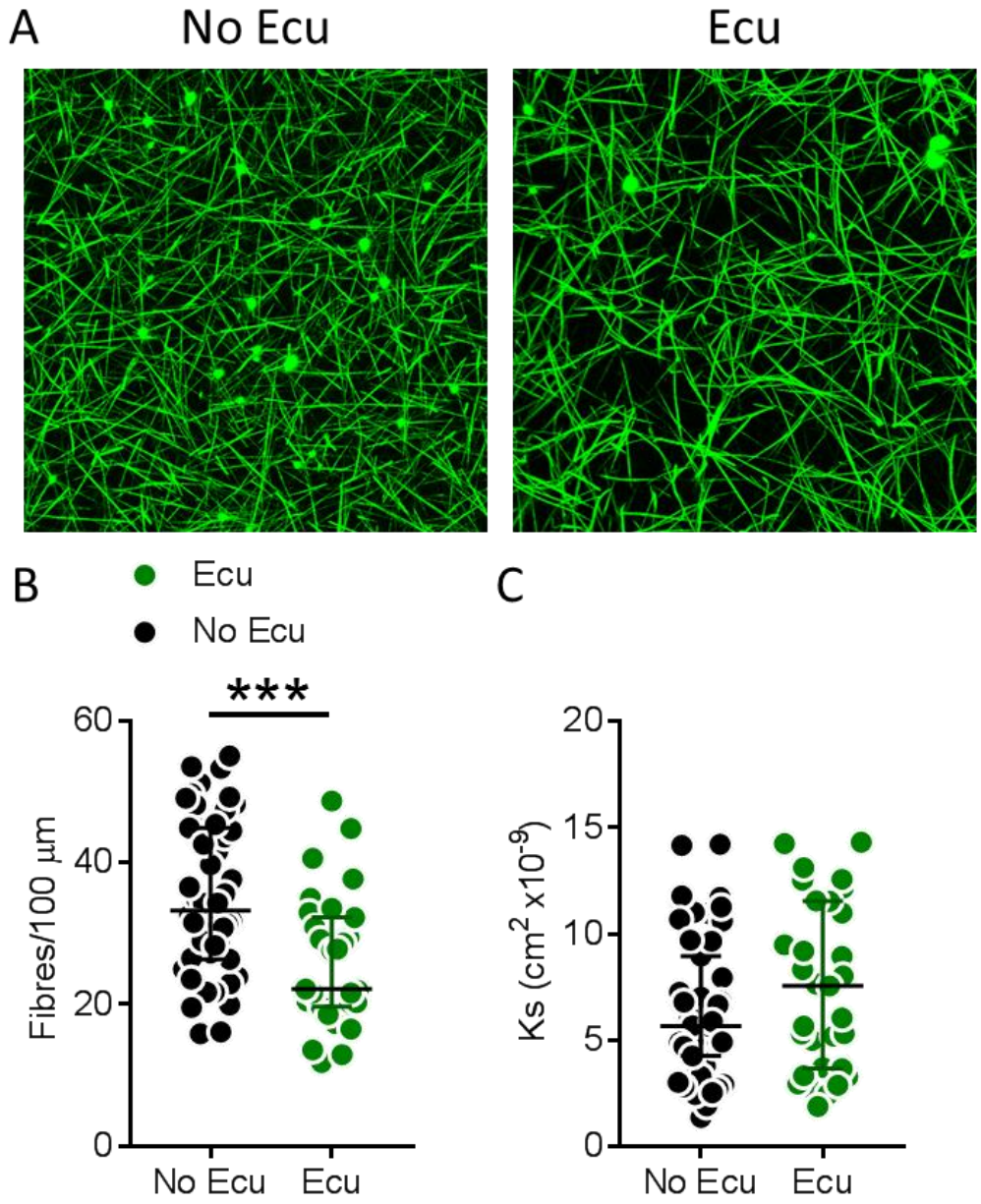

Figure 68 The effects of eculizumab treatment on clot structure. The effects of eculizumab treatment on clot structure and porosity were assessed. **A,** Representative confocal microscopy images of plasma clots from patients on or off eculizumab treatment. **B,** Effects of eculizumab treatment on fibres/100 µm. Spearman's rank correlation. **C,** Effect of eculizumab treatment on Ks (cm^2 $x10^{-9}$, permeation or Darcy constant). Mann-Whitney U test for pairwise comparisons. Ecu – eculizumab.

The effects of eculizumab treatment on clot formation and breakdown were investigated using turbidity and lysis assays. Treatment with eculizumab appeared to have no effect on lag time, time to maximum OD, time from 25-75 % of clot formation or the maximum rate of clotting (Figure 69A, C-E).

However, patients on eculizumab presented with a reduced maximum OD, 0.288 ± 0.068, compared to patients not on treatment, 0.355 ± 0.109, indicating the formation of less dense clots which is in agreement with the confocal data (p = 0.003, Figure 69B).

Treatment with eculizumab appeared to have no effect on clot breakdown, with no differences in time to 50 % lysis, time from 25-75 % of clot breakdown and maximum lysis rate found between patients on or off eculizumab (Figure 70A-C).

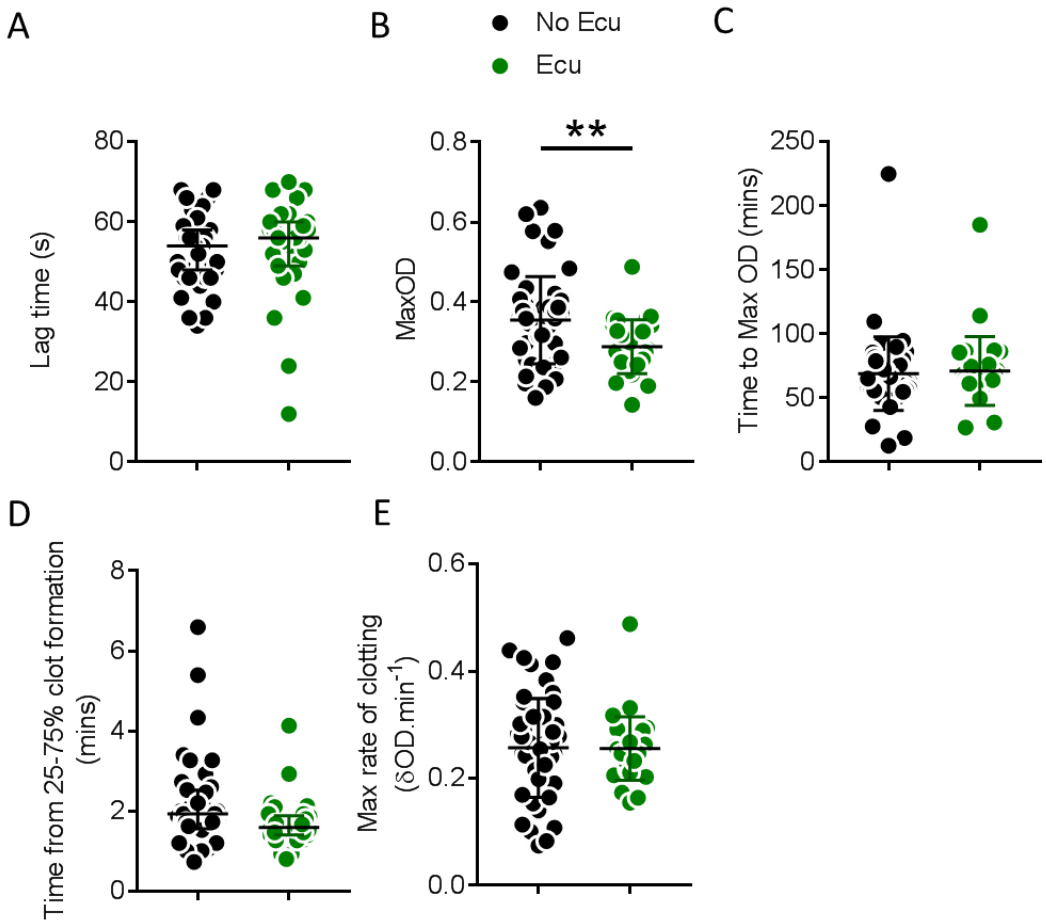

Figure 69 The effects of eculizumab treatment on clot formation. The effects of eculizumab treatment on different parameters of clot formation were assessed. **A,** Lag time (s). **B,** MaxOD. **C,** Time to MaxOD (mins). **D,** Time from 25-75 % clotting (mins). **E,** Max rate of clotting (δOD.min^{-1}). Ecu – eculizumab, OD – optical density. Mann-Whitney U test for pairwise comparisons – A, D. Unpaired student's t-test for pairwise comparison – B, C, and E.

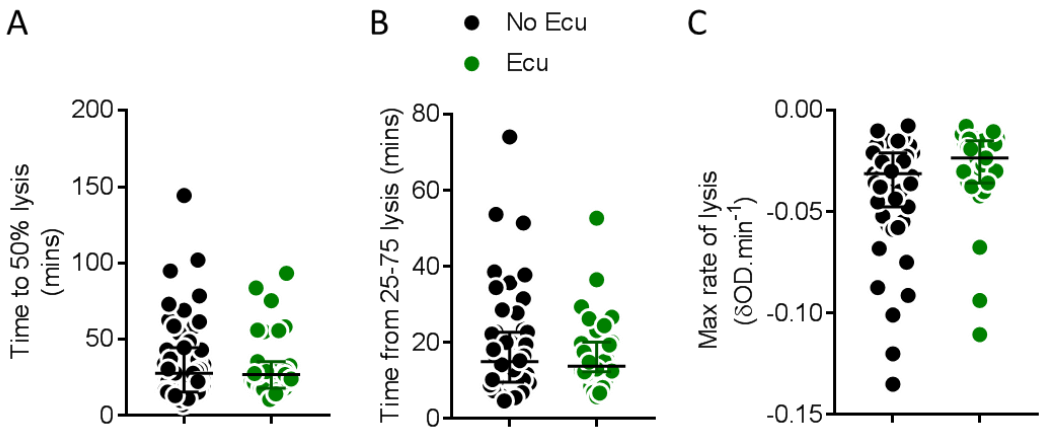

Figure 70 The effects of eculizumab treatment on clot breakdown. The effects of eculizumab treatment on different parameters of clot breakdown were assessed. **A,** Time to 50 % lysis (mins) **B,** Time from 25-75 % lysis (mins) **C,** Max rate of lysis ($\delta OD.min^{-1}$). Ecu – eculizumab, OD – optical density. Mann-Whitney U test for pairwise comparisons.

In view of the anti-thrombotic effects of treatment on clot structure, the effects of eculizumab on fibrinogen levels and thrombin production were investigated. Patients on eculizumab were found to have decreased fibrinogen levels, 2.87 $g.L^{-1}$ (IQR 2.30-3.38), when compared to patients not on treatment, 3.40 $g.L^{-1}$ (IQR 2.91-4.11, p = 0.0003, Figure 71A). When thrombin generation was examined, no difference was found in the time taken to begin thrombin production (Figure 71B). However, a significant decrease in endogenous thrombin potential (Ecu – 2644 ± 633 $nM.min^{-1}$ vs No Ecu – 3197 ± 625 $nM.min^{-1}$, p = 0.0002, Figure 71C) and peak thrombin production (Ecu – 421 nM (382-479) vs No Ecu – 486 nM (382-479), p = 0.0038, Figure 71D) was observed in the eculizumab group. This was in agreement with a small study on 11 patients with PNH that investigated the effect of complement C5 inhibition with eculizumab over 90 days (Weitz et al., 2012).

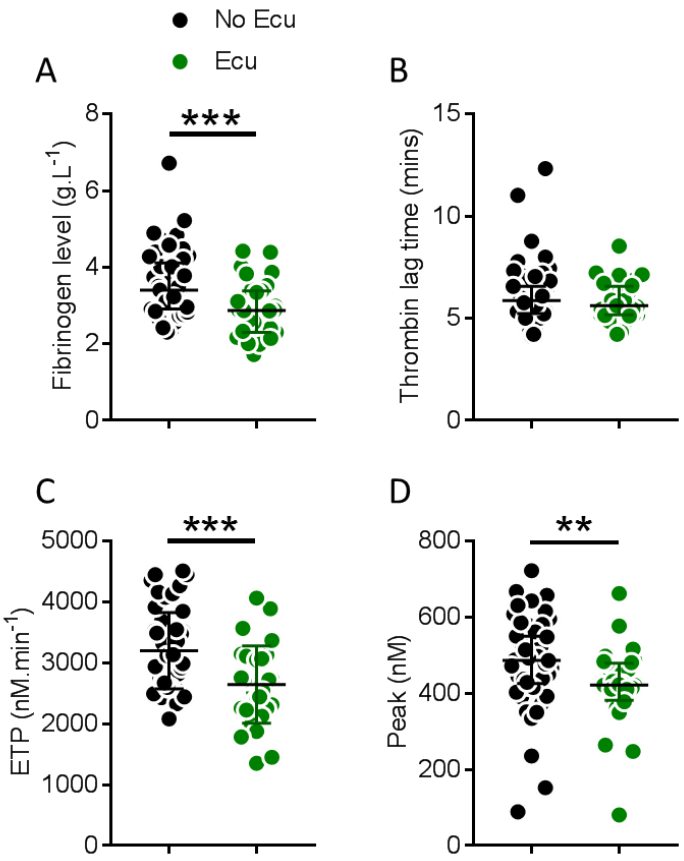

Figure 71 The effects of eculizumab treatment on fibrinogen and thrombin levels. The effects of eculizumab treatment on fibrinogen levels and thrombin generation were assessed. **A,** Fibrinogen levels ($g.L^{-1}$). **B,** Thrombin lag time (mins). **C,** ETP ($nM.min^{-1}$). **D,** Peak thrombin generation (nM). Ecu – eculizumab, ETP – Endogenous thrombin potential. Mann-Whitney U test for pairwise comparisons– A, B, D. Unpaired student's t-test for pairwise comparisons – C.

With eculizumab treatment leading to decreased fibrinogen and thrombin levels, the effects of eculizumab treatment time was investigated. In this population the length of time spent on eculizumab was independent of clone size, with no correlation between these two parameters (Figure 72A). As the length of eculizumab treatment time increased the levels of LDH decreased (Figure 72B).

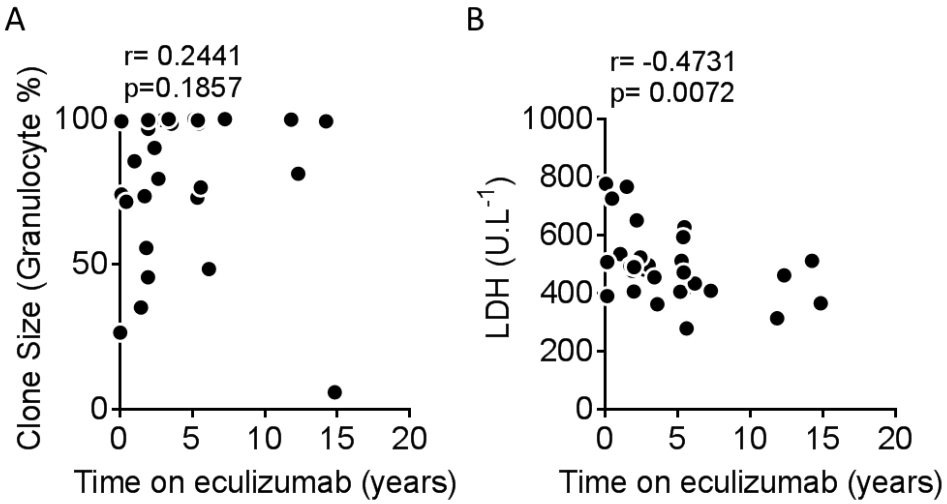

Figure 72 The relationship between time on eculizumab, clone size and LDH. The relationships between time on eculizumab with clone size and LDH were assessed**. A,** Clone size (Granulocyte %). **B,** LDH ($U.L^{-1}$). LDH - lactate dehydrogenase. Spearman's rank correlation.

Fibrinogen levels decreased as the length of time a patient had been treated with eculizumab increased (Figure 73A), mimicking the relationship of LDH with time on eculizumab. In agreement with this fibrinogen and LDH were also found to weakly correlate (Figure 73B) suggesting that their levels may be linked. In a similar manner, ETP decreased as the time spent on eculizumab increased (Figure 73C), with ETP also positively correlating with LDH levels (Figure 73D). ETP and fibrinogen levels were also correlated positively (Figure 73E). These data suggest that there is a link between LDH levels, fibrinogen levels and thrombin generation, and that the anti-thrombotic effects of eculizumab may, in part, be through changes in clot structure and reduction of fibrinogen and thrombin levels.

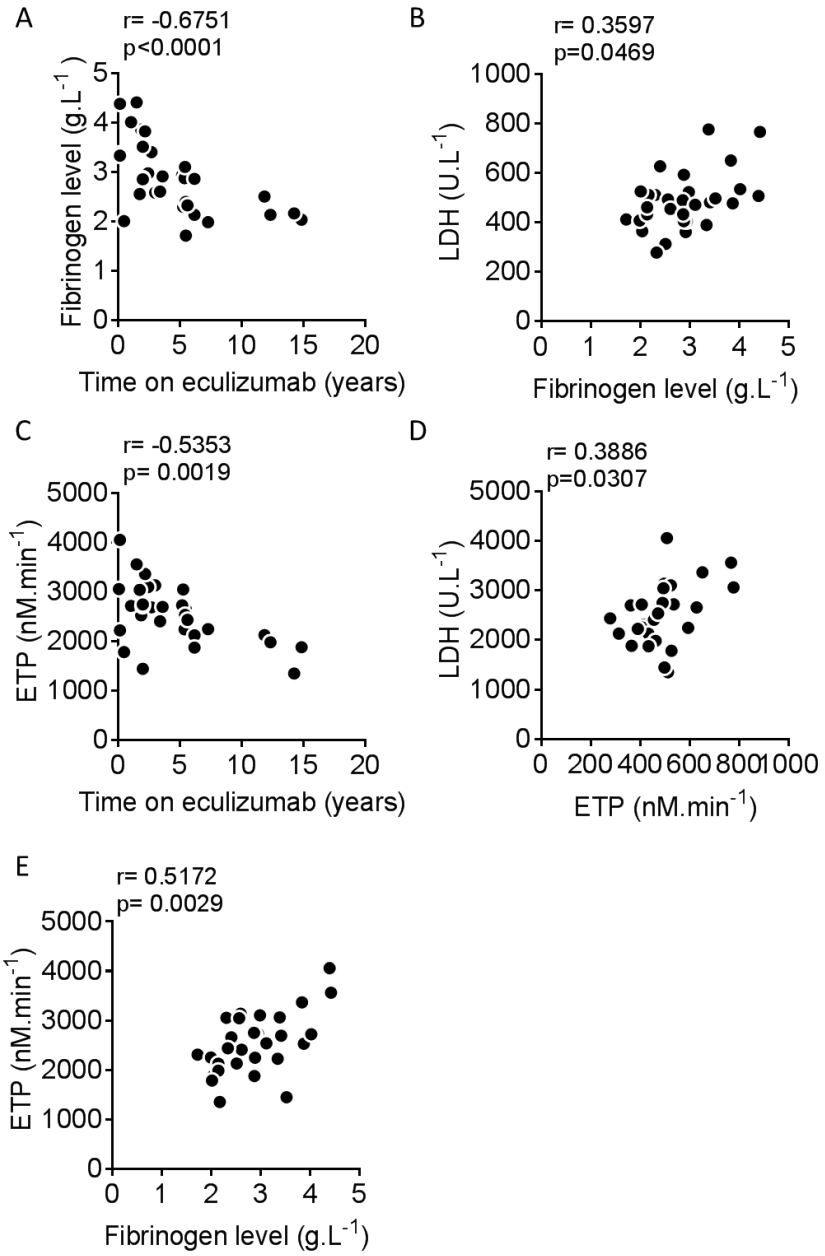

Figure 73 The relationship between time on eculizumab, fibrinogen levels and thrombin generation. The relationships between time on eculizumab with fibrinogen levels and thrombin generation were assessed**. A,** Fibrinogen levels ($g.L^{-1}$). **B,** LDH ($U.L^{-1}$).v Fibrinogen levels ($g.L^{-1}$). **C,** ETP ($nM.min^{-1}$). **D,** LDH ($U.L^{-1}$).v ETP ($nM.min^{-1}$). **E,** ETP ($nM.min^{-1}$) v Fibrinogen levels ($g.L^{-1}$). LDH - lactate dehydrogenase, ETP – Endogenous thrombin potential. Spearman's rank correlation.

7.4 Whole blood analysis

Previous studies have indicated that PNH has severe effects on blood cells involved in the clot formation process, including haemolysis of RBCs and the formation of more active platelets. We hypothesised that increasing granulocyte clone size resulting in increased complement activation would lead to a change in patient whole blood clot formation and firmness. To test this, exploratory experiments were carried out using ROTEM to analyse the mechanical properties of patient blood clots as they formed. So far, 15 whole blood samples from PNH patients have been analysed by ROTEM, and the group demographics are shown in Table 24. LDH levels in this group were found to correlate with clone size which was in agreement with the data from the whole PNH cohort presented earlier in this chapter (Figure 74).

ROTEM was carried out in 15 patients with PNH, using ex-tem or in-tem assays as described in chapter 2.1.9. Parameters from these measurements were correlated with granulocyte clone size to explore the relationship of clone size with clot formation.

Table 24 Demographics of PNH patients analysed by ROTEM.

	n=15
Age (years)†	47 (24, 64)
Weight (Kg)†	73 (53.6, 87.9)
Average granulocyte clone size (%)†	65 (0.4, 82.0)
LDH†	777 (331, 1448)
Systolic blood pressure (mmHg)§	133 (24..4)
Diastolic blood pressure (mmHg)§	79 (26.4)
On Eculizumab¥	0 (0%)
Smoker¥	3 (20%)

† = median (IQR)

§ = mean (SD)

¥ = n (%)

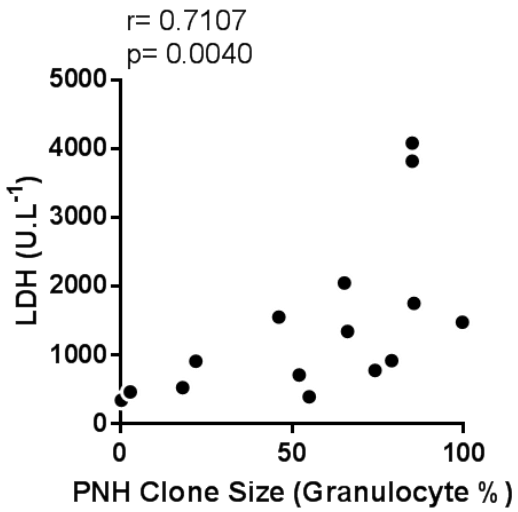

Figure 74 The relationship between clone size and LDH levels in ROTEM group. The effects of increasing granulocyte clone size on LDH levels were assessed in the subset of patients that were analysed by ROTEM. Spearman's rank correlation. LDH - lactate dehydrogenase.

No correlation was found between clone size and lag time with both ex-tem and in-tem. This suggests that increasing complement activation does not affect the initial speed of clot formation (Figure 75A). Positive correlations were found between clone size and MCF, average rate of clotting and maximum clotting rate with both ex-tem and in-tem assays (Figure 75B, D and E). There was also a negative correlation between clone size and time to MCF with in-tem assays, and a similar trend in the ex-tem assays (Figure 75C). This indicates that increases in clone size and complement activation may lead to more rapidly forming clots that are more stable and harder to breakdown. However, since numbers were small in this analysis, future studies with a larger number of patients should confirm these findings.

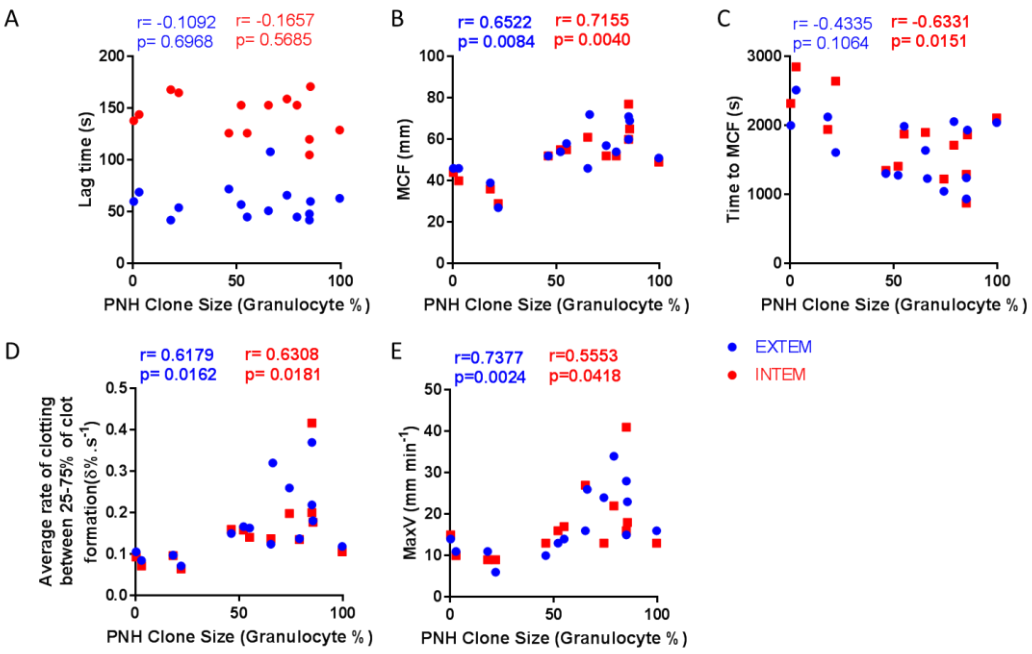

Figure 75 Ex-tem and in-tem ROTEM analysis of the relationship between granulocyte clone size and clot formation. The relationship between granulocyte clone size and ROTEM parameters of clot formation were assessed when clotting was initiated with ex-tem or in-tem (n = 15). Correlation of clone size with **A,** lag time (s), **B,** MCF (mm), **C,** Time to MCF (s), **D,** Average rate of clotting between 25-75 % of clot formation (δ%.s^{-1}), **E,** Maximum clotting rate (MaxV, mm.min^{-1}). A, D, E - Spearman's rank correlation. B, C – Pearson correlation. MCF – Maximum clot firmness.

7.5 Discussion

In this chapter, the role of fibrin clot structure in the development of thrombosis in patients with PNH and its treatment with eculizumab was investigated. This ongoing study is one of the first to investigate clot structure and the role of the fibrin clot in PNH related thrombosis, and is based on one of the largest collections of PNH patient plasma in the world.

Previous studies on patients with other thrombotic disorders have shown a link between changes in clot structure and thrombotic diseases. These changes include denser fibrin clots with thinner fibres that are less susceptible to fibrinolysis (Undas and Ariens, 2011). PNH is a pro-thrombotic disorder with many of the patients dying due to thrombotic complications (Hill et al., 2013), and a number of studies have shown that there is an increase in the risk of developing thrombosis with an increase in the proportion of PNH cells (Moyo et al., 2004, Hoekstra et al., 2009, Fowkes et al., 2003). PNH is particularly interesting to study with regards to thrombosis mechanisms, since uncontrolled complement activation appears to play a key role in driving thrombosis risk in these patients. Complement factors have previously been shown to influence clot structure (Hess et al., 2012, Hess et al., 2013). So it was hypothesized that an increase in the PNH granulocyte clone size in patients may result in a more pro-thrombotic clot structure.

Patients with a larger clone size were found to have markedly increased LDH levels, indicating increased intravascular haemolysis and tissue damage. However, in platelet poor plasma assays no links were found between changes in granulocyte clone size and the formation, structure or

breakdown of fibrin clots. Furthermore, as clone size increased there were no differences in thrombin generation or fibrinogen levels in plasma samples. However, patients on eculizumab were found to have decreased LDH and fibrinogen levels, and reduced clot density and reduced thrombin generation. Analysis of whole blood samples by ROTEM suggested a link between increasing clone size and faster forming, more stable clots most likely driven by the effects of complement activation on the cellular components of blood.

PNH differs from other thrombotic disorders as the increase in thrombotic risk is thought to be due to increased complement activation. A small number of studies have explored the link between the complement system and fibrin clot structure. One study has shown an association between complement activation via the alternative pathway and the formation of denser clots that are more resistant to lysis, but failed to uncover which complement proteins were involved (Shats-Tseytlina et al., 1994). Another study showed that MASP-1 can influence fibrin clot structure in a thrombin dependent manner (Hess et al., 2012). Complement protein C3 has also been linked to coagulation, with studies demonstrating that C3 is crosslinked into the fibrin clot which leads to prolonged fibrinolysis (Howes et al., 2012, Richardson et al., 2013). The data in this chapter helps to provide new information on the relationship between PNH and thrombosis, highlighting the potential role of intravascular haemolysis in the alteration of clot structure.

ROTEM was used to analyse the mechanical properties of blood clots from PNH patients. Changes in these properties have been shown in patients with

increased thrombotic risk (Spiezia et al., 2008, McCrath et al., 2005). In this study, MCF and clotting rate were increased as PNH clone size increased when clotting was initiated via the intrinsic or extrinsic pathway. This suggests a more prothrombotic state as clone size increases, which is in agreement with previous findings (Moyo et al., 2004, Hoekstra et al., 2009, Fowkes et al., 2003). Increases in MCF and clotting rates have previously been linked to thrombin generation, fibrinogen levels and platelet levels/activation (Kang et al., 1985, Schneider et al., 2015, Zuckerman et al., 1981), however there was no significant relationship seen between clone size and fibrinogen levels in this study. This would suggest that changes in MCF in PNH patients are most likely due to changes in platelet activation and thrombin generation. Despite the loss of CD55 and CD59, PNH platelets have been shown to have a normal lifespan, having increased complement mediated activation with increased FVa binding sites, resulting in increased thrombin generating capacity (Sims and Wiedmer, 1995, Wiedmer et al., 1993). Platelets have also been shown to be able to shed the MAC complex, avoiding complement mediated lysis (Sims and Wiedmer, 1991). Alternatively, the observed changes may be due to changes in cells in the blood other than platelets (e.g. neutrophils, monocytes and RBCs), either effecting polymerization via thrombin generation or altering clotting rates and firmness as they were incorporated into the clot. These characteristics may offer some explanation for the changes seen in clot properties in this study and the pro-thrombotic state in PNH.

Results from plasma assays showed no link between clone size and fibrin clot structure. These results may help to pinpoint where complement activation plays a role in clot formation. There are a few possible

explanations as to why no differences were seen in plasma samples, but changes in clot structure were seen in whole blood samples. ROTEM assays were carried out using whole blood, but all other clot structure assays were carried out using platelet poor plasma with all blood cells removed. Previous studies have demonstrated the multiple factors that contribute to a prothrombotic state in PNH and the majority of these involve blood cells (neutrophils, monocytes, platelets, RBCs). Therefore, most changes in clot structure in PNH patients may arise from changes to the cell components of blood.

Another variation between experimental setups to consider is the initiator of clotting. In all plasma assays except thrombin generation, clotting was initiated with thrombin bypassing the clotting cascade. However, in ROTEM assays, clotting was initiated with thromboplastin or ellagic acid, activating the extrinsic or intrinsic pathway respectively. The use of thrombin may have bypassed some effects that complement activation may have had on the coagulation cascade. Previous studies have suggested links between the complement and clotting cascades that may influence thrombin generation, but in this study no link was found between clone size and thrombin generation. It should be noted that thrombin generation assays were performed in the absence of cells, so this could indicate that complement activation may play a role in cell based thrombin generation.

A further point to consider is the presence or lack of activated complement proteins or mechanisms in the plasma samples. Complement proteins have varying half-lives ranging from 1 minute up to a couple of hours (Kirschfink and Mollnes, 2003). Whole blood samples were analysed within 4 hours of

the blood draw, so some activated complement proteins would still be present, and more may have been generated in the presence of complement affected cells or free haemoglobin (Wilson and Thomas, 1979). Plasma samples were generated by centrifugation of whole blood within 4 hours of the blood draw, and were then frozen and kept for between 2 months and a year before analysis was carried out. In this time there could have been degradation of complement proteins, resulting in absence of activated complement proteins or mechanisms present during the analysis of the samples.

Treatment with eculizumab appeared to show clear effects on clot structure. Treatment of PNH with eculizumab has been shown to drastically reduce thromboembolic events (Hillmen et al., 2007). It imparts its effects through the inhibition of C5 cleavage, preventing downstream complement activation. In this study, treatment with eculizumab had significant anti-thrombotic effects, with patients on eculizumab presenting with clots with reduced fibre density, decreased fibrinogen levels and reduced thrombin generation. Furthermore, as the length of time spent on eculizumab increased, the levels of LDH, fibrinogen and thrombin generation decreased.

LDH is a tetrameric enzyme that is expressed extensively throughout the body and is released during tissue damage and intravascular haemolysis, and because of this it is regularly used as a marker of intravascular damage. Previous studies have shown that an increase in granulocyte size leads to an increase in intravascular haemolysis and LDH levels (Schrezenmeier et al., 2014), and this was corroborated in this study, with LDH levels positively correlating with clone size. Treatment with eculizumab led to a decrease in

LDH which has previously been seen in clinical trials, with eculizumab treatment reducing intravascular haemolysis (Hillmen et al., 2007). The negative correlation of eculizumab treatment time with LDH levels supported previous findings that eculizumab has good long term effects against complement mediated intravascular haemolysis (Hill et al., 2005), and potentially points to improved or accumulative effects over long time periods.

The relationships found in this study between eculizumab treatment and changes in clot structure, fibrinogen levels and thrombin generation could be explained by the reduction in intravascular haemolysis brought about by C5 inhibition. Increased intravascular haemolysis has previously been linked to an increased inflammatory response including amplified IL-6 release (Almeida et al., 2015, Conran and Almeida, 2016). In a small study, patients treated with eculizumab were found to present with decreased IL-6 levels (Weitz et al., 2012). IL-6 is a known regulator of fibrinogen synthesis, with fibrinogen genes being highly responsive to changes in IL-6 levels (Heinrich et al., 1990), and so it is possible that a reduction in IL-6 levels could lead to a reduction in fibrinogen production. The reduction in fibrinogen levels in eculizumab treated patients in this study may be explained by a reduction in intravascular haemolysis, leading to a drop in inflammation resulting in a decrease in the stimulation of fibrinogen production.

A reduction in thrombin generation in patients treated with eculizumab has previously been reported (Helley et al., 2010, Weitz et al., 2012, van Bijnen et al., 2015), but the potential mechanisms underpinning reduced thrombin generation in patients on eculizumab are still unknown. The independent correlation of ETP with LDH and fibrinogen levels in this study suggest that

thrombin generation may be linked to one or both of these. Intravascular haemolysis is known to result in a pro-coagulant state through the formation of RBC fragments, which lead to increased thrombin generation (Stief, 2007). Reducing intravascular haemolysis with eculizumab treatment may lead to a reduction in thrombin generation. The reduction in thrombin generation could also be attributed to the reduction in fibrinogen levels. A number of studies have highlighted links between thrombin generation and fibrinogen levels (Stepien et al., 2007, Kremers et al., 2013, Zentai et al., 2016), indicating a relationship where increased fibrinogen levels lead to increased thrombin generation. This suggests that the opposite is possible, with a reduction in fibrinogen levels resulting in a reduction in thrombin generation.

Fibrin clot structure is dependent on many factors including fibrinogen concentration and thrombin generation, with increased fibrinogen levels and increased thrombin generation both leading to more densely packed clots (Machlus et al., 2011, Wolberg, 2007). A decrease in fibrinogen levels and thrombin generation could help to explain the changes in clot structure in patients on eculizumab, with these changes resulting in a decrease in fibrin network density and a less thrombotic state.

There are a few limiting factors in this study. The rarity of PNH makes it difficult to obtain large study numbers, with it taking four years to recruit 82 patients for this study. A greater number of patients both on and off treatment with a larger spread of clone sizes would have increased the power of this study. Also a larger number of patients with whole blood ROTEM analysis is required. The low number of patients means that the

statistical analysis of the ROTEM data may not represent the true effects of PNH on clot structure. The introduction of a control group would make it possible to compare clot structure to individuals without PNH, but choosing the selection criteria for the control group may be difficult. Patients with PNH can be split into three groups. Classical PNH, characterized by intravascular haemolysis with no evidence of an underlying bone marrow disorder. A second group have haemolytic PNH and a bone marrow disorder, such as aplastic anaemia. The third group can be defined as subclinical PNH where they possess a small proportion of PNH cells, but they have no evidence of haemolysis or thrombosis (Parker et al., 2005). There is potential that two control groups may be required. One that contains patients with an underlying bone marrow disorder and one with healthy controls. A larger patient demographic would also help to improve the study, and highlight the effects of confounding factors in the disease.

In summary, this chapter has shown that clots formed from whole blood from PNH patients with larger clone sizes had increased stability and formed at a quicker rate. However, these changes did not appear in clots formed from platelet poor plasma. Eculizumab treatment led to a reduction in LDH levels, fibrinogen levels, thrombin generation and clot density. This suggests that the anti-thrombotic effects of eculizumab may occur through a reduction in intravascular haemolysis, which in turn may lead to a less thrombotic clot structure.

7.6 Future work

This study has highlighted that more research is needed into the links between PNH and clot structure, and the mechanisms behind eculizumab treatment. PNH has a significant effect on blood cells which appears to play an important role in PNH driven thrombosis. In this study there was only a limited number of patient samples analysed by ROTEM. To increase the power of this data more patient samples could be analysed by ROTEM. Further whole blood analysis could also be carried out, but many of the clot structure experiments are not possible in whole blood. To further the understanding of PNH mechanisms in whole blood, whole blood flow assays and whole blood SEM could also be carried out, and the assessment of fibrinolysis in whole blood could also be investigated using the halo clot assay (Bonnard et al., 2017). Thrombin generation in whole blood could also be investigated using fluorogenic thrombin generation assays (Ninivaggi et al., 2012), this would help to uncover if thrombin generation is increased in PNH patients in whole blood, and also help to uncover the mechanisms by which eculizumab effects thrombin generation. As the levels of thrombin generation were decreased in patients on eculizumab, it would be important to measure levels of prothrombin in these patients to assess if reduced levels of prothrombin are the reason for reduced thrombin production. Measuring haemolysis levels in patient plasma samples could also be carried out. This would help to investigate the relationship between intravascular haemolysis levels and changes in coagulation factors and clot structure. The development of a longitudinal study with multiple follow up blood samples from each patient would be of great interest, allowing

analysis of changes in coagulation factors and clot structure as the disease progresses, and permitting the study of the long term effects of eculizumab treatment in more detail. Another line of research that could be followed to improve the understanding of PNH and thrombosis would be to stimulate complement activation in the blood of healthy volunteers. This would help show if complement activation has an immediate effect in blood and if this results in changes in clot formation and breakdown. The role of complement inhibitors in blood could also be more closely explored in this *in vitro* setting.

These studies would help to take a more in depth look at the link between complement activation and the coagulation cascade, helping to identify the cause of increased thrombosis in PNH. They would also help to develop new therapeutic targets for the treatment of PNH and improve the current treatments.

Chapter 8 - General discussion and conclusions

8.1 General Discussion

The aim of this thesis was to explore the role of fibrin(ogen) in the settings of thrombosis and haemostasis to uncover new mechanisms that cause or prevent disease. Fibrin(ogen) plays multiple roles in the body, including the facilitation of endothelial cell spreading, tissue fibroblast proliferation, capillary tube formation, and angiogenesis which all aid the wound healing process. However, its most notable and perhaps best known role is in the coagulation process. The formation of a fibrin clot is an important part of haemostasis, combining with platelets and other blood cells to form a seal at sites of vascular damage to prevent blood loss. When these clots form intravascularly it can lead to serious complications in the tissue or organ affected, leading to heart attacks and strokes. The role of coagulation and the fibrin clot in the initiation and progression of many CVDs is not fully understood. Multiple studies have found links between thrombotic disorders and changes in clot structure, but in many cases it is still unclear if these changes represent cause or effect. This thesis investigated different pathways that are known to influence clot structure in an attempt to uncover mechanisms involved in the pathophysiology of thrombosis and haemostasis. It also explored patients with thrombotic disorders to elucidate if changes in clot structure contribute to the formation and progression of the disease. By understanding the roles and mechanisms of fibrin(ogen) in both haemostatic and thrombotic clots, new targets for therapeutics may be uncovered.

One of the findings presented in this thesis has shown that fibrinogen γ' influences clot formation, structure and breakdown at physiological

concentrations. However, the influence of fibrinogen γ' on CVD is not clear-cut and the relationship may not be as simple as increasing γ' levels causing denser clots that are harder to break down. The effects of γ' on clotting and fibrinolysis rates in purified systems were not always consistent with those seen in patient plasma samples. This may have been due to the influence of other components within the patient plasmas, either by these components having a greater effect on clotting and masking the effects of γ', or due to interactions between γ' and plasma factors that were not seen in the purified system. A number of these relationships between γ' and plasma components, FXIII and thrombin for example, have already been investigated, but several of these studies disagree on the effects of these interactions. Without a better understanding of the interactions of fibrinogen γ' with other plasma proteins it is difficult to elucidate the mechanisms of γ' in thrombosis, and so further research is required to uncover this. Further insight into this relationship could be achieved with the use of arterial and venous thrombosis animal models. The preferred animal for thrombosis models is mice, but mice do not possess the fibrinogen γ' variant. So to examine the role of γ' in mice, thrombosis models would have to be carried out in Hu-γ' transgenic mouse models previously demonstrated by Mosesson et al. (Mosesson et al., 2009), or in fibrinogen deficient mice infused with human fibrinogen γ'. These models would both have limitations, but would provide useful information on the roles of γ' in a complex *in vivo* situation.

Another finding of interest presented in this thesis was the effects of fibrinogen γ' under flow and shear stress. Fibrinogen γA/γ' clots formed under venous flow rates were shown to form much quicker and have much

greater volume and height than those made with γA/γA fibrinogen under comparable conditions. Yet at higher flow rates clots from both γA/γ' and γA/γA fibrinogen variants formed at similar speed, with the difference in clot volume and height greatly reduced. These data suggest that there are flow rate specific changes in clot structure between fibrinogen γ' and γA, and that these changes could potentially influence thrombosis via different pathways. This is an important finding which may provide insight into previous studies that have shown associations of increased levels of γ' in arterial thrombotic disorders (Lovely et al., 2002, Cheung et al., 2008, Appiah et al., 2015) and decreased levels in venous thrombotic disorders (Uitte de Willige et al., 2005, Mosesson et al., 2007, Nowak-Gottl et al., 2009). Could the flow rate dependent changes seen with fibrinogen γ' provide an explanation for these apposing associations? In arterial thrombosis an increase in fibrinogen γ' could lead to the formation of larger clots with more branched fibres, that when combined with the increased pressure of high flow rates become very compact and difficult to breakdown. In venous thrombosis lower flow rates allow for the formation of larger more voluminous clots. Without the increased pressure, an increase in fibrinogen γ' in this situation could lead to less stable more porous clots that are more easily broken down. This highlights the need to explore the role of vascular flow rates on thrombosis, and investigate not only the role of fibrinogen γ' in flow conditions, but also other factors within the blood. This could be investigated in a similar fashion to the animal experiments mentioned previously with the use of arterial and venous thrombosis models in wildtype and transgenic mouse models.

Fibrinogen γ' levels do not always play a role in CVD. In Chapter 6 it was shown that there is no difference in fibrinogen γ' levels between AAA

patients and controls, suggesting that γ' levels have no influence on the incidence of AAA . However, AAA patients have previously been shown to suffer from increased thrombotic risk (Thompson et al., 2012) and altered clot structure (Scott et al., 2011). This, in part, may be due to the previously reported increase in overall fibrinogen levels in AAA patients (Al-Barjas et al., 2006, Scott et al., 2011), but changes in clot structure are not normally due to the fibrinogen molecule alone. FXIII is known to influence clot structure by crosslinking fibrin molecules together, increasing clot strength and stiffness, and alterations to this process can play a role in the pathogenesis of thrombosis (Hethershaw et al., 2014, Byrnes et al., 2016). However, there appears to be very little research into the role of FXIII in AAA. Research findings regarding coding FXIII sequence variants presented in Chapter 6 indicate that FXIII may indeed play a role in AAA. The allele frequency of the sequence variant FXIII-B His95Arg was found to be increased in patients with an AAA, indicating a small increase in the risk of developing an AAA when in possession of an Arg allele. FXIII-B His95Arg has been reported to influence FXIII subunit dissociation and activation rates (Komanasin et al., 2005), which in turn may alter clot stability. This presents a possible mechanism for the role of this sequence variant in AAA disease, but will need further studies, using suitable *in vitro* and *in vivo* models. FXIII-B His95Arg could influence ILT clot structure and/or other clots in the body which may contribute to the increased thrombotic risk. Further research is required to uncover the role of FXIII and other clot structure modulators in AAA.

Combined, these data are in clear agreement with the notion that thrombosis is not a "single gene" disease, and that many disorders that cause or

associate with thrombosis are multifactorial, with differential cellular and humoral driving mechanisms. These mechanisms are not always induced by changes in the clotting process alone, with the inflammatory and immune systems often contributing to the pathophysiology of the disease. A prime example of this is thrombosis in patients with PNH. A mutation in the PIG-A gene leads to increased complement activation which results in a significant increase in thrombotic risk (Brodsky, 2014), and this appears to be driven by multiple factors (Peacock-Young et al., 2018). In this study patients with increased granulocyte clone size were found to have faster forming and more stable clots, in agreement with the greater thrombotic risk. Previous findings also suggested that changes in fibrin clot structure were not a major contributor to thrombosis in this disease. However, this study did find that PNH patients treated with eculizumab showed reduced LDH levels, fibrinogen levels, thrombin generation and clot density. Eculizumab is known to prevent end stage complement activation, which in turn leads to a reduction in inflammation (Hillmen et al., 2004). Could this reduction in inflammation be the driving force behind the anti-thrombotic effects of eculizumab? This, in turn, may also suggest that inflammation may be a major component of thrombosis in PNH, and the use of anti-inflammatory treatments could be explored in the treatment of this disease. These data indicate that increases in platelet activity, haemolysis, inflammation and NETs, independent of changes in clot structure, may be the driving force behind thrombosis in PNH.

The lack of changes in fibrin clot structure in PNH patients may begin to provide insight into different types of thrombosis and their locations. PNH is relatively unique in that thrombosis can occur in just about any site in the

body, with common sites including the coronary and cerebral veins and arteries (Hill et al., 2012) and the hepatic vein, for reasons still unknown. Patients with other thrombotic disorders such as many types of thrombophilia (antiphospholipid syndrome, prothrombin and FV mutations and antithrombin, protein C and protein S deficiencies), the disease mostly presents as venous thromboembolism (Simioni et al., 2006). Previous studies data suggest that clot structure is altered in thrombophilia (Undas, 2017), and many studies have found altered clot structure in patients who have suffered a VTE (Undas and Ariens, 2011). This could suggest that the driving force behind the thrombosis is important to its location, with thrombosis driven in some part by changes in fibrin clot structure occurring in certain places more regularly. More research is needed to explore the connection between locations of thrombi and the underlying cause for its formation.

To fully understand the implications and mechanisms of fibrin clots in disease, a complete understanding of its role in normal coagulation is required. We have a vast understanding of many mechanisms of haemostasis, but it is clear that our knowledge is far from complete, with new information and mechanisms continually being uncovered. This thesis reveals a novel mechanism of haemostatic fibrin films that form at the air-blood interface of external injuries, preventing bacterial invasion. The data demonstrate that fibrin films may play an important role in the protection against infection. This could lead to new targets to prevent infection at sites of injury, preventing blood borne infections, sepsis and infection induced thrombosis. It may also provide new therapeutics that could improve tissue repair by reducing infections in wounds. Further research is required to

uncover the complete structure of the film, fully explore how changes in underlying clot structure influence film formation and if fibrin films can be exploited to improve wound healing. This may be particularly relevant for patients with diabetes, who suffer impaired wound healing (Goodson and Hunt, 1977). Furthermore, other diseases may also be targeted for improved treatment, e.g. PVD (Henry et al., 2014) and Obesity (Pierpont et al., 2014) which result in significant complications and burden to healthcare organisations due to wound healing complications.

This extraordinary finding also begins to raise questions about if these films may also be present in thrombosis. Do fibrin films form intravascularly? Previous studies with Langmuir-Blodgett experiments have shown film formation of fibrin(ogen) on phosphatidylcholine coated surfaces (Sankaranarayanan et al., 2010), suggesting fibrin film formation could occur on phospholipid surfaces intravascularly. My lab also already has indirect evidence of fibrin films forming on intravascular thrombi from murine $FeCl_3$ models of thrombosis. Others have also observed similar film structures at the clot boundaries of arterial intracranial thrombi extracted using stent-retriever in patients with stroke (van Es et al., 2017, Autar et al., 2018). Together these findings begin to support the formation of intravascular fibrin films, but further research is required to confirm this. So what effect would these films have on thrombosis? Initial studies have indicated that fibrin films would not slow lysis directly as they were found to breakdown with plasmin at the same rate as fibrin fibres. However, films within thrombi may play an indirect role on clot breakdown potentially slowing fibrinolysis rates by reducing perfusion of the fibrinolytic proteins through the clot network. It is also possible that fibrin films may play a key role in the mechanic stability of

thrombi, for example through the retention of RBCs in these thrombi and through other mechanisms. The formation of films in thrombi could have implications in many thrombotic diseases. Would these films play a bigger role in slower forming thrombi like ILTs in AAA, forming in multiple places throughout the thrombus, than in the rapid forming thrombi in PNH? Would these films form differently in arterial and venous flow rates? These findings highlight tantalising new opportunities for future research in this area, with the potential to transform our understanding of thrombosis and thrombus stability, leading to future novel therapeutic or diagnostic opportunities.

8.2 Conclusions

In summary, there are a number of main conclusions to be drawn from this thesis:

1. Fibrinogen γ' plays an important role in modulating clot structure at physiological concentrations, and it significantly influences the height and volume of clots produced under flow conditions.
2. The FXIII-B Arg95 variant is associated with an increased risk of AAA, suggesting a possible role for FXIII in AAA pathogenesis.
3. PNH patients with increased clone size have a more thrombotic phenotype, with faster forming, more stable clots. While changes in fibrin clot structure do not appear to be the primary cause of thrombosis in this disease, while complement inhibition with eculizumab normalises clot structure.
4. Formation of fibrin films on the blood clot exterior reveal a mechanism in haemostasis that helps retain blood cells and control microbial

infection, and it appears to be an important physiological process that should be exploited in the future.

This thesis has explored the changes, mechanisms and roles of fibrin clot formation, and it has demonstrated how multiple different pathways can lead to changes in clot structure. From small changes in the fibrin(ogen) molecule (fibrinogen γ') leading to faster forming larger clots, to the introduction of an interface which alters the polymerization process and structure of fibrin. These changes have then been shown to be either beneficial, protecting against infection, or harmful, promoting thrombosis. Together these data have highlighted new mechanisms and pathways that can be targeted for future therapeutic treatments. They also demonstrate how our current knowledge of fibrin clots in haemostasis and thrombosis is still far from complete, and that fibrin needs to remain an area of research interest in the future.

References

ADOLPH, R., VORP, D. A., STEED, D. L., WEBSTER, M. W., KAMENEVA, M. V. & WATKINS, S. C. 1997. Cellular content and permeability of intraluminal thrombus in abdominal aortic aneurysm. *J Vasc Surg,* 25**,** 916-26.

AILAWADI, G., ELIASON, J. L. & UPCHURCH, G. R., JR. 2003. Current concepts in the pathogenesis of abdominal aortic aneurysm. *J Vasc Surg,* 38**,** 584-8.

AJJAN, R., LIM, B. C., STANDEVEN, K. F., HARRAND, R., DOLLING, S., PHOENIX, F., GREAVES, R., ABOU-SALEH, R. H., CONNELL, S., SMITH, D. A., WEISEL, J. W., GRANT, P. J. & ARIENS, R. A. 2008. Common variation in the C-terminal region of the fibrinogen beta-chain: effects on fibrin structure, fibrinolysis and clot rigidity. *Blood,* 111**,** 643-50.

AL-BARJAS, H. S., ARIENS, R., GRANT, P. & SCOTT, J. A. 2006. Raised plasma fibrinogen concentration in patients with abdominal aortic aneurysm. *Angiology,* 57**,** 607-14.

ALCORN, H. G., WOLFSON, S. K., JR., SUTTON-TYRRELL, K., KULLER, L. H. & O'LEARY, D. 1996. Risk factors for abdominal aortic aneurysms in older adults enrolled in The Cardiovascular Health Study. *Arterioscler Thromb Vasc Biol,* 16**,** 963-70.

ALLAN, P., DE WILLIGE, S. U., ABOU-SALEH, R. H., CONNELL, S. D. & ARIENS, R. A. S. 2012. Evidence that fibrinogen gamma ' directly interferes with protofibril growth: implications for fibrin structure and clot stiffness. *Journal of Thrombosis and Haemostasis,* 10**,** 1072-1080.

ALMEIDA, C. B., SOUZA, L. E., LEONARDO, F. C., COSTA, F. T., WERNECK, C. C., COVAS, D. T., COSTA, F. F. & CONRAN, N. 2015. Acute hemolytic vascular inflammatory processes are prevented by nitric oxide replacement or a single dose of hydroxyurea. *Blood,* 126**,** 711-20.

AMELOT, A. A., TAGZIRT, M., DUCOURET, G., KUEN, R. L. & LE BONNIEC, B. F. 2007. Platelet factor 4 (CXCL4) seals blood clots by altering the structure of fibrin. *J Biol Chem,* 282**,** 710-20.

ANNABI, B., SHEDID, D., GHOSN, P., KENIGSBERG, R. L., DESROSIERS, R. R., BOJANOWSKI, M. W., BEAULIEU, E., NASSIF, E., MOUMDJIAN, R. & BELIVEAU, R. 2002. Differential regulation of matrix metalloproteinase activities in abdominal aortic aneurysms. *J Vasc Surg,* 35**,** 539-46.

APPIAH, D., HECKBERT, S. R., CUSHMAN, M., PSATY, B. M. & FOLSOM, A. R. 2016. Lack of association of plasma gamma prime (gamma') fibrinogen with incident cardiovascular disease. *Thromb Res,* 143**,** 50-2.

APPIAH, D., SCHREINER, P. J., MACLEHOSE, R. F. & FOLSOM, A. R. 2015. Association of Plasma gamma' Fibrinogen With Incident Cardiovascular Disease: The Atherosclerosis Risk in Communities (ARIC) Study. *Arterioscler Thromb Vasc Biol,* 35**,** 2700-6.

ARIENS, R. A., LAI, T. S., WEISEL, J. W., GREENBERG, C. S. & GRANT, P. J. 2002. Role of factor XIII in fibrin clot formation and effects of genetic polymorphisms. *Blood,* 100**,** 743-54.

ARIENS, R. A., PHILIPPOU, H., NAGASWAMI, C., WEISEL, J. W., LANE, D. A. & GRANT, P. J. 2000. The factor XIII V34L polymorphism accelerates thrombin activation of factor XIII and affects cross-linked fibrin structure. *Blood,* 96**,** 988-95.

ARIENS, R. A. S. 2016. Novel mechanisms that regulate clot structure/function. *Thrombosis Research,* 141**,** S25-S27.

AUTAR, A. S. A., HUND, H. M., RAMLAL, S. A., HANSEN, D., LYCKLAMA, A. N. G. J., EMMER, B. J., DE MAAT, M. P. M., DIPPEL, D. W. J., VAN DER LUGT, A., VAN ES, A., VAN BEUSEKOM, H. M. M. & INVESTIGATORS, M. C. R. 2018. High-Resolution Imaging of Interaction Between Thrombus and Stent-Retriever in Patients With Acute Ischemic Stroke. *J Am Heart Assoc,* 7.

BALLARIN, J., ARCE, Y., TORRA BALCELLS, R., DIAZ ENCARNACION, M., MANZARBEITIA, F., ORTIZ, A., EGIDO, J. & MORENO, J. A. 2011. Acute renal failure associated to paroxysmal nocturnal haemoglobinuria leads to intratubular haemosiderin accumulation and CD163 expression. *Nephrol Dial Transplant,* 26**,** 3408-11.

BARTLETT, J. W., DE STAVOLA, B. L. & MEADE, T. W. 2009. Assessing the contribution of fibrinogen in predicting risk of death in men with peripheral arterial disease. *J Thromb Haemost,* 7**,** 270-6.

BELCHER, J. D., CHEN, C., NGUYEN, J., MILBAUER, L., ABDULLA, F., ALAYASH, A. I., SMITH, A., NATH, K. A., HEBBEL, R. P. & VERCELLOTTI, G. M. 2014. Heme triggers TLR4 signaling leading to endothelial cell activation and vaso-occlusion in murine sickle cell disease. *Blood,* 123**,** 377-90.

BERGMEIER, W., PIFFATH, C. L., GOERGE, T., CIFUNI, S. M., RUGGERI, Z. M., WARE, J. & WAGNER, D. D. 2006. The role of platelet adhesion receptor GPIbalpha far exceeds that of its main ligand, von Willebrand factor, in arterial thrombosis. *Proc Natl Acad Sci U S A,* 103**,** 16900-5.

BESSLER, M., MASON, P., HILLMEN, P. & LUZZATTO, L. 1994. Somatic mutations and cellular selection in paroxysmal nocturnal haemoglobinuria. *Lancet,* 343**,** 951-3.

BEVERS, E. M., COMFURIUS, P., DEKKERS, D. W. C. & ZWAAL, R. F. A. 1999. Lipid translocation across the plasma membrane of mammalian cells. *Biochimica Et Biophysica Acta-Molecular and Cell Biology of Lipids,* 1439**,** 317-330.

BLAIR, P. & FLAUMENHAFT, R. 2009. Platelet alpha-granules: Basic biology and clinical correlates. *Blood Reviews,* 23**,** 177-189.

BLANCHARD, J. F., ARMENIAN, H. K. & FRIESEN, P. P. 2000. Risk factors for abdominal aortic aneurysm: Results of a case-control study. *American Journal of Epidemiology,* 151**,** 575-583.

BONNARD, T., LAW, L. S., TENNANT, Z. & HAGEMEYER, C. E. 2017. Development and validation of a high throughput whole blood thrombolysis plate assay. *Scientific Reports,* 7.

BREWSTER, D. C., CRONENWETT, J. L., HALLETT, J. W., JOHNSTON, K. W., KRUPSKI, W. C. & MATSUMURA, J. S. 2003. Guidelines for

the treatment of abdominal aortic aneurysms - Report of a subcommittee of the Joint Council of the American Association for Vascular Surgery and Society for Vascular Surgery. *Journal of Vascular Surgery,* 37**,** 1106-1117.

BRIDGE, K. I., PHILIPPOU, H. & ARIENS, R. 2014. Clot properties and cardiovascular disease. *Thromb Haemost,* 112**,** 901-8.

BRODSKY, R. A. 2014. Paroxysmal nocturnal hemoglobinuria. *Blood,* 124**,** 2804-11.

BRUMMEL, K. E., PARADIS, S. G., BUTENAS, S. & MANN, K. G. 2002. Thrombin functions during tissue factor-induced blood coagulation. *Blood,* 100**,** 148-52.

BYRNES, J. R., WILSON, C., BOUTELLE, A. M., BRANDNER, C. B., FLICK, M. J., PHILIPPOU, H. & WOLBERG, A. S. 2016. The interaction between fibrinogen and zymogen FXIII-A(2)B(2) is mediated by fibrinogen residues gamma 390-396 and the FXIII-B subunits. *Blood,* 128**,** 1969-1978.

CAMPBELL, R. A., ALEMAN, M., GRAY, L. D., FALVO, M. R. & WOLBERG, A. S. 2010. Flow profoundly influences fibrin network structure: implications for fibrin formation and clot stability in haemostasis. *Thromb Haemost,* 104**,** 1281-4.

CAMPBELL, R. A., OVERMYER, K. A., BAGNELL, C. R. & WOLBERG, A. S. 2008. Cellular Procoagulant Activity Dictates Clot Structure and Stability as a Function of Distance From the Cell Surface. *Arteriosclerosis Thrombosis and Vascular Biology,* 28**,** 2247-U194.

CARRELL, T. W., BURNAND, K. G., BOOTH, N. A., HUMPHRIES, J. & SMITH, A. 2006. Intraluminal thrombus enhances proteolysis in abdominal aortic aneurysms. *Vascular,* 14**,** 9-16.

CARTER, A. M., CATTO, A. J., KOHLER, H. P., ARIENS, R. A. S., STICKLAND, M. H. & GRANT, P. J. 2000. alpha-fibrinogen Thr312Ala polymorphism and venous thromboembolism. *Blood,* 96**,** 1177-1179.

CESARMAN-MAUS, G. & HAJJAR, K. A. 2005. Molecular mechanisms of fibrinolysis. *Br J Haematol,* 129**,** 307-21.

CHEUNG, E. Y., UITTE DE WILLIGE, S., VOS, H. L., LEEBEEK, F. W., DIPPEL, D. W., BERTINA, R. M. & DE MAAT, M. P. 2008. Fibrinogen gamma' in ischemic stroke: a case-control study. *Stroke,* 39**,** 1033-5.

CHEUNG, E. Y., VOS, H. L., KRUIP, M. J., DEN HERTOG, H. M., JUKEMA, J. W. & DE MAAT, M. P. 2009. Elevated fibrinogen gamma' ratio is associated with cardiovascular diseases and acute phase reaction but not with clinical outcome. *Blood,* 114**,** 4603-4; author reply 4604-5.

CHUNG, D. W., CHAN, W. Y. & DAVIE, E. W. 1983. Characterization of a complementary deoxyribonucleic acid coding for the gamma chain of human fibrinogen. *Biochemistry,* 22**,** 3250-6.

CHUNG, D. W. & DAVIE, E. W. 1984. gamma and gamma' chains of human fibrinogen are produced by alternative mRNA processing. *Biochemistry,* 23**,** 4232-6.

COLLEN, D. 1980a. Natural inhibitors of fibrinolysis. *J Clin Pathol Suppl (R Coll Pathol),* 14**,** 24-30.

COLLEN, D. 1980b. On the regulation and control of fibrinolysis. Edward Kowalski Memorial Lecture. *Thromb Haemost,* 43**,** 77-89.

COLLET, J. P., PARK, D., LESTY, C., SORIA, J., SORIA, C., MONTALESCOT, G. & WEISEL, J. W. 2000. Influence of fibrin network conformation and fibrin fiber diameter on fibrinolysis speed: dynamic and structural approaches by confocal microscopy. *Arterioscler Thromb Vasc Biol,* 20**,** 1354-61.

COLLET, J. P., SHUMAN, H., LEDGER, R. E., LEE, S. & WEISEL, J. W. 2005. The elasticity of an individual fibrin fiber in a clot. *Proc Natl Acad Sci U S A,* 102**,** 9133-7.

CONRAN, N. & ALMEIDA, C. B. 2016. Hemolytic vascular inflammation: an update. *Rev Bras Hematol Hemoter,* 38**,** 55-7.

COOKSON, P., SUTHERLAND, J. & CARDIGAN, R. 2004. A simple spectrophotometric method for the quantification of residual haemoglobin in platelet concentrates. *Vox Sang,* 87**,** 264-71.

COOPER, A. V., STANDEVEN, K. F. & ARIENS, R. A. 2003. Fibrinogen gamma-chain splice variant gamma' alters fibrin formation and structure. *Blood,* 102**,** 535-40.

COSTA, M. & ROBBS, J. V. 1986. Abdominal Aneurysms in a Black-Population - Clinicopathological Study. *British Journal of Surgery,* 73**,** 554-558.

COUTARD, M., TOUAT, Z., HOUARD, X., LECLERCQ, A. & MICHEL, J. B. 2010. Thrombus versus wall biological activities in experimental aortic aneurysms. *J Vasc Res,* 47**,** 355-66.

CURCI, J. A., LIAO, S., HUFFMAN, M. D., SHAPIRO, S. D. & THOMPSON, R. W. 1998. Expression and localization of macrophage elastase (matrix metalloproteinase-12) in abdominal aortic aneurysms. *J Clin Invest,* 102**,** 1900-10.

DA, Q., TERUYA, M., GUCHHAIT, P., TERUYA, J., OLSON, J. S. & CRUZ, M. A. 2015. Free hemoglobin increases von Willebrand factor-mediated platelet adhesion in vitro: implications for circulatory devices. *Blood,* 126**,** 2338-41.

DAHLBACK, B. 2000. Blood coagulation. *Lancet,* 355**,** 1627-32.

DALMON, J., LAURENT, M. & COURTOIS, G. 1993. The human beta fibrinogen promoter contains a hepatocyte nuclear factor 1-dependent interleukin-6-responsive element. *Mol Cell Biol,* 13**,** 1183-93.

DANESH, J., LEWINGTON, S., THOMPSON, S. G., LOWE, G. D. O., COLLINS, R. & COLLABORATION, F. S. 2005. Plasma fibrinogen level and the risk of major cardiovascular diseases and nonvascular mortality - An individual participant meta-analysis. *Jama-Journal of the American Medical Association,* 294**,** 1799-1809.

DARDIK, R., LOSCALZO, J. & INBAL, A. 2006. Factor XIII (FXIII) and angiogenesis. *Journal of Thrombosis and Haemostasis,* 4**,** 19-25.

DE BOSCH, N. B., MOSESSON, M. W., RUIZ-SAEZ, A., ECHENAGUCIA, M. & RODRIGUEZ-LEMOIN, A. 2002. Inhibition of thrombin generation in plasma by fibrin formation (Antithrombin I). *Thromb Haemost,* 88**,** 253-8.

DE WILLIGE, S. U., STANDEVEN, K. F., PHILIPPOU, H. & ARIENS, R. A. S. 2009. The pleiotropic role of the fibrinogen gamma ' chain in hemostasis. *Blood,* 114**,** 3994-4001.

DEGEN, J. L., BUGGE, T. H. & GOGUEN, J. D. 2007. Fibrin and fibrinolysis in infection and host defense. *Journal of Thrombosis and Haemostasis,* 5**,** 24-31.

DEVALET, B., MULLIER, F., CHATELAIN, B., DOGNE, J. M. & CHATELAIN, C. 2015. Pathophysiology, diagnosis, and treatment of paroxysmal nocturnal hemoglobinuria: a review. *Eur J Haematol,* 95**,** 190-8.

DEVINE, D. V. & ROSSE, W. F. 1987. Regulation of the Activity of Platelet-Bound C-3 Convertase of the Alternative Pathway of Complement by Platelet Factor-H. *Proceedings of the National Academy of Sciences of the United States of America,* 84**,** 5873-5877.

DILLAVOU, E. D., MULUK, S. C. & MAKAROUN, M. S. 2006. A decade of change in abdominal aortic aneurysm repair in the United States: Have we improved outcomes equally between men and women? *Journal of Vascular Surgery,* 43**,** 230-236.

DOMINGUES, M. M., MACRAE, F. L., DUVAL, C., MCPHERSON, H. R., BRIDGE, K. I., AJJAN, R. A., RIDGER, V. C., CONNELL, S. D., PHILIPPOU, H. & ARIENS, R. A. 2016. Thrombin and fibrinogen gamma' impact clot structure by marked effects on intrafibrillar structure and protofibril packing. *Blood,* 127**,** 487-95.

DOOLITTLE, R. F. 1984. Fibrinogen and fibrin. *Annu Rev Biochem,* 53**,** 195-229.

DUELLMAN, T., WARREN, C. L., PEISSIG, P., WYNN, M. & YANG, J. 2012. Matrix Metalloproteinase-9 Genotype as a Potential Genetic Marker for Abdominal Aortic Aneurysm. *Circulation-Cardiovascular Genetics,* 5**,** 529-537.

DUVAL, C., ALLAN, P., CONNELL, S. D., RIDGER, V. C., PHILIPPOU, H. & ARIENS, R. A. 2014. Roles of fibrin alpha- and gamma-chain specific cross-linking by FXIIIa in fibrin structure and function. *Thromb Haemost,* 111**,** 842-50.

ENGELMANN, B. & MASSBERG, S. 2013. Thrombosis as an intravascular effector of innate immunity. *Nature Reviews Immunology,* 13**,** 34-45.

ESMON, C. T. 2004. Interactions between the innate immune and blood systems coagulation. *Trends in Immunology,* 25**,** 536-542.

FALLS, L. A. & FARRELL, D. H. 1997. Resistance of gammaA/gamma' fibrin clots to fibrinolysis. *J Biol Chem,* 272**,** 14251-6.

FILARDO, G., POWELL, J. T., MARTINEZ, M. A. M. & BALLARD, D. J. 2012. Surgery for small asymptomatic abdominal aortic aneurysms. *Cochrane Database of Systematic Reviews*.

FOLEY, J. H. & CONWAY, E. M. 2016. Cross Talk Pathways Between Coagulation and Inflammation. *Circulation Research,* 118**,** 1392-1408.

FOLKESSON, M., SILVEIRA, A., ERIKSSON, P. & SWEDENBORG, J. 2011. Protease activity in the multi-layered intra-luminal thrombus of abdominal aortic aneurysms. *Atherosclerosis,* 218**,** 294-9.

FONTAINE, V., JACOB, M. P., HOUARD, X., ROSSIGNOL, P., PLISSONNIER, D., ANGLES-CANO, E. & MICHEL, J. B. 2002. Involvement of the mural thrombus as a site of protease release and activation in human aortic aneurysms. *Am J Pathol,* 161**,** 1701-10.

FORNACE, A. J., JR., CUMMINGS, D. E., COMEAU, C. M., KANT, J. A. & CRABTREE, G. R. 1984. Structure of the human gamma-fibrinogen

gene. Alternate mRNA splicing near the 3' end of the gene produces gamma A and gamma B forms of gamma-fibrinogen. *J Biol Chem,* 259**,** 12826-30.

FOWKES, F. J. I., PRICE, J. F. & FOWKES, F. G. R. 2003. Incidence of diagnosed deep vein thrombosis in the general population: Systematic review. *European Journal of Vascular and Endovascular Surgery,* 25**,** 1-5.

FOWLER, W. E., HANTGAN, R. R., HERMANS, J. & ERICKSON, H. P. 1981. Structure of the fibrin protofibril. *Proc Natl Acad Sci U S A,* 78**,** 4872-6.

FRANCIS, C. W., MARDER, V. J. & MARTIN, S. E. 1980. Demonstration of a large molecular weight variant of the gamma chain of normal human plasma fibrinogen. *J Biol Chem,* 255**,** 5599-604.

FRANCIS, C. W., NACHMAN, R. L. & MARDER, V. J. 1984. Plasma and platelet fibrinogen differ in gamma chain content. *Thromb Haemost,* 51**,** 84-8.

FRANCO, R. F., PAZIN, A., TAVELLA, M. H., SIMOES, M. V., MARIN-NETO, J. A. & ZAGO, M. A. 2000. Factor XIII Val34Leu and the risk of myocardial infarction. *Haematologica,* 85**,** 67-71.

FREDENBURGH, J. C., STAFFORD, A. R., LESLIE, B. A. & WEITZ, J. I. 2008. Bivalent binding to gammaA/gamma'-fibrin engages both exosites of thrombin and protects it from inhibition by the antithrombin-heparin complex. *J Biol Chem,* 283**,** 2470-7.

GAFFNEY, P. J. & WHITAKER, A. N. 1979. Fibrin crosslinks and lysis rates. *Thromb Res,* 14**,** 85-94.

GERSH, K. C., EDMONDSON, K. E. & WEISEL, J. W. 2010. Flow rate and fibrin fiber alignment. *J Thromb Haemost,* 8**,** 2826-8.

GERSH, K. C., LORD, S. T. & WOLBERG, A. S. 2006. An investigation of factor XIII binding to recombinant gamma'/gamma' and gamma/gamma' fibrinogen. *Blood,* 108**,** 485a-485a.

GOODSON, W. H. & HUNT, T. K. 1977. Studies of Wound-Healing in Experimental Diabetes-Mellitus. *Journal of Surgical Research,* 22**,** 221-227.

GRALNICK, H. R., VAIL, M., MCKEOWN, L. P., MERRYMAN, P., WILSON, O., CHU, I. & KIMBALL, J. 1995. Activated Platelets in Paroxysmal-Nocturnal Hemoglobinuria. *British Journal of Haematology,* 91**,** 697-702.

GREENBERG, C. S. & SHUMAN, M. A. 1982. The zymogen forms of blood coagulation factor XIII bind specifically to fibrinogen. *J Biol Chem,* 257**,** 6096-101.

GRUNBACHER, G., WEGER, W., MARX-NEUHOLD, E., PILGER, E., KOPPEL, H., WASCHER, T., MARZ, W. & RENNER, W. 2007. The fibrinogen gamma (FGG) 10034C > T polymorphism is associated with venous thrombosis. *Thrombosis Research,* 121**,** 33-36.

GRUNEWALD, M., SIEGEMUND, A., GRUNEWALD, A., SCHMID, A., KOKSCH, M., SCHOPFLIN, C., SCHAUER, S. & GRIESSHAMMER, M. 2003. Plasmatic coagulation and fibrinolytic system alterations in PNH: relation to clone size. *Blood Coagul Fibrinolysis,* 14**,** 685-95.

HALL, C., RICHARDS, S. & HILLMEN, P. 2003. Primary prophylaxis with warfarin prevents thrombosis in paroxysmal nocturnal hemoglobinuria (PNH). *Blood,* 102**,** 3587-3591.

HALL, C. E. & SLAYTER, H. S. 1959. The fibrinogen molecule: its size, shape, and mode of polymerization. *J Biophys Biochem Cytol,* 5**,** 11-6.

HANAOKA, N., KAWAGUCHI, T., HORIKAWA, K., NAGAKURA, S., MITSUYA, H. & NAKAKUMA, H. 2006. Immunoselection by natural killer cells of PIGA mutant cells missing stress-inducible ULBP. *Blood,* 107**,** 1184-91.

HANN, R. A. 1990. Molecules for Langmuir-Blodgett-Film Formation. *Philosophical Transactions of the Royal Society a-Mathematical Physical and Engineering Sciences,* 330**,** 141-152.

HANTGAN, R. R. & HERMANS, J. 1979. Assembly of fibrin. A light scattering study. *J Biol Chem,* 254**,** 11272-81.

HARBOE, M. 1959. A method for determination of hemoglobin in plasma by near-ultraviolet spectrophotometry. *Scand J Clin Lab Invest,* 11**,** 66-70.

HARFENIST, E. J., PACKHAM, M. A. & MUSTARD, J. F. 1984. Effects of variant gamma chains and sialic acid content of fibrinogen upon its interactions with ADP-stimulated human and rabbit platelets. *Blood,* 64**,** 1163-8.

HARR, J. N., MOORE, E. E., GHASABYAN, A., CHIN, T. L., SAUAIA, A., BANERJEE, A. & SILLIMAN, C. C. 2013. Functional fibrinogen assay indicates that fibrinogen is critical in correcting abnormal clot strength following trauma. *Shock,* 39**,** 45-9.

HARTER, L. P., GROSS, B. H., CALLEN, P. W. & BARTH, R. A. 1982. Ultrasonic Evaluation of Abdominal Aortic Thrombus. *Journal of Ultrasound in Medicine,* 1**,** 315-318.

HAWIGER, J., TIMMONS, S., KLOCZEWIAK, M., STRONG, D. D. & DOOLITTLE, R. F. 1982. gamma and alpha chains of human fibrinogen possess sites reactive with human platelet receptors. *Proc Natl Acad Sci U S A,* 79**,** 2068-71.

HE, C. M. & ROACH, M. R. 1994. The composition and mechanical properties of abdominal aortic aneurysms. *J Vasc Surg,* 20**,** 6-13.

HEINRICH, P. C., CASTELL, J. V. & ANDUS, T. 1990. Interleukin-6 and the Acute Phase Response. *Biochemical Journal,* 265**,** 621-636.

HELLEY, D., DE LATOUR, R. P., PORCHER, R., RODRIGUES, C. A., GALY-FAUROUX, I., MATHERON, J., DUVAL, A., SCHVED, J. F., FISCHER, A. M., SOCIE, G. & HEMATOLOGY, F. S. 2010. Evaluation of hemostasis and endothelial function in patients with paroxysmal nocturnal hemoglobinuria receiving eculizumab. *Haematologica-the Hematology Journal,* 95**,** 574-581.

HEMKER, H. C. & BEGUIN, S. 1995. Thrombin generation in plasma: its assessment via the endogenous thrombin potential. *Thromb Haemost,* 74**,** 134-8.

HEMKER, H. C., GIESEN, P., AL DIERI, R., REGNAULT, V., DE SMEDT, E., WAGENVOORD, R., LECOMPTE, T. & BEGUIN, S. 2003. Calibrated automated thrombin generation measurement in clotting plasma. *Pathophysiol Haemost Thromb,* 33**,** 4-15.

HENRY, J. C., PETERSON, L., SCHLANGER, R. E., GO, M. R., SEN, C. K. & HIGGINS, R. S. 2014. Wound healing in peripheral arterial disease: current and future therapy. *Journal of Vascular Medicine & Surgery,* 2.

HENSCHEN, A. & MCDONAGH, J. 1986. Chapter 7 Fibrinogen, fibrin and factor XIII. *In:* NEUBERGER, A. & VAN DEENEN, L. L. M. (eds.) *New Comprehensive Biochemistry.* Elsevier.

HERNANDEZ, E. M. & FRANSES, E. I. 2003. Adsorption and surface tension of fibrinogen at the air/water interface. *Colloids Surf A Physicochem Eng Asp,* 214**,** 249-262.

HESS, K., AJJAN, R., PHOENIX, F., DOBO, J., GAL, P. & SCHROEDER, V. 2012. Effects of MASP-1 of the complement system on activation of coagulation factors and plasma clot formation. *PLoS One,* 7**,** e35690.

HESS, K. A., KURDEE, Z., OXLEY, N., PHOENIX, F., MARX, N., KING, R., STOREY, R. F., GRANT, P. J. & AJJAN, R. A. 2013. Modulation of complement C3 levels and fibrin clot structure: the role of aspirin dose. *European Heart Journal,* 34**,** 891-891.

HETHERSHAW, E. L., CILIA LA CORTE, A. L., DUVAL, C., ALI, M., GRANT, P. J., ARIENS, R. A. & PHILIPPOU, H. 2014. The effect of blood coagulation factor XIII on fibrin clot structure and fibrinolysis. *J Thromb Haemost,* 12**,** 197-205.

HILL, A., HILLMEN, P., RICHARDS, S. J., ELEBUTE, D., MARSH, J. C., CHAN, J., MOJCIK, C. F. & ROTHER, R. P. 2005. Sustained response and long-term safety of eculizumab in paroxysmal nocturnal hemoglobinuria. *Blood,* 106**,** 2559-65.

HILL, A., KELLY, R. J. & HILLMEN, P. 2013. Thrombosis in paroxysmal nocturnal hemoglobinuria. *Blood,* 121**,** 4985-96; quiz 5105.

HILL, A., KELLY, R. J., KULASEKARARAJ, A. G., GANDHI, S. A., MITCHELL, L. D., ELEBUTE, M., RICHARDS, S. J., CULLEN, M., ARNOLD, L. M., LARGE, J., WOOD, A., BROOKSBANK, G. L., DOWNING, T., MCKINLEY, C., COHEN, D., GREGORY, W. M., MARSH, J. C. W., MUFTI, G. J. & HILLMEN, P. 2012. Eculizumab in Paroxysmal Nocturnal Hemoglobinuria (PNH): A Report of All 153 Patients Treated in the UK. *Blood,* 120.

HILL, A., REID, S. A., ROTHER, R. P., GLADWIN, M. T., COLLINSON, P. O., GAZE, D. C., LOWE, A., GUTHRIE, A., SIVANANTHAN, M. U. & HILLMEN, P. 2007a. High definition contrast-enhanced MR imaging in paroxysmal nocturnal hemoglobinuria suggests a high frequency of subclinical thrombosis. *Haematologica-the Hematology Journal,* 92**,** 24-25.

HILL, A., RICHARDS, S. J. & HILLMEN, P. 2007b. Recent developments in the understanding and management of paroxysmal nocturnal haemoglobinuria. *Br J Haematol,* 137**,** 181-92.

HILLMEN, P., HALL, C., MARSH, J. C., ELEBUTE, M., BOMBARA, M. P., PETRO, B. E., CULLEN, M. J., RICHARDS, S. J., ROLLINS, S. A., MOJCIK, C. F. & ROTHER, R. P. 2004. Effect of eculizumab on hemolysis and transfusion requirements in patients with paroxysmal nocturnal hemoglobinuria. *N Engl J Med,* 350**,** 552-9.

HILLMEN, P., MUUS, P., DUHRSEN, U., RISITANO, A. M., SCHUBERT, J., LUZZATTO, L., SCHREZENMEIER, H., SZER, J., BRODSKY, R. A.,

HILL, A., SOCIE, G., BESSLER, M., ROLLINS, S. A., BELL, L., ROTHER, R. P. & YOUNG, N. S. 2007. Effect of the complement inhibitor eculizumab on thromboembolism in patients with paroxysmal nocturnal hemoglobinuria. *Blood,* 110**,** 4123-8.

HILLMEN, P., MUUS, P., ROTH, A., ELEBUTE, M. O., RISITANO, A. M., SCHREZENMEIER, H., SZER, J., BROWNE, P., MACIEJEWSKI, J. P., SCHUBERT, J., URBANO-ISPIZUA, A., DE CASTRO, C., SOCIE, G. & BRODSKY, R. A. 2013. Long-term safety and efficacy of sustained eculizumab treatment in patients with paroxysmal nocturnal haemoglobinuria. *British Journal of Haematology,* 162**,** 62-73.

HOEKSTRA, J., LEEBEEK, F. W. G., PLESSIER, A., RAFFA, S., MURAD, S. D., HELLER, J., HADENGUE, A., CHAGNEAU, C., ELIASG, E., PRIMIGNANI, M., GARCIA-PAGAN, J. C., VALLA, D. C., JANSSEN, H. L. A. & LI, E. N. V. D. 2009. Paroxysmal nocturnal hemoglobinuria in Budd-Chiari Syndrome: Findings from a cohort study. *Journal of Hepatology,* 51**,** 696-706.

HOUARD, X., ROUZET, F., TOUAT, Z., PHILIPPE, M., DOMINGUEZ, M., FONTAINE, V., SARDA-MANTEL, L., MEULEMANS, A., LE GULUDEC, D., MEILHAC, O. & MICHEL, J. B. 2007. Topology of the fibrinolytic system within the mural thrombus of human abdominal aortic aneurysms. *J Pathol,* 212**,** 20-8.

HOWES, J. M., RICHARDSON, V. R., SMITH, K. A., SCHROEDER, V., SOMANI, R., SHORE, A., HESS, K., AJJAN, R., PEASE, R. J., KEEN, J. N., STANDEVEN, K. F. & CARTER, A. M. 2012. Complement C3 is a novel plasma clot component with anti-fibrinolytic properties. *Diab Vasc Dis Res,* 9**,** 216-25.

HUBER-LANG, M., SARMA, J. V., ZETOUNE, F. S., RITTIRSCH, D., NEFF, T. A., MCGUIRE, S. R., LAMBRIS, J. D., WARNER, R. L., FLIERL, M. A., HOESEL, L. M., GEBHARD, F., YOUNGER, J. G., DROUIN, S. M., WETSEL, R. A. & WARD, P. A. 2006. Generation of C5a in the absence of C3: a new complement activation pathway. *Nature Medicine,* 12**,** 682-687.

HUGEL, B., SOCIE, G., VU, T., TOTI, F., GLUCKMAN, E., FREYSSINET, J. M. & SCROBOHACI, M. L. 1999. Elevated levels of circulating procoagulant microparticles in patients with paroxysmal nocturnal hemoglobinuria and aplastic anemia. *Blood,* 93**,** 3451-6.

HUI, K. Y., HABER, E. & MATSUEDA, G. R. 1983. Monoclonal antibodies to a synthetic fibrin-like peptide bind to human fibrin but not fibrinogen. *Science,* 222**,** 1129-32.

INOUE, N., IZUI-SARUMARU, T., MURAKAMI, Y., ENDO, Y., NISHIMURA, J., KUROKAWA, K., KUWAYAMA, M., SHIME, H., MACHII, T., KANAKURA, Y., MEYERS, G., WITTWER, C., CHEN, Z., BABCOCK, W., FREI-LAHR, D., PARKER, C. J. & KINOSHITA, T. 2006. Molecular basis of clonal expansion of hematopoiesis in 2 patients with paroxysmal nocturnal hemoglobinuria (PNH). *Blood,* 108**,** 4232-6.

INZOLI, F., BOSCHETTI, F., ZAPPA, M., LONGO, T. & FUMERO, R. 1993. Biomechanical factors in abdominal aortic aneurysm rupture. *Eur J Vasc Surg,* 7**,** 667-74.

IULIANO, L., PEDERSEN, J. Z., PRATICO, D., ROTILIO, G. & VIOLI, F. 1994. Role of Hydroxyl Radicals in the Activation of Human Platelets. *European Journal of Biochemistry,* 221**,** 695-704.

IWATA, H., KITANO, T., UMETSU, K., YUASA, I., YAMAZAKI, K., KEMKES-MATTHES, B. & ICHINOSE, A. 2009. Distinct C-terminus of the B subunit of factor XIII in a population-associated major phenotype: the first case of complete allele-specific alternative splicing products in the coagulation and fibrinolytic systems. *Journal of Thrombosis and Haemostasis,* 7**,** 1084-1091.

JANKOWSKA, A. M., SZPURKA, H., CALABRO, M., MOHAN, S., SCHADE, A. E., CLEMENTE, M., SILVERSTEIN, R. L. & MACIEJEWSKI, J. P. 2011. Loss of expression of neutrophil proteinase-3: a factor contributing to thrombotic risk in paroxysmal nocturnal hemoglobinuria. *Haematologica,* 96**,** 954-62.

JOHANSEN, K. & KOEPSELL, T. 1986. Familial Tendency for Abdominal Aortic-Aneurysms. *Jama-Journal of the American Medical Association,* 256**,** 1934-1936.

JOHNSTON, K. W., RUTHERFORD, R. B., TILSON, M. D., SHAH, D. M., HOLLIER, L. & STANLEY, J. C. 1991. Suggested standards for reporting on arterial aneurysms. Subcommittee on Reporting Standards for Arterial Aneurysms, Ad Hoc Committee on Reporting Standards, Society for Vascular Surgery and North American Chapter, International Society for Cardiovascular Surgery. *J Vasc Surg,* 13**,** 452-8.

JONES, G. T., TROMP, G., KUIVANIEMI, H., GRETARSDOTTIR, S., BAAS, A. F., GIUSTI, B., STRAUSS, E., VAN'T HOF, F. N., WEBB, T. R., ERDMAN, R., RITCHIE, M. D., ELMORE, J. R., VERMA, A., PENDERGRASS, S., KULLO, I. J., YE, Z., PEISSIG, P. L., GOTTESMAN, O., VERMA, S. S., MALINOWSKI, J., RASMUSSEN-TORVIK, L. J., BORTHWICK, K. M., SMELSER, D. T., CROSSLIN, D. R., DE ANDRADE, M., RYER, E. J., MCCARTY, C. A., BOTTINGER, E. P., PACHECO, J. A., CRAWFORD, D. C., CARRELL, D. S., GERHARD, G. S., FRANKLIN, D. P., CAREY, D. J., PHILLIPS, V. L., WILLIAMS, M. J., WEI, W., BLAIR, R., HILL, A. A., VASUDEVAN, T. M., LEWIS, D. R., THOMSON, I. A., KRYSA, J., HILL, G. B., ROAKE, J., MERRIMAN, T. R., OSZKINIS, G., GALORA, S., SARACINI, C., ABBATE, R., PULLI, R., PRATESI, C., SARATZIS, A., VERISSIMO, A. R., BUMPSTEAD, S., BADGER, S. A., CLOUGH, R. E., COCKERILL, G., HAFEZ, H., SCOTT, D. J., FUTERS, T. S., ROMAINE, S. P., BRIDGE, K., GRIFFIN, K. J., BAILEY, M. A., SMITH, A., THOMPSON, M. M., VAN BOCKXMEER, F. M., MATTHIASSON, S. E., THORLEIFSSON, G., THORSTEINSDOTTIR, U., BLANKENSTEIJN, J. D., TEIJINK, J. A., WIJMENGA, C., DE GRAAF, J., KIEMENEY, L. A., LINDHOLT, J. S., HUGHES, A., BRADLEY, D. T., STIRRUPS, K., GOLLEDGE, J., NORMAN, P. E., POWELL, J. T., HUMPHRIES, S. E., HAMBY, S. E., GOODALL, A. H., NELSON, C. P., SAKALIHASAN, N., COURTOIS, A., FERRELL, R. E., ERIKSSON, P., FOLKERSEN, L., FRANCO-CERECEDA, A., EICHER, J. D., JOHNSON, A. D., BETSHOLTZ, C., RUUSALEPP, A., FRANZEN, O., SCHADT, E. E., BJORKEGREN, J. L., et al. 2017.

Meta-Analysis of Genome-Wide Association Studies for Abdominal Aortic Aneurysm Identifies Four New Disease-Specific Risk Loci. *Circ Res,* 120**,** 341-353.

JUVONEN, J., SURCEL, H. M., SATTA, J., TEPPO, A. M., BLOIGU, A., SYRJALA, H., AIRAKSINEN, J., LEINONEN, M., SAIKKU, P. & JUVONEN, T. 1997. Elevated circulating levels of inflammatory cytokines in patients with abdominal aortic aneurysm. *Arterioscler Thromb Vasc Biol,* 17**,** 2843-7.

KAIN, K., BLAXILL, J. M., CATTO, A. J., GRANT, P. J. & CARTER, A. M. 2002. Increased fibrinogen levels among South Asians versus Whites in the United Kingdom are not explained by common polymorphisms. *Am J Epidemiol,* 156**,** 174-9.

KANT, J. A., FORNACE, A. J., JR., SAXE, D., SIMON, M. I., MCBRIDE, O. W. & CRABTREE, G. R. 1985. Evolution and organization of the fibrinogen locus on chromosome 4: gene duplication accompanied by transposition and inversion. *Proc Natl Acad Sci U S A,* 82**,** 2344-8.

KAPLAN, A. P., JOSEPH, K. & SILVERBERG, M. 2002. Pathways for bradykinin formation and inflammatory disease. *Journal of Allergy and Clinical Immunology,* 109**,** 195-209.

KATONA, E., PENZES, K., CSAPO, A., FAZAKAS, F., UDVARDY, M. L., BAGOLY, Z., OROSZ, Z. Z. & MUSZBEK, L. 2014. Interaction of factor XIII subunits. *Blood,* 123**,** 1757-1763.

KAWAGUCHI, T. & NAKAKUMA, H. 2007. New insights into molecular pathogenesis of bone marrow failure in paroxysmal nocturnal hemoglobinuria. *Int J Hematol,* 86**,** 27-32.

KAZI, M., THYBERG, J., RELIGA, P., ROY, J., ERIKSSON, P., HEDIN, U. & SWEDENBORG, J. 2003. Influence of intraluminal thrombus on structural and cellular composition of abdominal aortic aneurysm wall. *J Vasc Surg,* 38**,** 1283-92.

KIM, P. Y., VU, T. T., LESLIE, B. A., STAFFORD, A. R., FREDENBURGH, J. C. & WEITZ, J. I. 2014. Reduced plasminogen binding and delayed activation render gamma'-fibrin more resistant to lysis than gammaA-fibrin. *J Biol Chem,* 289**,** 27494-503.

KIRSCHFINK, M. & MOLLNES, T. E. 2003. Modern complement analysis. *Clin Diagn Lab Immunol,* 10**,** 982-9.

KLOCZEWIAK, M., TIMMONS, S. & HAWIGER, J. 1982. Localization of a site interacting with human platelet receptor on carboxy-terminal segment of human fibrinogen gamma chain. *Biochem Biophys Res Commun,* 107**,** 181-7.

KLOVAITE, J., NORDESTGAARD, B. G., TYBJAERG-HANSEN, A. & BENN, M. 2013. Elevated fibrinogen levels are associated with risk of pulmonary embolism, but not with deep venous thrombosis. *Am J Respir Crit Care Med,* 187**,** 286-93.

KNOX, J. B., SUKHOVA, G. K., WHITTEMORE, A. D. & LIBBY, P. 1997. Evidence for altered balance between matrix metalloproteinases and their inhibitors in human aortic diseases. *Circulation,* 95**,** 205-12.

KOH, T. J. & DIPIETRO, L. A. 2011. Inflammation and wound healing: the role of the macrophage. *Expert Rev Mol Med,* 13**,** e23.

KOLLMAN, J. M., PANDI, L., SAWAYA, M. R., RILEY, M. & DOOLITTLE, R. F. 2009. Crystal structure of human fibrinogen. *Biochemistry,* 48**,** 3877-86.

KOMANASIN, N., CATTO, A. J., FUTERS, T. S., VAN HYLCKAMA VLIEG, A., ROSENDAAL, F. R. & ARIENS, R. A. 2005. A novel polymorphism in the factor XIII B-subunit (His95Arg): relationship to subunit dissociation and venous thrombosis. *J Thromb Haemost,* 3**,** 2487-96.

KOOLE, D., ZANDVOORT, H. J., SCHONEVELD, A., VINK, A., VOS, J. A., VAN DEN HOOGEN, L. L., DE VRIES, J. P., PASTERKAMP, G., MOLL, F. L. & VAN HERWAARDEN, J. A. 2013. Intraluminal abdominal aortic aneurysm thrombus is associated with disruption of wall integrity. *J Vasc Surg,* 57**,** 77-83.

KREM, M. M. & DI CERA, E. 2002. Evolution of enzyme cascades from embryonic development to blood coagulation. *Trends Biochem Sci,* 27**,** 67-74.

KREMERS, R., WAGENVOORD, R. & HEMKER, C. 2013. Fibrinogen Attentuates Thrombin Decay In a Concentration-Dependent Manner. *Blood,* 122.

KREMERS, R. M., WAGENVOORD, R. J. & HEMKER, H. C. 2014. The effect of fibrin(ogen) on thrombin generation and decay. *Thromb Haemost,* 112**,** 486-94.

L'ACQUA, C. & HOD, E. 2015. New perspectives on the thrombotic complications of haemolysis. *British Journal of Haematology,* 168**,** 175-185.

LADENVALL, C., CSAJBOK, L., NYLEN, K., JOOD, K., NELLGARD, B. & JERN, C. 2009. Association between factor XIII single nucleotide polymorphisms and aneurysmal subarachnoid hemorrhage Clinical article. *Journal of Neurosurgery,* 110**,** 475-481.

LANCELLOTTI, S., RUTELLA, S., DE FILIPPIS, V., POZZI, N., ROCCA, B. & DE CRISTOFARO, R. 2008. Fibrinogen-elongated gamma chain inhibits thrombin-induced platelet response, hindering the interaction with different receptors. *J Biol Chem,* 283**,** 30193-204.

LANE, A., GRAHAM, L., COOK, M., CHANTRY, D., GREEN, F., NIGON, F. & HUMPHRIES, S. E. 1991. Cytokine production by cholesterol-loaded human peripheral monocyte-macrophages: the effect on fibrinogen mRNA levels in a hepatoma cell-line (HepG2). *Biochim Biophys Acta,* 1097**,** 161-5.

LANGMUIR, I. 1917. The Shapes of Group Molecules Forming the Surfaces of Liquids. *Proc Natl Acad Sci U S A,* 3**,** 251-7.

LARSSON, E., GRANATH, F., SWEDENBORG, J. & HULTGREN, R. 2009. A population-based case-control study of the familial risk of abdominal aortic aneurysm. *Journal of Vascular Surgery,* 49**,** 47-51.

LEDERLE, F. A., JOHNSON, G. R., WILSON, S. E., CHUTE, E. P., LITTOOY, F. N., BANDYK, D., KRUPSKI, W. C., BARONE, G. W., ACHER, C. W. & BALLARD, D. J. 1997. Prevalence and associations of abdominal aortic aneurysm detected through screening. *Annals of Internal Medicine,* 126**,** 441-+.

LEUNG, L. L. & MORSER, J. 2016. Plasmin as a complement C5 convertase. *EBioMedicine,* 5**,** 20-1.

LI, X., ZHAO, G., ZHANG, J., DUAN, Z. Q. & XIN, S. J. 2013. Prevalence and Trends of the Abdominal Aortic Aneurysms Epidemic in General Population - A Meta-Analysis. *Plos One,* 8.

LIM, B. C., ARIENS, R. A., CARTER, A. M., WEISEL, J. W. & GRANT, P. J. 2003. Genetic regulation of fibrin structure and function: complex gene-environment interactions may modulate vascular risk. *Lancet,* 361**,** 1424-31.

LINDHOLT, J. S. & SHI, G. P. 2006. Chronic inflammation, immune response, and infection in abdominal aortic aneurysms. *Eur J Vasc Endovasc Surg,* 31**,** 453-63.

LINNE, A., LINDSTROM, D. & HULTGREN, R. 2012. High prevalence of abdominal aortic aneurysms in brothers and sisters of patients despite a low prevalence in the population. *Journal of Vascular Surgery,* 56**,** 305-310.

LIU, W., CARLISLE, C. R., SPARKS, E. A. & GUTHOLD, M. 2010. The mechanical properties of single fibrin fibers. *J Thromb Haemost,* 8**,** 1030-6.

LIU, W., JAWERTH, L. M., SPARKS, E. A., FALVO, M. R., HANTGAN, R. R., SUPERFINE, R., LORD, S. T. & GUTHOLD, M. 2006. Fibrin fibers have extraordinary extensibility and elasticity. *Science,* 313**,** 634-634.

LORAND, L. 2001. Factor XIII: structure, activation, and interactions with fibrinogen and fibrin. *Ann N Y Acad Sci,* 936**,** 291-311.

LOVELY, R. S., BOSHKOV, L. K., MARZEC, U. M., HANSON, S. R. & FARRELL, D. H. 2007. Fibrinogen gamma' chain carboxy terminal peptide selectively inhibits the intrinsic coagulation pathway. *British Journal of Haematology,* 139**,** 494-503.

LOVELY, R. S., FALLS, L. A., AL-MONDHIRY, H. A., CHAMBERS, C. E., SEXTON, G. J., NI, H. & FARRELL, D. H. 2002. Association of gammaA/gamma' fibrinogen levels and coronary artery disease. *Thromb Haemost,* 88**,** 26-31.

LOVELY, R. S., MOADDEL, M. & FARRELL, D. H. 2003. Fibrinogen gamma' chain binds thrombin exosite II. *J Thromb Haemost,* 1**,** 124-31.

LUNETTA, K. L. 2008. Genetic association studies. *Circulation,* 118**,** 96-101.

LYAKISHEVA, A., FELDA, O., GANSER, A., SCHMIDT, R. E. & SCHUBERT, J. 2002. Paroxysmal nocturnal hemoglobinuria: Differential gene expression of EGR-1 and TAXREB107. *Exp Hematol,* 30**,** 18-25.

MACHLUS, K. R., CARDENAS, J. C., CHURCH, F. C. & WOLBERG, A. S. 2011. Causal relationship between hyperfibrinogenemia, thrombosis, and resistance to thrombolysis in mice. *Blood,* 117**,** 4953-4963.

MACRAE, F. L., DOMINGUES, M. M., CASINI, A. & ARIENS, R. A. 2016. The (Patho)physiology of Fibrinogen gamma'. *Semin Thromb Hemost,* 42**,** 344-55.

MACRAE, F. L., DUVAL, C., PAPAREDDY, P., BAKER, S. R., YULDASHEVA, N., KEARNEY, K. J., MCPHERSON, H. R., ASQUITH, N., KONINGS, J., CASINI, A., DEGEN, J. L., CONNELL, S. D., PHILIPPOU, H., WOLBERG, A. S., HERWALD, H. & ARIENS, R. A. 2018. A fibrin biofilm covers blood clots and protects from microbial invasion. *J Clin Invest,* 128**,** 3356-3368.

MACRAE, F. L., EVANS, H. L., BRIDGE, K. I., JOHNSON, A., SCOTT, D. J. & ARIENS, R. A. 2014. Common FXIII and fibrinogen polymorphisms in abdominal aortic aneurysms. *PLoS One,* 9**,** e112407.

MALINAUSKAS, R. A. 1997. Plasma hemoglobin measurement techniques for the in vitro evaluation of blood damage caused by medical devices. *Artif Organs,* 21**,** 1255-67.

MANNILA, M. N., LOVELY, R. S., KAZMIERCZAK, S. C., ERIKSSON, P., SAMNEGARD, A., FARRELL, D. H., HAMSTEN, A. & SILVEIRA, A. 2007. Elevated plasma fibrinogen gamma' concentration is associated with myocardial infarction: effects of variation in fibrinogen genes and environmental factors. *J Thromb Haemost,* 5**,** 766-73.

MAO, D., LEE, J. K., VANVICKLE, S. J. & THOMPSON, R. W. 1999. Expression of collagenase-3 (MMP-13) in human abdominal aortic aneurysms and vascular smooth muscle cells in culture. *Biochem Biophys Res Commun,* 261**,** 904-10.

MARDER, V. J., SHULMAN, N. R. & CARROLL, W. R. 1969. High molecular weight derivatives of human fibrinogen produced by plasmin. I. Physicochemical and immunological characterization. *J Biol Chem,* 244**,** 2111-9.

MATRAS, H. 1985. Fibrin seal: the state of the art. *J Oral Maxillofac Surg,* 43**,** 605-11.

MCEVER, R. P., BECKSTEAD, J. H., MOORE, K. L., MARSHALL-CARLSON, L. & BAINTON, D. F. 1989. GMP-140, a platelet alpha-granule membrane protein, is also synthesized by vascular endothelial cells and is localized in Weibel-Palade bodies. *J Clin Invest,* 84**,** 92-9.

MCPHERSON, H., DUVAL, C., ASQUITH, N., DOMINGUES, M. M., BAKER, S., RIDGER, V. C., CONNELL, S., PHILIPPOU, H., AJJAN, R. & ARIENS, R. 2017. Role of Fibrinogen αC Domain in Fibrin Fibre Lateral Aggregation and αC Connector Region In Longitudinal Fibre Growth; Complex Interactions of the αC Region that Regulate Clot Structure and Function. *Congress of the International Society on Thrombosis and Haemostasis.* Berlin: Res Pract Thromb Haemost.

MIHALYI, E. 1968. Physicochemical studies of bovine fibrinogen. IV. Ultraviolet absorption and its relation to the structure of the molecule. *Biochemistry,* 7**,** 208-23.

MIYATA, T., TAKEDA, J., IIDA, Y., YAMADA, N., INOUE, N., TAKAHASHI, M., MAEDA, K., KITANI, T. & KINOSHITA, T. 1993. The cloning of PIG-A, a component in the early step of GPI-anchor biosynthesis. *Science,* 259**,** 1318-20.

MOADDEL, M., FALLS, L. A. & FARRELL, D. H. 2000. The role of gamma A/gamma ' fibrinogen in plasma factor XIII activation. *J Biol Chem,* 275**,** 35656.

MONROE, D. M. & HOFFMAN, M. 2006. What does it take to make the perfect clot? *Arterioscler Thromb Vasc Biol,* 26**,** 41-8.

MOSESSON, M. W., COOLEY, B. C., HERNANDEZ, I., DIORIO, J. P. & WEILER, H. 2009. Thrombosis risk modification in transgenic mice containing the human fibrinogen thrombin-binding gamma' chain sequence. *J Thromb Haemost,* 7**,** 102-10.

MOSESSON, M. W. & FINLAYSON, J. S. 1963. Biochemical and chromatographic studies of certain activities associated with human fibrinogen preparations. *J Clin Invest,* 42**,** 747-55.

MOSESSON, M. W., FINLAYSON, J. S. & UMFLEET, R. A. 1972. Human fibrinogen heterogeneities. 3. Identification of chain variants. *J Biol Chem,* 247**,** 5223-7.

MOSESSON, M. W., HERNANDEZ, I., RAIFE, T. J., MEDVED, L., YAKOVLEV, S., SIMPSON-HAIDARIS, P. J., UITTE, D. E. W. S. & BERTINA, R. M. 2007. Plasma fibrinogen gamma' chain content in the thrombotic microangiopathy syndrome. *J Thromb Haemost,* 5**,** 62-9.

MOWER, W. R., QUINONES, W. J. & GAMBHIR, S. S. 1997. Effect of intraluminal thrombus on abdominal aortic aneurysm wall stress. *J Vasc Surg,* 26**,** 602-8.

MOYO, V. M., MUKHINA, G. L., GARRETT, E. S. & BRODSKY, R. A. 2004. Natural history of paroxysmal nocturnal haemoglobinuria using modern diagnostic assays. *British Journal of Haematology,* 126**,** 133-138.

MURAKAMI, Y., INOUE, N., SHICHISHIMA, T., OHTA, R., NOJI, H., MAEDA, Y., NISHIMURA, J., KANAKURA, Y. & KINOSHITA, T. 2012. Deregulated expression of HMGA2 is implicated in clonal expansion of PIGA deficient cells in paroxysmal nocturnal haemoglobinuria. *British Journal of Haematology,* 156**,** 383-387.

MUSZBEK, L., ADANY, R. & MIKKOLA, H. 1996. Novel aspects of blood coagulation factor XIII. I. Structure, distribution, activation, and function. *Crit Rev Clin Lab Sci,* 33**,** 357-421.

MUTCH, N. J., ENGEL, R., UITTE DE WILLIGE, S., PHILIPPOU, H. & ARIENS, R. A. 2010a. Polyphosphate modifies the fibrin network and down-regulates fibrinolysis by attenuating binding of tPA and plasminogen to fibrin. *Blood,* 115**,** 3980-8.

MUTCH, N. J., KOIKKALAINEN, J. S., FRASER, S. R., DUTHIE, K. M., GRIFFIN, M., MITCHELL, J., WATSON, H. G. & BOOTH, N. A. 2010b. Model thrombi formed under flow reveal the role of factor XIII-mediated cross-linking in resistance to fibrinolysis. *Journal of Thrombosis and Haemostasis,* 8**,** 2017-2024.

MUTHARD, R. W., WELSH, J. D., BRASS, L. F. & DIAMOND, S. L. 2015. Fibrin, gamma'-fibrinogen, and transclot pressure gradient control hemostatic clot growth during human blood flow over a collagen/tissue factor wound. *Arterioscler Thromb Vasc Biol,* 35**,** 645-54.

NAIMUSHIN, Y. A. & MAZUROV, A. V. 2004. Von Willebrand factor can support platelet aggregation via interaction with activated GPIIb-IIIa and GPIb. *Platelets,* 15**,** 419-25.

NAKAKUMA, H. & KAWAGUCHI, T. 2003. Pathogenesis of selective expansion of PNH clones. *Int J Hematol,* 77**,** 121-4.

NICKERSON, D. 2003. SeattleSNPs: NHLBI Program for Genomic Applications, UW-FHCRC, Seattle, WA.

NINIVAGGI, M., APITZ-CASTRO, R., DARGAUD, Y., DE LAAT, B., HEMKER, H. C. & LINDHOUT, T. 2012. Whole-Blood Thrombin

Generation Monitored with a Calibrated Automated Thrombogram-Based Assay. *Clinical Chemistry,* 58**,** 1252-1259.

NISHIMURA, J. & KANAKURA, Y. 2015. [The C5 gene polymorphism in patients with PNH]. *Rinsho Ketsueki,* 56**,** 103-10.

NOWAK-GOTTL, U., WEILER, H. & STOLL, M. 2009. Elevated fibrinogen gamma ' ratios and clinical outcomes Response. *Blood,* 114**,** 4604-4605.

O'BRIEN, E. T., FALVO, M. R., MILLARD, D., EASTWOOD, B., TAYLOR, R. M. & SUPERFINE, R. 2008. Ultrathin self-assembled fibrin sheets. *Proceedings of the National Academy of Sciences of the United States of America,* 105**,** 19438-19443.

OLSEN, S. B., TANG, D. B., JACKSON, M. R., GOMEZ, E. R., AYALA, B. & ALVING, B. M. 1996. Enhancement of platelet deposition by cross-linked hemoglobin in a rat carotid endarterectomy model. *Circulation,* 93**,** 327-32.

OMAROVA, F., DE WILLIGE, S. U., ARIENS, R. A. S., ROSING, J., BERTINA, R. M. & CASTOLDI, E. 2013a. Inhibition of thrombin-mediated factor V activation contributes to the anticoagulant activity of fibrinogen gamma '. *Journal of Thrombosis and Haemostasis,* 11**,** 1669-1678.

OMAROVA, F., DE WILLIGE, S. U., SIMIONI, P., ARIENS, R., BERTINA, R. M., ROSING, J. & CASTOLDI, E. 2013b. Fibrinogen ?' increases the sensitivity to activated protein C in normal and FV Leiden plasma. *Journal of Thrombosis and Haemostasis,* 11**,** 43-44.

PARKER, C., OMINE, M., RICHARDS, S., NISHIMURA, J., BESSLER, M., WARE, R., HILLMEN, P., LUZZATTO, L., YOUNG, N., KINOSHITA, T., ROSSE, W., SOCIE, G. & INTERNATIONAL, P. N. H. I. G. 2005. Diagnosis and management of paroxysmal nocturnal hemoglobinuria. *Blood,* 106**,** 3699-709.

PARRY, D. J., AL-BARJAS, H. S., CHAPPELL, L., RASHID, T., ARIENS, R. A. & SCOTT, D. J. 2009. Haemostatic and fibrinolytic factors in men with a small abdominal aortic aneurysm. *Br J Surg,* 96**,** 870-7.

PEACOCK-YOUNG, B., MACRAE, F. L., NEWTON, D. J., HILL, A. & ARIENS, R. A. S. 2018. The prothrombotic state in paroxysmal nocturnal hemoglobinuria: a multifaceted source. *Haematologica,* 103**,** 9-17.

PEERSCHKE, E. I., FRANCIS, C. W. & MARDER, V. J. 1986. Fibrinogen binding to human blood platelets: effect of gamma chain carboxyterminal structure and length. *Blood,* 67**,** 385-90.

PIERPONT, Y. N., DINH, T. P., SALAS, R. E., JOHNSON, E. L., WRIGHT, T. G., ROBSON, M. C. & PAYNE, W. G. 2014. Obesity and surgical wound healing: a current review. *ISRN Obes,* 2014**,** 638936.

PIETERS, M., KOTZE, R. C., JERLING, J. C., KRUGER, A. & ARIENS, R. A. 2013. Evidence that fibrinogen gamma' regulates plasma clot structure and lysis and relationship to cardiovascular risk factors in black Africans. *Blood,* 121**,** 3254-60.

PINEDA, A. O., CHEN, Z. W., MARINO, F., MATHEWS, F. S., MOSESSON, M. W. & DI CERA, E. 2007. Crystal structure of thrombin in complex with fibrinogen gamma' peptide. *Biophys Chem,* 125**,** 556-9.

PRASAD, J. M., GORKUN, O. V., RAGHU, H., THORNTON, S., MULLINS, E. S., PALUMBO, J. S., KO, Y. P., HOOK, M., DAVID, T., COUGHLIN, S. R., DEGEN, J. L. & FLICK, M. J. 2015. Mice expressing a mutant form of fibrinogen that cannot support fibrin formation exhibit compromised antimicrobial host defense. *Blood,* 126**,** 2047-2058.

PRETORIUS, E., OBERHOLZER, H. M., VAN DER SPUY, W. J., SWANEPOEL, A. C. & SOMA, P. 2012. Scanning electron microscopy of fibrin networks in rheumatoid arthritis: a qualitative analysis. *Rheumatology International,* 32**,** 1611-1615.

RASMUSSEN-TORVIK, L. J., CUSHMAN, M., TSAI, M. Y., ZHANG, Y., HECKBERT, S. R., ROSAMOND, W. D. & FOLSOM, A. R. 2007. The association of alpha-fibrinogen Thr312Ala polymorphism and venous thromboembolism in the LITE study. *Thromb Res,* 121**,** 1-7.

RAZUMOVSKY, L. & DAMODARAN, S. 1999. Surface activity-compressibility relationship of proteins at the air-water interface. *Langmuir,* 15**,** 1392-1399.

REEPS, C., PELISEK, J., SEIDL, S., SCHUSTER, T., ZIMMERMANN, A., KUEHNL, A. & ECKSTEIN, H. H. 2009. Inflammatory infiltrates and neovessels are relevant sources of MMPs in abdominal aortic aneurysm wall. *Pathobiology,* 76**,** 243-52.

RENNE, T., SCHMAIER, A. H., NICKEL, K. F., BLOMBACK, M. & MAAS, C. 2012. In vivo roles of factor XII. *Blood,* 120**,** 4296-4303.

RICHARDS, S. J. & BARNETT, D. 2007. The role of flow cytometry in the diagnosis of paroxysmal nocturnal hemoglobinuria in the clinical laboratory. *Clin Lab Med,* 27**,** 577-90, vii.

RICHARDSON, V. R., SCHROEDER, V., GRANT, P. J., STANDEVEN, K. F. & CARTER, A. M. 2013. Complement C3 is a substrate for activated factor XIII that is cross-linked to fibrin during clot formation. *Br J Haematol,* 160**,** 116-9.

RITCHIE, H., LAWRIE, L. C., MOSESSON, M. W. & BOOTH, N. A. 2001. Characterization of crosslinking sites in fibrinogen for plasminogen activator inhibitor 2 (PAI-2). *Fibrinogen,* 936**,** 215-218.

RIZAS, K. D., IPPAGUNTA, N. & TILSON, M. D., 3RD 2009. Immune cells and molecular mediators in the pathogenesis of the abdominal aortic aneurysm. *Cardiol Rev,* 17**,** 201-10.

ROLLINS, S. A. & SIMS, P. J. 1990. The complement-inhibitory activity of CD59 resides in its capacity to block incorporation of C9 into membrane C5b-9. *J Immunol,* 144**,** 3478-83.

ROSKAM, J., HUGUES, J., BOUNAMEAUX, Y. & SALMON, J. 1959. The part played by platelets in the formation of an efficient hemostatic plug. *Thromb Diath Haemorrh,* 3**,** 510-9.

ROSTI, V., TREMML, G., SOARES, V., PANDOLFI, P. P., LUZZATTO, L. & BESSLER, M. 1997. Murine embryonic stem cells without pig-a gene activity are competent for hematopoiesis with the PNH phenotype but not for clonal expansion. *J Clin Invest,* 100**,** 1028-36.

ROURKE, C., CURRY, N., KHAN, S., TAYLOR, R., RAZA, I., DAVENPORT, R., STANWORTH, S. & BROHI, K. 2012. Fibrinogen levels during trauma hemorrhage, response to replacement therapy, and association with patient outcomes. *J Thromb Haemost,* 10**,** 1342-51.

RUIGROK, Y. M., SLOOTER, A. J., RINKEL, G. J., WIJMENGA, C. & ROSENDAAL, F. R. 2010. Genes influencing coagulation and the risk of aneurysmal subarachnoid hemorrhage, and subsequent complications of secondary cerebral ischemia and rebleeding. *Acta Neurochir (Wien),* 152**,** 257-62.

RYAN, A. W., HUGHES, D. A., TANG, K., KELLEHER, D. P., RYAN, T., MCMANUS, R. & STONEKING, M. 2009. Natural selection and the molecular basis of electrophoretic variation at the coagulation F13B locus. *Eur J Hum Genet,* 17**,** 219-27.

SABO, T. M., FARRELL, D. H. & MAURER, M. C. 2006. Conformational analysis of gamma' peptide (410-427) interactions with thrombin anion binding exosite II. *Biochemistry,* 45**,** 7434-45.

SANDFORD, R. M., BOWN, M. J., LONDON, N. J. & SAYERS, R. D. 2007. The genetic basis of abdominal aortic aneurysms: A review. *European Journal of Vascular and Endovascular Surgery,* 33**,** 381-390.

SANKARANARAYANAN, K., DHATHATHREYAN, A. & MILLER, R. 2010. Assembling Fibrinogen at Air/Water and Solid/Liquid Interfaces Using Langmuir and Langmuir-Blodgett Films. *Journal of Physical Chemistry B,* 114**,** 8067-8075.

SCHREZENMEIER, H., MUUS, P., SOCIE, G., SZER, J., URBANO-ISPIZUA, A., MACIEJEWSKI, J. P., BRODSKY, R. A., BESSLER, M., KANAKURA, Y., ROSSE, W., KHURSIGARA, G., BEDROSIAN, C. & HILLMEN, P. 2014. Baseline characteristics and disease burden in patients in the International Paroxysmal Nocturnal Hemoglobinuria Registry. *Haematologica,* 99**,** 922-9.

SCHROEDER, V., CHATTERJEE, T. & KOHLER, H. P. 2001. Influence of blood coagulation factor XIII and FXIII Val34Leu on plasma clot formation measured by thrombelastography. *Thromb Res,* 104**,** 467-74.

SCHUBERT, J. & ROTH, A. 2015. Update on paroxysmal nocturnal haemoglobinuria: on the long way to understand the principles of the disease. *Eur J Haematol,* 94**,** 464-73.

SCHWARTZ, M. L., PIZZO, S. V., HILL, R. L. & MCKEE, P. A. 1973. Human Factor XIII from plasma and platelets. Molecular weights, subunit structures, proteolytic activation, and cross-linking of fibrinogen and fibrin. *J Biol Chem,* 248**,** 1395-407.

SCOTT, D. J., PRASAD, P., PHILIPPOU, H., RASHID, S. T., SOHRABI, S., WHALLEY, D., KORDOWICZ, A., TANG, Q., WEST, R. M., JOHNSON, A., WOODS, J., AJJAN, R. A. & ARIENS, R. A. 2011. Clot architecture is altered in abdominal aortic aneurysms and correlates with aneurysm size. *Arterioscler Thromb Vasc Biol,* 31**,** 3004-10.

SEREGINA, E. A., TSVETAEVA, N. V., NIKULINA, O. F., ZAPARIY, A. P., ERASOV, A. V., GRIBKOVA, I. V., OREL, E. B., ATAULLAKHANOV, F. I. & BALANDINA, A. N. 2015. Eculizumab effect on the hemostatic state in patients with paroxysmal nocturnal hemoglobinuria. *Blood Cells Mol Dis,* 54**,** 144-50.

SHAINOFF, J. R. & DARDIK, B. N. 1983. Fibrinopeptide B in fibrin assembly and metabolism: physiologic significance in delayed release of the peptide. *Ann N Y Acad Sci,* 408**,** 254-68.

SHATS-TSEYTLINA, E. A., NAIR, C. H. & DHALL, D. P. 1994. Complement activation: a new participant in the modulation of fibrin gel characteristics and the progression of atherosclerosis? *Blood Coagul Fibrinolysis,* 5**,** 529-35.

SHEN, L. & LORAND, L. 1983. Contribution of fibrin stabilization to clot strength. Supplementation of factor XIII-deficient plasma with the purified zymogen. *J Clin Invest,* 71**,** 1336-41.

SIEBENLIST, K. R., MEH, D. A. & MOSESSON, M. W. 1996. Plasma factor XIII binds specifically to fibrinogen molecules containing gamma chains. *Biochemistry,* 35**,** 10448-53.

SIEBENLIST, K. R., MEH, D. A. & MOSESSON, M. W. 2001. Protransglutaminase (factor XIII) mediated crosslinking of fibrinogen and fibrin. *Thromb Haemost,* 86**,** 1221-8.

SIEBENLIST, K. R. & MOSESSON, M. W. 1994. Progressive cross-linking of fibrin gamma chains increases resistance to fibrinolysis. *J Biol Chem,* 269**,** 28414-9.

SIEBENLIST, K. R., MOSESSON, M. W., HERNANDEZ, I., BUSH, L. A., DI CERA, E., SHAINOFF, J. R., DI ORIO, J. P. & STOJANOVIC, L. 2005. Studies on the basis for the properties of fibrin produced from fibrinogen-containing gamma' chains. *Blood,* 106**,** 2730-6.

SIMAO DA SILVA, E., RODRIGUES, A. J., MAGALHAES CASTRO DE TOLOSA, E., RODRIGUES, C. J., VILLAS BOAS DO PRADO, G. & NAKAMOTO, J. C. 2000. Morphology and diameter of infrarenal aortic aneurysms: a prospective autopsy study. *Cardiovasc Surg,* 8**,** 526-32.

SIMIONATTO, C. S., CABAL, R., JONES, R. L. & GALBRAITH, R. A. 1988. Thrombophlebitis and Disturbed Hemostasis Following Administration of Intravenous Hematin in Normal Volunteers. *American Journal of Medicine,* 85**,** 538-540.

SIMIONI, P., TORMENE, D., SPIEZIA, L., TOGNIN, G., ROSSETTO, V., RADU, C. & PRANDONI, P. 2006. Inherited thrombophilia and venous thromboembolism. *Semin Thromb Hemost,* 32**,** 700-8.

SIMS, P. J. & WIEDMER, T. 1991. The Response of Human Platelets to Activated Components of the Complement-System. *Immunology Today,* 12**,** 338-342.

SIMS, P. J. & WIEDMER, T. 1995. Induction of Cellular Procoagulant Activity by the Membrane Attack Complex of Complement. *Seminars in Cell Biology,* 6**,** 275-282.

SINGH, K., BONAA, K. H., JACOBSEN, B. K., BJORK, L. & SOLBERG, S. 2001. Prevalence of and risk factors for abdominal aortic aneurysms in a population-based study : The Tromso Study. *Am J Epidemiol,* 154**,** 236-44.

SMITH, E. L., CARDINALI, B., PING, L., ARIENS, R. & PHILIPPOU, H. 2013. Elimination of coagulation factor XIII from fibrinogen preparations. *Journal of Thrombosis and Haemostasis,* 11**,** 1053-1053.

SMITH, S. A., TRAVERS, R. J. & MORRISSEY, J. H. 2015. How it all starts: Initiation of the clotting cascade. *Crit Rev Biochem Mol Biol,* 50**,** 326-36.

SOCIE, G., MARY, J. Y., DE GRAMONT, A., RIO, B., LEPORRIER, M., ROSE, C., HEUDIER, P., ROCHANT, H., CAHN, J. Y. & GLUCKMAN, E. 1996. Paroxysmal nocturnal haemoglobinuria: long-term follow-up and prognostic factors. French Society of Haematology. *Lancet,* 348**,** 573-7.

SPRAGGON, G., EVERSE, S. J. & DOOLITTLE, R. F. 1997. Crystal structures of fragment D from human fibrinogen and its crosslinked counterpart from fibrin. *Nature,* 389**,** 455-462.

STACKELBERG, O., BJORCK, M., SADR-AZODI, O., LARSSON, S. C., ORSINI, N. & WOLK, A. 2013. Obesity and abdominal aortic aneurysm. *British Journal of Surgery,* 100**,** 360-366.

STANDEVEN, K. F., ARIENS, R. A. & GRANT, P. J. 2005. The molecular physiology and pathology of fibrin structure/function. *Blood Rev,* 19**,** 275-88.

STANDEVEN, K. F., CARTER, A. M., GRANT, P. J., WEISEL, J. W., CHERNYSH, I., MASOVA, L., LORD, S. T. & ARIENS, R. A. 2007. Functional analysis of fibrin {gamma}-chain cross-linking by activated factor XIII: determination of a cross-linking pattern that maximizes clot stiffness. *Blood,* 110**,** 902-7.

STANDEVEN, K. F., GRANT, P. J., CARTER, A. M., SCHEINER, T., WEISEL, J. W. & ARIENS, R. A. 2003. Functional analysis of the fibrinogen Aalpha Thr312Ala polymorphism: effects on fibrin structure and function. *Circulation,* 107**,** 2326-30.

STENBAEK, J., KALIN, B. & SWEDENBORG, J. 2000. Growth of thrombus may be a better predictor of rupture than diameter in patients with abdominal aortic aneurysms. *Eur J Vasc Endovasc Surg,* 20**,** 466-9.

STEPIEN, E., PLICNER, D., BRANICKA, A., STANKIEWICZ, E., PAZDAN, A., SNIEZEK-MACIEJEWSKA, M., GORKIEWICZ, I., KAPELAK, B. & SADOWSKI, J. 2007. [Factors influencing thrombin generation measured as thrombin-antithrombin complexes levels and using calibrated automated thrombogram in patients with advanced coronary artery disease]. *Pol Arch Med Wewn,* 117**,** 297-305.

STIEF, T. W. 2007. Thrombin generation by hemolysis. *Blood Coagulation & Fibrinolysis,* 18**,** 61-66.

STUDT, J. D., KREMER HOVINGA, J. A., ANTOINE, G., HERMANN, M., RIEGER, M., SCHEIFLINGER, F. & LAMMLE, B. 2005. Fatal congenital thrombotic thrombocytopenic purpura with apparent ADAMTS13 inhibitor: in vitro inhibition of ADAMTS13 activity by hemoglobin. *Blood,* 105**,** 542-4.

SUENSON, E., LUTZEN, O. & THORSEN, S. 1984. Initial plasmin-degradation of fibrin as the basis of a positive feed-back mechanism in fibrinolysis. *Eur J Biochem,* 140**,** 513-22.

SUH, T. T., HOLMBACK, K., JENSEN, N. J., DAUGHERTY, C. C., SMALL, K., SIMON, D. I., POTTER, S. & DEGEN, J. L. 1995. Resolution of spontaneous bleeding events but failure of pregnancy in fibrinogen-deficient mice. *Genes Dev,* 9**,** 2020-33.

SUNTHARALINGAM, J., GOLDSMITH, K., VAN MARION, V., LONG, L., TREACY, C. M., DUDBRIDGE, F., TOSHNER, M. R., PEPKE-ZABA, J., EIKENBOOM, J. C. & MORRELL, N. W. 2008. Fibrinogen Aalpha Thr312Ala polymorphism is associated with chronic thromboembolic pulmonary hypertension. *Eur Respir J,* 31**,** 736-41.

TAMAKI, T. & AOKI, N. 1981. Cross-Linking of Alpha-2-Plasmin Inhibitor and Fibronectin to Fibrin by Fibrin-Stabilizing Factor. *Biochimica Et Biophysica Acta,* 661**,** 280-286.

THOMPSON, M. M., JONES, L., NASIM, A., SAYERS, R. D. & BELL, P. R. 1996. Angiogenesis in abdominal aortic aneurysms. *Eur J Vasc Endovasc Surg,* 11**,** 464-9.

THOMPSON, R. W., LIAO, S. & CURCI, J. A. 1997. Vascular smooth muscle cell apoptosis in abdominal aortic aneurysms. *Coron Artery Dis,* 8**,** 623-31.

THORSEN, S. 1992. The mechanism of plasminogen activation and the variability of the fibrin effector during tissue-type plasminogen activator-mediated fibrinolysis. *Ann N Y Acad Sci,* 667**,** 52-63.

TIEDE, C., BEDFORD, R., HESELTINE, S. J., SMITH, G., WIJETUNGA, I., ROSS, R., ALQALLAF, D., ROBERTS, A. P., BALLS, A., CURD, A., HUGHES, R. E., MARTIN, H., NEEDHAM, S. R., ZANETTI-DOMINGUES, L. C., SADIGH, Y., PEACOCK, T. P., TANG, A. A., GIBSON, N., KYLE, H., PLATT, G. W., INGRAM, N., TAYLOR, T., COLETTA, L. P., MANFIELD, I., KNOWLES, M., BELL, S., ESTEVES, F., MAQBOOL, A., PRASAD, R. K., DRINKHILL, M., BON, R. S., PATEL, V., GOODCHILD, S. A., MARTIN-FERNANDEZ, M., OWENS, R. J., NETTLESHIP, J. E., WEBB, M. E., HARRISON, M., LIPPIAT, J. D., PONNAMBALAM, S., PECKHAM, M., SMITH, A., FERRIGNO, P. K., JOHNSON, M., MCPHERSON, M. J. & TOMLINSON, D. C. 2017. Affimer proteins are versatile and renewable affinity reagents. *Elife,* 6.

TREMML, G., DOMINGUEZ, C., ROSTI, V., ZHANG, Z., PANDOLFI, P. P., KELLER, P. & BESSLER, M. 1999. Increased sensitivity to complement and a decreased red blood cell life span in mice mosaic for a nonfunctional Piga gene. *Blood,* 94**,** 2945-54.

TSUI, J. C. 2010. Experimental models of abdominal aortic aneurysms. *Open Cardiovasc Med J,* 4**,** 221-30.

UITTE DE WILLIGE, S., DE VISSER, M. C., HOUWING-DUISTERMAAT, J. J., ROSENDAAL, F. R., VOS, H. L. & BERTINA, R. M. 2005. Genetic variation in the fibrinogen gamma gene increases the risk for deep venous thrombosis by reducing plasma fibrinogen gamma' levels. *Blood,* 106**,** 4176-83.

UITTE DE WILLIGE, S., RIETVELD, I. M., DE VISSER, M. C., VOS, H. L. & BERTINA, R. M. 2007. Polymorphism 10034C>T is located in a region regulating polyadenylation of FGG transcripts and influences the fibrinogen gamma'/gammaA mRNA ratio. *J Thromb Haemost,* 5**,** 1243-9.

UNDAS, A. 2017. Prothrombotic Fibrin Clot Phenotype in Patients with Deep Vein Thrombosis and Pulmonary Embolism: A New Risk Factor for Recurrence. *Biomed Research International*.

UNDAS, A. & ARIENS, R. A. 2011. Fibrin clot structure and function: a role in the pathophysiology of arterial and venous thromboembolic diseases. *Arterioscler Thromb Vasc Biol,* 31**,** e88-99.

VALNICKOVA, Z. & ENGHILD, J. J. 1998. Human procarboxypeptidase U, or thrombin-activable fibrinolysis inhibitor, is a substrate for transglutaminases - Evidence for transglutaminase-catalyzed cross-linking to fibrin. *Journal of Biological Chemistry,* 273**,** 27220-27224.

VAN BIJNEN, S. T. A., OSTERUD, B., BARTELING, W., VERBEEK-KNOBBE, K., WILLEMSEN, M., VAN HEERDE, W. L. & MUUS, P. 2015. Alterations in markers of coagulation and fibrinolysis in patients with Paroxysmal Nocturnal Hemoglobinuria before and during treatment with eculizumab. *Thrombosis Research,* 136**,** 274-281.

VAN DEN HERIK, E. G., CHEUNG, E. Y. L., DE LAU, L. M. L., DEN HERTOG, H. M., LEEBEEK, F. W., DIPPEL, D. W. J., KOUDSTAAL, P. J. & DE MAAT, M. P. M. 2011. gamma '/total fibrinogen ratio is associated with short-term outcome in ischaemic stroke. *Thrombosis and Haemostasis,* 105**,** 430-434.

VAN DER BOM, J. G., DE MAAT, M. P., BOTS, M. L., HAVERKATE, F., DE JONG, P. T., HOFMAN, A., KLUFT, C. & GROBBEE, D. E. 1998. Elevated plasma fibrinogen: cause or consequence of cardiovascular disease? *Arterioscler Thromb Vasc Biol,* 18**,** 621-5.

VAN ES, A. C., AUTAR, A. S., EMMER, B. J., LYCKLAMA, A. N. G. J., VAN DER KALLEN, B. F. & VAN BEUSEKOM, H. M. 2017. Imaging stent-thrombus interaction in mechanical thrombectomy. *Neurology,* 88**,** 216-217.

VAN HOLTEN, T. C., WAANDERS, L. F., DE GROOT, P. G., VISSERS, J., HOEFER, I. E., PASTERKAMP, G., PRINS, M. W. & ROEST, M. 2013. Circulating biomarkers for predicting cardiovascular disease risk; a systematic review and comprehensive overview of meta-analyses. *PLoS One,* 8**,** e62080.

VAN KRUCHTEN, R., COSEMANS, J. M. E. M. & HEEMSKERK, J. W. M. 2012. Measurement of whole blood thrombus formation using parallel-plate flow chambers - a practical guide. *Platelets,* 23**,** 229-242.

VAN OSS, C. J. 1990. Surface properties of fibrinogen and fibrin. *J Protein Chem,* 9**,** 487-91.

VELNAR, T., BAILEY, T. & SMRKOLJ, V. 2009. The wound healing process: an overview of the cellular and molecular mechanisms. *J Int Med Res,* 37**,** 1528-42.

VORP, D. A., LEE, P. C., WANG, D. H., MAKAROUN, M. S., NEMOTO, E. M., OGAWA, S. & WEBSTER, M. W. 2001. Association of intraluminal thrombus in abdominal aortic aneurysm with local hypoxia and wall weakening. *J Vasc Surg,* 34**,** 291-9.

VORP, D. A., RAGHAVAN, M. L. & WEBSTER, M. W. 1998. Mechanical wall stress in abdominal aortic aneurysm: influence of diameter and asymmetry. *J Vasc Surg,* 27**,** 632-9.

VORP, D. A. & VANDE GEEST, J. P. 2005. Biomechanical determinants of abdominal aortic aneurysm rupture. *Arterioscler Thromb Vasc Biol,* 25**,** 1558-66.

VU, T. T., STAFFORD, A. R., LESLIE, B. A., KIM, P. Y., FREDENBURGH, J. C. & WEITZ, J. I. 2011. Histidine-rich Glycoprotein Binds Fibrin(ogen) with High Affinity and Competes with Thrombin for Binding to the gamma '-Chain. *Journal of Biological Chemistry,* 286**,** 30314-30323.

WANG, D. H., MAKAROUN, M. S., WEBSTER, M. W. & VORP, D. A. 2002. Effect of intraluminal thrombus on wall stress in patient-specific models of abdominal aortic aneurysm. *J Vasc Surg,* 36**,** 598-604.

WEISEL, J. W. 1986. The electron microscope band pattern of human fibrin: various stains, lateral order, and carbohydrate localization. *J Ultrastruct Mol Struct Res,* 96**,** 176-88.

WEISEL, J. W. 2005. Fibrinogen and fibrin. *Adv Protein Chem,* 70**,** 247-99.

WEISEL, J. W. & MEDVED, L. 2001. The structure and function of the alpha C domains of fibrinogen. *Fibrinogen,* 936**,** 312-327.

WEISEL, J. W. & NAGASWAMI, C. 1992. Computer modeling of fibrin polymerization kinetics correlated with electron microscope and turbidity observations: clot structure and assembly are kinetically controlled. *Biophys J,* 63**,** 111-28.

WEISEL, J. W., STAUFFACHER, C. V., BULLITT, E. & COHEN, C. 1985. A Model for Fibrinogen - Domains and Sequence. *Science,* 230**,** 1388-1391.

WEITZ, I. C., RAZAVI, P., ROCHANDA, L., ZWICKER, J., FURIE, B., MANLY, D., MACKMAN, N., GREEN, R. & LIEBMAN, H. A. 2012. Eculizumab therapy results in rapid and sustained decreases in markers of thrombin generation and inflammation in patients with PNH independent of its effects on hemolysis and microparticle formation. *Thrombosis Research,* 130**,** 361-368.

WELLS, P. S., ANDERSON, J. L., SCARVELIS, D. K., DOUCETTE, S. P. & GAGNON, F. 2006. Factor XIII Val34Leu variant is protective against venous thromboembolism: A HuGE review and meta-analysis. *American Journal of Epidemiology,* 164**,** 101-109.

WERB, Z., UNDERWOOD, J. L. & RAPPOLEE, D. A. 1992. The Role of Macrophage-Derived Growth-Factors in Tissue-Repair. *Mononuclear Phagocytes***,** 404-409.

WESTON-DAVIES, W. H., NUNN, M. A., PINTO, F. O., MACKIE, I. J., RICHARDS, S. J., MACHIN, S. J., PRUDO, R. & HILLMEN, P. 2014. Clinical and Immunological Characterisation of Coversin, a Novel Small Protein Inhibitor of Complement C5 with Potential As a Therapeutic Agent in PNH and Other Complement Mediated Disorders. *Blood,* 124.

WIEDMER, T., ESMON, C. T. & SIMS, P. J. 1986. Complement Proteins C5b-9 Stimulate Procoagulant Activity through the Platelet Prothrombinase. *Federation Proceedings,* 45**,** 1072-1072.

WIEDMER, T., HALL, S. E., ORTEL, T. L., KANE, W. H., ROSSE, W. F. & SIMS, P. J. 1993. Complement-induced vesiculation and exposure of membrane prothrombinase sites in platelets of paroxysmal nocturnal hemoglobinuria. *Blood,* 82**,** 1192-6.

WILGUS, T. A., ROY, S. & MCDANIEL, J. C. 2013. Neutrophils and Wound Repair: Positive Actions and Negative Reactions. *Adv Wound Care (New Rochelle),* 2**,** 379-388.

WILSON, W. A. & THOMAS, E. J. 1979. Activation of the Alternative Pathway of Human-Complement by Hemoglobin. *Clinical and Experimental Immunology,* 36**,** 140-144.

WOLBERG, A. S. 2007. Thrombin generation and fibrin clot structure. *Blood Reviews,* 21**,** 131-142.

WOLBERG, A. S. 2010. Plasma and cellular contributions to fibrin network formation, structure and stability. *Haemophilia,* 16**,** 7-12.

WOLF, Y. G., THOMAS, W. S., BRENNAN, F. J., GOFF, W. G., SISE, M. J. & BERNSTEIN, E. F. 1994. Computed tomography scanning findings associated with rapid expansion of abdominal aortic aneurysms. *J Vasc Surg,* 20**,** 529-35; discussion 535-8.

WOLFENSTEIN-TODEL, C. & MOSESSON, M. W. 1980. Human plasma fibrinogen heterogeneity: evidence for an extended carboxyl-terminal sequence in a normal gamma chain variant (gamma'). *Proc Natl Acad Sci U S A,* 77**,** 5069-73.

WOLFENSTEIN-TODEL, C. & MOSESSON, M. W. 1981. Carboxy-terminal amino acid sequence of a human fibrinogen gamma-chain variant (gamma'). *Biochemistry,* 20**,** 6146-9.

WOODHEAD, J. L., NAGASWAMI, C., MATSUDA, M., AROCHA-PINANGO, C. L. & WEISEL, J. W. 1996. The ultrastructure of fibrinogen Caracas II molecules, fibers, and clots. *J Biol Chem,* 271**,** 4946-53.

ZASADZINSKI, J. A., VISWANATHAN, R., MADSEN, L., GARNAES, J. & SCHWARTZ, D. K. 1994. Langmuir-Blodgett films. *Science,* 263**,** 1726-33.

ZENTAI, C., SOLOMON, C., VAN DER MEIJDEN, P. E. J., SPRONK, H. M. H., SCHNABEL, J., ROSSAINT, R. & GROTTKE, O. 2016. Effects of Fibrinogen Concentrate on Thrombin Generation, Thromboelastometry Parameters, and Laboratory Coagulation Testing in a 24-Hour Porcine Trauma Model. *Clinical and Applied Thrombosis-Hemostasis,* 22**,** 749-759.

ZHOU, Z., HAN, H., CRUZ, M. A., LOPEZ, J. A., DONG, J. F. & GUCHHAIT, P. 2009. Haemoglobin blocks von Willebrand factor proteolysis by ADAMTS-13: a mechanism associated with sickle cell disease. *Thromb Haemost,* 101**,** 1070-7.

ZHU, S., CHEN, J. & DIAMOND, S. L. 2018. Establishing the Transient Mass Balance of Thrombosis: From Tissue Factor to Thrombin to Fibrin Under Venous Flow. *Arterioscler Thromb Vasc Biol,* 38**,** 1528-1536.

ZIAKAS, P. D., POULOU, L. S., ROKAS, G. I., BARTZOUDIS, D. & VOULGARELIS, M. 2007. Thrombosis in paroxysmal nocturnal hemoglobinuria: sites, risks, outcome. An overview. *Journal of Thrombosis and Haemostasis,* 5**,** 642-645.

Appendices

Appendix 1 - Protocol

Background

An abdominal aortic aneurysm (AAA)
is a focal dilatation of the abdominal aorta greater than three centimetres in maximal diameter. The condition spontaneously evolves towards rupture, which confers a mortality risk in the region of 80 % despite emergency surgery. The current principles of management involve watchful waiting with targeted intervention once the annual risk of rupture outweighs the mortality risks of intervention. This treatment threshold is currently set at 5.5 cm in otherwise fit patients. Open aneurysm repair (OAR) or endovascular aneurysm repair (EVAR) are both suitable treatment modalities.

The clinical risk factors for AAA include male sex, smoking, high blood pressure and age; diabetes is thought to be protective. Although atherosclerosis clusters with AAA, its precise role in aneurysm development remains unclear. The pathobiology of AAA incorporates transmural inflammation, loss of vascular smooth muscle from the arterial media, over production of matrix metalloproteinases which destroy collagen and elastin. Acting in concert these factors lead to aneurysm formation, but the precise event that precipitates this process remains unknown. Furthermore, the factors which influence the ongoing growth of AAA once established are debated. It is also apparent that patients with AAA are at increased cardiac risk, but how this cardiac risk is related to the presence of AAA is also unclear.

Aims

The overall aim of the LEADS project is to investigate AAA development, growth and outcomes, and thus identify novel treatments. In order to do this, a Leeds based AAA database will collect demographic and diagnostic information on AAA and control patients and store patients‟ blood, DNA, RNA, protein, plasma and AAA tissue.

History

The Leeds Aneurysm Development Study (LEADS) (Leeds East 03/142) was first established in 2003 as a small case-control study (AAA vs. Controls) focused on the differences in inflammatory and coagulation markers in male patients with AAA and controls. The important novel findings stemming from this work led to the continuation of the study and widening of the inclusion criteria. In 2005 women were invited to participate in the study and in 2006 the study minimum age limit was reduced from 65 years to 55 years. As the project grew it became apparent that links should be made between the blood results observed at recruitment, and aneurysm tissue and post-operative blood samples. Thus, following an amendment to the protocol in 2006, these samples were collected for further study.

As the study grew in size and the findings were disseminated locally, the opportunity arose to collaborate with other researchers within and outside of the faculty at The University of Leeds. These new members of the research team offered fresh hypotheses relating to the development and growth of AAA. As a result, and again following amendments to the protocol in 2008 – 2010 data collected now includes aneurysm imaging and growth, genetics, survival and arterial stiffness (pulse wave velocity), with an aim of recruiting a total of 1500 aneurysm and 1500 control patients. As specified in the consent form, all participants are followed prospectively from the time of recruitment. This offers extensive information as to the dynamics of aneurysm expansion (by analysing serial USS and CT scans), AAA prognosis and patient survival. In addition, an application has been submitted to link to the Office of National Statistics data set in order to collect reliable mortality data for our cohort.

As a result of increasing public health awareness, particularly with regard to smoking and changes in medications (statins and ACE-inhibitors), the number of patients with AAA has declined over the last ten years. As a result of decreasing patient numbers, but more significantly as a consequence of huge advances in endovascular aneurysm repair, the number of people in the UK undergoing open AAA repair has vastly decreased. Hence, a collection of aneurysm tissue linked to a data set which includes peripheral blood samples, patient characteristics and imaging is undeniably of importance internationally as a resource for further research in this area. Thus even upon completion of recruitment for this study, we will have established a valuable resource for continued research into the cause of AAA disease, which can be utilized for future medical students, BSc, MD and PhD projects through the Light Laboratories and the University of Leeds.

Study Design and Methodology

This is a prospective observational study recruiting cases (patients with AAA) and control (patients with normal diameter aorta) from a variety of sources. We aim to recruit a minimum of 1500 AAA patients and 1500 age and sex matched controls in order to allow the use of multilevel mixed effects modelling as part of the growth analysis.

This target will also provide sufficient patients for the genetic polymorphism analysis, which also requires significant patient numbers. Depending on the frequency of the genetic mutation of interest, in order to achieve at least 80 % power with 95 % confidence, at least 1000 patients are typically required per analysis. In addition, we aim to compare the AAA patient group with a control group to assess the overall impact of the risk factors such as cardiovascular disease history or e.g. smoking on the development of AAA. We seek to recruit 1500 controls in order to allow effective use of propensity score methods when applied to AAA patient subgroups.

Recruitment of Subjects

AAA

Patients undergoing routine ultrasound surveillance for small AAA (3-5.4 cm AAA) and those admitted for elective/semi-urgent AAA intervention (> 5.4cms) will be recruited from a variety of sources.

Inclusion criteria for AAA:

- Caucasian
- Age ≥ 55 years
- Aortic Diameter on Ultrasound (≥30mm)
- Able to provide informed consent.

Exclusion criteria for AAA:

- Non Caucasian – very low incidence
- Age < 55 years – very low incidence

Control

Controls will be recruited from a variety of sources comparable with the initial source of referral of the AAA. These will include Vascular Surgery Out-patients Department (OPD), General Surgery OPD, Urology OPD, Cardiology OPD, Neurology and Diabetes OPD and General Practitioners in addition to volunteers who come forward as a result of advertisements in Trust and local media. All controls will have imaging of their abdominal aorta (ultrasound or CT scan) to confirm an anterio-posterior diameter of less than 30 mm. From the results of previous ultrasound screening programmes, a normal aorta (< 30mm) at age 65 ensures that the patient is most likely to be free of an aneurysmal dilatation for life. The exact scanning protocol for control subjects may be changed in order to match with guidelines laid out by the National Abdominal Aortic Aneurysm Screening Programme.

Inclusion criteria for controls:

- Caucasian
- Age ≥ 55 years
- Normal Aortic Diameter on Ultrasound (< 30mm)
- Able to provide informed consent.

Exclusion criteria for controls:

- Non Caucasian – very low incidence
- Age < 55 years

Consent

Participants will be welcomed to take part at any time. Typically, participants are invited to participate at an outpatient clinic and provided with the patient information leaflet (enclosed). They are then given at least 24 hours (but typically one week) to consider participation before being contacted by the senior research nurse to arrange recruitment. Written, informed consent will be obtained at recruitment (usually during a recruitment visit or occasionally on attendance for vascular surgery inpatient treatment) using a standardised written consent form (as enclosed). Consent will be taken by the Lead Research Nurse, by the Chief Investigator and by the Chief investigators research fellows, as he deems appropriate. All those taking consent will have undergone NIHR approved Informed Consent training, as well as Good Clinical Practice training. Should an individual who has given consent to take part lose

capacity during the study, they would be would be withdrawn from the follow up process. Identifiable data or tissue already collected with consent would be retained and used in the study. No further data or tissue would be collected or any other research procedures carried out on or in relation to the participant.

Demographics, Medical History, Anthropometrics, Haemodynamics, Doppler & Arterial Stiffness

At the recruitment visit, patients will complete a standard proforma (enclosed) documenting demographics, medical history, drug history, social history and family history. The questionnaire is completed via structured face to face interview with a member of the research team. Following this, a full patient assessment is undertaken. This comprises:

- Measurement of systolic and diastolic blood pressure with oscillometric cuff
- Measurement of height and weight, and calculation of Body Mass Index (BMI)
- Measurement of abdominal circumference, hip circumference and waist circumference
- Ultrasound scan of the abdominal aorta (see below)
- ECG
- Palpation of peripheral pulses, Doppler of peripheral pulses and calculation of ankle-brachial pressure index (ABI)
- Arterial Stiffness measurement using Vicorder (see below)

Blood Sampling & Analysis

Venous blood is taken from the antero-cubital vein from the non-dominant arm. A tourniquet is applied to aid identification of the vein, and inflated to 40mmHg. Once the needle position is confirmed within the vein, the tourniquet is released, and the first 10mls of blood are discarded, as per the laboratory protocol for all clotting studies. 50mls of free flowing venous blood is collected.

As part of their routine clinical care, blood samples are sent to the Leeds Teaching Hospitals NHS Trust Pathology Lab for routine tests. These results are then fed back to the supervising clinician or general practitioner. The remainder is transferred within 30mins to the Laboratory for processing and storage prior to experiments. This consists of 11ml of blood on room temperature citrate, two 6ml samples on EDTA, 10ml of blood on cold citrate and 3ml of blood on cold heparin.

1.2ml of the room temperature blood is put through the ROTEM device in order to elicit an immediate measurement of coagulation through the intrinsic and extrinsic pathways. The remainder is then centrifuged; the two cold samples are spun at 4000rpm for 30mins at 4 °C and the room temperature sample at 4000rpm for 20mins at room temperature. The resultant plasma is aliquoted and flash frozen in liquid nitrogen, before being stored at -80°C.

This plasma is used for all coagulation studies and screens for biomarkers of AAA and cardiovascular disease.

The two EDTA tubes each containing 6mls of whole blood are stored at -20°C to be used for DNA and RNA extraction. A grade D research technician (Myself) is responsible for the processing and initial analysis of blood samples.

For patients and controls who fulfil any of the following secondary exclusion criteria, blood is only taken for DNA, RNA and protein extraction and analysis, so as not to bias results of any coagulation studies. These criteria are:

- Recent Surgery (less than 3 months)
- Active chronic inflammatory conditions
- Recent Thrombotic (arterial and venous) event (less than 3 months)
- Anticoagulation treatments; Warfarin, Factor Xa inhibitors, Therapeutic Tinzaparin
- Active malignancy

Vicorder

The Vicorder device will be used to measure arterial compliance and elasticity. This is done by simultaneously recording a pulse wave from the carotid brachial and femoral and ankle sites by using an oscillometric method. First a neck pad is applied over the carotid artery to prevent compression of the trachea and compression of both carotid arteries at the same time. Next the cuff is placed around the patient's right thigh. Both carotid and femoral cuffs are inflated automatically to 65mmHg and the corresponding oscillometric signal from each cuff is digitally analysed to extract, in real time, the pulse delay. After acquiring several steady pulses the recording is frozen on the display and the transit time in milliseconds presented. The distance between the upper edge of the right femoral cuff and the sternal notch minus the distance between the lower edge of the carotid cuff and the sternal notch is recorded and entered into the computer and displayed as PWVcf (pulse wave velocity common femoral). The procedure is then repeated with the cuff at (i) brachial and femoral and (ii) brachial and ankle. If the pulse

wave is poor on one side the cuffs will be switched to the opposite side. Further details can be seen at www.dopstudio.co.uk. The recording takes just over one hour and no patients have reported any adverse effects.

Imaging

All subjects (AAA and controls) will undergo ultrasound examination of the abdominal aorta (maximum anteroposterior (AP) diameter, position and area of ILT) at the university. The results of these scans are initially stored on the hard drive of the ultrasound machine in an anonymised format, before being transferred to a secure university server for long term storage. This ultrasound examination at recruitment will be separate to any AAA surveillance the patient undergoes at the Leeds Teaching Hospitals NHS Trust. We will ensure all patients with AAA are enrolled in a suitable surveillance programme if they wish as part of the National Abdominal Aortic Aneurysm Screening programme (NAAASP). Following recruitment in the study and initial USS examination at the University, subsequent aortic imaging (USS, Colour Doppler USS, CTA, MRA, Angiography) reports will be obtained from the Leeds Teaching Hospitals NHS Trust secured results server and added to the anonymised database held within the University.

As patients reach their intervention threshold all patients will undergo further imaging, usually CT, or if contraindicated, MRA, as part of the routine NHS care within the Leeds Teaching Hospitals NHS Trust. The images are stored on a secured, limited access PACS system. We will transfer anonymised CT images to CD to allow transfer of images to the University where they will be analysed in the department of Biomechanical Engineering using relevant software. This work involves the segmentation, mapping and ultimately geometric analysis of the AAA and the ILT in three dimensions. The aims of this work are: (1) compare the ultrasound and CT/MRI, (2) to study the force and stresses upon the wall, (3) to study the flow through the aorta and (4) to model the impact of a metal stent on the aorta. Non-identifiable patient images will be stored on the encrypted University server only. The CDs containing these images will be stored in a limited access locked room in the University accessible to the lead research nurse and the PI.

All patients recruited as control subjects will also undergo USS at the University. They will be counselled as to the potential implications of finding an incidental AAA in the same manner as patients attending NAAASP visits at the Leeds Teaching Hospitals NHS Trust. Any control patients found to have an AAA will pass into the AAA group and will be enrolled in the Leeds Teaching Hospitals NHS Trust AAA surveillance

protocol.

Growth modelling

It is well established that once an AAA has developed it tends to grow with time, however, the pattern of growth is much more unclear. AAA measurements obtained from the Leeds Teaching Hospitals NHS Trust server from patients enrolled in the study will be used for this analysis by a team of biostatisticians led by Dr Paul Baxter. The statistics team will only have remote access to blinded data (see below) for their analyses. Growth modelling work will use multilevel mixed effects models to characterise the growth of AAAs within patients. Linear mixed models with random slopes and intercepts can be considered a reasonable basic model. However, more complex non-linear mixed models of quadratic and logistic growth are also of interest. As an alternative, allowing for autocorrelation in residuals from a linear mixed model will be used as a simple strategy for modelling non-linearity in growth. Autocorrelation can be addressed by Box-Jenkins autoregressive moving average (ARMA) structures or contrasted with a spatial autocorrelation model that allows for unequal spacing of observations through time. Growth mixture modelling will provide an alternative, experimental strategy, for characterising growth. Modelling with propensity score matched controls is likely to use techniques including linear and generalised linear models with multilevel and latent variable techniques, where appropriate, to respect complex data structures.

Operative Samples

In those patients who require open surgery, the following samples will be taken (1) abdominal aortic wall, (2) Intra-luminal thrombus, and (3) blood from the AAA sac. All of these samples are normally discarded at the time of surgery.

In those patients who require endovascular stenting a blood sample will be obtained from (i) the sheath placed in the femoral artery and (ii) a catheter placed in the AAA sac. The sheath and passage of the catheter through the AAA are part of the normal procedure; blood is normally aspirated from these sheaths /catheters and then flushed with heparinised saline.

Follow-up

1. **Control patients**

There is no routine follow up for the purposes of this study.

2. Small AAA 30-54mm

In addition to the NHS follow up US scans (see above), those patients with a small AAA 30-54mm will be invited to return at yearly intervals (until the AAA exceeds 55mm) to update their demographic data and medications and to give a repeat blood sample.

3. Large AAA > 55mm at recruitment in those suitable for elective repair

Those patients who undergo a successful AAA operation (Open or Endovascular) will be recalled back to the LIGHT, University of Leeds (if they are fit and well) or we can visit them at home after 3 and 12 months for a repeat blood sample and a repeat ultrasound examination of the AAA repair site. Previous large scale studies have demonstrated that patients return back to a normal quality of life after 3 months and as such the majority would be fit enough to travel. Post-operative imaging undertaken as part of routine clinical care as outlined by LTHT protocols will be accessed electronically by the research team.

4. Large AAA > 55mm in patients who have declined/been turned down for intervention

The medical results server held by the LTHT will be accessed annually for blood results (including Hb, WCC, Plts, Clotting, U&E, CRP and Creatinine and Lipid Profile) and/or any subsequent relevant imaging in order to track AAA growth. In addition, should they wish to return, these patients are also invited back on a yearly basis in order to update their demographic data and medications and to give a repeat blood sample.

At recruitment, consent is taken for all patients and controls to be followed up through Hospital Episode Statistics (HES), Office of National Statistics mortality data (ONS) and The Myocardial Infarction National Audit Project (MINAP) to allow collection of relevant information regarding patient outcomes, specifically relating to cardiovascular morbidity, and mortality.

Laboratory Methods

Plasma levels of TAT, F1+F2, D-dimer, TAFI, PAI-I AG, tPA Ag, plasminogen, alpha2-antiplamin, MMP‟s, insulin and proinsulin are be measured using ELISA kits as well as commercially available antibodies, and fibrinogen is assayed using the Clauss Method. Thrombin generation is measured using the Calibrated Automated Thrombogram (CAT). Other coagulation factors (FVII, FIX, vWF, FXI, FXII) may also be measured by ELISA.

Cardiovascular Disease (CVD) biomarkers would be analysed using relevant biochemical and immunological methods.

Measurement of plasma glucose and lipid sub-fractions are carried out in the routine laboratories of the Chemical Pathology department of the LGI.

Insulin resistance is assessed using the HOMA model with fasting insulin/glucose product, which we have found to be a subtle indicator of insulin resistance in relatives of type 2 diabetic subjects compared to controls. In addition there is evidence that proinsulin is inadequately processed in the presence of insulin resistance and that the insulin: proinsulin ratio is a good indicator of underlying insulin resistance. This will be investigated as a marker of insulin resistance in these subjects.

Factor XIII activity is assayed by a method which employs cadaverine incorporation as a surrogate for fibrin cross-linking and which has been developed in the Unit of Molecular Vascular Medicine in Leeds. Factor XIII A and B subunit antigens will be assayed by in house ELISA. These assays have a sensitivity of 0.4ng/ml of Factor XIII A and B subunits with an intra-assay coefficient of variation of 4 % and 6 % respectively.

Assessment of fibrin structure/function; Fibrin permeation characteristics

Measurement of the permeability of fully polymerised and cross-linked fibrin provides structural data regarding fibre thickness and the mass-length ratio. This is done by assessing the permeation or Darcy constant Ks. The Ks represent the surface of the gel allowing flow through a network and thus provides information on the pore structure will be calculated using the following formula: $Ks = {}^{Q.\,L\,.\eta}/_{A\,t\,\Delta P}$ where Q Is the volume of liquid (ml) with the viscosity η (10^{-2} poise) flowing through a clot with length L (1.3 cm) and a cross-sectional area A (0.049 cm^2) in time t (sec) under pressure Δ P (dyne/cm^2). Duplicate clots are formed for each plasma sample, using human thrombin and calcium. Samples are incubated in a moist atmosphere for 2 hours to allow for full clot formation and cross-linking. The fibrin clots will be washed with 0.05 mol/L Tris-Cl, pH 7.5, 0.1 mol/L NaCl, and permeated with the same buffer at a pressure drop of 4 cm. Flow rate of the buffer through the clots is analysed by measuring total buffer filtrate at 30minute intervals.

Fibrin polymerisation

Fibrin polymerisation will be studied by following generation of turbidity at 350 nm over

the time course of clot formation. Turbidity analysis provides kinetic information regarding the lag period and rate of fibrin polymerisation, in addition to fibre thickness, which can be calculated from the maximum absorbency at complete clot formation. Clot formation of each sample will be triggered in duplicate with thrombin and calcium in microtiter plate. Immediately upon addition of thrombin/calcium, absorbency will be read every 7 seconds at 350 nm for 15 minutes using a Dynex MRX-TC2 plate reader in kinetic mode. Parameters such as lag phase before start of fibrin polymerisation slope of the polymerisation curve (A/min) and maximum absorbency at full polymerisation will be recorded. The addition of a fibrinolytic agent (tPA) allows for analysis of lysis of the fibrin clot, again reading the absorbency every 7seconds over a period of up to 8 hours until full lysis has occurred.

Visco-Elastic properties

Fibrin cross-linking by FXIIIa is a strong determinant of the elasticity of the fibrin clot. We have recently purchased ROTEM equipment. The ROTEM provides a fully automated method to measure visco-elastic properties of the fibrin clot in whole blood samples or in blood plasma. In collaboration with physics (Leeds University) we have also developed magnetic tweezers equipment which we may use to investigate visco-elastic properties in more detail.

Confocal Microscopy

Fibrin clot structure will be imaged using confocal microscopy. In brief, thrombin and FITC fibrinogen will be added to plasma samples, and placed into a 6 channel confocal microscopy plate. After an incubation period to ensure full clot formation and fibrin cross linking, the clots can be imaged using the confocal microscope. This provides both 2dimensional and 3 dimensional images. In addition to providing detailed pictorial representations of the clot, this will also allow accurate measurement of fibre thickness and pore size (by taking relevant measurements at known magnifications).

Scanning electron microscopy

Fibrin clot structure will be further investigated by scanning electron microscopy. We will make use of electron microscopes (Camscan Series 4 and Camscan CS-44-EX) available in the microscopy suit of the Department of Material Sciences at the University of Leeds. Clots will be made as previously described. The clot will be extensively washed with 0.067 mol/l Na-cacodylate buffer pH 7.2, fixed with 2 % glutaraldehyde in cacodylate buffer overnight. Samples will be further processed dehydration using a stepwise acetone gradient, critical point drying and sputter coating

with palladium-gold. Each sample will be observed in at least 6 different areas for digital image analysis. Overall clot structure will be analysed, in addition to measurement of fibre image analysis. Overall clot structure will be analysed, in addition to measurement of fibre thickness and number of branch points per area using Image software version 1.24 (Wayne Rasband, National Institutes of Health, USA).

Molecular Biology

DNA extraction

DNA is extracted from the whole blood samples taken at recruitment. Prior to extraction, samples are defrosted in a room temperature water bath.

The process uses a commercially available DNA extraction kit (QIAGEN maxi spin kit). In brief, protease and a lysis buffer are added to the whole blood samples, and then incubated at 75°C for 10minutes. 100 % ethanol is added, and following a thorough mixing stage, the samples are decanted into the QIAGEN spin column. They are centrifuged at 3000rpm for 2minutes, and the filtrate discarded. The column is then washed in a two-stage process, before being transferred into a clean centrifuge tube. The elution buffer is added, the column incubated to ensure DNA binding, and two final centrifugation stages are undertaken.

The concentration of the resulting DNA sample solution is elicited using the Nanodrop reader, at an absorbance of 260nm. Samples are diluted to a final concentration of 10ng/μL using DNAase and RNAase free TBS, and stored at 4°C. Long term storage of concentrated DNA for future work is at -20°C.

RNA Extraction

RNA will be extracted using a standardized TRIreagent protocol. Total RNA is extracted from VSMC using Tri- reagent (Sigma), bromocriptine and glycogen. RNA precipitates were re-suspended in water followed by DNase 1 turbo digestion at 37oC for one hour. RNA can be quantified using Ribogreen® (Molecular Probes, Invitrogen). 0.6ug of RNA is reverse transcribed to cDNA using the Applied Biosystems High Capacity RNA to cDNA kit (RT+). 0.6ug is also used for a genomic DNA control in a reaction without reverse transcriptase (RT-). Real time PCR is performed using SYBR Green I on a LightCycler (Roche). The specificity of PCR is confirmed by performing RT negative control experiments and melt curve analysis of PCR products. PCR cycle crossing points (Cp) are determined using a fit points methodology (Light Cycler Software 3.5). Relative abundance of target RNA is quantified as compared to the

housekeeper gene beta actin.

Protein Extraction

Vascular smooth muscle cells are collected on ice cold phosphate buffered saline and pelleted at 4oC before lysis using Laemmli sample buffer supplemented with complete protease inhibitor (Roche). The lysate is centrifuged to remove particulate matter and equal amounts of protein are separated by 8 % sodium dodecyl sulphate polyacrylamide gel electrophoresis and transferred onto nitrocellulose membrane. Membranes are incubated with blocking buffer for two hours at room temperature followed by incubation with primary antibodies of interest overnight at 4oC. Membranes are washed and incubated with the secondary antibody of interest. Signals are detected using super signal west pico chemiluminescent.

Genotyping

Currently, DNA samples are genotyped for known polymorphisms of Fibrinogen, Factor XIII and TAFI. Commercially available probes are used (Taqman Genotyping Assays). Genetic polymorphisms in other coagulation and fibrinolysis related proteins will also be investigated.

In brief, the probe is added to TaqMan Genotyping MasterMix in a 20:1 ratio (henceforth referred to as MasterProbe). 2.7μL of MasterProbe and 2.2μL of the diluted DNA (10ng/μL) are added to each well of a 384 well plate. Two no template controls (containing only MasterProbe) are included on each plate. A LightCycler480 is used for programming the real time PCR. Each run consists of 50 amplifications, with end-point genotyping following cooling.

Operative Samples

Participants undergoing open aneurysm repair at Leeds Teaching Hospitals NHS Trust as part of their usual care will be given the opportunity to donate tissue samples as part of the study. All tissue taken as part of this process would usually be discarded during the operation.

Aortic Wall

A segment of anterior aortic wall will be biopsied at the time of surgery and divided into different transport media as follows: (1) Dulbecco"s Modified Eagle Medium supplemented with 10 % foetal calf serum and 1 % penicillin/streptomycin transported on ice to Dr Porter's primary tissue culture lab and (2) sterile 0.9 % saline, transported

at room temperature to the lab for histological analysis.

Dr Porter and her team will undertake Smooth muscle cell isolation & culture. An explant technique will be used to acquire primary vascular smooth muscle cells (vSMC). The media will be isolated and dissected into small fragments ($1mm^3$) and transferred in 2ml of culture medium to tissue culture flasks and maintained at 37^oC in a humidified incubator in 5 % CO_2 in air. After 1-2 weeks, vSMC will be observed to migrate out from the explants and passaged in order for experimentation. The primary cells will be confirmed as SMC by staining for intracellular smooth muscle-actin and myosin heavy chain-2 fibres. Isolated vSMC can be used for DNA, mRNA and protein characterisation, in addition to functional and phenotypic analysis studies. Functional studies include proliferation, invasion, migration and apoptosis assays. Secretory function can be demonstrated with the use of zymography. Phenotypic studies will allow the identification of extracellular markers that will help characterise the vSMC.

Our early work suggests that vSMC isolated from AAA exhibit poor proliferation, reduced migration and we have observed a flatter more rhomboid phenotype compared to vSMC isolated from internal mammary artery in use in the lab. To further understand the driving forces behind this altered phenotype, the vSMC will be used for calcium signalling experiments in conjunction with Prof. Beech using a range of pharmacological agents, RNA interference strategies and antibodies. This work will involve isolation of mRNA/protein from the cultured vSMC in addition to functional assays as previously described.

Intraluminal Thrombus

The material will be fixed in formalin before sectioning on a microtome to allow immunohistochemical analysis of blood coagulation and fibrinolysis related proteins. Blood and tissue samples taken from the same patient will be appropriately coded to allow them to be matched during analysis.

Data Management

The LEADS database itself is managed by Thomas Fleming, Data Management Technology Group, University of Leeds. All information stored on this database is anonymised. The master database of information is stored on a password protected computer in an access-limited area of the university. Access to the original database is limited to the database manager, the lead research nurse, and the vascular research administrative assistant who works alongside her (David Watson). Access-only use is

granted to members of the research team at the discretion of the principal investigator.

Identifiable patient information is held only as paper copies, and is kept in a secure, locked drawer in a limited access area of the University of Leeds. The lead research nurse (Mrs Anne Johnson) acts as the custodian for this information, and is the only one to have access to the identifiable data. Personal identifiable information will be destroyed five years after the end of the study.

Appendix 2 - Patient Information Sheet

THE LEEDS ANEURYSM DEVELOPMENT STUDY

A Study of risk factors in patients with Abdominal Aortic Aneurysms (AAA)

You are being invited to take part in a RESEARCH study. Before you decide, it is important for you to understand why the research is being done and what it will involve. Please read the following information carefully and discuss it with friends, relatives and your GP if you wish. Ask us if there is anything that is not clear, or if you would like more information. A leaflet is produced by INVOLVE (Promoting public involvement in NHS, public health and social care research) - www.invo.org.uk gives information about medical research and looks at some questions you may want to ask.

What is the purpose of the study?

Aortic aneurysm is a common condition where the major blood vessel (aorta) in the tummy dilates like a balloon. The vast majority of patients have no symptoms. There is some evidence that abdominal aortic aneurysms (AAA) run in families and it is unclear whether this risk is due to environmental factors (e.g. diet, smoking, high blood pressure etc.) or whether a person's genes may contribute.

Given time, however, the aneurysm expands and may burst. Of all the cases of ruptured AAA only 10 % survive emergency surgery compared to 95 % who survive elective surgery. The wider availability of ultrasound scans as a simple non-invasive method to accurately assess the presence of aneurysms and the National Aortic Aneurysm Screening means that in future it is likely that we will identify large numbers of subjects with early disease.

At the present time patients with small Aortic Aneurysms (3.0 – 5.0cm) are followed up by routine ultrasound scans every 6-12 months depending upon their size. Once the Aortic Aneurysm exceeds 5.0cms patients are referred by their consultants for more specialised scanning to assess the suitability for treatment. This can be either a CT or

MRI/MRA scan. A CT (Computerised Tomography) scan is a type of x-ray examination where a cross sectional picture of the area scanned is produced. Magnetic Resonance Scanning (known as MRI/MRA)) is a way of looking inside your body without the use of x-rays. Instead it uses a large magnet, radio waves and a computer to scan your body and produce a detailed picture.

Surgery in the form of open or stenting (minimally invasive) is reserved for those patients in whom the abdominal aortic aneurysm exceeds 5.5cms in diameter.

The aim of this project is to investigate the cause of abdominal aortic aneurysm, and in particular the proteins that cause weakening of the wall of the aorta and the genes for those proteins.

The project should provide us with important information about the cause of abdominal aortic aneurysms and may identify relatives at risk of developing the condition.

The study may also identify further areas of study in the development of new drug treatments to stop the abdominal aorta from increasing in size.

Why have I been chosen?

You have been chosen because you have an Abdominal Aortic Aneurysm so called “triple A”

Do I have to take part?

It is up to you to decide whether or not to take part. If you do decide to take part, you will be given this information sheet to keep and be asked to sign a consent form. If you do decide to take part, you are still free to withdraw at any time and without giving a reason. This will not affect the standard of care you receive.

What will happen if I take part?

If you are happy to help us with this research project this is what will happen

You will have nothing to eat or drink after midnight before your visit.

You should try not to smoke during this period.

You will be asked some simple questions about your health.

You will have cuffs placed around your arm, leg and a pad on your neck which will be used to measure the stiffness of your blood vessels.

You will have a heart tracing.

You will give a sample of blood (50mls, about 4 tablespoons). These samples will allow us to study the levels of blood sugar, fat and factors in the blood, which cause it to clot. We will also look at the genes which are involved in the development of aortic aneurysms and the formation of new blood vessels and blood clotting

You will have a simple ultrasound test (very similar to the scans that pregnant women have) to measure the size of the abdominal aorta. This is painless and takes 5-10 minutes. In those cases where it is difficult to see the aorta we will arrange a separate ultrasound scan at St James' Hospital, this will be undertaken by Dr Michael Weston, Consultant Radiologist.

The above tests will take place in the clinical research unit of the LIGHT laboratories of the University of Leeds. You will be asked to attend for an appointment with a research nurse, which will last about one hour. We will write to you to confirm a suitable day and time for the assessment. We will send you details of how to get to the LIGHT building either by local transport or taxi.

We will access your electronically held medical records annually. We will register your data with the NHS Information Centre and the NHS Central Register so that we can track your progress over the study time period. As such your data will be identifiable to us.

We will write to you on a yearly basis to ask if you would be prepared to return for a further a repeat assessment.

If your aortic aneurysm is larger than 5.0cms your consultant will arrange for you to have either a CT scan or an MRI scan. This is part of the normal workup to assess how best to treat your aortic aneurysm. We would like to have your permission to store these anonymised images and use them at a later date to study (1) the comparison between ultrasound and CT/MRI, (2) the force and stresses upon the aortic wall, (3) the flow through the aorta and (4) the impact of a metal stent on the aorta. This work will be undertaken by Dr Peter Walker (Department of Mechanical Engineering, University of Leeds)

If you are having an operation for your aortic aneurysm we would ask permission to collect the following samples:

Fluid between the aortic aneurysm wall and the blood clot

A blood sample (20 ml) from the aneurysm sac,

A sample of the wall of the aortic aneurysm and

The blood clot within the aneurysm.

All of these tissues are usually discarded at the time of surgery

Post operation

You will be seen in the outpatient department at approximately six weeks following surgery.

At this stage we will ask if you would be happy for a further sample to be taken at 3 to 6 months post operatively. This could be arranged as a home visit.

You will have nothing to eat or drink after midnight before your visit.

You should try not to smoke during this period.

You will give a sample of blood (50mls, about 4 tablespoons). These samples will allow us to study the levels of blood sugar, fat and factors in the blood, which cause it to clot.

What are the potential risks from taking part?

Taking a blood sample is unlikely to cause any problems, although some people experience minor discomfort or bruising.

What are the potential benefits from taking part?

There are no direct benefits to you for taking part. In the future we hope that the information we get from this study may help us to improve the treatment of patients with abdominal aortic aneurysms. We will be able to assess whether life-style changes and or new drug treatments may help those patients with small abdominal aortic aneurysms and relatives at highest risk of developing abdominal aortic aneurysms.

What if new information becomes available?

Sometimes during the course of a research project, new information becomes available. In your case this may be an increase in the size of your abdominal aorta. If this happens, your research nurse will tell you about it and discuss with you whether you want to continue in the study. If you decide to withdraw, arrangements will be made for your care to continue. If you decide to continue in the study you will be asked to sign an updated consent form and the necessary information passed onto your consultant surgeon and general practitioner.

What if something goes wrong?

If taking part in this research project harms you, there are no special compensation arrangements. If you are harmed due to someone's clinical negligence, then you may have grounds for a legal action but you may have to pay for legal advice. Regardless of this, if you wish to complain about any aspect of the way you have been approached or treated during the course of this study, the normal National Health Service complaints mechanisms should be available to you.

Will my taking part in this study be kept confidential?

All information, which is collected, about you during the course of this research will be kept *strictly confidential.* Any information that leaves the laboratory will have your name

and address removed so that you cannot be recognised from it. The blood, fluid and tissue samples taken to look at the proteins and genes will be given a study number so that it is impossible in any way to identify you from them.

You should be aware that the samples of blood, fluid and tissue will be stored in a freezer and may be used for future studies at a later date.

Any abnormalities detected in your blood sugar or fat will be forwarded to you and your general practitioner.

What will happen to the results of the study?

The results of the study will be published in a variety of surgical journals and discussed at surgical meetings. Please note that you will not be identified in any report or publication.

Who is organising and funding the research?

The study is based in the Division of Cardiovascular and Diabetes Research at the Leeds Institute of Genetics, Therapeutics and Health at the University of Leeds. The study is currently funded by The Garfield Weston Trust, Circulation Foundation, British Heart Foundation and Wellcome Trust.

Who has reviewed the study?

Leeds (East) Research Ethics Committee has reviewed the study.

Contact for further information.

Any further questions regarding the study can be easily answered by calling Anne Johnson Vascular **Research Nurse 0113 343 7702** or by writing to Professor Julian Scott, Leeds Vascular Institute, Leeds General Infirmary, Leeds LS1 3EX Version 10 01/02/2012

Thank you for considering whether to take part in this research

Appendix 3 - Patient Consent Form

THE LEEDS ANEURYSM DEVELOPMENT STUDY

Subject Identification Number: Name of researcher: Prof D J A Scott

Anne Johnson

I confirm that I have read and understand the study information sheet dated.../../…., and have had the opportunity to discuss it with relatives and friends, and ask any questions.

I understand and accept that if I take part in the study I may not gain any direct personal benefit from it.

I understand that all information collected in the study will be held in confidence and that, if it is presented or published, all my personal details will be removed from it.

I confirm that I will be taking part in this study of my own free will. I understand that I may withdraw from it, at any time and for any reason, without my medical care or my legal rights being affected.

I understand that any blood and tissue samples collected as part of the study are given freely as a gift. I consent to my samples being examined for genetic factors which are thought to influence the formation of aneurysms. I agree to transfer any property rights to the samples I provide to the University of Leeds on the understanding that it is only used for research.

I agree to my electronically held medical records being accessed annually by the research nurses assigned to the study

I understand my details will be registered with the NHS Information Centres

I agree to participate in this study.

Name	Signature	Date
Name of Person taking consent	Signature	Date

One copy for patient, 1 copy for researcher, 1 copy to be kept with hospital records

Appendix 4 – Purification of fibrinogen γA/γ' and γA/γA - Concave gradient for elution

Sample elution: Gradient from 0 % to 100 % Buffer B1, over 13.4CV, 2ml/min (3.5ml fractions, +6°c)

5 % Buffer B1, 3.16 CV

10 % Buffer B1, 3.63 CV

15 % Buffer B1, 3.63 CV

20 % Buffer B1, 3.63 CV

25 % Buffer B1, 3.63 CV

30 % Buffer B1, 3.63 CV

40 % Buffer B1, 3.63 CV

10 % Buffer B1, 3.63 CV

10 % Buffer B1, 3.63 CV

10 % Buffer B1, 3.63 CV

10 % Buffer B1, 3.63 CV

10 % Buffer B1, 3.63 CV

10 % Buffer B1, 3.63 CV

Column wash: Buffer B1, 5 CV, 2 ml/min

Column equilibration: Buffer A1, 5 CV, 2 ml/min

Run time ~ 350 min

Pool peaks fractions and store at -80 °c

Store column at +4 °c

Appendix 5 – In-house fibre density macro

I produced a macro using image J (v2.0, NIH), which runs through the following steps:

Maximum intensity projection of a 20 µm (all layers of Z-stack flattened into one), and subtraction of background (Figure 76A).

The resulting image is made binary (Figure 76B)

A vertical line is drawn across the image (Figure 76C)

All parts of the image are removed except for the sections of the clot fibres that cross the yellow line (Figure 76).

The number of points that crossed the line is quantified and this represents the number of fibres that crossed the yellow line

This is repeated 9 more times vertically at different points across the image, and then 10 times horizontally down the image.

From this the average number of fibres/100 µm can be calculated.

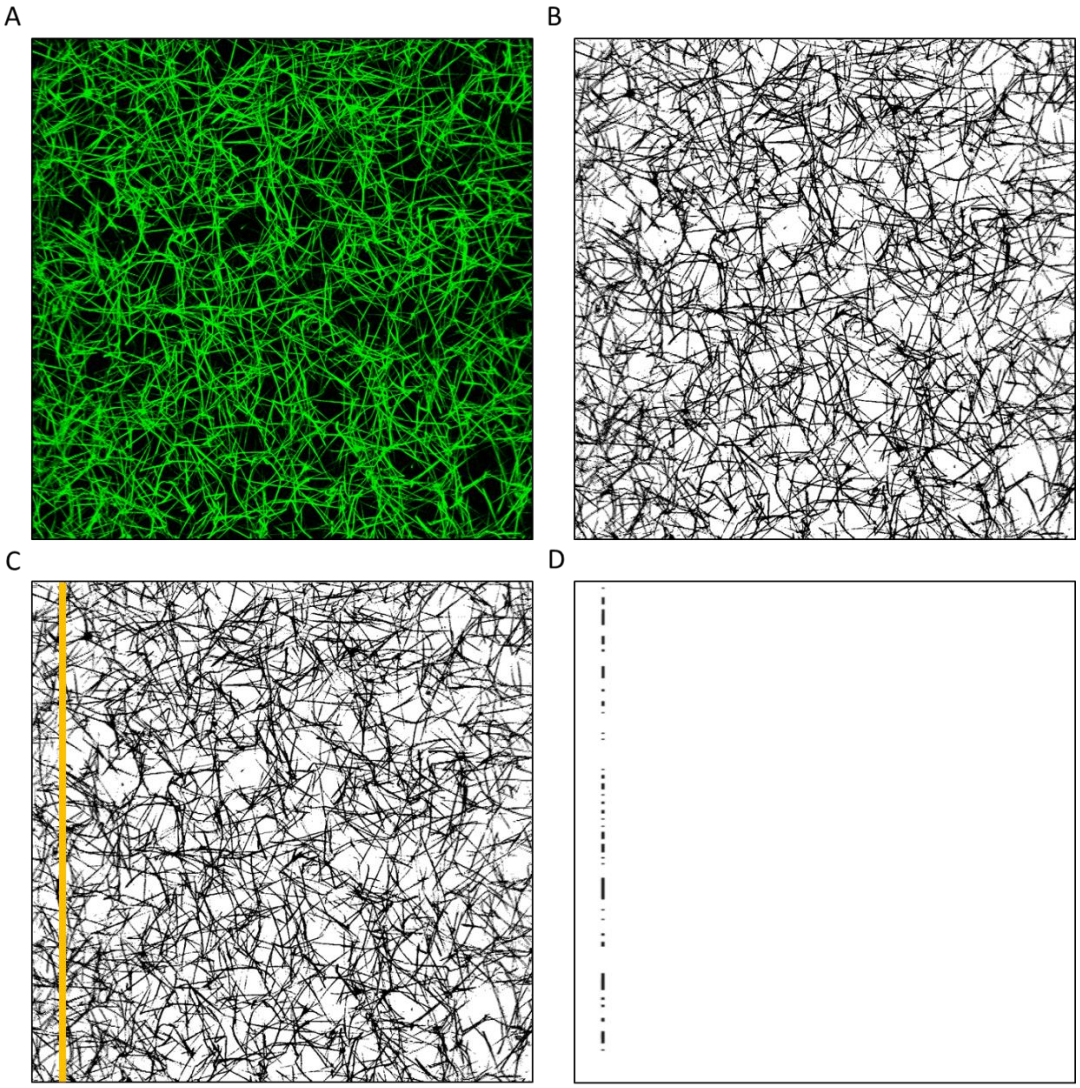

Figure 76 Fibre density macro. The multiple stages of the macro have been separated. **A,** Z-stacks are flattened. **B,** Images are made binary. **C,** 10 vertical and 10 horizontal lines are drawn across the image at different points. **D,** For each line all areas of the image are deleted except the sections of fibre that intersect the line. These are then quantified.

Appendix 6 - DNA extraction from whole blood using the QIAGEN Maxi-Column Kit

Before starting

Prepare a 70°C water bath

Buffer AW1 should be prepared (mixed with ethanol as indicated on the bottle)

Stored at room temp

Buffer AW2 should be prepared (mixed with ethanol as indicated on the bottle)

Stored at room temp

QIAGEN protease should be prepared (Add 5.5mls of distilled water)

Blood should be defrosted in a room temperature water bath

Procedure

Pipette 500µL QIAGEN protease into the bottom of a 50ml centrifuge tube (each vial of protease will be enough for 11 blood samples)

Add 6ml of blood (one full pink topped tube)

Add 4ml of PBS

Mix briefly

Add 12ml of Buffer AL (provided in kit), mix thoroughly by inverting the tube 15 times then shaking vigorously for a minute.

Incubate at 70°C for 10minutes (incubating for longer will not adversely affect the DNA yield)

Add 10ml of ethanol (96-100 %) to each sample

Mix by inverting 10 times and then shaking vigorously again

Transfer half of the solution into the QIAamp maxi column within a 50ml centrifuge tube.

Ensure the rim is dry and close the cap

Centrifuge at 1850 x g or 3000 rpm for 3 minutes

Remove the maxi-column from the centrifuge tube, discard the filtrate, ensure the tube is dry and replace the column

Transfer the remaining solution into the maxi-column

Centrifuge again at 1850 x g or 3000 rpm for 3 minutes

Remove the maxi-column from the centrifuge tube, discard the filtrate, ensure the tube is dry and replace the column

Add 5ml of Buffer AW1 to the QIAamp maxi column. Pipette carefully, without moistening the rim. Pipette to the side of the column (not directly onto the membrane)

Centrifuge at 4500 x g or 5000 rpm for 1 minute.

Without discarding the filtrate, add 5 ml of buffer AW2 to the QIAamp maxi column.

Centrifuge at 4500 x g or 5000 rpm for 15minutes

Place the QIAamp maxi column in a clean 50 ml centrifuge tube.

Discard the collection tube containing the filtrate

Pipette 1 ml of Buffer AE directly onto the membrane of the QIAamp maxi-column. Incubate at room temperature for 5 minutes.

Centrifuge at 4500 x g or 5000 rpm for 2 minutes.

Two final steps:

For maximum concentration of DNA – reload the eluate containing the DNA onto the maxi column. Incubate for 5 mins at room temperature. Centrifuge at 4500 x g or 5000 rpm for 5 minutes.